Current-Density Functionals in Extended Systems

Arjan Berger

Het promotieonderzoek beschreven in dit proefschrift werd uitgevoerd in de theoretische chemie groep van het Materials Science Centre (MSC) aan de Rijksuniversiteit Groningen, Nijenborgh 4, 9747 AG Groningen. Het onderzoek werd financieel mogelijk gemaakt door de Stichting voor Fundamenteel Onderzoek der Materie (FOM).

Arjan Berger,

Current-Density Functionals in Extended Systems,

Proefschrift Rijksuniversiteit Groningen.

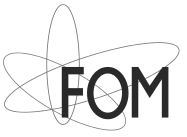

RIJKSUNIVERSITEIT GRONINGEN

Current-Density Functionals in Extended Systems

Proefschrift

ter verkrijging van het doctoraat in de
Wiskunde en Natuurwetenschappen
aan de Rijksuniversiteit Groningen
op gezag van de
Rector Magnificus, dr. F. Zwarts,
in het openbaar te verdedigen op
maandag 2 oktober 2006
om 16.15 uur

door

Jan Adriaan Berger

geboren op 24 februari 1978
te Steenwijk

Promotor:	prof. dr. R. Broer
Copromotores:	dr. R. van Leeuwen
	dr. ir. P. L. de Boeij

Beoordelingscommissie:	prof. dr. A. Görling
	prof. dr. J. Knoester
	prof. dr. G. Vignale

ISBN: 90-367-2758-8

voor mijn ouders

Contents

General Introduction **xi**
0.1 Introduction . . . xi
0.2 Overview of the Thesis . . . xiv

1 Density-Functional Theory **1**
1.1 Introduction . . . 1
1.2 Preliminaries . . . 1
1.3 Hohenberg-Kohn Theorem for Nondegenerate Ground States . . . 3
1.4 The Functional Derivative . . . 6
1.5 Kohn-Sham Theory . . . 7
1.6 Hohenberg-Kohn Theorem for Degenerate Ground States . . . 10
1.7 The Lieb Functional and Noninteracting v-Representability . . . 13
1.8 Exchange-Correlation Functionals . . . 17

2 Time-Dependent (Current-)Density-Functional Theory **21**
2.1 Introduction . . . 21
2.2 Preliminaries . . . 21
2.3 The Runge-Gross Theorem . . . 23
2.4 Time-Dependent Kohn-Sham Theory . . . 26
2.5 The Adiabatic Local Density Approximation . . . 27
2.6 Time-Dependent Current-Density-Functional Theory . . . 28
2.7 The Keldysh Action Functional . . . 34
2.8 Exact Constraints . . . 40

3 Linear Response within TD(C)DFT **43**
3.1 Introduction . . . 43
3.2 Linear Response Theory . . . 43
3.3 The Linear Response Kohn-Sham Equations . . . 46

3.4 The Exchange-Correlation Kernel in TDDFT 49
3.5 Exact Constraints within the Linear Response Formulation of TDDFT 50
3.6 Examples of Approximate Exchange-Correlation Kernels 51
3.7 The Ultra-Nonlocality Problem 52
3.8 The Exchange-Correlation Kernel in TDCDFT 53
3.9 Exact Constraints within the Linear Response Formulation of TDCDFT 56

4 The Vignale-Kohn Functional 59
4.1 Introduction 59
4.2 Summary of the Main Results 59
4.2.1 The Exchange-Correlation Kernel of the Homogeneous Electron Gas 59
4.2.2 The Weakly Inhomogeneous Electron Gas 60
4.2.3 The Exhange-Correlation Kernel to First Order in γ 61
4.2.4 The Vignale-Kohn Functional in Real Space 62
4.3 The Homogeneous Electron gas 63
4.4 TDCDFT for the Homogeneous Electron Gas 66
4.5 The Weakly Inhomogeneous Electron Gas 68
4.5.1 The Expansion of the Exchange-Correlation Kernel 68
4.5.2 First Order in the Inhomogeneity and the Ward Identity 69
4.5.3 The Onsager Relation and the Conservation Laws 72
4.5.4 Explicit Form of the Exchange-Correlation Kernel to First Order in γ 75
4.5.5 Construction of the Vignale-Kohn Functional in Real Space . . 77
4.6 The Response Coefficients $f^h_{xcL,T}(\rho,\omega)$ 84

5 Analysis of the Viscoelastic Coefficients in the Vignale-Kohn Functional: The Cases of One- and Three-Dimensional Polyacetylene 93
5.1 Introduction 94
5.2 Theory 98
5.2.1 TDCDFT 98
5.2.2 Linear Response 99
5.2.3 The Vignale-Kohn Functional 102
5.2.4 The Response Coefficients 104
5.3 Implementation 108
5.4 Computational Details 111
5.5 Results 112
5.6 Conclusions 119

6 A Physical Model for the Longitudinal Polarizabilities of Polymer Chains 123
6.1 Introduction . . . 124
6.2 Theory . . . 127
6.2.1 Extrapolation Methods . . . 127
6.2.2 Infinite Quasi-one-dimensional Dielectric Media . . . 128
6.2.3 The Dielectric Needle . . . 130
6.2.4 Approximate Solution of the Fredholm Equation . . . 134
6.3 Computational Details . . . 137
6.3.1 Periodic Boundary Calculations . . . 137
6.3.2 Extrapolation . . . 138
6.4 Results . . . 138
6.5 Conclusions . . . 142

7 Analysis of the Vignale-Kohn Current Functional in the Calculation of the Optical Spectra of Semiconductors 147
7.1 Introduction . . . 147
7.2 Theory . . . 149
7.2.1 TDCDFT Linear Response Equations . . . 149
7.2.2 The Vignale-Kohn Functional . . . 152
7.2.3 Limiting behavior of $f^h_{xcL,T}$ . . . 155
7.2.4 Parametrizations for $f^h_{xcL,T}$ . . . 157
7.3 Computational Details . . . 158
7.4 Results . . . 159
7.5 Conclusions . . . 162

8 Performance of the Vignale-Kohn Functional in the Linear Response of Metals 163
8.1 Introduction . . . 164
8.2 Theory . . . 166
8.2.1 Time-Dependent Current-Density-Functional Theory . . . 166
8.2.2 Linear Response . . . 167
8.2.3 The Vignale-Kohn Functional . . . 171
8.2.4 Relativistic Corrections . . . 174
8.3 Implementation . . . 176
8.4 Results . . . 178
8.5 Conclusions . . . 183

9 A Nonlocal Current-Density Functional **191**
9.1 Introduction . . . 191
9.2 Theory . . . 193
9.2.1 TDCDFT . . . 193
9.2.2 Zero-Force and Zero-Torque Theorems . . . 194
9.2.3 The Exchange-Correlation Vector Potential of the Homogeneous Electron Gas . . . 197
9.2.4 A Nonlocal Current-Denstity Functional . . . 199
9.2.5 The Exchange-Correlation Kernel of the Homogeneous Electron Gas . . . 201
9.3 Implementation . . . 203
9.3.1 Evaluation of the Exchange-Correlation Vector Potential . . . 203
9.3.2 Fitfunctions . . . 204
9.4 Computational Details . . . 207
9.5 Results . . . 207
9.6 Conclusions . . . 211

List of Acronyms **213**

Samenvatting **215**

List of Publications **223**

Dankwoord **225**

Bibliography **227**

General Introduction

0.1 Introduction

In quantum chemistry we are interested in the physical properties of many-particle systems like atoms, molecules and solids. These systems consist of electrons, protons and neutrons which are all spin-1/2 fermions. The protons and neutrons together form the nuclei of these systems. A complete (nonrelativistic) description of the physics of these many-particle systems is governed by the quantum-mechanical wave function $\Psi(\mathbf{x}_1, \mathbf{x}_2, \cdots, \mathbf{x}_n, t)$, where n is the number of particles in the system and the coordinates $\mathbf{x}_i$ consist of the space-coordinate $\mathbf{r}_i$ and the spin-coordinate σ_i. This n-particle wave function can be obtained by solving the time-dependent Schrödinger equation,

$$\hat{H}(t)\Psi(\mathbf{x}_1, \mathbf{x}_2, \cdots, \mathbf{x}_n, t) = i\frac{\partial}{\partial t}\Psi(\mathbf{x}_1, \mathbf{x}_2, \cdots, \mathbf{x}_n, t), \tag{1}$$

where $\hat{H}(t)$ is the Hamiltonian which consists of a kinetic energy operator and a potential operator. Its expectation value describes the total energy of the system. The exact form of the potential operator depends on the physical problem at hand. If the potential is time-independent then the Schrödinger equation can be solved by the method of separation of variables for separable initial states. The solution is then a simple product of a purely time-dependent function and a function that only depends on the positions of the particles. The solution for the latter function can be obtained from the time-independent Schrödinger equation,

$$\hat{H}\Psi(\mathbf{x}_1, \mathbf{x}_2, \cdots, \mathbf{x}_n) = E\Psi(\mathbf{x}_1, \mathbf{x}_2, \cdots, \mathbf{x}_n), \tag{2}$$

where E is an eigenenergy of the n-particle system. The solution for the time-dependent function is simply a phase factor. The expectation values of any operator can therefore be obtained without knowledge of this phase factor since it cancels out. To obtain these expectation values one can therefore solve Eq. (2) for $\Psi(\mathbf{x}_1, \mathbf{x}_2, \cdots, \mathbf{x}_n)$. However, for many-particle systems this equation is still much too

difficult to solve. A widely used and accepted approximation to simplify this equation is the so-called Born-Oppenheimer approximation. This approximation is based on the large difference in mass of the electrons and nuclei. Since the nuclei are much heavier than the electrons their movement is much slower than that of the electrons. This means that for each instantaneous configuration of the nuclei the electrons are approximately in a stationary state. We can therefore consider the nuclei to provide a fixed frame for the electrons. The Schrödinger equation for the electronic system in principle has to be solved for all possible configurations of the nuclei. However, since the nuclei are very localized around their equilibrium positions in the body-fixed frame we can consider them to be fixed at these positions, i.e., we replace their probability distributions by delta functions. We have now reduced the problem to solving the electronic part of Eq. (2). This problem cannot be solved exactly for many-electron systems and in practice we need to make approximations by using perturbation theory or variational methods. A well-known variational method is the Hartree-Fock method. The main idea of this approach is that each electron moves in a mean field generated by all other electrons and the external potential (e.g. the nuclear potential). This means that the potential in the Hamiltonian can be approximated by an effective single-particle potential. Consequently we can write the wave function as a Slater determinant of single-particle orbitals. We can then use the Rayleigh-Ritz variational theorem to minimize the expectation value of the Hamiltonian with respect to this Slater determinant. This leads to the so-called Hartree-Fock equations from which we can obtain the effective single-particle potential that gives the lowest energy, the Hartree-Fock potential. Since this potential itself depends on the single-particle orbitals of the Slater determinant the problem has to be solved self-consistently. The Hartree-Fock wave function is often used as a reference wave function in other methods like, for example, the configuration interaction method. In this method one writes the exact wave function as an expansion of Slater determinants of single-particle orbitals. The coefficients are determined by minimization of the energy according to the variational theorem. In practice this expansion has to be truncated at some point. Since the Hartree-Fock wave function is the Slater determinant of single-particle orbitals that gives an energy closest to the true energy it is a good starting point for this expansion. The remaining Slater determinants in the expansion can then be obtained from all the possible excitations of one or more electrons from occupied orbitals to unoccupied orbitals.

A different way to obtain the properties of many-electron systems without making any explicit reference to the wave function was formulated in the 1960's by Hohenberg, Kohn and Sham [1, 2]. This method called density-functional theory (DFT) has as fundamental quantity the electron density. Hohenberg and Kohn showed in

1964 that the external potential is a functional of the electron density. As a consequence every ground-state property, and in particular the ground-state energy, is a functional of the electron density. The advantages of such a theory are clear. Whereas the complicated many-body wave function depends on three spatial variables for each of the N electrons, the electron density is a collective variable which only depends on three spatial variables, making the electron density a quantity that is easier to deal with in practice. Furthermore, the electron density is also easier to deal with from a conceptual point of view. Shortly after, in 1965, Kohn and Sham formulated the idea that the electron density of a system of interacting particles under the influence of some external potential can be reproduced in a system of noninteracting particles under the influence of an effective potential, the so-called Kohn-Sham potential. According to the Hohenberg-Kohn theorem this Kohn-Sham potential is also a functional of the electron density. The Kohn-Sham formulation of DFT allows one to write the Schrödinger equation as a set of single-particle equations that together with the electron density can be solved in a self-consistent manner. Assuming that indeed such a Kohn-Sham system of noninteracting particles exists this theory is exact. The Kohn-Sham potential consists of the external potential, the Hartree potential, which is the average Coulomb potential generated by all the electrons, and the so-called exchange-correlation potential which contains all the remaining contributions. The latter potential is the functional derivative of the exchange-correlation energy with respect to the electron density. In practice we have to find approximations for the exchange-correlation energy and the corresponding potential. We discuss the main aspects of DFT in chapter 1.

In 1984 Runge and Gross formulated the time-dependent extension of the Hohenberg-Kohn theorem [3]. They showed that for two densities evolving from a common initial state and generated by two external potentials that differ by more than a purely time-dependent function and that both have a Taylor expansion around the initial time cannot be the same. Therefore, for a given initial state, the expectation value of any quantum mechanical operator is a unique functional of the density. One can then introduce a time-dependent Kohn-Sham system to obtain equations that can be solved in practice. This method is called time-dependent density-functional theory (TDDFT). However, TDDFT can only be used to describe systems that are under the influence of time-dependent fields that can be described by a time-dependent scalar potential. A similar theory can be formulated for systems under the influence of general time-dependent fields which need to be described by a time-dependent vector potential. However, this theory has to be formulated in terms of the current density instead of the density [4–6]. This theory is therefore called time-dependent current-density-functional theory (TDCDFT). It has some other advantages as well

when compared to TDDFT, especially when considering infinite systems. An efficient way to describe infinite systems is by using periodic boundary conditions (PBC). However, PBC artificially remove the effects of density changes at the surface [7]. For example, when a system is perturbed by an electric field there will be a macroscopic response of the system and there will be a current flowing through the interior with a nonzero average. This macroscopic current is directly related through the continuity equation to a density change at the outer surface of the system but does not correspond to a density change in the bulk of the system. The density change at the surface of the system leads to a macroscopic screening field in the bulk of the system. When using periodic boundary conditions this phenomenon cannot be described with a functional of the bulk density alone [7] but it can be described by a functional of the current density in the bulk. Some of these difficulties can be circumvented by use of an expression which relates the density-density response function to the trace of the current-current response function [8–10]. However, for anisotropic materials this relation only provides enough information to extract the trace of the dielectric tensor and not its individual components. Furthermore, Vignale and Kohn showed that in the case of time-dependent linear response theory, where one is interested in the response to a small external perturbation, a local approximation of the exchange-correlation potential, in general, does not exist if one wants to describe its dynamics in terms of the density [11–13]. They also show that a local approximation for time-dependent linear response theory does exist for the exchange-correlation vector potential in terms of the current density. Therefore it can be more convenient and more efficient to use a local functional of the current density instead of a nonlocal functional of the density. We discuss TDDFT and TDCDFT in chapter 2.

In order to use TDCDFT in practice we need to have an approximation for the exchange-correlation part of the vector potential. By studying a weakly perturbed electron gas Vignale and Kohn derived an exchange-correlation vector potential that is a local functional of the current density [12, 13]. By construction this functional satisfies several conservation laws and symmetry relations. In this thesis we give a discussion of the Vignale-Kohn functional in its application to extended systems. Furthermore, we indicate in what way this functional may be improved upon.

0.2 Overview of the Thesis

As mentioned above an introduction to DFT and TD(C)DFT is given in chapters 1 and 2, respectively. Since we are interested in studying the response of a many-particle system to a small external perturbation it is convenient to formulate the Kohn-Sham equations within the linear response regime. In chapter 3 we show how to derive

these equations. In chapter 4 we discuss the Vignale-Kohn (VK) expression for the exchange-correlation vector potential. We show a derivation of this expression and discuss the longitudinal and transverse parts of the exchange-correlation kernels of the homogeneous electron gas that enter the VK functional. Furthermore, we discuss the parametrizations for these kernels that were formulated by Conti, Nifosì, and Tosi (CNT) [14] and by Qian and Vignale (QV) [15].

In chapter 5 we compare the influence of the CNT and QV parametrizations for longitudinal and transverse exchange-correlation kernels of the homogeneous electron gas on the linear response properties of one-dimensional and three-dimensional polyacetylene. We show that the results strongly depend on the values of the exchange-correlation part of the shear modulus. The spectra obtained with the CNT parametrization are relatively close to the spectra obtained in the adiabatic local density approximation (ALDA), while the spectra obtained with the QV parametrization largely differ from the ALDA spectra. We obtain roughly the same results when we neglect the frequency dependence of the two parametrizations. This means that the explanation for the difference between the QV spectra and the ALDA spectra is in the dependence of the results on the transverse exchange-correlation kernel of the homogeneous electron gas in the limit of vanishing frequency, since the longitudinal part reduces to the ALDA in this limit. The transverse exchange-correlation kernel is related to the exchange-correlation part of the shear modulus in the limit of vanishing frequency. Unfortunately this quantity is only known approximately.

In chapter 6 we introduce an extrapolation method in order to compare our results for the polarizability per unit cell of infinite polymer chains with results obtained for finite polymer chains. In contrast to many extrapolation methods in the literature our model is based on the physical properties of polymer chains. In our model we assume that a polymer chain is well-described by a nonconducting cylinder with a radius much smaller than its length, the so-called dielectric needle model. We show that within this model the macroscopic screening disappears in the limit of a rod of infinite length. This means that we can obtain the polarizability per unit chain of an infinite polymer chain directly from a periodic boundary calculation. Furthermore we show that end effects, which ultimately vanish in the infinite polymer chain, decrease only slowly with increasing chain length. The dielectric needle also provides us with a procedure to extrapolate the results for the polarizability per unit chain of finite polymer chains to infinite length. We test our dielectric needle model on polyacetylene and the hydrogen chain and we found values for the polarizability per unit cell obtained with the two methods are in good agreement. This means that our dielectric needle model is a good approximation to describe the dielectric properties of long polymer chains.

In chapter 7 we apply the VK functional to the calculation of the optical spectra of

semiconductors. We discuss the results for silicon which is a typical case. If we use the QV parametrization for the longitudinal and transverse exchange-correlation kernels of the homogeneous electron gas the optical spectra collapse. We discuss possible reasons for this failure. We show that the constraints on the degree of nonuniformity of the ground-state density and the degree of spatial variation of the external potential for which the VK functional is derived, are almost all violated. Furthermore, we argue that the VK functional which is derived for a weakly perturbed electron gas in the region above the particle-hole continuum is not suited to calculate optical spectra since they are closely related to the particle-hole continuum. If we make the approximation that the exchange-correlation part of the shear modulus is equal to zero, as was done in the CNT parametrization we obtain optical spectra that are close to the spectra obtained within the ALDA. This is simply a consequence of the fact that in this approximation the VK functional reduces to the ALDA in the limit of vanishing frequency and the fact that for the relevant frequencies in optical spectra the values of the longitudinal and transverse exchange-correlation kernels of the homogeneous electron gas are not very different from their values at zero frequency.

In chapter 8 we show how we include the VK expression in our formulation of the linear response of metals. Since this functional is nonlocal in time we can take into account relaxation effects due to electron-electron scattering in this way. We discuss de different behavior of the inter- and intraband processes when the wave vector of the perturbation is small. In the optical limit, where this wave vector vanishes, the two sets of self-consistent equations are coupled when we include the VK functional in our formulation. Because of the results mentioned above for the optical spectra of semiconductors and the fact that we are mainly interested in the frequency dependence of the exchange-correlation vector potential to describe relaxation effects we make the approximation that the exchange-correlation part of the shear modulus is equal to zero in all our calculations. In this way we obtain the dielectric function and the electron energy loss spectra (EELS) of copper, silver and gold. The obtained results are in good agreement with the results obtained in experiment. In contrast to the ALDA results we obtain the Drude-like tail in the low-frequency part of the imaginary part of the dielectric function. Furthermore, we now obtain the experimentally observed sharp plasmon peak in the EELS of silver.

In chapter 9 we relieve the constraints on the wave vector of the perturbation which restricts the formal application of the local VK functional by introducing a nonlocal functional of the current density with a similar viscoelastic structure as the VK functional. This nonlocal functional is constructed such that it satisfies the same conservation laws and symmetry relations as the VK functional. In contrast to the VK functional this nonlocal functional is almost completely determined by the

longitudinal exchange-correlation kernel for low frequencies whereas the VK functional is mainly determined by its transverse exchange-correlation kernel in this frequency range. The optical spectra of silicon and gallium phosphide calculated with this nonlocal functional collapse in a similar way as the spectra obtained with the VK functional. If we use our nonlocal functional in which we only take into account the uniform component of the current density we obtain results close to those obtained in experiment provided we use an empirical prefactor. We therefore conclude that we are considering the correct physics by using a functional of the current density instead of a functional of the density but that a good current-density functional is not available at the moment.

Chapter 1

Density-Functional Theory

1.1 Introduction

The aim of density-functional theory (DFT) as formulated by Hohenberg, Kohn and Sham [1,2] is to describe the properties of the ground state of a many-electron system solely by the electron density without making any explicit reference to the many-body wave function. In other words every ground-state property, and in particular the ground-state energy, is a functional of the electron density. The advantages of such a theory are clear. Whereas the complicated many-body wave function depends on three spatial variables for each of the N electrons, the electron density is a collective variable which only depends on three spatial variables, making the electron density a quantity that is easier to deal with in practice. Furthermore, the electron density is also easier to deal with from a conceptual point of view. That the ground-state properties of a many-electron system can be obtained from the electron density alone is, however, not obvious. We will present the proof of this fact, originally given in the famous paper by Hohenberg and Kohn [1], in section 1.3.

An overview of the key concepts of DFT giving some background to the mathematics involved can be found in Ref. [16]. Also several books have appeared on the subject of DFT, two of which are listed in Refs. [17,18].

1.2 Preliminaries

Consider a non-relativistic Hamiltonian $\hat{H}$ of a stationary many-body system

$$\hat{H} = \hat{T} + \hat{V} + \hat{W}, \tag{1.1}$$

where $\hat{T}$, $\hat{V}$ and $\hat{W}$ are the operators corresponding to the kinetic energy, the external potential and the two-particle interaction, respectively. They are explicitly given by:

$$\hat{T} = \sum_{i=1}^{N} -\frac{1}{2}\nabla_i^2 \tag{1.2}$$

$$\hat{V} = \sum_{i=1}^{N} v(\mathbf{r}_i) \tag{1.3}$$

$$\hat{W} = \sum_{i>j}^{N} w(|\mathbf{r}_i - \mathbf{r}_j|), \tag{1.4}$$

where N is the number of electrons. We assume that the two-particle interaction $w(|\mathbf{r}|)$ is specified. In this work, for example, it will always be the Coulomb potential $w(|\mathbf{r}|) = 1/|\mathbf{r}|$. We note that atomic units are used throughout this work. So both $\hat{T}$ and $\hat{W}$ are identical for all electronic systems, i.e., atoms, molecules and solids. They differ only in the expression for the external potential $v(\mathbf{r})$ and the number of electrons N. Therefore, we can regard the properties of these systems as functionals of the external potential v and the number of electrons N. In particular we can consider the ground-state wave function $|\Psi[v]\rangle$ and the ground-state energy $E[v]$ to be functionals of v. They are related by the time-independent Schrödinger equation

$$\hat{H}_v|\Psi[v]\rangle = (\hat{T} + \hat{V} + \hat{W})|\Psi[v]\rangle = E[v]|\Psi[v]\rangle, \tag{1.5}$$

where we added the subscript v to the Hamiltonian to indicate that we consider $\hat{H}$ to be a functional of $v(\mathbf{r})$. Our objective now is to switch from $v(\mathbf{r})$ as the basic variable to the electron density $\rho(\mathbf{r})$. This is possible because $v(\mathbf{r})$ and $\rho(\mathbf{r})$ are so-called conjugate variables. We will show what we mean by this concept in the following. We can write $\hat{V}$ as

$$\hat{V} = \int d\mathbf{r} v(\mathbf{r})\hat{\rho}(\mathbf{r}), \tag{1.6}$$

where we defined the density operator $\hat{\rho}(\mathbf{r})$ as

$$\hat{\rho}(\mathbf{r}) = \sum_{i=1}^{N} \delta(\mathbf{r} - \mathbf{r}_i). \tag{1.7}$$

The expectation value of $\hat{V}$ is given by

$$\langle\Psi|\hat{V}|\Psi\rangle = \int d\mathbf{r} v(\mathbf{r})\rho(\mathbf{r}), \tag{1.8}$$

where $\rho(\mathbf{r})$ is the electron density. The expectation value of the density operator $\hat{\rho}(\mathbf{r})$ is obtained from the many-body wave function $|\Psi\rangle$ according to

$$\rho(\mathbf{r}) = \langle\Psi|\hat{\rho}|\Psi\rangle = N \sum_{\sigma_1\cdots\sigma_N} \int d\mathbf{r}_2 \cdots d\mathbf{r}_N |\Psi(\mathbf{r}\sigma_1 \cdots \mathbf{r}_N\sigma_N)|^2, \tag{1.9}$$

where we used the antisymmetry property of the many-body wavefunction. In the above expression σ_i indicates the spin coordinate belonging to electron i. From Eq. (1.8) we see that $v(\mathbf{r})$ and $\rho(\mathbf{r})$ are conjugate variables, i.e., the contribution of the external potential $v(\mathbf{r})$ to the energy is simply an integral of the product of the external potential with the density $\rho(\mathbf{r})$. It is this relation that makes it possible to prove that the density of a ground state uniquely determines the external potential up to an arbitrary constant and hence we can regard the ground-state properties of electronic systems as functionals of the density ρ. For nondegenerate ground states this proof is given in the famous paper by Hohenberg and Kohn [1]. We will show it in the next section. The proof for degenerate ground states will be given in section 1.6.

1.3 Hohenberg-Kohn Theorem for Nondegenerate Ground States

The Hohenberg-Kohn theorem states that the density $\rho(\mathbf{r})$ of a nondegenerate ground state uniquely determines the external potential $v(\mathbf{r})$ up to an arbitrary constant. This means one cannot find two potentials differing by more than a constant that yield the same density. In the following proof of this theorem we will only consider potentials in the Banach space $L^{3/2} + L^{\infty}$, because for those potentials we can rigorously prove the Hohenberg-Kohn theorem. We have the usual physical constraints on the density,

$$\rho(\mathbf{r}) \geq 0 \tag{1.10}$$

$$\int d\mathbf{r}\rho(\mathbf{r}) = N, \tag{1.11}$$

and furthermore we require that the expectation values for the kinetic energy and the external potential of the many-body system are finite. The latter requirement is explicitly given as

$$\left| \int d\mathbf{r}\rho(\mathbf{r})v(\mathbf{r}) \right| < \infty. \tag{1.12}$$

Without going into the mathematical details we just like to mention that these four constraints imply that we have potentials in the space $L^{3/2} + L^{\infty}$ [19]. That the constraints on the density lead to constraints on the external potential is a consequence

of the fact that the density and external potential are conjugate variables. Finally, we note that the Coulomb potential is in the space $L^{3/2} + L^{\infty}$.

Consider now the set of potentials $\mathcal{V} \subset L^{3/2} + L^{\infty}$ that leads to a set of nondegenerate normalizable ground states Φ through the solutions of the Schrödinger equation. Since we only consider nondegenerate ground states every external potential $v(\mathbf{r}) \in \mathcal{V}$ uniquely determines the ground-state wave function $|\Psi[v]\rangle \in \Phi$ up to an arbitrary phase factor. We have thus obtained the map

$$C : \mathcal{V} \to \Phi. \tag{1.13}$$

We now define the set $\mathcal{A}$ as the set of densities that can be constructed from the set of nondegenerate ground states Φ through Eq. (1.9). This immediately gives a second map

$$D : \Phi \to \mathcal{A}. \tag{1.14}$$

We will now prove that the maps C and D are invertible. Both proofs go by *reductio ad absurdum*. In the case of map C we have to prove that two potentials $v_1(\mathbf{r}), v_2(\mathbf{r}) \in \mathcal{V}$ that differ by more than a constant c, i.e., $v_1(\mathbf{r}) \neq v_2(\mathbf{r}) + c$, always yield two different ground states $|\Psi[v_1]\rangle$ and $|\Psi[v_2]\rangle$, that is $|\Psi[v_1]\rangle$ and $|\Psi[v_2]\rangle$ differ by more than a phase factor. Consider the Schrödinger equations for $|\Psi[v_1]\rangle$ and $|\Psi[v_2]\rangle$,

$$(\hat{T} + \hat{V}_1 + \hat{W})|\Psi[v_1]\rangle = E[v_1]|\Psi[v_1]\rangle, \tag{1.15}$$

and

$$(\hat{T} + \hat{V}_2 + \hat{W})|\Psi[v_2]\rangle = E[v_2]|\Psi[v_2]\rangle. \tag{1.16}$$

We now make the assumption $|\Psi[v_1]\rangle = |\Psi[v_2]\rangle = |\Psi\rangle$. Subtraction of the two equations then leads to

$$(\hat{V}_1 - \hat{V}_2)|\Psi\rangle = (E[v_1] - E[v_2])|\Psi\rangle. \tag{1.17}$$

Since $\hat{V}_1$ and $\hat{V}_2$ are multiplicative operators we see from Eq. (1.6) that if in some region $v_1(\mathbf{r}) \neq v_2(\mathbf{r}) + c$ then $|\Psi\rangle$ must vanish in that region for the above equation to hold. However, it is guaranteed by the unique continuation theorem that if $v_1(\mathbf{r}), v_2(\mathbf{r}) \in L^{3/2} + L^{\infty}$ then $|\Psi\rangle$ cannot vanish on a set with nonzero measure. This argument is explained in Ref. [19]. We have arrived at a contradiction which means that $|\Psi[v_1]\rangle$ and $|\Psi[v_2]\rangle$ differ by more than a phase factor. We have thus proved that the map C is invertible. Note that the above argument is valid only because $v(\mathbf{r})$ and $\rho(\mathbf{r})$ are conjugate variables.

To prove that the map D is invertible we have to show that two nondegenerate ground states $|\Psi[v_1]\rangle$ and $|\Psi[v_2]\rangle$ that correspond to potentials $v_1(\mathbf{r}), v_2(\mathbf{r}) \in \mathcal{V}$ and

that differ by more than a phase factor cannot lead to the same density, i.e., $\rho_1(\mathbf{r}) \neq \rho_2(\mathbf{r})$. The proof makes use of the Rayleigh-Ritz variation principle. We have

$$\begin{aligned} E[v_1] &= \langle\Psi[v_1]|(\hat{T}+\hat{V}_1+\hat{W})|\Psi[v_1]\rangle \\ &< \langle\Psi[v_2]|(\hat{T}+\hat{V}_1+\hat{W})|\Psi[v_2]\rangle \\ &= \langle\Psi[v_2]|(\hat{T}+\hat{V}_2+\hat{W})|\Psi[v_2]\rangle + \int d\mathbf{r}[v_1(\mathbf{r})-v_2(\mathbf{r})]\rho_2(\mathbf{r}) \\ &= E[v_2] + \int d\mathbf{r}[v_1(\mathbf{r})-v_2(\mathbf{r})]\rho_2(\mathbf{r}). \end{aligned} \tag{1.18}$$

By a similar argument we obtain the inequality

$$E[v_2] < E[v_1] + \int d\mathbf{r}[v_2(\mathbf{r})-v_1(\mathbf{r})]\rho_1(\mathbf{r}). \tag{1.19}$$

We now make the assumption $\rho_1(\mathbf{r}) = \rho_2(\mathbf{r})$. Adding the two inequalities then leads to the contradiction

$$E[v_1] + E[v_2] < E[v_1] + E[v_2]. \tag{1.20}$$

Therefore, two nondegenerate ground states that differ by more than a phase factor cannot lead to the same density and we have thus proved that the map D is invertible. Since both maps C and D are invertible we have shown that the density of a nondegenerate ground state uniquely determines the external potential up to a constant, thereby proving the Hohenberg-Kohn theorem.

Since according to the Hohenberg-Kohn theorem the density uniquely determines the ground-state wave function up to a phase factor every ground-state expectation value of an operator $\hat{O}$ is a unique functional of the density according to

$$O[\rho] = \langle\Psi[\rho]|\hat{O}|\Psi[\rho]\rangle. \tag{1.21}$$

We can now define the universal Hohenberg-Kohn functional F_{HK} as

$$F_{\mathrm{HK}}[\rho] = \langle\Psi[\rho]|\hat{T}+\hat{W}|\Psi[\rho]\rangle. \tag{1.22}$$

It is universal in the sense that F_{HK} does not include the system-dependent external potential $v(\mathbf{r})$ and we consider $\hat{W}$ to be fixed. The energy functional then becomes

$$E[\rho] = \int d\mathbf{r} v(\mathbf{r})\rho(\mathbf{r}) + F_{\mathrm{HK}}[\rho]. \tag{1.23}$$

Consider now a ground-state density $\rho_1(\mathbf{r})$ corresponding to an external potential $v_1(\mathbf{r})$ and an energy E_1. Then for any ground-state density $\rho_2(\mathbf{r})$ we have

$$\begin{aligned} E_{v_1}[\rho_2] &= \int d\mathbf{r} v_1(\mathbf{r})\rho_2(\mathbf{r}) + F_{\mathrm{HK}}[\rho_2] = \langle\Psi[\rho_2]|\hat{T}+\hat{V}_1+\hat{W}|\Psi[\rho_2]\rangle \\ &\geq \langle\Psi[\rho_1]|\hat{T}+\hat{V}_1+\hat{W}|\Psi[\rho_1]\rangle = E_{v_1}[\rho_1] = E_1. \end{aligned} \tag{1.24}$$

We can thus obtain the ground-state energy E_0 corresponding to a Hamiltonian with external potential $v_0(\mathbf{r})$ by minimization of the functional $E_{v_0}[\rho]$, i.e.,

$$E_0 = \inf_{\rho \in \mathcal{A}} E_{v_0}[\rho] = \inf_{\rho \in \mathcal{A}} \left[\int d\mathbf{r} v_0(\mathbf{r}) \rho(\mathbf{r}) + F_{\mathrm{HK}}[\rho] \right]. \tag{1.25}$$

This result for the energy functional is analogous to the Rayleigh-Ritz variational principle for ground-state wave functions.

However, we do not have criteria from which we can know whether a given density $\rho(\mathbf{r})$ is in the set $\mathcal{A}$. This is known as the v-representability problem. A density $\rho(\mathbf{r})$ is called v-representable if it is the density of a ground state of the Hamiltonian (1.1) (with N and $\hat{W}$ specified) with some external potential $v(\mathbf{r})$. By construction the functionals $F_{\mathrm{HK}}[\rho]$ and $E_{v_0}[\rho]$ are defined only for v-representable densities. In practice we need approximations for $F_{\mathrm{HK}}[\rho]$. Good approximations can be obtained using the Kohn-Sham approach [2]. This approach makes use of functional derivatives. Before we will discuss the Kohn-Sham theory in section 1.5 we will, therefore, first give the definition of the functional derivative in the next section.

1.4 The Functional Derivative

Let G be a functional from a normed Banach space B to the real numbers $\mathcal{R}$. If for every h and positive number ϵ there exists a continuous linear functional $\delta G/\delta f$ of h in $f \in B$ defined by

$$\frac{\delta G}{\delta f}[h] = \lim_{\epsilon \to 0} \frac{G[f + \epsilon h] - G[f]}{\epsilon}, \tag{1.26}$$

then $\delta G/\delta f$ is called the Gâteaux derivative in f. The derivative $\delta G/\delta f$ then only depends on the point f where the derivative is taken. If the linear functional $\delta G/\delta f$ can be written in the following form,

$$\frac{\delta G}{\delta f}[h] = \int d\mathbf{r} g(\mathbf{r}) h(\mathbf{r}), \tag{1.27}$$

then we write

$$g(\mathbf{r}) = \frac{\delta G}{\delta f(\mathbf{r})}, \tag{1.28}$$

and call this the functional derivative of $G[f]$ with respect to $f(\mathbf{r})$. Note that if all $h(\mathbf{r})$ are subject to the constraint

$$\int d\mathbf{r} h(\mathbf{r}) = 0, \tag{1.29}$$

as is the case for $\delta\rho(\mathbf{r})$ for example, then according to Eq. (1.27) the functional derivative $\delta G/\delta f(\mathbf{r})$ is uniquely defined up to a constant.

1.5 Kohn-Sham Theory

Hohenberg and Kohn have provided us with an elegant approach to obtain the ground-state density and energy through the minimum principle, Eq. (1.25). However, we do not know any practically applicable forms of $F_{\mathrm{HK}}[\rho]$. Kohn and Sham thought of a scheme that leads to an expression for $F_{\mathrm{HK}}[\rho]$ [2], of which only a specific part of $F_{\mathrm{HK}}[\rho]$, the so-called exchange-correlation energy $E_{xc}[\rho]$, requires approximation. Their idea was that the density $\rho(\mathbf{r})$ of a system of interacting particles with external potential $v(\mathbf{r})$ could be reproduced in a system of noninteracting particles with some external potential $v_s(\mathbf{r})$. In the following we will show how this concept leads to the so-called Kohn-Sham equations, a set of equations that can be solved in practice once a choice for $E_{xc}[\rho]$ is made. We do this by means of a Legendre transform as was shown by van Leeuwen [16, 20].

Starting from Eq. (1.5) we see that we can write the ground-state energy as a functional of the external potential $v(\mathbf{r})$ according to

$$E[v] = \langle \Psi[v] | \hat{H}_v | \Psi[v] \rangle. \tag{1.30}$$

Our goal is now to switch from the external potential as the basic variable to the electron density $\rho(\mathbf{r})$. Again we will see that the reason this is possible is because the potential and the density are conjugate variables. We make use of this relation now that we will take the functional derivative of Eq. (1.30) with respect to the potential $v(\mathbf{r})$. We obtain

$$\begin{aligned} \frac{\delta E}{\delta v(\mathbf{r})} &= \left\langle \frac{\delta \Psi}{\delta v(\mathbf{r})} \middle| \hat{H}_v \middle| \Psi \right\rangle + \left\langle \Psi \middle| \hat{H}_v \middle| \frac{\delta \Psi}{\delta v(\mathbf{r})} \right\rangle + \left\langle \Psi \middle| \frac{\hat{H}_v}{\delta v(\mathbf{r})} \middle| \Psi \right\rangle \\ &= E[v] \frac{\delta}{\delta v(\mathbf{r})} \langle \Psi | \Psi \rangle + \langle \Psi | \hat{\rho}(\mathbf{r}) | \Psi \rangle = \rho(\mathbf{r}), \end{aligned} \tag{1.31}$$

where we used the Schrödinger equation (1.5) and the fact that the wave function $|\Psi\rangle$ is normalized, i.e., $\langle \Psi | \Psi \rangle = 1$. Note that the equation above is just a functional generalization of the Hellmann-Feynman theorem [21]. The above result now allows us to switch from the external potential $v(\mathbf{r})$ to the electron density $\rho(\mathbf{r})$ as the basic variable by defining the Legendre transform

$$F[\rho] = E[v] - \int d\mathbf{r} v(\mathbf{r}) \rho(\mathbf{r}) = \langle \Psi[v] | \hat{T} + \hat{W} | \Psi[v] \rangle, \tag{1.32}$$

where $v(\mathbf{r})$ must now be regarded as a functional of ρ. The Hohenberg-Kohn theorem guarantees that this mapping is unique. Since $v(\mathbf{r})$ is a unique functional of ρ we see from Eq. (1.22) that we have the identity

$$F[\rho] \equiv F_{\mathrm{HK}}[\rho]. \tag{1.33}$$

Remember that $F_{\rm HK}[\rho]$ is defined only for the set of v-representable densities. With the result obtained in Eq. (1.31) we can now derive the functional derivative of $F_{\rm HK}[\rho]$ with respect to $\rho(\mathbf{r})$. We obtain

$$\begin{aligned}\frac{\delta F_{\rm HK}}{\delta\rho(\mathbf{r})} &= \int d\mathbf{r}'\frac{\delta E}{\delta v(\mathbf{r}')}\frac{\delta v(\mathbf{r}')}{\delta\rho(\mathbf{r})} - \frac{\delta}{\delta\rho(\mathbf{r})}\int d\mathbf{r}'\rho(\mathbf{r}')v(\mathbf{r}') \\ &= \int d\mathbf{r}'\rho(\mathbf{r}')\frac{\delta v(\mathbf{r}')}{\delta\rho(\mathbf{r})} - \int d\mathbf{r}'\frac{\delta\rho(\mathbf{r}')}{\delta\rho(\mathbf{r})}v(\mathbf{r}') - \int d\mathbf{r}'\rho(\mathbf{r}')\frac{\delta v(\mathbf{r}')}{\delta\rho(\mathbf{r})} \\ &= -\int d\mathbf{r}'\delta(\mathbf{r}-\mathbf{r}')v(\mathbf{r}') = -v(\mathbf{r}), \end{aligned} \tag{1.34}$$

where in the first line we used the functional generalization of the chain rule. In the above expression we left implicit that the functional derivative of $F_{\rm HK}$ with respect to the density is defined up to a constant as discussed in the previous section. To arrive at the Kohn-Sham equations we do similar derivations for a system of noninteracting particles. Starting from the energy functional for a system of noninteracting particles with external potential $v_s(\mathbf{r})$ and with ground-state wave function $\Phi[v_s]$ according to

$$E_s[v_s] = \langle\Phi[v_s]|\hat{T} + \hat{V}_s|\Phi[v_s]\rangle, \tag{1.35}$$

we obtain its Legendre transform

$$F_s[\rho] = E_s[v_s] - \int d\mathbf{r}v_s(\mathbf{r})\rho(\mathbf{r}) = \langle\Phi[v_s]|\hat{T}|\Phi[v_s]\rangle, \tag{1.36}$$

and the functional derivatives

$$\frac{\delta E_s}{\delta v_s(\mathbf{r})} = \rho(\mathbf{r}), \tag{1.37}$$

$$\frac{\delta F_s}{\delta\rho(\mathbf{r})} = -v_s(\mathbf{r}). \tag{1.38}$$

Since $F_s[\rho]$ in Eq. (1.36) is just the kinetic energy of a system of noninteracting particles with potential $v_s(\mathbf{r})$ and density $\rho(\mathbf{r})$ it is usually denoted by T_s. In the following we will adopt this convention. We now define the exchange-correlation functional $E_{xc}[\rho]$ by the equation

$$F_{\rm HK}[\rho] = T_s[\rho] + \frac{1}{2}\int d\mathbf{r}d\mathbf{r}'\rho(\mathbf{r})\rho(\mathbf{r}')w(|\mathbf{r}-\mathbf{r}'|) + E_{xc}[\rho]. \tag{1.39}$$

Here an important assumption has been made, namely that the functionals $F[\rho]$ and $T_s[\rho]$ are defined on the same domain of densities. We thus assume that for a given ground-state density of an interacting system with potential $v(\mathbf{r})$ there is a noninteracting system with potential $v_s(\mathbf{r})$ that has the same density. In other

words, we assume that the density of the interacting system is noninteracting v-representable. We will discuss whether this assumption is justified in section 1.7. Taking the functional derivative with respect to the density $\rho(\mathbf{r})$ of Eq. (1.39) leads to

$$v_s(\mathbf{r}) = v(\mathbf{r}) + \int d\mathbf{r}'\rho(\mathbf{r}')w(|\mathbf{r}-\mathbf{r}'|) + v_{xc}(\mathbf{r}), \tag{1.40}$$

where we defined

$$v_{xc}(\mathbf{r}) = \frac{\delta E_{xc}}{\delta\rho(\mathbf{r})} \tag{1.41}$$

as the exchange-correlation potential. Since $|\Phi\rangle$ is the ground-state wave function of a system of noninteracting particles we can write it as an anti-symmetrized product of single-particle orbitals $\phi_i(\mathbf{r})$, i.e., a Slater determinant. Combining Eqs. (1.32) and (1.39) we obtain

$$\begin{aligned} E[v] &= \sum_{i=1}^{N} -\frac{1}{2}\int d\mathbf{r}\phi_i^*(\mathbf{r})\nabla^2\phi_i(\mathbf{r}) + \int d\mathbf{r}v(\mathbf{r})\rho(\mathbf{r}) \\ &+ \frac{1}{2}\int d\mathbf{r}d\mathbf{r}'\rho(\mathbf{r})\rho(\mathbf{r}')w(|\mathbf{r}-\mathbf{r}'|) + E_{xc}[\rho]. \end{aligned} \tag{1.42}$$

Furthermore, the Schrödinger equation can now be written as a set of single-particle equations according to

$$\left(-\frac{1}{2}\nabla^2 + v(\mathbf{r}) + \int d\mathbf{r}'\rho(\mathbf{r}')w(|\mathbf{r}-\mathbf{r}'|) + v_{xc}(\mathbf{r})\right)\phi_i(\mathbf{r}) = \epsilon_i\phi_i(\mathbf{r}), \tag{1.43}$$

where the ϵ_i are the Kohn-Sham orbital eigenvalues and the ground-state density $\rho(\mathbf{r})$ is given by

$$\rho(\mathbf{r}) = \sum_{i=1}^{N}|\phi_i(\mathbf{r})|^2, \tag{1.44}$$

The above three equations constitute the Kohn-Sham equations [2]. If we have an approximation for $E_{xc}[\rho]$ we can calculate the exchange-correlation potential $v_{xc}(\mathbf{r})$ and solve the orbital equations (1.43) and (1.44) self-consistently. With the density obtained in this way we can then find the ground-state energy of the system from Eq. (1.42). To summarize, we have converted the ground-state problem into the problem of solving the Kohn-Sham equations. This means we no longer need to approximate the whole functional $F_{\mathrm{HK}}[\rho]$ but instead we need to find good approximations for its exchange correlation part $E_{xc}[\rho]$ and its functional derivative $v_{xc}(\mathbf{r})$.

Finally, we note that the Kohn-Sham wave function constructed from the N lowest Kohn-Sham orbitals is not intended to be an approximation to the true ground-state wave function and the Kohn-Sham eigenvalues are not generally related to the excitation energies of the system. However, the eigenvalue corresponding to the highest

occupied Kohn-Sham orbital has a clear physical meaning. In finite systems it is equal to the negative of the true ionization potential provided that the Kohn-Sham potential vanishes at infinity [22, 23]. Furthermore, it can be shown that the eigenvalues of the other occupied Kohn-Sham orbitals are close to the true ionization energies [24]. In the case of a metal it can be proved rigorously that it is equal to the true Fermi energy of the system [25]. However, the shape of the Kohn-Sham Fermi surface is, in general, different from that of the true Fermi surface [26].

1.6 Hohenberg-Kohn Theorem for Degenerate Ground States

In this section we will extend the Hohenberg-Kohn theorem to systems that have a degenerate ground state. For these systems the external potential $v(\mathbf{r})$ no longer uniquely determines the ground-state wave function. Instead, one obtains a linearly independent set of q different ground states. This means that the expectation value of any operator (except of course the total energy) depends on the choice we make from which ground state out of the ground-state manifold this expectation value is calculated. In particular, we have for the density operator that, in general, different ground states out of the ground-state manifold do not lead to the same density. Therefore, the ground-state density is no longer a unique functional of the external potential in the case of systems that have a degenerate ground state. However, we will show that every ground state density still uniquely determines the external potential that generated it up to an arbitrary constant. This means that the Hohenberg-Kohn theorem as formulated in the case of nondegenerate ground states still holds in the case of degenerate ground states. Before we come to proof the Hohenberg-Kohn theorem for degenerate ground states we start by giving a generalization of the densities that we will consider. Instead of pure-state densities, which are densities that come from an eigenstate of the Hamiltonian $\hat{H}$, we will now consider ensemble densities. In order to define these densities we introduce for a q-fold degenerate ground state $\{|\Psi_i\rangle, i = 1 \cdots q\}$ the density matrix

$$\hat{D} = \sum_{i=1}^{q} \lambda_i |\Psi_i\rangle\langle\Psi_i| \qquad \sum_{i}^{q} \lambda_i = 1 \qquad (0 \leq \lambda_i \leq 1), \tag{1.45}$$

where the ground-state wave functions $|\Psi_i\rangle$ are chosen to be orthonormal. We now define the ground-state expectation value of an operator $\hat{O}$ by

$$\langle O \rangle = \mathrm{Tr}\hat{D}\hat{O}, \tag{1.46}$$

in which the trace operation Tr is defined as

$$\mathrm{Tr}\hat{A} = \sum_{i=1}^{\infty} \langle \Phi_i | \hat{A} | \Phi_i \rangle, \tag{1.47}$$

where the $|\Phi_i\rangle$'s form an arbitrary complete set of orthonormal states. The trace is independent of the complete set of states that is chosen. Therefore, we can choose that complete set to be the set of eigenstates of the Hamiltonian $\hat{H}$. We then obtain

$$\mathrm{Tr}\hat{D}\hat{O} = \sum_{i}^{\infty} \langle \Psi_i | \hat{D}\hat{O} | \Psi_i \rangle = \sum_{i}^{q} \lambda_i \langle \Psi_i | \hat{O} | \Psi_i \rangle, \tag{1.48}$$

which defines the expectation value of an operator $\hat{O}$ in an ensemble described by density matrix $\hat{D}$. For the expectation value of the density operator $\hat{\rho}$ we thus obtain

$$\rho(\mathbf{r}) = \mathrm{Tr}\hat{D}\hat{\rho} = \sum_{i}^{q} \lambda_i \langle \Psi_i | \hat{\rho} | \Psi_i \rangle = \sum_{i=1}^{q} \lambda_i \rho_i(\mathbf{r}), \tag{1.49}$$

where $\rho_i(\mathbf{r})$ is the density corresponding to the ground state $|\Psi_i\rangle$. The densities $\rho(\mathbf{r})$ obtained in this way from an orthonormal set of ground states $\{|\Psi_i\rangle, i = 1 \cdots q\}$ corresponding to an external potential $v(\mathbf{r})$ we will call ensemble v-representable densities. We denote the set of ensemble v-representable densities generated by external potentials in the space $L^{3/2} + L^{\infty}$ by $\mathcal{B}$. If a density can be written as $\rho(\mathbf{r}) = \langle \Psi | \hat{\rho} | \Psi \rangle$ with $|\Psi\rangle$ a ground state corresponding to an external potential $v(\mathbf{r})$, then we will call $\rho(\mathbf{r})$ a pure-state v-representable density. Therefore, the set of pure-state v-representable densities is a subset of the set of ensemble v-representable densities. The Hohenberg-Kohn theorem for degenerate ground states now reads: Every ensemble v-representable density uniquely determines the external potential that generated it up to an arbitrary constant. This means that if two density matrices $\hat{D}_1$ and $\hat{D}_2$ that lead to the ensemble densities $\rho_1(\mathbf{r})$ and $\rho_2(\mathbf{r})$ correspond to the ground-state ensembles for external potentials $v_1(\mathbf{r})$ and $v_2(\mathbf{r})$ with $v_1(\mathbf{r}) \neq v_2(\mathbf{r}) + c$, then $\rho_1(\mathbf{r}) \neq \rho_2(\mathbf{r})$. The proof is analogous to that for the nondegenerate case.

Suppose we have an external potential $v_1(\mathbf{r})$ that generates the ground-state multiplet $A_1 = \{|\Phi_i\rangle, i = 1 \cdots q_1\}$ and an external potential $v_2(\mathbf{r})$ that generates the ground-state multiplet $A_2 = \{|\Psi_i\rangle, i = 1 \cdots q_2\}$. Without loss of generality, we can choose all the wave functions within the multiplets to be orthonormal. Since the expectation value for the ground-state energy is the same for every ground state $|\Phi_i\rangle$ in A_1 and likewise the expectation value for the ground-state energy is the same for every ground state $|\Psi_i\rangle$ in A_2, we can use the same arguments we used in the proof of the invertibility of the map $\mathcal{C}$ in section 1.3. We thus immediately see that none of

the ground-state wave functions in the sets A_1 and A_2 are the same. In particular, since the sets A_1 and A_2 are only defined to within a unitary transformation, there is no $|\Psi_i\rangle$ in A_2 that is a linear combination of the $|\Phi_i\rangle$ in A_1. As a consequence, two ground-state ensemble density matrices generated from the ground-state wave functions in A_1 and A_2 are different, i.e.,

$$\hat{D}_1 = \sum_{i=1}^{q_1} \lambda_i |\Phi_i\rangle\langle\Phi_i| \neq \sum_{i=1}^{q_2} \mu_i |\Psi_i\rangle\langle\Psi_i| = \hat{D}_2 \qquad \sum_{i=1}^{q_1} \lambda_i = \sum_{i=1}^{q_2} \mu_i = 1. \tag{1.50}$$

This follows, for instance, by taking the inner product on both sides with $|\Psi_m\rangle$ since the $|\Psi_i\rangle$ are not linear combinations of the $|\Phi_i\rangle$. We have thus proved that the sets of ground-state density matrices corresponding to two different external potentials $v_1(\mathbf{r})$ and $v_2(\mathbf{r})$ are disjoint. We are left to prove that the ground-state density matrices in these sets lead to different densities. Consider the Hamiltonians $\hat{H}_1 = \hat{T} + \hat{V}_1 + \hat{W}$ and $\hat{H}_2 = \hat{T} + \hat{V}_2 + \hat{W}$. For $\hat{H}_2$ we now show that we have the following inequality

$$\mathrm{Tr}\hat{D}_1\hat{H}_2 > \mathrm{Tr}\hat{D}_2\hat{H}_2. \tag{1.51}$$

This follows immediately from

$$\begin{aligned} \mathrm{Tr}\hat{D}_1\hat{H}_2 &= \sum_{i=1}^{q_1} \lambda_i \langle\Phi_i|\hat{H}_2|\Phi_i\rangle \\ &> \sum_{i=1}^{q_1} \lambda_i \langle\Psi_i|\hat{H}_2|\Psi_i\rangle = \sum_{i=1}^{q_1} \lambda_i E[v_2] = E[v_2] \qquad (1.52) \\ &= \sum_{i=1}^{q_2} \mu_i \langle\Psi_i|\hat{H}_2|\Psi_i\rangle = \mathrm{Tr}\hat{D}_2\hat{H}_2. \qquad (1.53) \end{aligned}$$

We can now again proceed in a similar as we did for the nondegenerate case. We have

$$\begin{aligned} E[v_1] = \mathrm{Tr}\hat{D}_1\hat{H}_1 = \mathrm{Tr}\hat{D}_1(\hat{H}_2 + \hat{V}_1 - \hat{V}_2) = \mathrm{Tr}\hat{D}_1\hat{H}_2 + \int d\mathbf{r}(v_1(\mathbf{r}) - v_2(\mathbf{r}))\rho_1(\mathbf{r}) \\ > \mathrm{Tr}\hat{D}_2\hat{H}_2 + \int d\mathbf{r}(v_1(\mathbf{r}) - v_2(\mathbf{r}))\rho_1(\mathbf{r}) = E[v_2] + \int d\mathbf{r}(v_1(\mathbf{r}) - v_2(\mathbf{r}))\rho_1(\mathbf{r}). \end{aligned} \tag{1.54}$$

Similarly we obtain the inequality

$$E[v_2] > E[v_1] + \int d\mathbf{r}(v_2(\mathbf{r}) - v_1(\mathbf{r}))\rho_2(\mathbf{r}). \tag{1.55}$$

We now make the assumption $\rho_1(\mathbf{r}) = \rho_2(\mathbf{r})$. Adding the two inequalities then leads again to the contradiction

$$E[v_1] + E[v_2] < E[v_1] + E[v_2]. \tag{1.56}$$

Therefore, $\hat{D}_1$ and $\hat{D}_2$ must yield different densities. This concludes the proof of the Hohenberg-Kohn theorem for degenerate ground states.

We note that within a given set of ensemble ground-state density matrices two different matrices corresponding to the same potential (modulo a constant) can yield the same density. However, if two ensemble ground-state density matrices yield the same density then also the energy $\mathrm{Tr}\hat{D}\hat{H}$ is the same for both density matrices. This means we can now define a universal functional F_{EHK} according to

$$F_{\mathrm{EHK}} = \mathrm{Tr}\hat{D}[\rho](\hat{T} + \hat{W}), \tag{1.57}$$

which is simply an extension of F_{HK}, i.e.,

$$F_{\mathrm{EHK}}[\rho] = F_{\mathrm{HK}}[\rho] \qquad \text{if} \rho \in \mathcal{A}. \tag{1.58}$$

Similarly, we can now define an extension of the energy functional $E_v[\rho]$ to the set of ensemble-v-representable densities as

$$E_v[\rho] = \int d\mathbf{r} v(\mathbf{r})\rho(\mathbf{r}) + F_{\mathrm{EHK}} = \mathrm{Tr}\hat{D}[\rho]\hat{H}. \tag{1.59}$$

Furthermore, it is easy to prove that we also have a minimization condition for F_{EHK} which is given by

$$E_0 = \inf_{\rho\in\mathcal{B}} E_{v_0}[\rho] = \inf_{\rho\in\mathcal{B}} \left[\int d\mathbf{r} v_0(\mathbf{r})\rho(\mathbf{r}) + F_{\mathrm{EHK}}[\rho]\right]. \tag{1.60}$$

Finally, we note that it can be shown that there exist ensemble v-representable densities that are not pure-state v-representable densities [19, 27].

1.7 The Lieb Functional and Noninteracting v-Representability

In the case that we have a system with a degenerate ground state it is clear that, with the exception of the energy, the expectation values of all observables depend on the ground state of the manifold we choose to calculate them from. This then obviously leads to a serious problem for the definition of general density functionals and their functional derivatives. For example, the functional derivative of the total energy E with respect to the potential $v(\mathbf{r})$ as calculated in Eq. (1.31) does not have an equivalent in the case of a degenerate ground state because the outcome of Eq. (1.26) then depends on the particular choice we make for the function h. This can be seen from the definition in Eq. (1.26), where ϵh lifts the degeneracy favoring a

particular state out of the manifold to have the lowest energy. Taking the limit $\epsilon \to 0$ then leads to a functional derivative that is equal to the density corresponding to the state h has picked out. The question now is whether the functional derivative of $F_{\rm EHK}$ with respect to the density exists. The existence of such a functional derivative will enable us to set up the Kohn-Sham equations for ensemble v-representable densities in a similar way as in the nondegenerate case. It can be shown using linear response theory [16] that for a system with a degenerate ground state and external potential $v(\mathbf{r})$ there exists the functional derivative of $F_{\rm EHK}$ with respect to the density $\rho(\mathbf{r})$ only for a certain set of ground-state densities. The densities in this set correspond to pure states that can be obtained from a perturbed system with potential $v(\mathbf{r})+\epsilon\delta v(\mathbf{r})$ in the limit $\epsilon \to 0$. However, as we noted in the previous section there are ensemble v-representable densities that are not a pure-state v-representable density. Consider now an ensemble corresponding to such a density with external potential $v(\mathbf{r})$. If we lift the degeneracy by changing the potential to $v(\mathbf{r}) + \epsilon\delta v(\mathbf{r})$ then for $\epsilon > 0$ the ensemble will become a pure state and the density will change abruptly. Therefore, the functional derivative of $F_{\rm EHK}$ with respect to a general ensemble v-representable density $\rho(\mathbf{r})$ does not exist. As was shown in the numerical studies of Schipper *et al.* this poses a serious problem [28, 29]. For they showed that there exist ground-state densities of interacting systems that are not pure-state densities of a noninteracting system. This means that the formulation of a Kohn-Sham approach for arbitrary ensemble v-representable densities is needed. However, using the constrained search approached introduced by Levy [30] we can define an extension of the functional $F_{\rm EHK}$ to a larger set of densities that does have a functional derivative with respect to a general ensemble v-representable density $\rho(\mathbf{r})$. This is the Lieb functional $F_{\rm L}$ [19] which is defined as

$$F_{\rm L}[\rho] = \inf_{\hat{D}\to\rho} {\rm Tr}\hat{D}(\hat{T} + \hat{W}), \tag{1.61}$$

where the infimum is searched over all N-particle density matrices

$$\hat{D} = \sum_{i=1}^{\infty} \lambda_i |\Psi\rangle\langle\Psi_i| \qquad \sum_{i=1}^{\infty} \lambda_i = 1, \tag{1.62}$$

which yield the prescribed density $\rho(\mathbf{r}) = {\rm Tr}\hat{D}\hat{\rho}(\mathbf{r})$. The N-particle functions $|\Psi_i\rangle$ form an orthonormal set. One can prove that the infimum is in fact a minimum [19]. This means that one can always find a minimizing density matrix. Obviously $F_{\rm L}$ is equal to $F_{\rm EHK}$ for all ensemble v-representable densities, i.e.,

$$F_{\rm L}[\rho] = F_{\rm EHK}[\rho] \qquad \rho \in \mathcal{B}, \tag{1.63}$$

which follows immediately from the minimization condition. We now define the energy functional

$$E_v[\rho] = \int d\mathbf{r} v(\mathbf{r})\rho(\mathbf{r}) + F_{\mathrm{L}}[\rho]. \tag{1.64}$$

It is easy to show that $E_v[\rho]$ assumes its minimum value at the correct ground-state density $\rho_0(\mathbf{r})$ corresponding to the external potential $v(\mathbf{r})$. This follows from

$$E_v[\rho] = \inf_{\hat{D}\to\rho} \mathrm{Tr}\hat{D}\hat{H} \geq \mathrm{Tr}\hat{D}[\rho_0]\hat{H} = E_v[\rho_0]. \tag{1.65}$$

We have thus shown that F_{L} is a proper extension of F_{EHK}.

It turns out that F_{L} has some convenient properties that will allow us to put the Kohn-Sham theory on a rigorous basis. It can be proved that F_{L} is differentiable with respect to all ensemble v-representable densities and nowhere else [31]. The functional derivative of F_{L} with respect to a given ensemble v-representable density $\rho(\mathbf{r})$ is

$$\frac{\delta F_{\mathrm{L}}}{\delta\rho(\mathbf{r})} = -v(\mathbf{r}), \tag{1.66}$$

where $v(\mathbf{r})$ is the external potential that generated the density $\rho(\mathbf{r})$. For practical purposes we would of course like to know which densities are ensemble v-representable. It turns out that one can prove that the set of ensemble v-representable densities is dense in the set of all admissable densities [16]. In other words one can always find an ensemble v-representable density arbitrarily close to any admissable density. This result will enable us to justify the assumption made by Kohn and Sham that there exists an auxiliary noninteracting system which yields the same ground-state density as the true interacting system. We define the functional $T_{\mathrm{L}}[\rho]$ as

$$T_{\mathrm{L}}[\rho] = \inf_{\hat{D}\to\rho} \mathrm{Tr}\hat{D}\hat{T}, \tag{1.67}$$

which is simply the Lieb functional $F_{\mathrm{L}}[\rho]$ with the two-particle interaction $\hat{W}$ omitted. The functional $T_{\mathrm{L}}[\rho]$ has the same properties as $F_{\mathrm{L}}[\rho]$ because the properties derived for $F_{\mathrm{L}}[\rho]$ do not depend on $\hat{W}$. Therefore, $T_{\mathrm{L}}[\rho]$ is differentiable with respect to all non-interacting ensemble v-representable densities and nowhere else. This set of non-interacting densities we will denote by $\mathcal{B}_0$. The functional derivative of $T_{\mathrm{L}}[\rho]$ with respect to a noninteracting ensemble v-representable density $\rho(\mathbf{r})$ is given by

$$\frac{\delta T_{\mathrm{L}}}{\delta\rho(\mathbf{r})} = -v_s(\mathbf{r}), \tag{1.68}$$

where the potential $v_s(\mathbf{r})$ generates the density $\rho(\mathbf{r})$ in a system of noninteracting particles. The results (1.66) and (1.68) enable us to set up the Kohn-Sham equations for

general ensemble v-representable densities along the same lines as in section 1.5. The question remains, however, if a general interacting ensemble v-representable density is non-interacting ensemble v-representable, that is, are the sets $\mathcal{B}$ and $\mathcal{B}_0$ the same? So far this has not been rigorously proved. However, it can be proved that the set $\mathcal{B}_0$ is dense in the set $\mathcal{B}$, and vice versa [16]. In other words, for every density in the set of interacting ensemble v-representable densities $\mathcal{B}$ there is a non-interacting ensemble v-representable density in the set $\mathcal{B}_0$ that is arbitrarily close to it. This means that we can now set up a Kohn-Sham scheme that generates a given interacting ensemble v-representable density to arbitrary accuracy. As in section 1.5 we start by defining the exchange-correlation functional $E_{xc}[\rho]$ for the Lieb functional according to

$$F_{\rm L}[\rho] = T_L[\rho] + \frac{1}{2}\int d\mathbf{r}d\mathbf{r}'\rho(\mathbf{r})\rho(\mathbf{r}')w(|\mathbf{r}-\mathbf{r}'|) + E_{xc}[\rho]. \tag{1.69}$$

Since $F_{\rm L}[\rho]$ is differentiable on the set $\mathcal{B}$ and nowhere else and $T_{\rm L}[\rho]$ is differentiable on the set $\mathcal{B}_0$ and nowhere else it follows that $E_{xc}[\rho]$ is differentiable on the set $\mathcal{B}\cap\mathcal{B}_0$ and nowhere else. Taking the functional derivative with respect to the density $\rho(\mathbf{r})$ of Eq. (1.69) on the set $\mathcal{B}\cap\mathcal{B}_0$ leads to

$$v_s(\mathbf{r}) = v(\mathbf{r}) + \int d\mathbf{r}'\rho(\mathbf{r}')w(|\mathbf{r}-\mathbf{r}'|) + v_{xc}(\mathbf{r}), \tag{1.70}$$

where the exchange-correlation potential is defined in Eq. (1.41). Both the density and the expectation value of $T_{\rm L}[\rho]$ now have to be calculated from the ground-state ensemble $\hat{D}_s[\rho]$ of the Kohn-Sham system given by

$$\hat{D}_s[\rho] = \sum_{i=1}^{q}\mu_i|\Phi_i\rangle\langle\Phi_i|, \tag{1.71}$$

which consists of q degenerate ground states $|\Phi_i\rangle$. The Kohn-Sham equations now become [32]

$$\begin{aligned} E[v] \;=\; & \sum_{i=1}^{M}\sum_{i=1}^{q} -\frac{1}{2}\tilde{\mu}_i\int d\mathbf{r}\phi_i^*(\mathbf{r})\nabla^2\phi_i(\mathbf{r}) + \int d\mathbf{r}v(\mathbf{r})\rho(\mathbf{r}) + \\ & \frac{1}{2}\int d\mathbf{r}d\mathbf{r}'\rho(\mathbf{r})\rho(\mathbf{r}')w(|\mathbf{r}-\mathbf{r}'|) + E_{xc}[\rho] \qquad \sum_{i}^{M}\tilde{\mu}_i = N \quad (M\geq N) \end{aligned} \tag{1.72}$$

$$\left(-\frac{1}{2}\nabla^2 + v(\mathbf{r}) + \int d\mathbf{r}'\rho(\mathbf{r}')w(|\mathbf{r}-\mathbf{r}'|) + v_{xc}(\mathbf{r})\right)\phi_i = \epsilon_i\phi_i \tag{1.73}$$

$$\rho(\mathbf{r}) = {\rm Tr}\hat{D}_s[\rho]\hat{\rho}(\mathbf{r}) = \sum_{i=1}^{q}\mu_i\langle\Phi_i|\hat{\rho}(\mathbf{r})|\Phi_i\rangle = \sum_{i=1}^{M}\tilde{\mu}_i|\phi_i(\mathbf{r})|^2, \tag{1.74}$$

where $0 \leq \tilde{\mu}_i \leq 1$. Again, the latter two equations have to be solved self-consistently for a given approximation of $E_{xc}[\rho]$ and $v_{xc}(\mathbf{r})$. With the density obtained in this way the ground-state energy can obtained from Eq. (1.72). Finally, we note that so far we required that an ensemble v-representable density can be generated by a ground-state ensemble of a noninteracting system. Whether such a density can be generated by an ensemble of ground-state Slater determinants, or even by a single Slater determinant, remains on open question.

1.8 Exchange-Correlation Functionals

In order to apply the theory outlined in the previous sections we need an approximations for the exchange-correlation functional $E_{xc}[\rho]$. The first approximation that was widely used is the so-called local density approximation (LDA). In this approximation $E_{xc}[\rho]$ is given by

$$E_{xc}^{LDA}[\rho] = \int d\mathbf{r} \epsilon_{xc}^{h}(\rho(\mathbf{r})), \tag{1.75}$$

where $\epsilon_{xc}^{h}(\rho)$ is the exchange-correlation energy per unit volume of a homogeneous electron gas of density ρ. The corresponding exchange-correlation potential is given by

$$v_{xc}^{LDA}[\rho] = \left. \frac{d\epsilon_{xc}^{h}(\rho)}{d\rho} \right|_{\rho(\mathbf{r})}. \tag{1.76}$$

From the above expressions it is clear that the LDA approximates the true inhomogeneous system locally by a homogeneous electron gas. This is a very crude approximation and therefore one would expect that it will only work well in systems with a slowly varying density. However, it turns out that this simple approximation works rather well even in very inhomogeneous systems such as atoms and molecules. It is believed that the main reason for its success is that the LDA satisfies the following important sum rule

$$\int d\mathbf{r}' [g(\mathbf{r}, \mathbf{r}') - 1] \rho(\mathbf{r}') = -1, \tag{1.77}$$

where $g(\mathbf{r}, \mathbf{r}')$ is the so-called pair-correlation function which is defined as the normalized probability of finding an electron at $\mathbf{r}'$ given that at the same time there is another electron at $\mathbf{r}$. The integrand in Eq. (1.77) is commonly referred to as the exchange-correlation hole. It describes the change of the average density at $\mathbf{r}'$ due to the presence of an electron at $\mathbf{r}$. When integrated over all space it should give -1 because the electron at $\mathbf{r}$ is nowhere else in space which means that there is a net deficiency of exactly one electron in the rest of the system.

There are also some notable failures of the LDA. We will briefly discuss two of them. Since the exchange-correlation potential is proportional to the density it falls of exponentially at large distances from the nucleus instead of approaching zero as $-1/r$. This is the correct behavior because at large distance the electron sees the Coulomb potential of the positively charged ion that it has left behind which is equal to $-1/r$. Since at large distance the nuclear potential and the Hartree potential cancel each other the exchange-correlation potential must decay as $-1/r$. A second well-known failure of the LDA is the systematic underestimation of the band gap of semiconductors and insulators due to the absence of derivative discontinuities in the LDA. This means that the LDA exchange-correlation energy functional does not show a jump in its magnitude upon removal or addition of an infinitesimal fraction of the integer number of electrons [18]. It is clear from the definition in Eq. (1.75) that the LDA exchange-correlation energy functional changes continuously upon such a removal or addition. The exact derivative discontinuity Δ_{xc} in the exchange-correlation energy functional is given by the difference between the true gap E_g and the Kohn-Sham gap $E_{g,s}$,

$$\Delta_{xc} = E_g - E_{g,s}. \tag{1.78}$$

The gap E_g is defined as the difference between the ionization energy and the electron affinity energy of the true interacting system and $E_{g,s}$ is the equivalent quantity for the noninteracting Kohn-Sham system.

The obvious way to go beyond the LDA is to extend the exchange-correlation functional with terms containing gradients of the density. Through the inclusion of these gradients changes in the density can be measured and this can then be expected to lead to an improvement of the results. This so-called gradient expansion approximation (GEA) [1, 33, 34] has the following form

$$E_{xc}^{GEA}[\rho] = E_{xc}^{LDA}[\rho] + \int d\mathbf{r} f_1(\rho(\mathbf{r}))(\nabla\rho(\mathbf{r}))^2 + \int d\mathbf{r} f_2(\rho(\mathbf{r}))(\nabla^2\rho(\mathbf{r}))^2 + \cdots, \tag{1.79}$$

where the functions $f_i(\rho)$ are uniquely determined by the density response functions of the homogeneous electron gas. In practice, however, the GEA is often found to give results that are less accurate than that obtained with the LDA. The reason is that although the short-range behavior of the exchange-correlation hole is improved in the GEA the long-range behavior becomes worse leading to the violation of the sum rule (1.77). This problem of the GEA has been cured in the so-called generalized-gradient approximations (GGA). They have the following form for the exchange-correlation functional

$$E_{xc}^{GGA}[\rho] = \int d\mathbf{r} f(\rho(\mathbf{r}), \nabla\rho(\mathbf{r})). \tag{1.80}$$

The function f is then chosen in such a way that it corrects the improper long-range behavior of the exchange-correlation hole in the GEA and satisfies again the sum rule (1.77) as well as other exact constraints. Several forms of f have been proposed. For an overview of GGA functionals see Ref. [35]. Finally, we note that van Leeuwen en Baerends [36] introduced an exchange-correlation potential with the correct $1/r$ long-range behavior, thereby solving one of the shortcomings of the LDA (and GGA). Unfortunately, as of yet no systemic way has been proposed to introduce derivative discontinuities in the exchange-correlation energy functional.

Chapter 2

Time-Dependent (Current-)Density-Functional Theory

2.1 Introduction

In stationary DFT the Hohenberg-Kohn theorem guarantees that the ground-state density uniquely determines the external potential up to an arbitrary constant. One may wonder if a similar statement can be made for time-dependent densities and potentials. The proof that indeed there is such a statement was given by Runge and Gross and will be presented in section 2.3. It is not just a simple extension of the Hohenberg-Kohn theorem since that relies on the Rayleigh-Ritz variational principle for the energy of which there is no equivalent in the time-dependent case. As we will show the Runge-Gross proof is based directly on the time-dependent Schrödinger equation. The Runge-Gross theorem provides the basis for time-dependent density functional theory (TDDFT). A review of TDDFT can be found in Ref. [37]. An overview of the key concepts of TDDFT is given in Ref. [20].

2.2 Preliminaries

Consider a particle system under the influence of some time-dependent external field. For the moment we will only consider systems in which this time-dependent external field can be described by a time-dependent scalar potential $v(\mathbf{r}, t)$. The time-

dependent Hamiltonian of such a many-particle system is given by

$$\hat{H}(t) = \hat{T} + \hat{V}(t) + \hat{W}, \tag{2.1}$$

where the kinetic energy $\hat{T}$ and the two-particle interaction $\hat{W}$ are defined in Eqs. (1.2) and (1.4). The time-dependent external potential $\hat{V}(t)$ is given by

$$\hat{V}(t) = \int d\mathbf{r} v(\mathbf{r}, t)\hat{\rho}(\mathbf{r}), \tag{2.2}$$

where the density operator $\hat{\rho}(\mathbf{r})$ is defined in Eq. (1.7). The dynamics of this system can be obtained by solving the time-dependent Schrödinger equation

$$i\frac{\partial}{\partial t}|\Psi(t)\rangle = \hat{H}(t)|\Psi(t)\rangle, \tag{2.3}$$

evolving from a fixed initial state $|\Psi(t_0)\rangle = |\Psi_0\rangle$. This initial state is often taken to be the ground state. The time-dependent density $\rho(\mathbf{r}, t)$ is obtained as the expectation value of the density operator with the time-dependent many-particle wave function $|\Psi(t)\rangle$,

$$\rho(\mathbf{r}, t) = \langle\Psi(t)|\hat{\rho}(\mathbf{r})|\Psi(t)\rangle. \tag{2.4}$$

Using the quantum mechanical equation of motion for the expectation value of an arbitrary operator $\hat{A}(t)$,

$$\frac{\partial}{\partial t}\langle\Psi(t)|\hat{A}(t)|\Psi(t)\rangle = \langle\Psi(t)|\left(\frac{\partial\hat{A}(t)}{\partial t} - i[\hat{A}(t), \hat{H}(t)]\right)|\Psi(t)\rangle, \tag{2.5}$$

we obtain for the time-dependent density the well-known continuity equation

$$\frac{\partial}{\partial t}\rho(\mathbf{r}, t) = -i\langle\Psi(t)|[\hat{\rho}(\mathbf{r}), \hat{H}(t)]|\Psi(t)\rangle = -\nabla\cdot\mathbf{j}_p(\mathbf{r}, t) = -\nabla\cdot\mathbf{j}(\mathbf{r}, t), \tag{2.6}$$

where the paramagnetic current-density operator is defined by

$$\hat{\mathbf{j}}_p(\mathbf{r}) = \frac{1}{2}\sum_{i=1}^{N}(\hat{\mathbf{p}}_i\delta(\mathbf{r} - \mathbf{r}_i) + \delta(\mathbf{r} - \mathbf{r}_i)\hat{\mathbf{p}}_i), \tag{2.7}$$

in which $\hat{\mathbf{p}}_i = -i\nabla_i$ is the momentum operator, and has expectation value

$$\mathbf{j}_p(\mathbf{r}, t) = \langle\Psi(t)|\hat{\mathbf{j}}_p(\mathbf{r})|\Psi(t)\rangle = \mathbf{j}(\mathbf{r}, t). \tag{2.8}$$

We note that the current density $\mathbf{j}(\mathbf{r}, t)$ is equal to the paramagnetic current density $\mathbf{j}_p(\mathbf{r}, t)$ because we only consider external fields that can be described by scalar potentials. When we will consider general external fields the current density acquires

an extra term, the so-called diamagnetic current density. In that case also the Hamiltonian will have a different form and the continuity equation will still hold. The continuity equation gives an important constraint on time-dependent densities and current densities since it assures that there is locally a conservation of the number of particles. As we will see in the next section it plays an important role in the proof of the Runge-Gross theorem.

2.3 The Runge-Gross Theorem

The Runge-Gross theorem [3] states that two densities $\rho_1(\mathbf{r},t)$ and $\rho_2(\mathbf{r},t)$ evolving from a common initial state $|\Psi_0\rangle = |\Psi(t_0)\rangle$ and generated by external potentials $v_1(\mathbf{r},t)$ and $v_2(\mathbf{r},t)$ that both have a Taylor expansion around the initial time t_0 cannot be the same, provided that the external potentials differ by more than a purely time-dependent function, i.e.,

$$v_1(\mathbf{r},t) \neq v_2(\mathbf{r},t) + C(t). \tag{2.9}$$

We start the proof by using the constraint that the external potentials $v_1(\mathbf{r},t)$ and $v_2(\mathbf{r},t)$ have a Taylor expansion around t_0, i.e.,

$$v_1(\mathbf{r},t) = \sum_{k=0}^{\infty} \frac{1}{k!} v_{1k}(\mathbf{r})(t-t_0)^k \tag{2.10}$$

$$v_2(\mathbf{r},t) = \sum_{k=0}^{\infty} \frac{1}{k!} v_{2k}(\mathbf{r})(t-t_0)^k. \tag{2.11}$$

From this we see that Eq. (2.9) is equivalent to the statement that for the expansion coefficients there exists a smallest integer $k \geq 0$ for which

$$w_k = v_{1k}(\mathbf{r}) - v_{2k}(\mathbf{r}) = \frac{\partial^k}{\partial t^k}(v_1(\mathbf{r},t) - v_2(\mathbf{r},t))\bigg|_{t=t_0} \neq \text{const.} \tag{2.12}$$

We can now use the quantum mechanical equation of motion given in Eq. (2.5) for the current densities $\mathbf{j}_1(\mathbf{r},t)$ and $\mathbf{j}_2(\mathbf{r},t)$. We obtain

$$\frac{\partial}{\partial t}\mathbf{j}_1(\mathbf{r},t) = \frac{\partial}{\partial t}\langle\Psi_1(t)|\hat{\mathbf{j}}_p(\mathbf{r})|\Psi_1(t)\rangle = -i\langle\Psi_1(t)|[\hat{\mathbf{j}}_p(\mathbf{r}), \hat{H}_1(t)]|\Psi_1(t)\rangle \tag{2.13}$$

$$\frac{\partial}{\partial t}\mathbf{j}_2(\mathbf{r},t) = \frac{\partial}{\partial t}\langle\Psi_2(t)|\hat{\mathbf{j}}_p(\mathbf{r})|\Psi_2(t)\rangle = -i\langle\Psi_2(t)|[\hat{\mathbf{j}}_p(\mathbf{r}), \hat{H}_2(t)]|\Psi_2(t)\rangle \tag{2.14}$$

Since the wave functions $|\Psi_1(t)\rangle$ and $|\Psi_2(t)\rangle$ evolve from the same initial state we have that $|\Psi_1(t_0)\rangle = |\Psi_2(t_0)\rangle = |\Psi_0\rangle$ and therefore we can write

$$\begin{aligned}\frac{\partial}{\partial t}(\mathbf{j}_1(\mathbf{r},t) - \mathbf{j}_2(\mathbf{r},t))\bigg|_{t=t_0} &= -i\langle\Psi_0|[\hat{\mathbf{j}}_p(\mathbf{r}), \hat{H}_1(t_0) - \hat{H}_2(t_0)]|\Psi_0\rangle \\ &= -\rho_0(\mathbf{r})\nabla(v_1(\mathbf{r},t_0) - v_2(\mathbf{r},t_0)), \end{aligned} \tag{2.15}$$

where $\rho_0(\mathbf{r}) = \rho(\mathbf{r},t_0)$ is the initial density. If condition (2.12) is satisfied for $k=0$ then the right-hand side of Eq. (2.15) cannot vanish and the current densities $\mathbf{j}_1(\mathbf{r},t)$ and $\mathbf{j}_2(\mathbf{r},t)$ will become different infinitesimally later then t_0. If condition (2.12) is not satisfied for $k=0$ then one can always find a smallest $k>0$ for which it is satisfied. Applying Eq. (2.5) $k+1$ times we obtain

$$\left(\frac{\partial}{\partial t}\right)^{k+1}(\mathbf{j}_1(\mathbf{r},t) - \mathbf{j}_2(\mathbf{r},t))\bigg|_{t=t_0} = -\rho_0(\mathbf{r})\nabla w_k(\mathbf{r}) \neq 0 \tag{2.16}$$

We can therefore conclude that $\mathbf{j}_1(\mathbf{r},t) \neq \mathbf{j}_2(\mathbf{r},t)$. To prove an analogous statement for the corresponding densities $\rho_1(\mathbf{r})$ and $\rho_2(\mathbf{r})$ we make use of the continuity equation. We have

$$\frac{\partial}{\partial t}(\rho_1(\mathbf{r},t) - \rho_2(\mathbf{r},t)) = -\nabla\cdot(\mathbf{j}_1(\mathbf{r},t) - \mathbf{j}_2(\mathbf{r},t)). \tag{2.17}$$

Taking the derivative of the above expression $k+1$ times at $t=t_0$ we arrive at

$$\left(\frac{\partial}{\partial t}\right)^{k+2}(\rho_1(\mathbf{r},t) - \rho_2(\mathbf{r},t))\bigg|_{t=t_0} = \nabla\cdot(\rho_0(\mathbf{r})\nabla w_k(\mathbf{r})). \tag{2.18}$$

To prove that the densities $\rho_1(\mathbf{r})$ and $\rho_2(\mathbf{r})$ will become different infinitesimally later than t_0 we have to show that the right-hand side of Eq. (2.18) cannot vanish identically. Therefore, consider the integral

$$\begin{aligned}\int d\mathbf{r}\rho_0(\mathbf{r})(\nabla w_k(\mathbf{r}))^2 = &- \int d\mathbf{r} w_k(\mathbf{r})\nabla\cdot(\rho_0(\mathbf{r})\nabla w_k(\mathbf{r})) \\ &+ \oint d\mathbf{S}\cdot(\rho_0(\mathbf{r})w_k(\mathbf{r})\nabla w_k(\mathbf{r})), \end{aligned} \tag{2.19}$$

where we used Green's theorem.

For physically realistic potentials, i.e., potentials that arise from normalizable external charge densities, the $w_k(\mathbf{r})$'s go to zero at least as $1/r$ at large distance and the density itself decays exponentially. As a consequence the surface integral vanishes for these potentials . This immediately leads to the conclusion that $\nabla\cdot(\rho_0(\mathbf{r})\nabla w_k(\mathbf{r})) \neq 0$ because if it were equal to zero, it would imply that $(\nabla w_k)^2 = 0$ which is in contradiction to the assumption made in (2.12) that $w(\mathbf{r})$ is not constant. This

completes the proof. We note that in the case of an extended system defined as a finite system with a volume approaching infinity the Runge-Gross proof holds for all volumes.

Another important result can be obtained from the Runge-Gross proof. According to Eq. (2.18) the difference $\rho_1(\mathbf{r},t) - \rho_2(\mathbf{r},t)$ is linear in $w_k(\mathbf{r})$. Hence, this difference is already nonvanishing to first order in $v_1(\mathbf{r},t) - v_2(\mathbf{r},t)$. This ensures that the linear density response function is invertible.

The constraint that the two densities should evolve from the same initial state leaves open the possibility that there are two potentials that differ by more than a constant yielding the same density but evolve from different initial states. We note that if the system is initially in its ground state the Hohenberg-Kohn theorem guarantees that the initial state is uniquely determined by the initial density [1]. Furthermore, we note that the constraint that the external potentials should have a Taylor expansion around the initial time t_0 excludes potentials that are adiabatically switched on, since they do not have a Taylor expansion around $t_0 = -\infty$.

For a given initial state Ψ_0 we have shown that the time-dependent density $\rho(\mathbf{r},t)$ uniquely determines the time-dependent external potential $v(\mathbf{r},t)$ up to a purely time-dependent function. Since the external potential determines the time-dependent wave function $|\Psi\rangle$ it can be regarded as a functional of the time-dependent density that is unique up to a purely time-dependent phase. Therefore, the expectation value of any quantum mechanical operator $\hat{A}(t)$ is a unique functional of the density according to

$$A[\rho](t) = \langle \Psi[\rho](t) | \hat{A}(t) | \Psi[\rho](t) \rangle, \tag{2.20}$$

since the ambiguity of the phase cancels out.

An important generalization of the Runge-Gross theorem was given by van Leeuwen [38]. The van Leeuwen theorem can be summarized in the following statement:

Let $\hat{H}_1$ and $\hat{H}_2$ be two Hamiltonians with different two-particle interactions $\hat{W}_1$ and $\hat{W}_2$ and different external potentials $v_1(\mathbf{r},t)$ and $v_2(\mathbf{r},t)$ that both have a Taylor expansion around the initial time t_0. Let $\rho(\mathbf{r},t)$ be the density that evolves from the initial state $|\Psi_1(t_0)\rangle$ under the influence of $\hat{H}_1$ and let $|\Psi_2(t_0)\rangle$ be an initial state of finite momentum with the same density and the same initial time-derivative of the density. Then the time-dependent density $\rho(\mathbf{r},t)$ uniquely determines, up to a purely time-dependent function, the external potential $v_2(\mathbf{r},t)$ that generates $\rho(\mathbf{r},t)$ evolving from $|\Psi_2(t_0)\rangle$ under the influence of $\hat{H}_2$.

We will not prove this theorem here. However, we will proof a generalization of this theorem by Vignale in section 2.6. It can easily be seen that in the case

$|\Psi_1(t_0)\rangle = |\Psi_2(t_0)\rangle$ and $\hat{W}_1 = \hat{W}_2$ the van Leeuwen theorem reduces to the Runge-Gross theorem. Now consider the case $\hat{W}_2 = 0$. Then the theorem asserts that for a given initial state $|\Psi_2(t_0)\rangle$ of finite momentum with the correct density and initial time-derivative of the density there is a unique potential $v_s(\mathbf{r}, t)$ (up to a purely time-dependent function) in a noninteracting system that generates the given density $\rho(\mathbf{r}, t)$ at all times. Therefore, if we can find an initial state with the correct properties mentioned above we have solved the noninteracting v-representability problem. Whether this initial state can be chosen to be the ground state of a non-interacting system is equivalent to the unresolved noninteracting v-representability problem of stationary DFT. The above result gives a good basis for the construction of the time-dependent Kohn-Sham equations.

2.4 Time-Dependent Kohn-Sham Theory

In this section our goal is to generalize the Kohn-Sham equations of stationary DFT in such a way that they generate the time-dependent densities at all times. From the previous section we know that, under some assumptions, there exists for any interacting system with time-dependent density $\rho(\mathbf{r}, t)$ a noninteracting system that yields the same time-dependent density. Furthermore, the external potential $v_s(\mathbf{r}, t)$ that generates this density in the noninteracting system is unique and therefore $v_s(\mathbf{r}, t)$ is a unique functional (up to a purely time-dependent function) of $\rho(\mathbf{r}, t)$. In analogy with stationary Kohn-Sham theory it can be written as

$$v_s(\mathbf{r}, t) = v(\mathbf{r}, t) + \int d\mathbf{r}' \rho(\mathbf{r}', t) w(|\mathbf{r} - \mathbf{r}'|) + v_{xc}(\mathbf{r}, t). \tag{2.21}$$

We now make the assumption that the initial state of the noninteracting system can be written as a single Slater determinant. Usually this will be the ground-state Kohn-Sham wave function obtained from stationary DFT. The time-dependent Kohn-Sham equations then take the form

$$i\frac{\partial}{\partial t}\phi_i(\mathbf{r}, t) = \left(-\frac{1}{2}\nabla^2 + v_s(\mathbf{r}, t)\right)\phi_i(\mathbf{r}, t), \tag{2.22}$$

$$\rho(\mathbf{r}, t) = \sum_{i=1}^{N} |\phi_i(\mathbf{r}, t)|^2. \tag{2.23}$$

So for a given approximation of $v_{xc}(\mathbf{r}, t)$ we can construct $v_s(\mathbf{r}, t)$ from the initial density which can then be used to compute the density at an infinitesimally later time, and so on.

In stationary DFT approximations for the exchange-correlation potential can be obtained from the knowledge that it is the functional derivative of the exchange-correlation energy functional with respect to the density. Unfortunately, it turns out that in time-dependent DFT it is not possible to write $v_{xc}(\mathbf{r},t)$ as the functional derivative with respect to the density of any functional. This can be understood from the following argument. Assume that $v_{xc}(\mathbf{r},t)$ can be written as the functional derivative with respect to the density of some action functional $\mathcal{A}_{xc}[\rho]$ according to

$$v_{xc}(\mathbf{r},t) = \frac{\delta \mathcal{A}_{xc}[\rho]}{\delta \rho(\mathbf{r},t)}. \tag{2.24}$$

However, this equation implies that

$$\frac{\delta v_{xc}(\mathbf{r},t)}{\delta \rho(\mathbf{r}',t')} = \frac{\delta^2 \mathcal{A}_{xc}[\rho]}{\delta \rho(\mathbf{r},t)\delta \rho(\mathbf{r}',t')}. \tag{2.25}$$

Since the right-hand side is symmetric under the interchange of the coordinates $\mathbf{r},t$ and $\mathbf{r}',t'$, the left-hand side must also be symmetric for this equation to hold. However, we know from the principle of causality that the Kohn-Sham potential $v_s(\mathbf{r},t)$ only depends on the density $\rho(\mathbf{r}',t')$ for times $t' < t$. This means that the left-hand side of Eq. (2.25) should vanish for $t' > t$ which is in contradiction to the symmetry requirement. From this we conclude that $v_{xc}(\mathbf{r},t)$ cannot be written as the functional derivative with respect to the density of any functional. Similar arguments lead to the conclusion that the potentials $v(\mathbf{r},t)$ and $v_s(\mathbf{r},t)$ cannot be written as the functional derivative of any functional. This means that for the practical application of TDDFT we cannot use the symmetry of the action in the search for good approximations of $v_{xc}(\mathbf{r},t)$. However, some exact constraints are known for $v_{xc}(\mathbf{r},t)$ from which we can obtain approximations. We will discuss these exact constraints in section 2.8. Finally, we note that the contradiction between causality and symmetry can be resolved by the construction of an action functional defined on a Keldysh contour [39] as is shown in Ref. [20]. One can then define a functional of the time-dependent density on the contour as a Legendre transform, in a similar manner as was done in Eq. (1.32) for stationary DFT. The exchange-correlation potential on the contour can then be written as the functional derivative of this Legendre transform with respect to the density on the contour. We will discuss this approach in section 2.7 within time-dependent current-density-functional theory.

2.5 The Adiabatic Local Density Approximation

The simplest approximation for the exchange-correlation potential $v_{xc}(\mathbf{r},t)$ is the so-called adiabatic local density approximation (ALDA) which is just a simple extension

of the LDA potential we encountered in stationary DFT to include time-dependent densities. It is given by

$$v_{xc}^{ALDA}(\mathbf{r},t) = \left.\frac{d\epsilon_{xc}^{h}[\rho]}{d\rho}\right|_{\rho=\rho(\mathbf{r},t)}. \tag{2.26}$$

By comparison with Eq. (1.76) we see that $v_{xc}^{ALDA}(\mathbf{r},t)$ is equal to the functional form of $v_{xc}^{LDA}(\mathbf{r})$ evaluated at the instantaneous time-dependent density $\rho(\mathbf{r},t)$. Therefore, $v_{xc}^{ALDA}(\mathbf{r},t)$ is both local in space and local in time. Thereby it neglects so-called memory effects arising from the dependence of the exchange-correlation potential at a time t on the density at times $t' < t$. Like the LDA in stationary DFT, the ALDA gives surprisingly good results even for systems that are not slowly varying in space and time. For examples see Ref. [37] and references therein. Because of the similarity between the LDA and the ALDA, the latter suffers from some of the same shortcomings as the former, e.g., the incorrect long-range behavior.

2.6 Time-Dependent Current-Density-Functional Theory

So far we have only considered systems in which the time-dependent external field can be described by a time-dependent scalar potential $v(\mathbf{r},t)$. We will now generalize this to arbitrary time-dependent external fields. General electromagnetic fields can be represented according to the following two relations

$$\mathbf{E}(\mathbf{r},t) = \nabla v(\mathbf{r},t) - \frac{\partial \mathbf{A}(\mathbf{r},t)}{\partial t} \tag{2.27}$$

$$\mathbf{B}(\mathbf{r},t) = \nabla \times \mathbf{A}(\mathbf{r},t), \tag{2.28}$$

where $\mathbf{A}(\mathbf{r},t)$ is a vector potential, and $\mathbf{E}(\mathbf{r},t)$ and $\mathbf{B}(\mathbf{r},t)$ are the electric and magnetic field, respectively. These fields are invariant under a so-called gauge transformation given by

$$\begin{aligned} v(\mathbf{r},t) &\rightarrow v(\mathbf{r},t) + \frac{\partial \Lambda(\mathbf{r},t)}{\partial t} \\ \mathbf{A}(\mathbf{r},t) &\rightarrow \mathbf{A}(\mathbf{r},t) + \nabla\Lambda(\mathbf{r},t), \end{aligned} \tag{2.29}$$

where $\Lambda(\mathbf{r},t)$ is a differentiable but otherwise arbitrary function of $\mathbf{r}$ and t. In order to leave the physical results unchanged a gauge transformation according given Eq. (2.29) should be accompanied by a transformation of the wave function according to

$$\Psi(t) \rightarrow \Psi(t) e^{-i\Lambda(\mathbf{r},t)}. \tag{2.30}$$

From the gauge transformation in Eq. (2.29) we observe that we can always eliminate the scalar potential by requiring $\Lambda(\mathbf{r},t)$ to be a solution of the differential equation

$$\frac{\partial\Lambda(\mathbf{r},t)}{\partial t} = -v(\mathbf{r},t), \tag{2.31}$$

with initial condition $\Lambda(\mathbf{r},t_0)=0$. We see that such a transformation leads to a vector potential of which a part is written as the gradient of the scalar function $\Lambda(\mathbf{r},t)$. In general, that part of the vector potential that can be written as the gradient of a scalar function is called longitudinal. This is because its Fourier transform $\mathbf{A}(\mathbf{q})$ is parallel to $\mathbf{q}$ for all $\mathbf{q}$. The remaining part of the vector potential is called transverse because its Fourier transform is perpendicular to $\mathbf{q}$ for all $\mathbf{q}$.

The time-dependent Hamiltonian now takes the form

$$\hat{H}_{\mathbf{A}}(t) = \sum_{i=1}^{N}\left(\frac{1}{2}\left[\hat{\mathbf{p}}_i + \mathbf{A}(\mathbf{r}_i,t)\right]^2\right) + \hat{V}(t) + \hat{W}, \tag{2.32}$$

where the first term on the right-hand side is just the kinetic-energy operator plus extra terms involving the vector potential $\mathbf{A}(\mathbf{r},t)$. The operators $\hat{V}(t)$ and $\hat{W}$ are defined as before. With the subscript in $\hat{H}_{\mathbf{A}}(t)$ we make explicit the dependence of the Hamiltonian on the vector potential $\mathbf{A}(\mathbf{r},t)$ in order to distinguish it from the Hamiltonian $\hat{H}(t)$ in Eq. (2.1). We can express $\hat{H}_{\mathbf{A}}(t)$ in terms of $\hat{H}(t)$ according to

$$\begin{aligned}\hat{H}_{\mathbf{A}}(t) &= \hat{H}(t) + \int d\mathbf{r}\hat{\mathbf{j}}_p(\mathbf{r})\cdot\mathbf{A}(\mathbf{r},t) + \frac{1}{2}\int d\mathbf{r}\hat{\rho}(\mathbf{r})\mathbf{A}^2(\mathbf{r},t) &(2.33)\\ &= \hat{H}(t) + \int d\mathbf{r}\hat{\mathbf{j}}(\mathbf{r})\cdot\mathbf{A}(\mathbf{r},t) - \frac{1}{2}\int d\mathbf{r}\hat{\rho}(\mathbf{r})\mathbf{A}^2(\mathbf{r},t), &(2.34)\end{aligned}$$

where the current-density operator $\hat{\mathbf{j}}(\mathbf{r},t)$ is defined by

$$\hat{\mathbf{j}}(\mathbf{r},t) = \frac{1}{2}\sum_{i=1}^{N}(\hat{\mathbf{v}}_i(t)\delta(\mathbf{r}-\mathbf{r}_i) + \delta(\mathbf{r}-\mathbf{r}_i)\hat{\mathbf{v}}_i(t)), \tag{2.35}$$

in which the velocity operator $\hat{\mathbf{v}}_i(t)$ is given by

$$\hat{\mathbf{v}}_i(t) = \hat{\mathbf{p}}_i + \mathbf{A}(\mathbf{r}_i,t). \tag{2.36}$$

The expectation value of the current-density operator is the physical (i.e., gauge invariant) current density $\mathbf{j}(\mathbf{r},t)$ according to

$$\mathbf{j}(\mathbf{r},t) = \langle\Psi(t)|\hat{\mathbf{j}}(\mathbf{r})|\Psi(t)\rangle = \mathbf{j}_p(\mathbf{r},t) + \rho(\mathbf{r},t)\mathbf{A}(\mathbf{r},t), \tag{2.37}$$

where the second term on the right-hand side is the diamagnetic current density. Note that the continuity equation (2.6) still holds, i.e.,

$$\frac{\partial}{\partial t}\rho(\mathbf{r},t) = -i\langle\Psi(t)|[\hat{\rho}(\mathbf{r}),\hat{H}_{\mathbf{A}}(t)]|\Psi(t)\rangle = -\nabla\cdot\mathbf{j}(\mathbf{r},t). \tag{2.38}$$

The question now is whether there exists an equivalent of the Runge-Gross theorem for systems under the influence of general time-dependent fields, or, even better, whether there exists an equivalent of the van Leeuwen theorem for these systems. It were Ghosh and Dhara [4, 5] that provided us with a generalization of the Runge-Gross theorem for arbitrary fields. Under similar constraints used in the proof of the Runge-Gross theorem, they showed that two current densities $\mathbf{j}_1(\mathbf{r},t)$ and $\mathbf{j}_2(\mathbf{r},t)$ evolving from a common initial state $|\Psi(t_0)\rangle$ and generated by the set of potentials $\{v_1(\mathbf{r},t),\mathbf{A}_1(\mathbf{r},t)\}$ and $\{v_2(\mathbf{r},t),\mathbf{A}_2(\mathbf{r},t)\}$, where all potentials have a Taylor expansion around the initial time t_0, cannot be the same, provided that the sets of potentials differ by more than a gauge transformation of the form (2.29). The density is then uniquely determined by the current density through the continuity equation (2.38). However, the density no longer uniquely determines the current density, i.e., the map $\rho(\mathbf{r},t) \rightarrow \mathbf{j}(\mathbf{r},t)$ does not exist. Therefore, it is more convenient to reformulate the theory in terms of the current density $\mathbf{j}(\mathbf{r},t)$ giving rise to so-called time-dependent current-density-functional theory (TDCDFT). Recently, Vignale [6] generalized the van Leeuwen theorem to include general time-dependent fields. In the following we will give the proof of this theorem. Vignale's theorem can be summarized in the following statement:

Let $\rho(\mathbf{r},t)$ and $\mathbf{j}(\mathbf{r},t)$ be the density and current density of a many-particle system that evolves from an initial state $|\Psi_1(t_0)\rangle$ under the influence of the Hamiltonian

$$\hat{H}_1(t) = \sum_{i=1}^{N}\left(\frac{1}{2}\left[\hat{\mathbf{p}}_i + \mathbf{A}_1(\mathbf{r}_i,t)\right]^2\right) + \hat{V}_1(t) + \hat{W}_1, \tag{2.39}$$

where $\hat{V}_1(t)$ and $\hat{W}_1$ are the external potential operator and the two-particle operator defined in a similar way as in Eqs. (2.2) and (1.4), respectively. Let the potentials $v_1(\mathbf{r},t)$ and $\mathbf{A}_1(\mathbf{r},t)$ have Taylor expansions around the initial time t_0. Then, under reasonable assumptions defined below, the same density and current density can be obtained from a many-particle system with Hamiltonian

$$\hat{H}_2(t) = \sum_{i=1}^{N}\left(\frac{1}{2}\left[\hat{\mathbf{p}}_i + \mathbf{A}_2(\mathbf{r}_i,t)\right]^2\right) + \hat{V}_2(t) + \hat{W}_2, \tag{2.40}$$

evolving from an initial state $|\Psi_2(t_0)\rangle$ that yields the same density and current density as $|\Psi_1(t_0)\rangle$, provided that $v_2(\mathbf{r},t)$ and $\mathbf{A}_2(\mathbf{r},t)$ have a Taylor expansion around the initial time t_0. The set of potentials $\{v_2(\mathbf{r},t),\mathbf{A}_2(\mathbf{r},t)\}$ is then uniquely determined by $\{v_1(\mathbf{r},t),\mathbf{A}_1(\mathbf{r},t)\}$ and the initial states $|\Psi_1(t_0)\rangle$ and $|\Psi_2(t_0)\rangle$ up to gauge transformations of the form (2.29).

In the following proof we will assume that a gauge transformation has been done for both systems 1 and 2 with $\Lambda(\mathbf{r},t)$ a solution of Eq. (2.31), so that the scalar potentials $v_1(\mathbf{r},t)$ and $v_2(\mathbf{r},t)$ are zero for all times t. We start the proof by considering the quantum mechanical equation of motion of $\mathbf{j}(\mathbf{r},t)$ for system 1. Using Eq. (2.5) we then obtain what might be called the continuity equation for the current density,

$$\frac{\partial \mathbf{j}(\mathbf{r},t)}{\partial t} = \left\langle \frac{\partial \hat{\mathbf{j}}(\mathbf{r},t)}{\partial t} - i[\hat{\mathbf{j}}(\mathbf{r},t), \hat{H}_1(t)] \right\rangle_1 \tag{2.41}$$

$$= \rho(\mathbf{r},t)\frac{\partial \mathbf{A}_1(\mathbf{r},t)}{\partial t} - \mathbf{j}(\mathbf{r},t)\times[\nabla\times\mathbf{A}_1(\mathbf{r},t)] + \mathcal{F}_1(\mathbf{r},t) + \nabla\cdot\sigma_1(\mathbf{r},t), \tag{2.42}$$

where $\langle\hat{A}(t)\rangle_1$ denotes the expectation value of an operator $\hat{A}(t)$ at time t for system 1. The internal force density $\mathcal{F}_1(\mathbf{r},t)$ and the stress tensor $\sigma_1(\mathbf{r},t)$ are defined as

$$\mathcal{F}_1(\mathbf{r},t) = -\left\langle \sum_{i=1}^{N}\delta(\mathbf{r}-\mathbf{r}_i)\sum_{j\neq i}^{N}\nabla_i w_1(|\mathbf{r}_i-\mathbf{r}_j|)\right\rangle_1 \tag{2.43}$$

$$\sigma_{1,\alpha\beta}(\mathbf{r},t) = -\left\langle \frac{1}{4}\sum_{i=1}^{N}\{\hat{v}_{1\alpha}(t),\{\hat{v}_{1\beta}(t),\delta(\mathbf{r}-\mathbf{r}_i)\}\}\right\rangle_1, \tag{2.44}$$

where $\{\hat{A},\hat{B}\} = \hat{A}\hat{B}+\hat{B}\hat{A}$ denotes the anticommutator of two operators $\hat{A}$ and $\hat{B}$. With the notation $\nabla\cdot\sigma_1(\mathbf{r},t)$ we mean that $[\nabla\cdot\sigma_1(\mathbf{r},t)]_\alpha = \sum_\beta \partial\sigma_1(\mathbf{r},t)/\partial r_\beta$. Note that in Eq. (2.42) the quantities $-\partial\mathbf{A}_1(\mathbf{r},t)/\partial t$ and $\nabla\times\mathbf{A}_1(\mathbf{r},t)$ are the electric and magnetic field, respectively, since $v_1(\mathbf{r},t)=0$ for all t. According to Vignale's theorem the same current density should also obey the following equation of motion

$$\frac{\partial \mathbf{j}(\mathbf{r},t)}{\partial t} = \rho(\mathbf{r},t)\frac{\partial \mathbf{A}_2(\mathbf{r},t)}{\partial t} - \mathbf{j}(\mathbf{r},t)\times[\nabla\times\mathbf{A}_2(\mathbf{r},t)] + \mathcal{F}_2(\mathbf{r},t) + \nabla\cdot\sigma_2(\mathbf{r},t), \tag{2.45}$$

where $\mathcal{F}_2(\mathbf{r},t)$ and $\sigma_2(\mathbf{r},t)$ are defined in an analogous manner to $\mathcal{F}_1(\mathbf{r},t)$ and $\sigma_1(\mathbf{r},t)$. The difference of the two equations of motion for the current density $\mathbf{j}(\mathbf{r},t)$ is given by

$$\rho(\mathbf{r},t)\frac{\partial \Delta\mathbf{A}(\mathbf{r},t)}{\partial t} = \mathbf{j}(\mathbf{r},t)\times[\nabla\times\Delta\mathbf{A}(\mathbf{r},t)] + Q_1(\mathbf{r},t) - Q_2(\mathbf{r},t), \tag{2.46}$$

where $\Delta\mathbf{A}(\mathbf{r},t) \equiv \mathbf{A}_2(\mathbf{r},t) - \mathbf{A}_1(\mathbf{r},t)$ and

$$Q_1(\mathbf{r},t) \equiv \mathcal{F}_1(\mathbf{r},t) + \nabla\cdot\sigma_1(\mathbf{r},t). \tag{2.47}$$

The expression for $Q_2(\mathbf{r},t)$ is analogous to that for $Q_1(\mathbf{r},t)$. Equation (2.46) determines the vector potential $\mathbf{A}_2(\mathbf{r},t)$ that yields the same current density as $\mathbf{A}_1(\mathbf{r},t)$. The question is whether Eq. (2.46) has a solution and, if so, whether this solution is

unique. For general vector potentials this is not easy to prove since Eq. (2.46) not only depends on $\mathbf{A}_2(\mathbf{r},t)$ explicitly but also implicitly through $Q_2(\mathbf{r},t)$. For this reason we required that the vector potentials $\mathbf{A}_1(\mathbf{r},t)$ and $\mathbf{A}_2(\mathbf{r},t)$ have a Taylor expansion around $t=t_0$. Also the difference of the two vector potentials, $\Delta\mathbf{A}(\mathbf{r},t)$, has a Taylor expansion around the initial time t_0 according to

$$\Delta\mathbf{A}(\mathbf{r},t)=\sum_{k=0}^{\infty}\Delta\mathbf{A}_k(\mathbf{r})(t-t_0)^k, \tag{2.48}$$

with

$$\Delta\mathbf{A}_k(\mathbf{r})\equiv\frac{1}{k!}\left.\frac{\partial^k\Delta\mathbf{A}(\mathbf{r},t)}{\partial t^k}\right|_{t=t_0}. \tag{2.49}$$

Substituting this expansion into Eq. (2.46) and equating the lth term of the expansion we obtain

$$\sum_{k=0}^{l}\rho_{l-k}(\mathbf{r})\left[\frac{\partial\Delta\mathbf{A}(\mathbf{r},t)}{\partial t}\right]_k=\sum_{k=0}^{l}\{\mathbf{j}_{l-k}(\mathbf{r},t)\times[\nabla\times\Delta\mathbf{A}_k(\mathbf{r})]\}+[Q_1(\mathbf{r},t)]_l-[Q_2(\mathbf{r},t)]_l, \tag{2.50}$$

where $\rho_k(\mathbf{r})$ and $\mathbf{j}_k(\mathbf{r})$ are the kth coefficients in the Taylor expansions of $\rho(\mathbf{r},t)$ and $\mathbf{j}(\mathbf{r},t)$ around $t=t_0$ and $[f(\mathbf{r},t)]_l$ is the lth coefficient (a function of $\mathbf{r}$ alone) in the Taylor expansion of a function $f(\mathbf{r},t)$ around $t=t_0$. It is a consequence of the analyticity of the vector potential and the time-dependent Schrödinger equation (2.1) that all the quantities entering Eq. (2.50) have a Taylor expansion around $t=t_0$. Since we have that

$$\left[\frac{\partial\Delta\mathbf{A}(\mathbf{r},t)}{\partial t}\right]_k=(k+1)\Delta\mathbf{A}_{k+1}(\mathbf{r}), \tag{2.51}$$

we can write Eq. (2.50) as follows

$$\begin{aligned}\rho_0(\mathbf{r})(l+1)\Delta\mathbf{A}_{l+1}(\mathbf{r})= &-\sum_{k=0}^{l-1}\rho_{l-k}(\mathbf{r})(k+1)\Delta\mathbf{A}_{k+1}(\mathbf{r})\\ &+\sum_{k=0}^{l}\{\mathbf{j}_{l-k}(\mathbf{r},t)\times[\nabla\times\Delta\mathbf{A}_k(\mathbf{r})]\}\\ &+[Q_1(\mathbf{r},t)]_l-[Q_2(\mathbf{r},t)]_l,\end{aligned} \tag{2.52}$$

where the $k=l$ term of the sum in the left-hand side of Eq. (2.50) has been isolated on the left-hand side. Equation (2.52) is a recursion relation for the coefficients of the Taylor expansion of $\Delta\mathbf{A}(\mathbf{r},t)$, i.e., the coefficient $\Delta\mathbf{A}_{l+1}(\mathbf{r})$ is solely determined by the coefficients $\Delta\mathbf{A}_k(\mathbf{r})$ with $k\leq l$. This is clear for the coefficients that enter Eq. (2.52) explicitly. For the coefficients $\Delta\mathbf{A}_k(\mathbf{r})$ that enter Eq. (2.52) implicitly

through the coefficients of the expansion of $Q_2(\mathbf{r},t)$ this is a consequence of the time-dependend Schrödinger equation (2.1). Since it is of first order in time it guarantees that the lth coefficient in the expansion of the states $|\Psi_1(t)\rangle$ and $|\Psi_2(t)\rangle$ are solely determined by the coefficients $\Delta\mathbf{A}_k(\mathbf{r})$ with $k<l$. This means that if we know the initial value of $\Delta\mathbf{A}_k(\mathbf{r})$, i.e., $\Delta\mathbf{A}(\mathbf{r},t)=\Delta\mathbf{A}_2(\mathbf{r},0)-\Delta\mathbf{A}_1(\mathbf{r},0)$, we can determine all coefficients through the recursion relation (2.52). This initial value can easily be determined from the knowledge that the density and current density of systems 1 and 2 are equal. Therefore, we see from Eq. (2.37) that

$$\rho(\mathbf{r},t_0)\Delta\mathbf{A}_0(\mathbf{r})=\langle\Psi_2(t_0)|\hat{\mathbf{j}}_p(\mathbf{r})|\Psi_2(t_0)\rangle-\langle\Psi_1(t_0)|\hat{\mathbf{j}}_p(\mathbf{r})|\Psi_1(t_0)\rangle, \tag{2.53}$$

where the paramagnetic current-density operator is defined in Eq. (2.7). The recursion relation (2.52) in combination with initial condition (2.53) now completely determines the coefficients in the Taylor expansion of vector potential $\mathbf{A}_2(\mathbf{r},t)$ that yields, in system 2, the same density $\rho(\mathbf{r},t)$ and current density $\mathbf{j}(\mathbf{r},t)$ as the vector potential $\mathbf{A}_1(\mathbf{r},t)$ yields in system 1. Since we required that $\mathbf{A}_1(\mathbf{r},t)$ and $\mathbf{A}_2(\mathbf{r},t)$ have a Taylor expansion around $t=t_0$, the coefficients in the Taylor expansion completely determine $\mathbf{A}_2(\mathbf{r},t)$ provided that this series converges within a nonvanishing convergence radius $t_c>0$. If this is the case then $\mathbf{A}_2(\mathbf{r},t)$ is uniquely determined, because $\mathbf{A}_2(\mathbf{r},t)$ can be determined up to t_c and then the procedure can be iterated with t_c as the initial time, and so on. If the convergence radius is zero this means that the kth derivative of $\mathbf{A}_2(\mathbf{r},t)$ with respect to time at $t=0$ grows more rapidly than $k!a^k$ with a an arbitrary positive constant. Because of the smooth dynamics of the Schrödinger equation it is very unlikely that the values of the initial derivatives will show such an explosion, and, therefore, we will exclude this option. This defines the reasonable assumptions mentioned in Vignale's theorem. We have thus proven Vignale's theorem. Note that the proof given above does not require the density or the current density to vanish at infinity.

We will now discuss two special cases of Vignale's theorem. First, let system 1 and 2 be the same, i.e., $\hat{W}_1=\hat{W}_2$ and $|\Psi_1(t_0)\rangle=|\Psi_2(t_0)\rangle$. Then, according to Eq. (2.53), $\Delta\mathbf{A}_0(\mathbf{r})=0$ and therefore, according to Eq. (2.52), $\Delta\mathbf{A}_k(\mathbf{r})=0$ for all k. This means that $\mathbf{A}_1(\mathbf{r},t)=\mathbf{A}_2(\mathbf{r},t)$ at all times t. We conclude that two vector potentials that evolve from the same initial state of a many-particle system and that yield the same current density must be equal, up to a gauge transformation. This is simply an analogue of the Runge-Gross theorem in the case of TDCDFT. Second, let system 2 be a system of noninteracting particles, i.e., $\hat{W}=0$. Then, Vignale's theorem asserts that for a given current density generated by a vector potential $\mathbf{A}_1(\mathbf{r},t)$ in an interacting system evolving from an initial state $|\Psi_1(t_0)\rangle$ there is a unique vector potential $\mathbf{A}_2(\mathbf{r},t)$ (up to a gauge transform) in a noninteracting system evolving from

an initial state $|\Psi_2(t_0)\rangle$ that yields this given current density at all times. Therefore, if we can find an initial state $|\Psi_2(t_0)\rangle$ with the correct initial density and current density we have solved the noninteracting **A**-representability problem. As mentioned before, whether this initial state can be chosen to be the ground state of a non-interacting system is equivalent to the unresolved noninteracting v-representability problem of stationary DFT. The above result gives a good basis for setting up the time-dependent Kohn-Sham equations for general time-dependent external fields. They are given by

$$i\frac{\partial}{\partial t}\phi_i(\mathbf{r},t) = \left(\frac{1}{2}[\hat{\mathbf{p}}+\mathbf{A}_s(\mathbf{r},t)]^2+v_s(\mathbf{r},t)\right)\phi_i(\mathbf{r},t) \tag{2.54}$$

$$\mathbf{j}(\mathbf{r},t) = \frac{1}{2i}\sum_{i=1}^{N}[\phi_i^*(\mathbf{r},t)\nabla\phi_i(\mathbf{r},t)-\nabla\phi_i^*(\mathbf{r},t)\phi_i(\mathbf{r},t)]+\rho(\mathbf{r},t)\mathbf{A}_s(\mathbf{r},t) \tag{2.55}$$

$$\rho(\mathbf{r},t) = \sum_{i=1}^{N}|\phi_i(\mathbf{r},t)|^2, \tag{2.56}$$

where we again made the assumption that the initial state of the noninteracting system can be written as a single Slater determinant. The set of Kohn-Sham potentials $\{v_s(\mathbf{r},t),\mathbf{A}_s(\mathbf{r},t)\}$ are defined, up to a gauge transform, by

$$v_s(\mathbf{r},t) = v(\mathbf{r},t)+\int d\mathbf{r}'\rho(\mathbf{r}',t)w(|\mathbf{r}-\mathbf{r}'|)+v_{xc}(\mathbf{r},t) \tag{2.57}$$

$$\mathbf{A}_s(\mathbf{r},t) = \mathbf{A}(\mathbf{r},t)+\mathbf{A}_{xc}(\mathbf{r},t). \tag{2.58}$$

We note that it has been shown that an interacting system under the influence of a time-dependent field that can be described by a scalar potential only, cannot, in general, be described by a Kohn-Sham system with solely a scalar potential [40]. That is, a v-representable current density is, in general, not noninteracting v-representable. However, the v-representable current density might be noninteracting **A**-representable since this is a much weaker condition. In the next section we will show that the potentials in Eqs. (2.57) and (2.58) can be written as functional derivatives with respect to the current density of the Legendre transform of an action functional defined on the Keldysh contour as was shown in Ref. [41].

2.7 The Keldysh Action Functional

Let us start this section by introducing the time-evolution operator $\hat{U}(t,t')$. It relates a state at time t' to a state at time t according to

$$|\Psi(t)\rangle = \hat{U}(t,t')|\Psi(t')\rangle. \tag{2.59}$$

From this expression we can derive that

$$\hat{U}(t,t') = \hat{T}\exp\left[-i\int_{t'}^{t} d\tau \hat{H}(\tau)\right], \tag{2.60}$$

where $\hat{T}$ is the time-ordering operator given by

$$\begin{aligned}\hat{T}\left[\hat{H}(\tau_1)\cdots\hat{H}(\tau_n)\right] &= \sum_P \Theta(\tau_{P(1)}-\tau_{P(2)})\cdots\Theta(\tau_{P(n-1)}-\tau_{P(n)}) \\ &\times \hat{H}(\tau_{P(1)})\cdots\hat{H}(\tau_{P(n)}),\end{aligned} \tag{2.61}$$

where P runs over all permutations of the numbers $1\cdots n$. If the Hamiltonian is time independent the evolution operator is simply given by

$$\hat{U}(t,t') = \exp\left[-i\hat{H}(t-t')\right]. \tag{2.62}$$

The time-evolution operator has the following properties

$$\hat{U}(t,t) = 1 \tag{2.63}$$

$$i\frac{\partial}{\partial t}\hat{U}(t,t') = \hat{H}(t)\hat{U}(t,t') \tag{2.64}$$

$$-i\frac{\partial}{\partial t}\hat{U}(t',t) = \hat{U}(t',t)\hat{H}(t). \tag{2.65}$$

The first property is obvious from Eq. (2.59). The second property is obtained by taking the derivative of Eq. (2.59) with respect to t and using the time-dependent Schrödinger equation

$$i\frac{\partial}{\partial t}|\Psi(t)\rangle = \hat{H}(t)|\Psi(t)\rangle. \tag{2.66}$$

This gives the result

$$i\frac{\partial}{\partial t}\hat{U}(t,t')|\Psi(t')\rangle = \hat{H}(t)\hat{U}(t,t')|\Psi(t')\rangle. \tag{2.67}$$

Since $|\Psi(t')\rangle$ is arbitrary we obtain Eq. (2.64). In a similar way we can obtain Eq. (2.65) by taking the time-derivative of Eq. (2.59) with respect to t'.

Consider a system that is described by the time-dependent Hamiltonian $\hat{H}_0(t)$ that has initial state $|\Psi_0\rangle$. At a certain time $t = t_0$ we switch on the time-dependent perturbation $\delta\hat{H}(t)$. The full time-dependent Hamiltonian $\hat{H}(t)$ then reads

$$\hat{H}(t) = \hat{H}_0(t) + \delta\hat{H}(t), \tag{2.68}$$

where $\delta H(t) = 0$ for $t < t_0$. The time-evolution operator can now be written as

$$\hat{U}'(t,t_0) = \hat{U}(t,t_0) + \delta\hat{U}(t,t_0). \tag{2.69}$$

Using Eqs. (2.63), (2.64), and (2.65) we obtain to first order in the perturbation

$$
\begin{aligned}
i\frac{\partial}{\partial t}\delta\hat{U}(t,t_0) &= \hat{H}_0(t)\delta\hat{U}(t,t_0) + \delta\hat{H}(t)\hat{U}(t,t_0) && (2.70)\\
-i\frac{\partial}{\partial t}\delta\hat{U}(t_0,t) &= \delta\hat{U}(t_0,t)\hat{H}_0(t) + \hat{U}(t_0,t)\delta\hat{H}(t) && (2.71)\\
\delta\hat{U}(t,t) &= 0. && (2.72)
\end{aligned}
$$

The above set of equations has the following solution

$$
\delta\hat{U}(t,t_0) = -i\int_{t_0}^{t} dt'\hat{U}(t,t')\delta\hat{H}(t')\hat{U}(t',t_0). \tag{2.73}
$$

We now define an operator $\hat{A}(t)$ in the Heisenberg picture as

$$
\hat{A}_H(t) = \hat{U}(t_0,t)\hat{A}(t)\hat{U}(t,t_0). \tag{2.74}
$$

The expectation value of the operator $\hat{A}(t)$ at time t can now be written as

$$
\langle\hat{A}(t)\rangle = \langle\Psi_0|\hat{A}_H(t)|\Psi_0\rangle = \langle\Psi_0|\hat{U}(t_0,t)\hat{A}(t)\hat{U}(t,t_0)|\Psi_0\rangle \tag{2.75}
$$

If we read the expression on the right-hand side from right to left we can say that the system evolves from t_0 to t after which the operator $\hat{A}(t)$ acts on the system and then the system evolves back again from t to t_0. A corresponding contour was introduced by Keldysh [39]. Using this contour we can write the following generalization for the expectation value of $\hat{A}(t)$

$$
\langle\hat{A}(t)\rangle = \frac{\langle\Psi_0|\hat{T}_C\left[\exp\left(-i\int_C d\tau\hat{H}(\tau)\right)\hat{A}(t)\right]|\Psi_0\rangle}{\langle\Psi_0|\hat{T}_C\left[\exp\left(-i\int_C d\tau\hat{H}(\tau)\right)\right]|\Psi_0\rangle} \tag{2.76}
$$

where we defined

$$
\begin{aligned}
\hat{T}_C\left[\exp\left(-i\int_C d\tau\hat{H}(\tau)\right)\hat{A}(t)\right] &\equiv \sum_n^{\infty}\frac{(-i)^n}{n!}\int_C d\tau_1\cdots d\tau_n \\
&\times\ \hat{T}_C\left[\hat{A}(t)\hat{H}(\tau_1)\cdots\hat{H}(\tau_n)\right]. \qquad (2.77)
\end{aligned}
$$

Here $\hat{T}_C$ is the time-ordering operator on the contour defined by

$$
\begin{aligned}
\hat{T}_C\left[\hat{A}_1(\tau_1)\cdots\hat{A}_n(\tau_n)\right] &= \sum_P \Theta_C(\tau_{P(1)},\tau_{P(2)})\cdots\Theta_C(\tau_{P(n-1)},\tau_{P(n)}) \\
&\times\ \hat{A}_{P(1)}(\tau_{P(1)})\cdots\hat{A}_{P(n)}(\tau_{P(n)}), \qquad (2.78)
\end{aligned}
$$

where $\Theta_C(t,t')$ is a generalization of the Heavside step function for time arguments that are on the contour, i.e., it is equal to 1 if time t is later than time t' on the contour and zero otherwise. In Eq. (2.76) we extended the definition of the Hamiltonian in such a way that it can be different on the forward and backward parts of the contour. If the Hamiltonian $H(t)$ is the same on the forward and backward parts of the contour, which is the case for physical perturbations, Eq. (2.76) reduces to Eq. (2.75).

Let us now consider systems under the influence of general time-dependent fields, i.e., systems that are described by the Hamiltonian in Eq. (2.32). We choose the gauge such that all perturbations are included in the vector potential, that is, for the scalar potential we have $v(\mathbf{r},t) = v(\mathbf{r},t_0)$ for all times t. We can therefore rewrite $H(t)$ according to

$$H(t) = \hat{H}_0(t) + \sum_{i=1}^{N} \frac{1}{2}\hat{\mathbf{p}}_i \cdot \mathbf{A}(\mathbf{r}_i,t) + \frac{1}{2}\mathbf{A}(\mathbf{r}_i,t)\cdot\hat{\mathbf{p}}_i + \frac{1}{2}\mathbf{A}^2(\mathbf{r}_i,t) \tag{2.79}$$

$$= \hat{H}_0(t) + \int d\mathbf{r}\hat{\mathbf{j}}_p(\mathbf{r})\cdot\mathbf{A}(\mathbf{r},t) + \frac{1}{2}\int d\mathbf{r}\hat{\rho}(\mathbf{r})\mathbf{A}^2(\mathbf{r},t). \tag{2.80}$$

We now define the following action functional of the vector potential $\mathbf{A}(\mathbf{r},t)$

$$\tilde{\mathcal{A}}[\mathbf{A}] = i\ln\langle\Psi_0|\hat{U}(t_0,t_0)|\Psi_0\rangle, \tag{2.81}$$

where we generalized the expression for the evolution operator to times on the contour according to

$$\hat{U}(t,t') = \hat{T}_C \exp\left(-i\int_{t'}^{t} d\tau \hat{H}(\tau)\right). \tag{2.82}$$

Since the Hamiltonian is a functional of the vector potential $\mathbf{A}(\mathbf{r},t)$ it is clear that if $\mathbf{A}(\mathbf{r},t)$ is the same on the forward and backward parts of the contour then $\hat{U}(t_0,t_0) = 1$ and the action functional vanishes. We will denote vector potentials of this kind as physical vector potentials. However, the functional derivatives of $\tilde{\mathcal{A}}[\mathbf{A}]$ with respect to $\mathbf{A}(\mathbf{r},t)$ taken at a physical vector potentials is, in general, nonzero. With the definition of the evolution operator in Eq. (2.82) we can rewrite Eq. (2.76) for the expectation value of $\hat{A}(t)$ as

$$\langle\hat{A}(t)\rangle = \frac{\langle\Psi_0|\hat{A}_H(t)|\Psi_0\rangle}{\langle\Psi_0|\hat{U}(t_0,t_0)|\Psi_0\rangle}. \tag{2.83}$$

From Eqs. (2.73) and (2.80) it is easy to see that the functional derivative of $\hat{U}(t,t_0)$ with respect to $\mathbf{A}(\mathbf{r},t)$ is given by

$$\frac{\delta\hat{U}(t,t_0)}{\delta\mathbf{A}(\mathbf{r},t')} = -i\hat{U}(t,t')\left[\hat{\mathbf{j}}_p(\mathbf{r}) + \hat{\rho}(\mathbf{r})\mathbf{A}(\mathbf{r},t')\right]\hat{U}(t',t_0) \tag{2.84}$$

With this result we obtain for the functional derivative of $\tilde{\mathcal{A}}[\mathbf{A}]$ with respect to $\mathbf{A}(\mathbf{r},t)$

$$\frac{\delta\tilde{\mathcal{A}}[\mathbf{A}]}{\delta\mathbf{A}(\mathbf{r},t)} = \frac{\langle\Psi_0|\hat{U}(t_0,t)\left[\hat{\mathbf{j}}_p(\mathbf{r})+\hat{\rho}(\mathbf{r})\mathbf{A}(\mathbf{r},t)\right]\hat{U}(t,t_0)|\Psi_0\rangle}{\langle\Psi_0|\hat{U}(t_0,t_0)|\Psi_0\rangle} \tag{2.85}$$

$$= \langle\hat{\mathbf{j}}_p(\mathbf{r},t)\rangle + \langle\hat{\rho}(\mathbf{r},t)\rangle\mathbf{A}(\mathbf{r},t) = \mathbf{j}(\mathbf{r},t). \tag{2.86}$$

From the above equation we see that the vector potential and the current density are conjugate variables. In a similar way as in stationary DFT we can now define the Legendre transform

$$\mathcal{A}[\mathbf{j}] = -\tilde{\mathcal{A}}[\mathbf{A}] + \int_C dtd\mathbf{r}\mathbf{j}(\mathbf{r},t)\cdot\mathbf{A}(\mathbf{r},t), \tag{2.87}$$

so that

$$\frac{\delta\mathcal{A}[\mathbf{j}]}{\delta\mathbf{j}(\mathbf{r},t)} = \mathbf{A}(\mathbf{r},t). \tag{2.88}$$

The Legendre transformation assumes that the current density uniquely determines the vector potential and vice versa which means that Eq. (2.86) should be invertible (up to a gauge). It can be proved by a generalization of the proof given in Ref. [20] for the density-density response function that for switch-on processes the Keldysh current-current response function is invertible for systems initially in their ground state. Similarly we have for the noninteracting Kohn-Sham system the Legendre transform

$$\mathcal{A}_s[\mathbf{j}] = -\tilde{\mathcal{A}}_s[\mathbf{A}] + \int_C dtd\mathbf{r}\mathbf{j}(\mathbf{r},t)\cdot\mathbf{A}_s(\mathbf{r},t) \tag{2.89}$$

We can now define the exchange-correlation part of the action functional $\mathcal{A}_{xc}$ by

$$\mathcal{A}[\mathbf{j}] = \mathcal{A}_s[\mathbf{j}] - \mathcal{A}_{xc}[\mathbf{j}] - \frac{1}{2}\int_C dtd\mathbf{r}d\mathbf{r}'\rho(\mathbf{r},t)\rho(\mathbf{r}',t)w(|\mathbf{r}-\mathbf{r}'|), \tag{2.90}$$

where the density $\rho(\mathbf{r},t)$ is a functional of the initial state and of the current density through the generalization of the continuity equation for times on the contour. In Eq. (2.90) we assume that $\mathcal{A}[\mathbf{j}]$ and $\mathcal{A}_s[\mathbf{j}]$ are defined on the same domain of current densities, i.e., $\mathbf{j}(\mathbf{r},t)$ is noninteracting $\mathbf{A}$-representable. In other words, we assume that there exists a generalization of Vignale's theorem for times on the contour. Taking the functional derivative of Eq. (2.90) with respect to the current density $\mathbf{j}(\mathbf{r},t)$ leads to

$$\mathbf{A}_s(\mathbf{r},t) = \mathbf{A}(\mathbf{r},t) + \mathbf{A}_{xc}(\mathbf{r},t) + \mathbf{A}_W(\mathbf{r},t), \tag{2.91}$$

where $\mathbf{A}_W(\mathbf{r},t)$ is defined by

$$\frac{\partial\mathbf{A}_W(\mathbf{r},t)}{\partial t} = -\nabla\int d\mathbf{r}\rho(\mathbf{r}',t)w(|\mathbf{r}-\mathbf{r}'|), \tag{2.92}$$

and the exchange-correlation vector potential is given by

$$\mathbf{A}_{xc}(\mathbf{r},t) = \frac{\delta \mathcal{A}_{xc}}{\delta \mathbf{j}(\mathbf{r},t)}. \tag{2.93}$$

It is easy to see that Eq. (2.91) and Eqs. (2.57) and (2.58) are the same up to a gauge transformation.

Finally, let us take a look at the causality and symmetry properties of the current-current response function on the contour. These properties have led to the paradox discussed in section 2.4 which led to the conclusion that it is not possible to write the scalar potentials $v(\mathbf{r},t)$, $v_s(\mathbf{r},t)$ and $v_{xc}(\mathbf{r},t)$ as functional derivatives with respect to the density of any functional. We will now show that this paradox is resolved in the case of the Keldysh action functional. In the following we will show the proof of this for the vector potential $\mathbf{A}(\mathbf{r},t)$. The proof for other potentials is analogous. From Eq. (2.85) we obtain for the current-current response function on the contour

$$\begin{aligned}
\chi_{C,mn}(\mathbf{r},t,\mathbf{r}',t') &= \frac{\delta^2 \tilde{\mathcal{A}}[\mathbf{A}]}{\delta A_m(\mathbf{r},t)\delta A_n(\mathbf{r}',t')} \\
&= \delta_{mn}\rho(\mathbf{r},t)\delta_C(t,t')\delta(\mathbf{r}-\mathbf{r}') \\
&- i\Theta_C(t,t')\langle \hat{\mathbf{j}}_p(\mathbf{r},t)\hat{\mathbf{j}}_p(\mathbf{r}',t')\rangle - i\Theta_C(t',t)\langle \hat{\mathbf{j}}_p(\mathbf{r}',t')\hat{\mathbf{j}}_p(\mathbf{r},t)\rangle \\
&+ i\langle \hat{\mathbf{j}}_p(\mathbf{r},t)\rangle\langle \hat{\mathbf{j}}_p(\mathbf{r}',t')\rangle,
\end{aligned} \tag{2.94}$$

where $\delta_C(t,t') = \partial_t \Theta_C(t,t')$ is the generalization of the delta function to times on the contour and we defined

$$\langle \hat{A}(t)\hat{B}(t')\rangle = \frac{\langle \Psi_0|\hat{A}_H(t)\hat{B}_H(t')|\Psi_0\rangle}{\langle \Psi_0|\hat{U}(t_0,t_0)|\Psi_0\rangle}. \tag{2.95}$$

The last term in Eq. (2.94) is due to the functional differentiation of the denominator in Eq. (2.85). If we define the fluctuation operator

$$\Delta\hat{\mathbf{j}}_p(\mathbf{r},t) = \hat{\mathbf{j}}_p(\mathbf{r},t) - \langle \hat{\mathbf{j}}_p(\mathbf{r},t)\rangle \tag{2.96}$$

we can rewrite Eq. (2.94) as

$$\chi_{C,mn}(\mathbf{r},t,\mathbf{r}',t') = \delta_{mn}\rho(\mathbf{r},t)\delta_C(t,t')\delta(\mathbf{r}-\mathbf{r}') - i\langle T_C[\Delta\hat{\mathbf{j}}_p(\mathbf{r},t)\Delta\hat{\mathbf{j}}_p(\mathbf{r}',t')]\rangle. \tag{2.97}$$

We observe that the current-current response function is a symmetric function of its arguments which it should be since it is a second order functional derivative. We will now show that it becomes a retarded function for physical current densities, i.e., current densities that are generated by physical vector potentials. The current density

response can be obtained from the current-current response function according to

$$\begin{aligned}\delta j_m(\mathbf{r},t) &= \sum_n \int_C dt' d\mathbf{r}' \chi_{C,mn}(\mathbf{r},t,\mathbf{r}',t')\delta A_n(\mathbf{r}',t') \\ &= \rho_0(\mathbf{r})\delta A_m(\mathbf{r},t) \\ &- \sum_n i\int_{t_0}^{t} dt' d\mathbf{r}' \langle \Delta\hat{\mathbf{j}}_{p,m}(\mathbf{r},t)\Delta\hat{\mathbf{j}}_{p,n}(\mathbf{r}',t')\rangle \delta A_n(\mathbf{r}',t') \\ &- \sum_n i\int_{t}^{t_0} dt' d\mathbf{r}' \langle \Delta\hat{\mathbf{j}}_{p,n}(\mathbf{r}',t')\Delta\hat{\mathbf{j}}_{p,m}(\mathbf{r},t)\rangle \delta A_n(\mathbf{r}',t') \qquad (2.98)\end{aligned}$$

For physical current densities this can be written according to

$$\delta j_m(\mathbf{r},t) = \sum_n \int_{t_0}^{\infty} dt' d\mathbf{r}' \chi_{mn}(\mathbf{r},t,\mathbf{r}',t')\delta A_n(\mathbf{r}',t'), \qquad (2.99)$$

where

$$\begin{aligned}\chi_{mn}(\mathbf{r},t,\mathbf{r}',t') &= \delta_{mn}\rho_0(\mathbf{r})\delta(t-t')\delta(\mathbf{r}-\mathbf{r}') \\ &- i\Theta(t-t')\langle\Psi_0|[\hat{\mathbf{j}}_{p,m}(\mathbf{r},t)_{H_0},\hat{\mathbf{j}}_{p,n}(\mathbf{r}',t')_{H_0}]|\Psi_0\rangle. \qquad (2.100)\end{aligned}$$

Here we used that the expectation value of the commutator of the fluctuation operators for the paramagnetic current density is the same as the expectation value of the commutator of the paramagnetic current operators. The function $\chi_{mn}(\mathbf{r},t,\mathbf{r}',t')$ is the retarded current-current response function as it usually appears in response theory. In the next section we will discuss some exact constraints that are known for the set of exchange-correlation potentials $\{v_{xc}(\mathbf{r},t),\mathbf{A}_{xc}(\mathbf{r},t)\}$.

2.8 Exact Constraints

In accordance with Newton's third law the net force and net torque acting on a system should have no contribution from the system itself. Since the net force and the net torque due to the potential corresponding to the two-particle interaction are equal to zero, the net force and the net torque due to the set of exchange correlation potentials $\{v_{xc}(\mathbf{r},t),\mathbf{A}_{xc}(\mathbf{r},t)\}$ should be equal to zero as well [42]. This leads to constraints on the form of $\{v_{xc}(\mathbf{r},t),\mathbf{A}_{xc}(\mathbf{r},t)\}$. These constraints are made explicit by the zero-force and zero-torque theorems which read

$$\mathbf{F}_{xc}(t) = \int d\mathbf{r}[\rho(\mathbf{r},t)\mathbf{E}_{xc}(\mathbf{r},t) + \mathbf{j}(\mathbf{r},t)\times\mathbf{B}_{xc}(\mathbf{r},t)] = 0 \qquad (2.101)$$

$$\mathbf{T}_{xc}(t) = \int d\mathbf{r}[\rho(\mathbf{r},t)\mathbf{r}\times\mathbf{E}_{xc}(\mathbf{r},t) + \mathbf{r}\times(\mathbf{j}(\mathbf{r},t)\times\mathbf{B}_{xc}(\mathbf{r},t))] = 0, \qquad (2.102)$$

where $\mathbf{F}_{xc}(t)$ and $\mathbf{T}_{xc}(t)$ are the exchange-correlation parts of the force and the torque, respectively. The exchange-correlation parts of the electric and magnetic fields are analogous to Eqs. (2.27) and (2.28). They are given by

$$\mathbf{E}_{xc}(\mathbf{r},t) = \nabla v_{xc}(\mathbf{r},t) - \frac{\partial}{\partial t}\mathbf{A}_{xc}(\mathbf{r},t) \tag{2.103}$$

$$\mathbf{B}_{xc}(\mathbf{r},t) = \nabla \times \mathbf{A}_{xc}(\mathbf{r},t). \tag{2.104}$$

We note that if the zero-force theorem is satisfied this automatically guarantees that the harmonic-potential theorem is satisfied. The harmonic-potential theorem states that the density of a system of electrons confined in a static parabolic potential well follows rigidly the classical motion of the center of mass when subjected to a uniform time-dependent perturbation [43].

Another constraint on the form of the exchange-correlation potentials is the so-called generalized translational invariance which, up to a gauge transform, can be expressed as

$$v_{xc}[\mathbf{j}'](\mathbf{r},t) = v_{xc}[\mathbf{j}](\mathbf{r}-\mathbf{x}(t),t) \tag{2.105}$$

$$\mathbf{A}_{xc}[\mathbf{j}'](\mathbf{r},t) = \mathbf{A}_{xc}[\mathbf{j}](\mathbf{r}-\mathbf{x}(t),t), \tag{2.106}$$

where

$$\mathbf{j}'(\mathbf{r},t) = \mathbf{j}(\mathbf{r}-\mathbf{x}(t),t) + \frac{\partial \mathbf{x}(t)}{\partial t}\rho(\mathbf{r}-\mathbf{x}(t),t), \tag{2.107}$$

with $\mathbf{x}(t)$ an arbitrary time-dependent function. The above equations simply state that a rigid translation of the current density implies the same rigid translation of the exchange-correlation potentials. The rigid translation of the current density implies a rigid translation of the density according to $\rho'(\mathbf{r},t) = \rho(\mathbf{r}-\mathbf{x}(t),t)$ through the continuity equation. Note that if $\mathbf{x}(t) = \mathbf{u}t$ the above equations guarantee that the exchange-correlation potentials satisfy Galileian invariance. In TDDFT where we consider time-dependent external fields that can be described by solely scalar potentials the above equations reduce to [42]

$$v_{xc}[\rho'](\mathbf{r},t) = v_{xc}[\rho](\mathbf{r}-\mathbf{x}(t),t), \tag{2.108}$$

where $\rho'(\mathbf{r},t) = \rho(\mathbf{r}-\mathbf{x}(t),t)$.

It is easy to see that the ALDA exchange-correlation potential given in Eq. (2.26) satisfies the generalized translation invariance (2.108). We will now show that the ALDA exchange-correlation potential also satisfies the zero-force and zero-torque the-

orems. The exchange-correlation force and torque are then given by

$$\mathbf{F}_{xc}^{ALDA}(\mathbf{r},t) = \int d\mathbf{r}\rho(\mathbf{r},t)\nabla\left\{\left.\frac{d\epsilon_{xc}(\rho)}{d\rho}\right|_{\rho=\rho(\mathbf{r},t)}\right\} \tag{2.109}$$

$$\mathbf{T}_{xc}^{ALDA}(\mathbf{r},t) = \sum_{ijk}\mathbf{e}_i\epsilon_{ijk}\int d\mathbf{r}\rho(\mathbf{r},t)r_j\partial_k\left\{\left.\frac{d\epsilon_{xc}(\rho)}{d\rho}\right|_{\rho=\rho(\mathbf{r},t)}\right\}, \tag{2.110}$$

where ϵ_{ijk} is the Levi-Civita antisymmetric tensor. Performing an integration by parts we obtain

$$\mathbf{F}_{xc}^{ALDA}(\mathbf{r},t) = -\int d\mathbf{r}[\nabla\rho(\mathbf{r},t)]\left.\frac{d\epsilon_{xc}(\rho)}{d\rho}\right|_{\rho=\rho(\mathbf{r},t)} \tag{2.111}$$

$$= -\int d\mathbf{r}\nabla\left\{\epsilon_{xc}(\rho)|_{\rho=\rho(\mathbf{r},t)}\right\} = 0 \tag{2.112}$$

$$\mathbf{T}_{xc}^{ALDA}(\mathbf{r},t) = -\sum_{ijk}\mathbf{e}_i\epsilon_{ijk}\int d\mathbf{r}\left\{\partial_k[r_j\rho(\mathbf{r},t)]\right\}\left.\frac{d\epsilon_{xc}(\rho)}{d\rho}\right|_{\rho=\rho(\mathbf{r},t)} \tag{2.113}$$

$$= -\sum_{ijk}\mathbf{e}_i\epsilon_{ijk}\int d\mathbf{r}r_j\left\{\partial_k[\rho(\mathbf{r},t)]\right\}\left.\frac{d\epsilon_{xc}(\rho)}{d\rho}\right|_{\rho=\rho(\mathbf{r},t)} \tag{2.114}$$

$$= -\sum_{ijk}\mathbf{e}_i\epsilon_{ijk}\int d\mathbf{r}\partial_k\left\{r_j\epsilon_{xc}(\rho)|_{\rho=\rho(\mathbf{r},t)}\right\} = 0, \tag{2.115}$$

where Eqs. (2.112) and (2.115) vanish due to Gauss' theorem.

Chapter 3

Linear Response within TD(C)DFT

3.1 Introduction

One is often interested in studying the response of a many-particle system to a small external perturbation, e.g., an electromagnetic field. The first term in the power expansion of the response in the strength of this perturbation gives the response as a linear function of the perturbation. If the perturbation is indeed small this linear response is a good approximation to the whole response. The linear response can be expressed in terms of so-called linear response functions. As we will show in the following they are completely determined by the eigenvalues and eigenfunctions of the unperturbed system.

3.2 Linear Response Theory

The equilibrium expectation value of an operator $\hat{A}$ in the grand canonical ensemble is defined by

$$\langle \hat{A} \rangle = \mathrm{Tr}\left\{ \hat{\rho} \hat{A} \right\}, \tag{3.1}$$

where

$$\hat{\rho} = \frac{e^{-\beta(\hat{H}-\mu\hat{N})}}{\mathrm{Tr}\{e^{-\beta(\hat{H}-\mu\hat{N})}\}}. \tag{3.2}$$

Here $\beta = 1/k_B T$ with k_B the Boltzmann constant and T the temperature, μ is the chemical potential and $\hat{N}$ is the total number operator. The definition of the trace

operator can be found in Eq. (1.47). Consider now a system that is described by the time-independent Hamiltonian $\hat{H}_0$ that has eigenstates $|\Psi_i\rangle$ with eigenvalues E_i. At a certain time $t = t_0$ we switch on a time-dependent perturbation $\delta\hat{H}(t)$. The full time-dependent Hamiltonian $\hat{H}(t)$ then reads,

$$\hat{H}(t) = \hat{H}_0 + \delta\hat{H}(t) \tag{3.3}$$

where $\delta H(t) = 0$ for $t < t_0$. The expectation value of the operator $\hat{A}$ at a time t is now given by

$$\langle\hat{A}(t)\rangle = \mathrm{Tr}\left\{\hat{\rho}\hat{A}_H(t)\right\}, \tag{3.4}$$

where $\hat{A}_H(t)$ is the operator $\hat{A}$ in the Heisenberg picture given by

$$\hat{A}_H(t) = \hat{U}(t_0,t)\hat{A}\hat{U}(t,t_0), \tag{3.5}$$

The change of the expectation value of $\hat{A}$ due to the perturbation is given by

$$\delta\langle\hat{A}(t)\rangle = \langle\hat{A}(t)\rangle - \langle\hat{A}(t_0)\rangle, \tag{3.6}$$

The time-evolution operator can now be written as

$$\hat{U}'(t,t_0) = \hat{U}(t,t_0) + \delta\hat{U}(t,t_0), \tag{3.7}$$

The expectation value of $\hat{A}$ at time t can then be written as

$$\begin{aligned}
\langle\hat{A}(t)\rangle &= \mathrm{Tr}\left\{\hat{\rho}\hat{U}'(t_0,t)\hat{A}\hat{U}'(t,t_0)\right\} && (3.8)\\
&= \mathrm{Tr}\left\{\hat{\rho}\hat{U}(t_0,t)\hat{A}\hat{U}(t,t_0)\right\} + \mathrm{Tr}\left\{\hat{\rho}\hat{U}(t_0,t)\hat{A}\delta\hat{U}(t,t_0)\right\}\\
&+ \mathrm{Tr}\left\{\hat{\rho}\delta\hat{U}(t_0,t)\hat{A}\hat{U}(t,t_0)\right\} + O(\delta\hat{H}^2) && (3.9)\\
&= \langle\hat{A}(t_0)\rangle + \mathrm{Tr}\left\{\hat{\rho}\delta\hat{U}(t_0,t)\hat{A}\hat{U}(t,t_0)\right\}\\
&+ \mathrm{Tr}\left\{\hat{\rho}\hat{U}(t_0,t)\hat{A}\delta\hat{U}(t,t_0)\right\} + O(\delta\hat{H}^2). && (3.10)
\end{aligned}$$

Substitution of Eq. (2.73) in the above equation then leads to the following expression for the linear response of $\hat{A}$ due to the perturbation $\delta\hat{H}(t)$,

$$\delta A(t) = -i\int_{t_0}^{t} dt'\langle[\hat{A}_{H_0}(t), \delta\hat{H}_{H_0}(t')]\rangle. \tag{3.11}$$

We now consider the following perturbation

$$\delta\hat{H}(t) = \sum_n \hat{A}_n F_n(t), \tag{3.12}$$

where the arbitrary operator $\hat{A}_n$ couples linearly to the corresponding field $F_n(t)$. Then the change of the equilibrium expectation value of $\hat{A}_m$ is given by

$$\delta A_m(t) = -i\int_{t_0}^{t} dt' \left\langle \left[\hat{A}_m(t)_{H_0}, \sum_n \hat{A}_n(t')_{H_0} F_n(t') \right] \right\rangle \tag{3.13}$$

$$= \sum_n \int_{t_0}^{\infty} dt' \chi_{mn}(t,t') F_n(t') \tag{3.14}$$

where the retarded linear response function $\chi_{mn}(t,t')$ is defined by

$$\chi_{mn}(t,t') = -i\Theta(t-t') \left\langle \left[\hat{A}_m(t)_{H_0}, \hat{A}_n(t')_{H_0} \right] \right\rangle, \tag{3.15}$$

where $\Theta(\tau)$ is the Heaviside step function that vanishes for $\tau > 0$ and is equal to 1 for $\tau > 0$ and thus ensures that the linear response function is retarded, or causal. This means that the response of the observable $\hat{A}_m$ at a time t is due only to perturbations that are coupled to the operator $\hat{A}_n$ at times $t' < t$.

If we insert two complete set of eigenstates of $\hat{H}_0$ in Eq. (3.15) we obtain

$$\chi_{mn}(t,t') = -i\Theta(t-t') \sum_{i,j,k}^{\infty} \Big\{ \langle \Psi_i|\hat{\rho}|\Psi_k\rangle \langle \Psi_k|\hat{A}_m(t)_{H_0}|\Psi_j\rangle \langle \Psi_j|\hat{A}_n(t')_{H_0}|\Psi_i\rangle \tag{3.16}$$

$$- \langle \Psi_i|\hat{\rho}|\Psi_k\rangle \langle \Psi_k|\hat{A}_n(t')_{H_0}|\Psi_j\rangle \langle \Psi_j|\hat{A}_m(t)_{H_0}|\Psi_i\rangle \Big\}. \tag{3.17}$$

We note that $\langle \Psi_i|\hat{\rho}|\Psi_k\rangle = \delta_{ik} P_i$, where P_i is simply the Boltzmann distribution defined by

$$P_i = \frac{e^{-\beta(E_i - \mu N_i)}}{\sum_j^{\infty} e^{-\beta(E_j - \mu N_j)}}. \tag{3.18}$$

Using this result together with Eq. (2.62) we obtain

$$\chi_{mn}(t,t') = -i\Theta(t-t') \sum_{i,j}^{\infty} P_i \Big\{ e^{i\omega_{ij}(t-t')} \langle \Psi_i|\hat{A}_m|\Psi_j\rangle \langle \Psi_j|\hat{A}_n|\Psi_i\rangle$$

$$- e^{i\omega_{ji}(t-t')} \langle \Psi_i|\hat{A}_n|\Psi_j\rangle \langle \Psi_j|\hat{A}_m|\Psi_i\rangle \Big\}, \tag{3.19}$$

where $\omega_{ij} = E_i - E_j$ are the excitation energies of the system. From the above expression we see that the response function depends only on the time difference $(t-t')$. Interchanging i and j in the second term on the right-hand side of Eq. (3.19) then yields

$$\chi_{mn}(t-t') = -i\Theta(t-t') \sum_{i,j}^{\infty} (P_i - P_j) e^{i\omega_{ij}(t-t')} \langle \Psi_i|\hat{A}_m|\Psi_j\rangle \langle \Psi_j|\hat{A}_n|\Psi_i\rangle. \tag{3.20}$$

Since the perturbation $\delta\hat{H}(t)$ vanishes for $t < t_0$ we can extend the time integration in Eq. (3.14) to $-\infty$ and subsequently do a Fourier transformation with respect to $(t-t')$. In general, we define the Fourier transform $\tilde{f}(\omega)$ of an arbitrary function $f(\tau)$ by

$$\tilde{f}(\omega) = \int_{-\infty}^{\infty} d\tau f(\tau) e^{i\omega\tau}. \tag{3.21}$$

For notational convenience we will drop the tilde on $\tilde{f}(\omega)$ in the following and assume that it is clear from the frequency dependence that we are dealing with a different quantity. We obtain for the Fourier transform of $\delta A_m(t)$,

$$\delta A_m(\omega) = \sum_n \chi_{mn}(\omega) F_n(\omega), \tag{3.22}$$

where the Fourier transform of the response function is given by

$$\chi_{mn}(\omega) = \lim_{\eta\to 0^+} \sum_{i,j}^{\infty} (P_i - P_j) \frac{\langle\Psi_i|\hat{A}_m|\Psi_j\rangle\langle\Psi_j|\hat{A}_n|\Psi_i\rangle}{\omega - \omega_{ji} + i\eta}, \tag{3.23}$$

where we used the integral representation of the heaviside step function

$$\Theta(\tau) = -\frac{1}{2\pi i} \lim_{\eta\to 0^+} \int_{-\infty}^{\infty} d\omega \frac{e^{-i\omega\tau}}{\omega + i\eta}. \tag{3.24}$$

We note that the limit to zero of the positive infinitesimal η in Eq. (3.23) should be taken after multiplication with $F_n(\omega)$. Equation (3.23) is known as the Lehmann representation [44] of the response function, the poles of which correspond to the exact excitation energies of the system.

3.3 The Linear Response Kohn-Sham Equations

With the theory of linear response formulated in the previous section we can now derive the linear response to an arbitrary field of the density and current density. In the previous chapters we saw that, under some assumptions, we can obtain the true ground-state density and the true time-dependent density and current density from a Kohn-Sham system of noninteracting particles. The ground-state Kohn-Sham Hamiltonian $\hat{H}_s$ is given by a sum of single-particle Hamiltonians $\hat{h}_s(\mathbf{r}_i)$ according to

$$\hat{H}_s = \sum_{i=1}^{N} \hat{h}_s(\mathbf{r}_i) = \sum_{i=1}^{N} -\frac{1}{2}\nabla_i^2 + v_s(\mathbf{r}_i). \tag{3.25}$$

Similarly we have the following expression for the time-dependent Kohn-Sham Hamiltonian $\hat{H}_s(t)$,

$$\hat{H}_s(t) = \sum_{i=1}^{N} \hat{h}_s(\mathbf{r}_i, t) = \sum_{i=1}^{N} \frac{1}{2}[\mathbf{p}_i + \mathbf{A}_s(\mathbf{r}_i, t)]^2 + v_s(\mathbf{r}_i, t). \tag{3.26}$$

Subtracting the ground-state Kohn-Sham Hamiltonian from the time-dependent Kohn-Sham Hamiltonian we obtain the following expression for the perturbation,

$$\begin{aligned}\delta\hat{H}_s(t) &= \sum_{i=1}^{N} \frac{1}{2}\hat{\mathbf{p}}_i \cdot \delta\mathbf{A}_s(\mathbf{r}_i, t) + \frac{1}{2}\delta\mathbf{A}_s(\mathbf{r}_i, t) \cdot \hat{\mathbf{p}}_i + \frac{1}{2}\delta\mathbf{A}_s^2(\mathbf{r}_i, t) + \delta v_s(\mathbf{r}_i, t) \quad (3.27)\\ &= \int d\mathbf{r}\hat{\mathbf{j}}_p(\mathbf{r}) \cdot \delta\mathbf{A}_s(\mathbf{r}, t) + \frac{1}{2}\int d\mathbf{r}\hat{\rho}(\mathbf{r})\delta\mathbf{A}_s^2(\mathbf{r}, t) + \int d\mathbf{r}\hat{\rho}(\mathbf{r})\delta v_s(\mathbf{r}, t), \quad (3.28)\end{aligned}$$

where we defined $\delta v_s(\mathbf{r}, t) = v_s(\mathbf{r}, t) - v_s(\mathbf{r}, t_0)$ and $\delta\mathbf{A}_s(\mathbf{r}, t) = \mathbf{A}_s(\mathbf{r}, t) - \mathbf{A}_s(\mathbf{r}, t_0)$. Since the ground-state equilibrium can be described solely by a scalar potential we assume that $\mathbf{A}_s(\mathbf{r}, t_0)$ vanishes. The linear response of the current density is therefore given by

$$\delta\mathbf{j}(\mathbf{r}, t) = \delta\mathbf{j}_p(\mathbf{r}, t) + \rho_0(\mathbf{r})\delta\mathbf{A}_s(\mathbf{r}, t), \tag{3.29}$$

where $\rho_0(\mathbf{r})$ is the ground-state density. Using Eqs. (3.12), (3.22), and (3.23) in the previous section we can now immediately write down the expressions for the linear response of the density and current density in the frequency domain. They are given by

$$\delta\rho(\mathbf{r}, \omega) = \int d\mathbf{r}'\chi_{s,\rho\mathbf{j}_p}(\mathbf{r}, \mathbf{r}', \omega) \cdot \delta\mathbf{A}_s(\mathbf{r}', \omega) + \int d\mathbf{r}'\chi_{s,\rho\rho}(\mathbf{r}, \mathbf{r}', \omega)\delta v_s(\mathbf{r}', \omega) \tag{3.30}$$

$$\begin{aligned}\delta\mathbf{j}(\mathbf{r}, \omega) = &\int d\mathbf{r}'[\chi_{s,\mathbf{j}_p\mathbf{j}_p}(\mathbf{r}, \mathbf{r}', \omega) + \rho_0(\mathbf{r})\delta(\mathbf{r} - \mathbf{r}')] \cdot \delta\mathbf{A}_s(\mathbf{r}', \omega)\\ &+ \int d\mathbf{r}'\chi_{s,\mathbf{j}_p\rho}(\mathbf{r}, \mathbf{r}', \omega)\delta v_s(\mathbf{r}', \omega), \quad (3.31)\end{aligned}$$

where we used that the density and current density in the Kohn-Sham system are equal to the true density and current density order by order as can be seen from the derivation of Vignale's theorem in the previous chapter. It remains to determine the Kohn-Sham response functions $\chi_{s,ab}(\mathbf{r}, \mathbf{r}', \omega)$ at $T = 0$. Since for the Kohn-Sham system of noninteracting particles the $|\Psi_i\rangle$'s in Eq. (3.23) are Slater determinants, the matrix element $\langle\Psi_i|\hat{A}_m|\Psi_j\rangle$ is only nonvanishing for $|\Psi_i\rangle$'s and $|\Psi_j\rangle$'s that differ by no more than one orbital if $\hat{A}_m$ is a single-particle operator such as the density and current-density operator. Since $(P_i - P_j)$ vanishes if $|\Psi_i\rangle$ is equal to $|\Psi_j\rangle$ it means that only $|\Psi_i\rangle$'s and $|\Psi_j\rangle$'s that differ by exactly one orbital contribute to $\chi_{s,ab}(\omega)$. If this is the case this matrix element is equal to $\langle\phi_i|\hat{A}_m|\phi_j\rangle$, where ϕ_i and ϕ_j are

the Kohn-Sham orbitals of $|\Psi_i\rangle$ and $|\Psi_j\rangle$ that are different. It is easy to see that the excitation energy ω_{ji} in Eq. (3.23) that corresponds to this matrix element is then equal to the difference of the orbital energies of ϕ_i and ϕ_j, i.e., $\omega_{ji} = (\epsilon_j - \epsilon_i)$. Furthermore, in the Kohn-Sham system the Boltzmann distribution P_i reduces to the Fermi-Dirac distribution which we will denote by f_i and is given by

$$f_i = \frac{1}{e^{\beta(\epsilon_i - \mu)} + 1}. \tag{3.32}$$

In the limit that the temperature goes to zero, and therefore $\beta \to \infty$, we see from the Fermi-Dirac distribution that $f_i = 1$ for $\epsilon_i < \mu$ and $f_i = 0$ for $\epsilon_i > \mu$, that is the orbitals with energies smaller than μ are occupied and and the orbitals with energies larger than μ are unoccupied. Furthermore, in the limit $T \to 0$ only the ground state $|\Psi_0\rangle$ is occupied in the initial equilibrium. Therefore, in this limit $|\Psi_i\rangle$ is simply equal to $|\Psi_0\rangle$ and the corresponding orbitals ϕ_i and orbital energies ϵ_i are properties of the ground state only. The Kohn-Sham response functions $\chi_{s,ab}(\mathbf{r}, \mathbf{r}', \omega)$ at $T = 0$ that enter Eqs. (3.30) and (3.31) are thus given by

$$\chi_{s,ab}(\mathbf{r}, \mathbf{r}', \omega) = \lim_{\eta \to 0^+} \sum_{i,j}^{\infty} (f_i - f_j) \frac{\langle \phi_i | \hat{a}(\mathbf{r}) | \phi_j \rangle \langle \phi_j | \hat{b}(\mathbf{r}') | \phi_i \rangle}{\omega - (\epsilon_j - \epsilon_i) + i\eta}, \tag{3.33}$$

where the operators $\hat{a}(\mathbf{r})$ and $\hat{b}(\mathbf{r})$ have to be substituted with the density operator $\hat{\rho}(\mathbf{r})$ and the paramagnetic current-density operator $\hat{\mathbf{j}}_p(\mathbf{r})$. Here the limit to zero of the positive infinitesimal η in Eq. (3.33) should be taken after integrating the response function with the potential $\delta v_s(\mathbf{r}, \omega)$ or $\delta \mathbf{A}_s(\mathbf{r}, \omega)$.

It is easy to see by doing a Fourier transformation of Eq. (2.38) that the continuity equation in the linear response regime becomes

$$i\omega \delta\rho(\mathbf{r}, \omega) = \nabla \cdot \delta\mathbf{j}(\mathbf{r}, \omega). \tag{3.34}$$

We note that for practical applications it is often useful to rewrite Eq. (3.31) for the induced current density $\delta\mathbf{j}(\mathbf{r}, \omega)$ using the conductivity sum rule

$$\left[\chi_{s,\mathbf{j}_p\mathbf{j}_p}(\mathbf{r}, \mathbf{r}', 0)\right]_{ij} + \rho_0(\mathbf{r})\delta_{ij}\delta(\mathbf{r} - \mathbf{r}') = 0. \tag{3.35}$$

The induced current density is then given by

$$\begin{aligned} \delta\mathbf{j}(\mathbf{r}, \omega) = & \int d\mathbf{r}' \left[\chi_{s,\mathbf{j}_p\mathbf{j}_p}(\mathbf{r}, \mathbf{r}', \omega) - \chi_{s,\mathbf{j}_p\mathbf{j}_p}(\mathbf{r}, \mathbf{r}', 0)\right] \cdot \delta\mathbf{A}_s(\mathbf{r}', \omega) \\ & + \int d\mathbf{r}' \chi_{s,\mathbf{j}_p\rho}(\mathbf{r}, \mathbf{r}', \omega)\delta v_s(\mathbf{r}', \omega). \end{aligned} \tag{3.36}$$

However, one then neglects the small Landau diamagnetic contribution for the transverse component of the induced current density [10].

3.4 The Exchange-Correlation Kernel in TDDFT

Within TDDFT where we only consider time-dependent external fields that can be reproduced by a scalar potential the only term that remains in Eqs. (3.30) and (3.31) is that involving the Kohn-Sham density-density response function $\chi_{s,\rho\rho}(\mathbf{r},\mathbf{r}',\omega)$. In this section we will show that within TDDFT the Kohn-Sham density-density response function can be related to the true density-density response function through the so-called exchange-correlation kernel. The exchange-correlation kernel is uniquely defined (up to a constant) by

$$f_{xc}(\mathbf{r},t,\mathbf{r}',t') = \frac{\delta v_{xc}(\mathbf{r},t)}{\delta\rho(\mathbf{r}',t')}. \tag{3.37}$$

This kernel describes the change in the exchange-correlation potential $v_{xc}(\mathbf{r},t)$ due to a change in the density $\rho(\mathbf{r},t)$. To obtain a relation between the Kohn-Sham density-density response function $\chi_{s,\rho\rho}(\mathbf{r},\mathbf{r}',\omega)$ and the true density-density response function $\chi_{\rho\rho}(\mathbf{r},\mathbf{r}',\omega)$ we start from the functional derivative of the density with respect to the external potential. We obtain

$$\frac{\delta\rho(\mathbf{r}_1,t_1)}{\delta v(\mathbf{r}_2,t_2)} = \int dt_3 d\mathbf{r}_3 \frac{\delta\rho(\mathbf{r}_1,t_1)}{\delta v_s(\mathbf{r}_3,t_3)} \frac{\delta v_s(\mathbf{r}_3,t_3)}{\delta v(\mathbf{r}_2,t_2)}, \tag{3.38}$$

where we used the functional generalization of the chain rule. The first term on the right-hand side is simply the density-density response function of the Kohn-Sham system which gives the change in the density due to a change in the Kohn-Sham potential. The second term on the right-hand side gives the change of the Kohn-Sham potential due to a change in the external potential. Using Eq. (2.21) we find

$$\begin{aligned}\frac{\delta v_s(\mathbf{r}_3,t_3)}{\delta v(\mathbf{r}_2,t_2)} &= \delta(\mathbf{r}_3-\mathbf{r}_2)\delta(t_3-t_2) \\ &+ \int dt_4 d\mathbf{r}_4 \left[w(|\mathbf{r}_3-\mathbf{r}_4|)\delta(t_3-t_4) + f_{xc}(\mathbf{r}_3,t_3,\mathbf{r}_4,t_4)\right] \frac{\delta\rho(\mathbf{r}_4,t_4)}{\delta v(\mathbf{r}_2,t_2)}\end{aligned} \tag{3.39}$$

Combining the above results we obtain the following relation between the Kohn-Sham density-density response function and the true density-density response function,

$$\begin{aligned}\chi_{\rho\rho}(\mathbf{r}_1,t_1,\mathbf{r}_2,t_2) = \chi_{s,\rho\rho}(\mathbf{r}_1,t_1,\mathbf{r}_2,t_2) + \int dt_3 d\mathbf{r}_3 dt_4 d\mathbf{r}_4 \chi_{s,\rho\rho}(\mathbf{r}_1,t_1,\mathbf{r}_3,t_3) \\ \times[w(|\mathbf{r}_3-\mathbf{r}_4|)\delta(t_3-t_4) + f_{xc}(\mathbf{r}_3,t_3,\mathbf{r}_4,t_4)]\chi_{\rho\rho}(\mathbf{r}_4,t_4,\mathbf{r}_2,t_2).\end{aligned} \tag{3.40}$$

Therefore, if we have an approximation for f_{xc} we can find the true density-density response function $\chi_{\rho\rho}$ from Eq. (3.40). Since both $\chi_{\rho\rho}$ and $\chi_{s,\rho\rho}$ only depend on the

difference of their time coordinates we can do a Fourier transformation according to Eq. (3.21) and obtain

$$\begin{aligned}\chi_{\rho\rho}(\mathbf{r}_1,\mathbf{r}_2,\omega) &= \chi_{s,\rho\rho}(\mathbf{r}_1,\mathbf{r}_2,\omega)+\int d\mathbf{r}_3 d\mathbf{r}_4 \chi_{s,\rho\rho}(\mathbf{r}_1,\mathbf{r}_3,\omega)\{w(|\mathbf{r}_3-\mathbf{r}_4|)\\ &+ f_{xc}(\mathbf{r}_3,\mathbf{r}_4,\omega)\}\chi_{\rho\rho}(\mathbf{r}_4,\mathbf{r}_2,\omega). \qquad (3.41)\end{aligned}$$

Therefore, if we have an approximation for f_{xc} we can find the true density-density response function $\chi_{\rho\rho}$ from Eq. (3.40) or Eq. (3.41) if we are in the linear response regime. Since f_{xc} only depends on the difference of its time coordinates we see from Eq. (3.37) that we can write

$$\delta v_{xc}(\mathbf{r},\omega)=\int d\mathbf{r}' f_{xc}(\mathbf{r},\mathbf{r}',\omega)\delta\rho(\mathbf{r}',\omega). \qquad (3.42)$$

It can readily be shown that $f_{xc}(\mathbf{r},\mathbf{r},\omega)$ can be written as

$$f_{xc}(\mathbf{r},\mathbf{r}',\omega)=\chi^{-1}_{s,\rho\rho}(\mathbf{r},\mathbf{r}',\omega)-\chi^{-1}_{\rho\rho}(\mathbf{r},\mathbf{r}',\omega)-w(|(\mathbf{r}-\mathbf{r}')|), \qquad (3.43)$$

which shows that $f_{xc}(\mathbf{r},\mathbf{r},\omega)$ is a causal function since $\chi^{-1}_{s,\rho\rho}(\mathbf{r},\mathbf{r}',\omega)$ and $\chi^{-1}_{\rho\rho}(\mathbf{r},\mathbf{r}',\omega)$ are causal functions.

3.5 Exact Constraints within the Linear Response Formulation of TDDFT

It is easy to see by doing Fourier transformations that within TDDFT the constraints mentioned in section 2.8 have the following equivalents in the linear response regime. We obtain for the zero-force and zero-torque theorems

$$\int d\mathbf{r}\,[\delta\rho(\mathbf{r},\omega)\nabla v_{xc,0}(\mathbf{r})+\rho_0(\mathbf{r})\nabla\delta v_{xc}(\mathbf{r},\omega)]=0 \qquad (3.44)$$

$$\int d\mathbf{r}\,[\delta\rho(\mathbf{r},\omega)\mathbf{r}\times\nabla v_{xc,0}(\mathbf{r})+\rho_0(\mathbf{r})\mathbf{r}\times\nabla\delta v_{xc}(\mathbf{r},\omega)]=0. \qquad (3.45)$$

The generalized translational invariance now reads

$$\begin{aligned} v_{xc,0}[\rho_0'](\mathbf{r}) &= v_{xc,0}[\rho_0](\mathbf{r}-\mathbf{x}(\omega)) \qquad (3.46)\\ \delta v_{xc}[\delta\rho'](\mathbf{r},\omega) &= \delta v_{xc}[\delta\rho](\mathbf{r}-\mathbf{x}(\omega),\omega), \qquad (3.47)\end{aligned}$$

where

$$\begin{aligned} \rho_0'(\mathbf{r}) &= \rho_0(\mathbf{r}-\mathbf{x}(\omega)) \qquad (3.48)\\ \delta\rho'(\mathbf{r},\omega) &= \delta\rho(\mathbf{r}-\mathbf{x}(\omega),\omega), \qquad (3.49)\end{aligned}$$

with $\mathbf{x}(\omega)$ an arbitrary frequency-dependent function.

If the unperturbed system is invariant under time reversal, that is in the absence of magnetic fields, the exchange-correlation kernel $f_{xc}(\mathbf{r},\mathbf{r}',\omega)$ satisfies the following symmetry relation

$$f_{xc}(\mathbf{r},\mathbf{r}',\omega) = f_{xc}(\mathbf{r}',\mathbf{r},\omega). \tag{3.50}$$

To prove this relation we start from the linear density-density response function which is given by

$$\chi_{\rho\rho}(\mathbf{r},\mathbf{r}',\omega) = \lim_{\eta\to 0^+}\sum_{i,j}^{\infty}(P_i - P_j)\frac{\langle\Psi_i|\hat{\rho}(\mathbf{r})|\Psi_j\rangle\langle\Psi_j|\hat{\rho}(\mathbf{r}')|\Psi_i\rangle}{\omega-\omega_{ji}+i\eta}. \tag{3.51}$$

If the unperturbed system is invariant under time reversal we can choose the wave functions corresponding to $|\Psi_i\rangle$ to be real which means that $\langle\Psi_i|\hat{\rho}(\mathbf{r})|\Psi_j\rangle = \langle\Psi_j|\hat{\rho}(\mathbf{r})|\Psi_i\rangle$. As a consequence we have the relation

$$\chi_{\rho\rho}(\mathbf{r},\mathbf{r}',\omega) = \chi_{\rho\rho}(\mathbf{r}',\mathbf{r},\omega). \tag{3.52}$$

The symmetry relation in Eq. (3.50) then follows immediately from Eq. (3.43).

We can rewrite the zero-force theorem in terms of the exchange-correlation kernel $f_{xc}(\mathbf{r},\mathbf{r}',\omega)$. Substitution of Eq. (3.42) into Eq. (3.44) followed by an integration by parts leads to the following expression for the zero-force theorem

$$\int d\mathbf{r}\nabla\rho_0(\mathbf{r})f_{xc}(\mathbf{r},\mathbf{r}',\omega) = \nabla' v_{xc,0}(\mathbf{r}'). \tag{3.53}$$

Using Eq. (3.50) we obtain the equivalent expression

$$\int d\mathbf{r}'\nabla'\rho_0(\mathbf{r}')f_{xc}(\mathbf{r},\mathbf{r}',\omega) = \nabla v_{xc,0}(\mathbf{r}). \tag{3.54}$$

In a similar way we can rewrite the zero-torque theorem given in Eq. (3.45) in terms of $f_{xc}(\mathbf{r},\mathbf{r}',\omega)$ as

$$\int d\mathbf{r}'\mathbf{r}'\times\nabla'\rho_0(\mathbf{r}')f_{xc}(\mathbf{r},\mathbf{r}',\omega) = \mathbf{r}\times\nabla v_{xc,0}(\mathbf{r}). \tag{3.55}$$

3.6 Examples of Approximate Exchange-Correlation Kernels

The exchange-correlation kernel of the ALDA can be obtained from Eq. (2.26). It is given by

$$f_{xc}^{ALDA}(\mathbf{r},t,\mathbf{r}',t) = \delta(t-t')\delta(\mathbf{r}-\mathbf{r}')\left.\frac{d^2\epsilon_{xc}}{d\rho^2}\right|_{\rho=\rho_0(\mathbf{r})}. \tag{3.56}$$

By doing a Fourier transformation we obtain the linear ALDA exchange-correlation kernel

$$f_{xc}^{ALDA}(\mathbf{r},\mathbf{r}',\omega) = \delta(\mathbf{r}-\mathbf{r}')\left.\frac{d^2\epsilon_{xc}}{d\rho^2}\right|_{\rho=\rho_0(\mathbf{r})}, \tag{3.57}$$

which is frequency independent.

In order to include the frequency dependence of $f_{xc}(\mathbf{r},\mathbf{r}',\omega)$ Gross and Kohn proposed to approximate the exchange-correlation kernel by the exchange-correlation kernel of the homogeneous electron gas $f_{xc}^h(|\mathbf{r}-\mathbf{r}'|,\omega)$ evaluated at the local density, an approximation in the spirit of the LDA [45]. Furthermore, they made the approximation that the induced density $\delta\rho(\mathbf{r},\omega)$ is sufficiently slowly varying that in the expression for the linear exchange-correlation potential $\delta v_{xc}(\mathbf{r},\omega)$ given in Eq. (3.42) it can be taken from underneath the integral according to

$$\delta v_{xc}(\mathbf{r},\omega) \simeq \delta\rho(\mathbf{r},\omega)\int d\mathbf{r}' f_{xc}(\mathbf{r},\mathbf{r}',\omega). \tag{3.58}$$

With slowly varying is meant that variations in in the ground-state density $\rho_0(\mathbf{r})$ are negligible over a length given by the range of $f_{xc}^h(|\mathbf{r}-\mathbf{r}'|,\omega)$, that is, outside this range $f_{xc}^h(|\mathbf{r}-\mathbf{r}'|,\omega)$ is close to zero. These approximations amount to the following expression for the linear exchange-correlation potential,

$$\begin{aligned}\delta v_{xc}^{GK}(\mathbf{r},\omega) &= \delta\rho(\mathbf{r},\omega)\int d\mathbf{r}' f_{xc}^h(\rho_0(\mathbf{r}),|\mathbf{r}-\mathbf{r}'|,\omega) &(3.59)\\ &= f_{xc}^h(\rho_0(\mathbf{r}),\omega)\delta\rho(\mathbf{r},\omega). &(3.60)\end{aligned}$$

The approximations mentioned above are equivalent to the following approximation for $f_{xc}(\mathbf{r},\mathbf{r}',\omega)$,

$$f_{xc}^{GK}(\mathbf{r},\mathbf{r}',\omega) = f_{xc}^h(\rho_0(\mathbf{r}),\omega)\delta(\mathbf{r}-\mathbf{r}'). \tag{3.61}$$

However, it turns out that the Gross Kohn approximation violates the zero-force theorem. This is easily seen by substitution of the Gross-Kohn approximation for $f_{xc}(\mathbf{r},\mathbf{r}',\omega)$ into Eq. (3.54). This leads to a left-hand side that is frequency dependent, which cannot be equal to the right-hand side that is frequency independent. Similar arguments lead to the conclusion that the Gross-Kohn approximation also violates the zero-torque theorem. Furthermore, it can be shown that the Gross-Kohn approximation also violates the constraint of generalized translational invariance [42].

3.7 The Ultra-Nonlocality Problem

In this section we show that Eq. (3.54) implies that the exchange-correlation kernel $f_{xc}(\mathbf{r},\mathbf{r}',\omega)$ is of infinite range in $|\mathbf{r}-\mathbf{r}'|$ and that therefore a frequency-dependent local

density approximation for $f_{xc}(\mathbf{r},\mathbf{r}',\omega)$ does not exist [12, 13]. Let us start the proof with the assumption that if the unperturbed density $\rho_0(\mathbf{r})$ is sufficiently slowly varying the exchange-correlation kernel $f_{xc}(\mathbf{r},\mathbf{r}',\omega)$ has a gradient expansion according to

$$\begin{aligned} f_{xc}(\mathbf{r},\mathbf{r}',\omega) &= f^h_{xc}(\rho_0(\mathbf{r}),\mathbf{r}-\mathbf{r}',\omega) \\ &+ g^h_{xc}(\rho_0(\mathbf{r}),\mathbf{r}-\mathbf{r}',\omega)\cdot\nabla\rho_0(\mathbf{r}) + O((\nabla\rho_0)^2,\nabla\otimes\nabla\rho_0), \end{aligned} \quad (3.62)$$

where f^h_{xc}, g^h_{xc}, etc., are properties of the homogeneous electron gas at the density $\rho_0(\mathbf{r})$. With slowly varying we mean that variations in $\rho_0(\mathbf{r})$ are negligible over a length given by the range of the kernels f^h_{xc}, g^h_{xc}, etc. The gradient expansion of the static exchange-correlation potential $v_{xc,0}(\mathbf{r})$ is given by

$$v_{xc,0}(\mathbf{r}) = \left.\frac{d\epsilon^h_{xc}(\rho)}{d\rho}\right|_{\rho=\rho_0(\mathbf{r})} + O((\nabla\rho)^2). \quad (3.63)$$

Upon substitution of the above expansions into Eq. (3.54) we obtain to first order in $\nabla\rho_0(\mathbf{r})$,

$$f^h_{xc}(\rho_0(\mathbf{r}),\omega)\nabla\rho_0(\mathbf{r}) = \left.\frac{d^2\epsilon^h_{xc}(\rho)}{d\rho^2}\right|_{\rho=\rho_0(\mathbf{r})}\nabla\rho_0(\mathbf{r}), \quad (3.64)$$

for all frequencies ω. Since we know that $f^h_{xc}(\rho_0(\mathbf{r}),\omega)$ depends on the frequency it cannot be equal to the frequency independent quantity $d^2\epsilon^h_{xc}(\rho)/d\rho^2$ and therefore we have arrived at a contradiction. This means that the gradient expansion given in Eq. (3.62) does not exist because $f_{xc}(\mathbf{r},\mathbf{r}',\omega)$ is of infinite range in $|\mathbf{r}-\mathbf{r}'|$.

Vignale and Kohn showed that the frequency-dependent exchange-correlation vector potential $\mathbf{A}_{xc}(\mathbf{r},\omega)$ does have a gradient expansion in terms of the current density [12, 13]. Hence, the ultra-nonlocality problem of time-dependent density-functional theory does not exist in time-dependent current-density-functional theory.

3.8 The Exchange-Correlation Kernel in TDCDFT

In the case of TDCDFT where we allow general time-dependent external fields we have to consider a vector potential $\mathbf{A}(\mathbf{r},t)$ and its conjugate variable the current density $\mathbf{j}(\mathbf{r},t)$. We now have to reconsider the meaning of Eq. (3.37). In this case we know that for general time-dependent external fields the set of potentials $\{v(\mathbf{r},t),\mathbf{A}(\mathbf{r},t)\}$ is uniquely determined (up to a gauge transformation) by the current denstity $\mathbf{j}(\mathbf{r},t)$ and not by the density $\rho(\mathbf{r},t)$ alone. It is easy to see that the same must be true for the set of exchange-correlation potentials $\{v_{xc}(\mathbf{r},t),\mathbf{A}_{xc}(\mathbf{r},t)\}$. However, for a given expression for the set of potentials $\{v_{xc}(\mathbf{r},t),\mathbf{A}_{xc}(\mathbf{r},t)\}$ it might be that there is a part of $v_{xc}(\mathbf{r},t)$ that only involves the divergence of the current density. This part can then

be written in terms of the time-derivative of the density according to the continuity equation. The variation of such a $v_{xc}(\mathbf{r},t)$ can then be written in the following form

$$\begin{aligned}\delta v_{xc}(\mathbf{r},t)[\rho,\mathbf{j}] &= \int d\mathbf{r}'dt' f_{xc}(\mathbf{r},t,\mathbf{r}',t')\delta\rho(\mathbf{r}',t') \\ &+ \int d\mathbf{r}'dt'\tilde{\mathbf{f}}_{xc}(\mathbf{r},t,\mathbf{r}',t')\cdot\delta\mathbf{j}(\mathbf{r}',t'),\end{aligned} \tag{3.65}$$

where we introduced a vector exchange-correlation kernel $\tilde{\mathbf{f}}_{xc}$. However, such an expression might be misleading as it may seem from Eq. (3.65) that the density and current density are independent variables which they are not since a variation in $\rho(\mathbf{r},t)$ implies a variation in $\mathbf{j}(\mathbf{r},t)$. Therefore the exchange-correlation kernel in Eq. (3.37) has lost its meaning within TDCDFT since it would suggest that we can obtain f_{xc} as the functional derivative of $v_{xc}(\mathbf{r},t)$ with respect to the density while keeping the current density fixed, i.e.,

$$f_{xc}(\mathbf{r},t,\mathbf{r}',t') = \left[\frac{\delta v_{xc}(\mathbf{r},t)}{\delta\rho(\mathbf{r}',t')}\right]_{\mathbf{j}}. \tag{3.66}$$

It is clear that a density with the property that upon variation it leaves the current density unchanged cannot be reproduced by any physical potential, i.e., it is not v-representable. However, since the density $\rho(\mathbf{r},t)$ is itself a functional of the current density $\mathbf{j}(\mathbf{r},t)$ through the continuity equation we could have written Eq. (3.65) as a functional of the current density only. Taking the functional derivative with respect to the current density then does not lead to any unphysical constraints on the density. The outcome of this procedure, however, still depends on the particular choice of gauge. Since we like to keep the discussion as general as possible we choose the gauge such that the scalar potentials in the true interacting system and the noninteracting Kohn-Sham system are zero at all times, i.e., we do a gauge transformation according to Eq. (2.29) with Λ a solution of Eq. (2.31). From Eqs. (2.57) and (2.58) we observe that the Kohn-Sham vector potential then has the form

$$\mathbf{A}_s(\mathbf{r},t) = \mathbf{A}(\mathbf{r},t) + \mathbf{A}_W(\mathbf{r},t) + \mathbf{A}_{xc}(\mathbf{r},t), \tag{3.67}$$

where $\mathbf{A}_W(\mathbf{r},t)$ is given by

$$\frac{\partial\mathbf{A}_W(\mathbf{r},t)}{\partial t} = -\nabla\int d\mathbf{r}'\rho(\mathbf{r}',t)w(|\mathbf{r}-\mathbf{r}'|). \tag{3.68}$$

We can now define a tensor exchange-correlation functional $\mathbf{f}_{xc}$ as the functional derivative of the exchange-correlation vector potential with respect to the current density,

$$\mathbf{f}_{xc}(\mathbf{r},t,\mathbf{r}',t') = \frac{\delta\mathbf{A}_{xc}(\mathbf{r},t)}{\delta\mathbf{j}(\mathbf{r}',t')}. \tag{3.69}$$

In a similar way as for the density-density response function we can now derive an expression that relates the true current-current response function $\chi_{\mathbf{jj}}$ to the Kohn-Sham current-current response function $\chi_{s,\mathbf{jj}}$ using Eq. (3.69). We obtain

$$\begin{aligned}\chi_{\mathbf{jj}}(\mathbf{r}_1,t_1,\mathbf{r}_2,t_2) &= \chi_{s,\mathbf{jj}}(\mathbf{r}_1,t_1,\mathbf{r}_2,t_2)\\ &+ \int dt_3 d\mathbf{r}_3 dt_4 d\mathbf{r}_4 \chi_{s,\mathbf{jj}}(\mathbf{r}_1,t_1,\mathbf{r}_3,t_3)\cdot\{\mathbf{f}_W(\mathbf{r}_3,t_3,\mathbf{r}_4,t_4)\\ &+ \mathbf{f}_{xc}(\mathbf{r}_3,t_3,\mathbf{r}_4,t_4)\}\cdot\chi_{\mathbf{jj}}(\mathbf{r}_4,t_4,\mathbf{r}_2,t_2), \end{aligned} \tag{3.70}$$

where we defined

$$\mathbf{f}_W(\mathbf{r}_3,t_3,\mathbf{r}_4,t_4) = \frac{\delta \mathbf{A}_W(\mathbf{r}_3,t_3)}{\delta \mathbf{j}(\mathbf{r}_4,t_4)}. \tag{3.71}$$

With the help of the continuity equation we can rewrite Eq. (3.68) as

$$\frac{\partial^2 \mathbf{A}_W(\mathbf{r},t)}{\partial t^2} = \nabla \int d\mathbf{r}' \nabla' \cdot \mathbf{j}(\mathbf{r}',t) w(|\mathbf{r}-\mathbf{r}'|). \tag{3.72}$$

Since both $\chi_{\mathbf{jj}}$ and $\chi_{s,\mathbf{jj}}$ only depend on the difference of their time coordinates we can use the above result to obtain the Fourier transform of Eq. (3.70). It is given by

$$\begin{aligned}\chi_{\mathbf{jj}}(\mathbf{r}_1,\mathbf{r}_2,\omega) = \chi_{s,\mathbf{jj}}(\mathbf{r}_1,\mathbf{r}_2,\omega) + \int d\mathbf{r}_3 d\mathbf{r}_4 \chi_{s,\mathbf{jj}}(\mathbf{r}_1,\mathbf{r}_3,\omega)\cdot\\ \times\left\{\mathbf{f}_{xc}(\mathbf{r}_3,\mathbf{r}_4,\omega) - \frac{1}{\omega^2}\nabla_{\mathbf{r_3}} w(|\mathbf{r}_3-\mathbf{r}_4|)\nabla_{\mathbf{r}_4}\right\}\cdot\chi_{\mathbf{jj}}(\mathbf{r}_4,\mathbf{r}_2,\omega). \end{aligned} \tag{3.73}$$

Since $\mathbf{f}_{xc}$ only depends on the difference of its time coordinates we see from Eq. (3.69) that we can write

$$\delta\mathbf{A}_{xc}(\mathbf{r},\omega) = \int d\mathbf{r}' \mathbf{f}_{xc}(\mathbf{r},\mathbf{r}',\omega)\cdot\delta\mathbf{j}(\mathbf{r}',\omega). \tag{3.74}$$

The tensor exchange-correlation kernel $\mathbf{f}_{xc}(\mathbf{r},\mathbf{r}',\omega)$ is defined as

$$\mathbf{f}_{xc}(\mathbf{r},\mathbf{r}',\omega) = \chi_{s,\mathbf{jj}}^{-1}(\mathbf{r},\mathbf{r}',\omega) - \chi_{\mathbf{jj}}^{-1}(\mathbf{r},\mathbf{r}',\omega) + \frac{1}{\omega^2}\nabla w(|(\mathbf{r}-\mathbf{r}')|)\nabla'. \tag{3.75}$$

Therefore, if we have an approximation for $\mathbf{f}_{xc}$ we can find the true current-current response function $\chi_{\mathbf{jj}}$ from Eq. (3.70) or Eq. (3.73) if we are in the linear response regime. We see that for the given gauge we only obtain a nonzero current-current response function. However, since the density and current density are gauge invariant this implies that a gauge transformation will lead to other response functions of the density and current density being nonzero. This can be easily checked for instance in the case of the linear response equations for $\delta\rho(\mathbf{r},\omega)$ and $\delta\mathbf{j}(\mathbf{r},\omega)$ of the Kohn-Sham system given in Eqs. (3.30) and Eq. (3.31).

3.9 Exact Constraints within the Linear Response Formulation of TDCDFT

Within TDCDFT the constraints mentioned in section 2.8 have the following equivalents within the linear response regime. For the zero-force and zero-torque theorems we obtain

$$\int d\mathbf{r}\,[\delta\rho(\mathbf{r},\omega)\nabla v_{xc,0}(\mathbf{r}) + \rho_0(\mathbf{r})\nabla\delta v_{xc}(\mathbf{r},\omega) + i\omega\rho_0(\mathbf{r})\delta\mathbf{A}_{xc}(\mathbf{r},\omega)] = 0 \tag{3.76}$$

$$\int d\mathbf{r}\,[\delta\rho(\mathbf{r},\omega)\mathbf{r}\times\nabla v_{xc,0}(\mathbf{r}) + \rho_0(\mathbf{r})\mathbf{r}\times\{\nabla\delta v_{xc}(\mathbf{r},\omega) + i\omega\delta\mathbf{A}_{xc}(\mathbf{r},\omega)\}] = 0 \tag{3.77}$$

The generalized translational invariance now reads

$$\begin{aligned} v_{xc,0}[\rho_0'](\mathbf{r}) &= v_{xc,0}[\rho_0](\mathbf{r}-\mathbf{x}(\omega)) && (3.78)\\ \delta v_{xc}[\delta\mathbf{j}'](\mathbf{r},\omega) &= \delta v_{xc}[\delta\mathbf{j}](\mathbf{r}-\mathbf{x}(\omega),\omega) && (3.79)\\ \delta\mathbf{A}_{xc}[\delta\mathbf{j}'](\mathbf{r},\omega) &= \delta\mathbf{A}_{xc}[\delta\mathbf{j}](\mathbf{r}-\mathbf{x}(\omega),\omega), && (3.80) \end{aligned}$$

where

$$\begin{aligned} \rho_0'(\mathbf{r}) &= \rho_0(\mathbf{r}-\mathbf{x}(\omega)) && (3.81)\\ \delta\mathbf{j}'(\mathbf{r},\omega) &= \delta\mathbf{j}(\mathbf{r}-\mathbf{x}(\omega),\omega) - i\omega\mathbf{x}(\omega)\rho_0(\mathbf{r}-\mathbf{x}(\omega)), && (3.82) \end{aligned}$$

with $\mathbf{x}(\omega)$ an arbitrary frequency-dependent function. The rigid translation of the current density implies a rigid translation of the density according to $\delta\rho'(\mathbf{r},\omega) = \delta\rho(\mathbf{r}-\mathbf{x}(\omega),\omega)$ through the continuity equation.

If the unperturbed system is invariant under time reversal, that is in the absence of magnetic fields, the tensor exchange-correlation kernel $\mathbf{f}_{xc}(\mathbf{r},\mathbf{r}',\omega)$ satisfies the Onsager symmetry relation given by

$$f_{xc,ij}(\mathbf{r},\mathbf{r}',\omega) = f_{xc,ji}(\mathbf{r}',\mathbf{r},\omega). \tag{3.83}$$

The proof is similar to that for the symmetry relation given in Eq. (3.50) for the scalar exchange-correlation kernel. We start from the linear current-current response function which is given by

$$\begin{aligned} \chi_{\mathbf{jj},ij}(\mathbf{r},\mathbf{r}',\omega) = \lim_{\eta\to 0^+}\sum_{k,l}^{\infty}(P_k - P_l)\frac{\langle\Psi_k|\hat{j}_{p,i}(\mathbf{r})|\Psi_l\rangle\langle\Psi_l|\hat{j}_{p,j}(\mathbf{r}')|\Psi_k\rangle}{\omega-\omega_{lk}+i\eta}\\ + \rho_0(\mathbf{r})\delta(\mathbf{r}-\mathbf{r}')\delta_{kl}. \end{aligned} \tag{3.84}$$

If the unperturbed system is invariant under time reversal we can choose the wave functions corresponding to $|\Psi_i\rangle$ to be real which means that $\langle\Psi_i|\hat{j}_{p,i}(\mathbf{r})|\Psi_j\rangle =$

$\langle\Psi_j|\hat{j}_{p,i}(\mathbf{r})|\Psi_i\rangle$. As a consequence we have the relation

$$\chi_{\mathbf{jj},ij}(\mathbf{r},\mathbf{r}',\omega) = \chi_{\mathbf{jj},ji}(\mathbf{r}',\mathbf{r},\omega). \tag{3.85}$$

The symmetry relation in Eq. (3.83) then follows immediately from Eq. (3.75).

If we choose the gauge such that all perturbations are included in the vector potential, i.e., $\delta v_{xc}(\mathbf{r},\omega) = 0$ for all ω, we can rewrite the zero-force and zero-torque theorems given in Eqs. (3.76) and (3.77) in terms of the exchange-correlation kernel $\mathbf{f}_{xc}(\mathbf{r},\mathbf{r}',\omega)$ according to

$$\int d\mathbf{r}' f_{xc,ij}(\mathbf{r},\mathbf{r}',\omega)\rho_0(\mathbf{r}') = \frac{\partial_i\partial_j v_{xc,0}(\mathbf{r})}{(i\omega)^2}, \tag{3.86}$$

$$\sum_{j,k}\int d\mathbf{r}'\epsilon_{ljk} f_{xc,ij}(\mathbf{r},\mathbf{r}',\omega)\rho_0(\mathbf{r}')(r'_k - r_k) = \frac{1}{(i\omega)^2}\sum_j \epsilon_{lji}\partial_j v_{xc,0}(\mathbf{r}). \tag{3.87}$$

The proofs of these relations are similar to that given in the derivation of Eq. (3.54). For the proof of Eq. (3.86) we start by substituting Eq. (3.74) into Eq. (3.76) which yields the following expression

$$\int d\mathbf{r}\frac{\nabla\cdot\delta\mathbf{j}(\mathbf{r},\omega)}{i\omega}\partial_i v_{xc,0}(\mathbf{r}) = -i\omega\sum_j\int d\mathbf{r}\int d\mathbf{r}'\rho_0(\mathbf{r}) f_{xc,ij}(\mathbf{r},\mathbf{r}',\omega)\delta j_j(\mathbf{r}',\omega), \tag{3.88}$$

where we used the continuity equation $\nabla\cdot\delta\mathbf{j}(\mathbf{r},\omega) = i\omega\delta\rho(\mathbf{r},\omega)$. Integration by parts on the left-hand side and interchange of $\mathbf{r}$ and $\mathbf{r}'$ on the right-hand side then gives

$$\sum_j\int d\mathbf{r}\delta j_j(\mathbf{r},\omega)\frac{\partial_i\partial_j v_{xc,0}(\mathbf{r})}{i\omega} = i\omega\sum_j\int d\mathbf{r}\int d\mathbf{r}'\rho_0(\mathbf{r}') f_{xc,ij}(\mathbf{r}',\mathbf{r},\omega)\delta j_j(\mathbf{r},\omega). \tag{3.89}$$

This then immediately leads to

$$\int d\mathbf{r}'\rho_0(\mathbf{r}') f_{xc,ij}(\mathbf{r}',\mathbf{r},\omega) = \frac{\partial_i\partial_j v_{xc,0}(\mathbf{r})}{(i\omega)^2}. \tag{3.90}$$

We see that the righthand side is symmetric in i and j. This must therefore also be true on the left-hand side. Interchanging i and j on the left-hand side and using the Onsager symmetry relation in Eq. (3.83) then yields the equivalent expression given in Eq. (3.86).

We can do similar manipulations for the zero-torque theorem. From Eq. (3.77) we obtain

$$\sum_{j,k}\epsilon_{ijk}\int d\mathbf{r}\frac{\nabla\cdot\delta\mathbf{j}(\mathbf{r},\omega)}{i\omega} r_j\partial_k v_{xc,0}(\mathbf{r}) =$$
$$-i\omega\sum_{j,k,l}\epsilon_{ijk}\int d\mathbf{r}\int d\mathbf{r}'\rho_0(\mathbf{r}) r_j f_{xc,kl}(\mathbf{r},\mathbf{r}',\omega)\delta j_l(\mathbf{r}',\omega). \tag{3.91}$$

Integration by parts on the left-hand side gives the equation

$$\sum_{j,k,l} \epsilon_{ijk} \int d\mathbf{r} \int d\mathbf{r}' \rho_0(\mathbf{r}) r_j f_{xc,kl}(\mathbf{r},\mathbf{r}',\omega) \delta j_l(\mathbf{r}',\omega) =$$
$$\sum_{j,k,l} \epsilon_{ijk} \int d\mathbf{r} \delta j_l(\mathbf{r},\omega) \frac{\partial_l (r_j \partial_k v_{xc,0}(\mathbf{r}))}{(i\omega)^2} +$$
$$\sum_{k,l} \epsilon_{ilk} \int d\mathbf{r} \delta j_l(\mathbf{r},\omega) \frac{\partial_k v_{xc,0}(\mathbf{r})}{(i\omega)^2} + \sum_{j,k,l} \epsilon_{ijk} \int d\mathbf{r} \delta j_l(\mathbf{r},\omega) r_j \frac{\partial_k \partial_l v_{xc,0}(\mathbf{r})}{(i\omega)^2}. \quad (3.92)$$

In the last term of this expression we can use the expression given in Eq. (3.90). If we insert this and bring it to the other side we find

$$\sum_{j,k,l} \epsilon_{ijk} \int d\mathbf{r} d\mathbf{r}' \rho_0(\mathbf{r}') (r'_j - r_j) f_{xc,kl}(\mathbf{r}',\mathbf{r},\omega) \delta j_l(\mathbf{r},\omega) =$$
$$\sum_{k} \epsilon_{ilk} \int d\mathbf{r} \delta j_l(\mathbf{r},\omega) \frac{\partial_k v_{xc,0}(\mathbf{r})}{(i\omega)^2}. \quad (3.93)$$

After relabeling ($k \leftrightarrow j, l \leftrightarrow i$) this gives the relation

$$\sum_{j,k} \epsilon_{lkj} \int d\mathbf{r}' \rho_0(\mathbf{r}') (r'_k - r_k) f_{xc,ji}(\mathbf{r}',\mathbf{r},\omega) = \frac{1}{(i\omega)^2} \sum_j \epsilon_{lij} \partial_j v_{xc,0}(\mathbf{r}). \quad (3.94)$$

Using the Onsager symmetry relation (3.83) this can then be rewritten according to Eq. (3.87).

In the next chapter we will show a derivation of the explicit expression that Vignale and Kohn derived for the exchange-correlation vector potential as a functional of the current density which makes use of the exact constraints given in this section [12,13].

Chapter 4

The Vignale-Kohn Functional

4.1 Introduction

In this chapter we will give a derivation of the Vignale-Kohn functional [12, 13]. The derivation contains two main steps which consist of first establishing some properties of the exchange-correlation kernel for the homogeneous electron gas and secondly using these properties together with basic conservation laws and other exact relations to construct an expression for the exchange-correlation kernel of the inhomogeneous electron gas. The main results of each of the steps are summarized in the next section. In the remaining sections we will show the derivation of these steps in some detail.

4.2 Summary of the Main Results

4.2.1 The Exchange-Correlation Kernel of the Homogeneous Electron Gas

In sections 4.3 and 4.4 we show that the exchange-correlation kernel of the homogeneous electron gas has the following structure

$$f^h_{xc,ij}(\mathbf{k},\omega) = \frac{1}{\omega^2}\left[f^h_{xcL}(\mathbf{k},\omega)k_ik_j + f^h_{xcT}(\mathbf{k},\omega)(|\mathbf{k}|^2\delta_{ij} - k_ik_j)\right], \tag{4.1}$$

where $f^h_{xcL}(\mathbf{k},\omega)$ and $f^h_{xcT}(\mathbf{k},\omega)$ are the longitudinal and transverse response kernels, respectively. Their explicit expressions are given in Eqs. (4.65) and (4.66). One can show that in the limit $\mathbf{k} \to 0$ the kernels $f^h_{xcL,T}(\mathbf{k},\omega)$ are finite functions of the

frequency according to

$$\lim_{\mathbf{k}\to 0} f^h_{xcL,T}(\mathbf{k},\omega) = f^h_{xcL,T}(\omega). \tag{4.2}$$

This relation is essential for the derivation of the Vignale-Kohn functional. With this relation one obtains that

$$f^h_{xc,ij}(\mathbf{k},\omega) = \frac{1}{\omega^2}\left[f^h_{xcL}(\omega)k_ik_j + f^h_{xcT}(\omega)(|\mathbf{k}|^2\delta_{ij} - k_ik_j)\right] \tag{4.3}$$

is a good approximation whenever $k \ll k_F, \omega/v_F$ where k_F is the Fermi momentum and v_F the Fermi velocity. We use Eq. (4.3) extensively in section 4.5 where we discuss the weakly inhomogeneous electron gas.

4.2.2 The Weakly Inhomogeneous Electron Gas

In section 4.5 we consider a weakly modulated electron gas with ground-state density

$$\rho_0(\mathbf{r}) = \rho(1 + 2\gamma\cos(\mathbf{q}\cdot\mathbf{r})) \tag{4.4}$$

with $\gamma \ll 1$. The parameter γ determines the amplitude of the density oscillation and the wave vector $\mathbf{q}$ is a parameter that determines the rapidity of the oscillation. The density is periodic in the direction $\mathbf{a}$ according to

$$\rho_0(\mathbf{r}+\mathbf{a}) = \rho_0(\mathbf{r}) \tag{4.5}$$

for $\mathbf{q}\cdot\mathbf{a} = 2\pi m$ where m is an integer. The exchange-correlation kernel then has the same periodicity

$$f_{xc,ij}(\mathbf{r}+\mathbf{a},\mathbf{r}'+\mathbf{a}) = f_{xc,ij}(\mathbf{r},\mathbf{r}'). \tag{4.6}$$

For this reason one can readily show that $f_{xc,ij}(\mathbf{r},\mathbf{r}',\omega)$ has the following expansion

$$f_{xc,ij}(\mathbf{r},\mathbf{r}',\omega) = \sum_{m=-\infty}^{\infty}\int \frac{d\mathbf{k}}{(2\pi)^3} f_{xc,ij}(\mathbf{k}+m\mathbf{q},\mathbf{k},\omega)e^{i(\mathbf{k}+m\mathbf{q})\cdot\mathbf{r}}e^{-i\mathbf{k}\cdot\mathbf{r}'}, \tag{4.7}$$

where the coefficients in this expansion are defined as

$$f_{xc,ij}(\mathbf{k}+m\mathbf{q},\mathbf{k},\omega) \equiv \frac{1}{V}\int d\mathbf{r}\int d\mathbf{r}' f_{xc,ij}(\mathbf{r},\mathbf{r}',\omega)e^{-i(\mathbf{k}+m\mathbf{q})\cdot\mathbf{r}}e^{i\mathbf{k}\cdot\mathbf{r}'}, \tag{4.8}$$

where V is the volume of the system. For these coefficients it is not difficult to see that to first order in γ only the coefficients for $m = 0, \pm 1$ contribute in the expansion (4.7). Furthermore, for $m = 0$ it is not difficult to see that to first order in γ

$$f_{xc,ij}(\mathbf{k},\mathbf{k},\omega) = f^h_{xc,ij}(\mathbf{k},\omega), \tag{4.9}$$

which can be obtained from Eq. (4.3). It therefore remains to find an explicit expression for $f_{xc,ij}(\mathbf{k}\pm\mathbf{q},\mathbf{k},\omega)$ that can be inserted into Eq. (4.7).

4.2.3 The Exhange-Correlation Kernel to First Order in γ

It turns out that to first order in γ the form of $f_{xc,ij}(\mathbf{k}\pm\mathbf{q},\mathbf{k},\omega)$ is completely determined by the following constraints

$$f_{xc,ij}(\mathbf{k}+m\mathbf{q},\mathbf{k},\omega) = f_{xc,ji}(-\mathbf{k},-\mathbf{k}-m\mathbf{q},\omega) \tag{4.10}$$

$$\lim_{\mathbf{q}\to 0} f_{xc,ij}(\mathbf{k}+\mathbf{q},\mathbf{k},\omega)(\omega) = \gamma\rho\frac{\partial f^h_{xc,ij}(\mathbf{k},\omega)}{\partial\rho} \tag{4.11}$$

$$= \frac{\gamma\rho}{\omega^2}\left[\frac{\partial f^h_{xcL}(\omega)}{\partial\rho}k_ik_j+\frac{\partial f^h_{xcT}(\omega)}{\partial\rho}(k^2\delta_{ij}-k_ik_j)\right] \tag{4.12}$$

$$\lim_{\mathbf{k}\to 0} f_{xc,ij}(\mathbf{k}+\mathbf{q},\mathbf{k},\omega) = -\frac{\gamma}{\omega^2}[\delta f^h_{xcL}(\omega)q_iq_j + f^h_{xcT}(\omega)(q^2\delta_{ij}-q_iq_j)] \tag{4.13}$$

$$\lim_{\mathbf{k}\to 0}\sum_{j,k}\epsilon_{ljk}\frac{\partial f_{xc,ij}(\mathbf{k},\mathbf{k}+\mathbf{q},\omega)}{\partial k_k} = -\frac{\gamma}{\omega^2}[\delta f^h_{xcL}(\omega)-3f^h_{xcT}(\omega)]\sum_k\epsilon_{lki}q_k. \tag{4.14}$$

The derivations of these constraints are given in sections 4.5.2 and 4.5.3. Equation (4.10) is obtained from the Onsager symmetry relation given in Eq. (3.83). Equation (4.12) is the Ward identity which follows directly by consideration of a system with a constant density change (as caused by a shift of the chemical potential). Equations (4.13) and Eq.(4.14) are derived from the zero-force and zero-torque theorems given in Eqs. (3.86) and (3.87). In section 4.5.4 we show that together these constraints lead to the following explicit expression for $f_{xc,ij}(\mathbf{k}+\mathbf{q},\mathbf{k},\omega)$ to first order in γ,

$$\begin{aligned} f_{xc,ij}(\mathbf{k}+\mathbf{q},\mathbf{k},\omega) &= -\frac{\gamma}{\omega^2}\Big\{(\delta f^h_{xcL}(\omega)-f^h_{xcT}(\omega))q_iq_j + f^h_{xcT}(\omega)\delta_{ij}q^2 \\ &\quad -\rho\frac{\partial f^h_{xcT}(\omega)}{\partial\rho}\delta_{ij}\mathbf{k}\cdot(\mathbf{k}+\mathbf{q}) + A(\rho,\omega)(k_i+q_i)k_j \\ &\quad -B(\rho,\omega)k_i(k_j+q_j)\Big\}, \end{aligned} \tag{4.15}$$

where

$$A(\rho,\omega) = \left[\rho(2\frac{\partial f^h_{xcT}(\omega)}{\partial\rho}-\frac{\partial f^h_{xcL}(\omega)}{\partial\rho})+3f^h_{xcT}(\omega)-\delta f^h_{xcL}(\omega)\right] \tag{4.16}$$

$$B(\rho,\omega) = \left[\rho\frac{\partial f^h_{xcT}(\omega)}{\partial\rho}+3f^h_{xcT}(\omega)-\delta f^h_{xcL}(\omega)\right]. \tag{4.17}$$

Here we defined

$$\delta f^h_{xcL}(\omega) = f^h_{xcL}(\omega)-\lim_{\mathbf{k}\to 0} f^h_{xcL}(\mathbf{k},\omega=0). \tag{4.18}$$

4.2.4 The Vignale-Kohn Functional in Real Space

In section 4.5.5 we show that we can obtain an expression for the exchange-correlation vector potential in real space from the explicit expression of the exchange-correlation kernel given in Eq. (4.15). We start from the first-order change in the exchange-corrrelation vector potential which is given by

$$\begin{aligned}\delta A_{xc,i}(\mathbf{r},\omega) &= \sum_j \int d\mathbf{r}' f_{xc,ij}(\mathbf{r},\mathbf{r}',\omega)\delta j_j(\mathbf{r}',\omega) \\ &= \sum_j \int \frac{d\mathbf{k}}{(2\pi)^3} f^h_{xc,ij}(\mathbf{k},\omega)\delta j_j(\mathbf{k},\omega)e^{i\mathbf{k}\cdot\mathbf{r}} \\ &+ \sum_{m=\pm 1} e^{im\mathbf{q}\cdot\mathbf{r}} \sum_j \int \frac{d\mathbf{k}}{(2\pi)^3} f_{xc,ij}(\mathbf{k}+m\mathbf{q},\mathbf{k},\omega)\delta j_j(\mathbf{k},\omega)e^{i\mathbf{k}\cdot\mathbf{r}}, \quad (4.19)\end{aligned}$$

where we used the expansion of the exchange-correlation kernel of Eq. (4.7) and where we defined the Fourier transform of the current density as

$$\delta j_j(\mathbf{k},\omega) = \int d\mathbf{r}\delta j_j(\mathbf{r},\omega)e^{-i\mathbf{k}\cdot\mathbf{r}}. \quad (4.20)$$

If we now insert the explict forms of Eqs. (4.3) and (4.15) into Eq. (4.19) and use the explicit form of the density of the weakly inhomogeneous electron gas given in Eq. (4.4) we obtain the expression of Vignale-Kohn in a form derived by Vignale, Ullrich and Conti [46],

$$\delta A_{xc,i}(\mathbf{r},\omega) = \frac{1}{i\omega}\partial_i \delta v^{ALDA}_{xc}(\mathbf{r},\omega) - \frac{1}{i\omega\rho_0(\mathbf{r})}\sum_j \partial_j \sigma_{xc,ij}(\mathbf{r},\omega) \quad (4.21)$$

where $\delta v^{ALDA}_{xc}(\mathbf{r},\omega)$ is the first order change in the ALDA exchange-correlation potential given in Eq. (2.26) and we defined the tensor $\sigma_{xc}(\mathbf{r},\omega)$ as

$$\sigma_{xc,ij}(\mathbf{r},\omega) = \tilde{\eta}_{xc}(\mathbf{r},\omega)\left[\partial_i u_j + \partial_j u_i - \frac{2}{3}\delta_{ij}(\nabla\cdot\mathbf{u})\right] + \tilde{\zeta}_{xc}(\mathbf{r},\omega)\delta_{ij}(\nabla\cdot\mathbf{u}), \quad (4.22)$$

where we defined the velocity field as $\mathbf{u}(\mathbf{r},\omega) = \delta\mathbf{j}(\mathbf{r},\omega)/\rho_0(\mathbf{r})$ and we defined the coefficients

$$\tilde{\eta}_{xc}(\mathbf{r},\omega) = -\frac{\rho_0^2(\mathbf{r})}{i\omega} f^h_{xcT}(\rho_0,\omega) \quad (4.23)$$

$$\tilde{\zeta}_{xc}(\mathbf{r},\omega) = -\frac{\rho_0^2(\mathbf{r})}{i\omega}\left[f^h_{xcL}(\rho_0,\omega) - \frac{4}{3}f^h_{xcT}(\rho_0,\omega) - f^h_{xcL}(\rho_0,\omega=0)\right]. \quad (4.24)$$

In the following sections we will go through the derivation of these steps in some detail.

4.3 The Homogeneous Electron gas

We see from Eq. (3.15) that the density-density response function and the current-current response function (at $T = 0$) are given by, respectively,

$$\begin{aligned}
\chi_{\rho\rho}(\mathbf{r},t,\mathbf{r}',t') &= -i\Theta(t-t')\langle\Psi_0|[\hat{\rho}(\mathbf{r},t)_{H_0},\hat{\rho}(\mathbf{r}',t')_{H_0}]|\Psi_0\rangle \qquad (4.25)\\
\chi_{\mathbf{jj},ij}(\mathbf{r},t,\mathbf{r}',t') &= -i\Theta(t-t')\langle\Psi_0|[\hat{\mathbf{j}}_{p,i}(\mathbf{r},t)_{H_0},\hat{\mathbf{j}}_{p,j}(\mathbf{r}',t')_{H_0}]|\Psi_0\rangle \\
&\quad +\rho_0(\mathbf{r})\delta_{ij}\delta(\mathbf{r}-\mathbf{r}')\delta(t-t'), \qquad (4.26)
\end{aligned}$$

where $|\Psi_0\rangle$ is the ground state. The electron gas represents a model physical system for which the many-body effects can be studied in detail. It is the starting point for many approximations in density functional theory. Because of translational symmetry all response functions of the electron gas depends only on the relative vector. For the current-density response from the ground state for instance we have

$$\delta j_i(\mathbf{r},t) = \sum_j \int d\mathbf{r}'dt'\chi_{ij}(\mathbf{r}-\mathbf{r}',t-t')\delta A_j(\mathbf{r}',t'), \qquad (4.27)$$

where for notational convenience we have left out the subindex **jj** of the current-current response function. We will continue to do so in the remaining of this chapter. Here we chose the gauge such that all perturbations are included in the vector potential, i.e., $\delta v(\mathbf{r},t)$ is equal to zero at all times t. Equation (4.27) is of convolution form and it is therefore convenient to do a Fourier transform in space and time

$$\delta j_i(\mathbf{k},\omega) = \sum_j \chi_{ij}(\mathbf{k},\omega)\delta A_j(\mathbf{k},\omega), \qquad (4.28)$$

where the Fourier transform and its inverse are given by

$$\begin{aligned}
f(\mathbf{k},\omega) &= \int d\mathbf{r}dt e^{-i(\mathbf{k}\cdot\mathbf{r}-\omega t)}f(\mathbf{r},t) \qquad (4.29)\\
f(\mathbf{r},t) &= \int \frac{d\mathbf{k}d\omega}{(2\pi)^4}e^{i(\mathbf{k}\cdot\mathbf{r}-\omega t)}f(\mathbf{k},\omega), \qquad (4.30)
\end{aligned}$$

and we use the convention that the arguments of Fourier transformed quantities are denoted by the symbols $\mathbf{k}$, $\mathbf{q}$ or $\mathbf{p}$. In Fourier space it is easy to characterize whether a vector field $\mathbf{A}(\mathbf{k})$ is tranverse or longitudinal. A field is called transverse if

$$\mathbf{A}(\mathbf{k})\cdot\mathbf{k} = 0, \qquad (4.31)$$

i.e., if the field is perpendicular to $\mathbf{k}$. On the other hand, if

$$\mathbf{k}\times\mathbf{A}(\mathbf{k}) = 0, \qquad (4.32)$$

i.e., if $\mathbf{A}(\mathbf{k}) = \alpha(\mathbf{k})\mathbf{k}$ for some function $\alpha(\mathbf{k})$, then the field is called longitudinal. For finite $\mathbf{k}$ an arbitrary field $\mathbf{A}(\mathbf{k})$ can always be split up into its transverse and longitudinal parts as follows

$$\begin{aligned} \mathbf{A}(\mathbf{k}) &= \mathbf{A}_T(\mathbf{k}) + \mathbf{A}_L(\mathbf{k}) && (4.33)\\ \mathbf{A}_L(\mathbf{k}) &= (\mathbf{A}(\mathbf{k})\cdot\mathbf{k})\frac{\mathbf{k}}{|\mathbf{k}|^2} && (4.34)\\ \mathbf{A}_T(\mathbf{k}) &= \mathbf{A}(\mathbf{k}) - (\mathbf{A}(\mathbf{k})\cdot\mathbf{k})\frac{\mathbf{k}}{|\mathbf{k}|^2} = \frac{1}{|\mathbf{k}|^2}\mathbf{k}\times(\mathbf{k}\times\mathbf{A}(\mathbf{k})). && (4.35) \end{aligned}$$

Because of the isotropy of the electron gas a longitudinal vector field induces a longitudinal current. This defines the longitudinal response function $\chi_L(\mathbf{k},\omega)$ by

$$\delta\mathbf{j}_L(\mathbf{k},\omega) = \chi_L(\mathbf{k},\omega)\delta\mathbf{A}_L(\mathbf{k},\omega). \tag{4.36}$$

Similarly, a transverse field induces a transverse current. This defines the transverse response function $\chi_T(\mathbf{k},\omega)$, i.e.,

$$\delta\mathbf{j}_T(\mathbf{k},\omega) = \chi_T(\mathbf{k},\omega)\delta\mathbf{A}_T(\mathbf{k},\omega). \tag{4.37}$$

The response to a general field can then be obtained by splitting it in its transverse and longitudinal parts as in Eqs. (4.34) and (4.35). So we obtain

$$\begin{aligned} \delta\mathbf{j}(\mathbf{k},\omega) &= \chi_L(\mathbf{k},\omega)\delta\mathbf{A}_L(\mathbf{k},\omega) + \chi_T(\mathbf{k},\omega)\delta\mathbf{A}_T(\mathbf{k},\omega)\\ &= \sum_j \chi_{ij}(\mathbf{k},\omega)\delta A_j(\mathbf{k},\omega), && (4.38) \end{aligned}$$

where

$$\chi_{ij}(\mathbf{k},\omega) = \chi_L(\mathbf{k},\omega)\frac{k_ik_j}{|\mathbf{k}|^2} + \chi_T(\mathbf{k},\omega)(\delta_{ij} - \frac{k_ik_j}{|\mathbf{k}|^2}). \tag{4.39}$$

It is readily seen that the inverse response function $\chi^{-1}_{ij}(\mathbf{k},\omega)$ has the same structure

$$\chi^{-1}_{ij}(\mathbf{k},\omega) = \frac{1}{\chi_L(\mathbf{k},\omega)}\frac{k_ik_j}{|\mathbf{k}|^2} + \frac{1}{\chi_T(\mathbf{k},\omega)}(\delta_{ij} - \frac{k_ik_j}{|\mathbf{k}|^2}). \tag{4.40}$$

It is instructive to work out the relation between $\chi_L(\mathbf{k},\omega)$ and the density-density response function for the case that we only have an external scalar potential $\delta v(\mathbf{r},t)$. In that case the induced density is given by

$$\delta\rho(\mathbf{r},t) = \int d\mathbf{r}'dt'\chi_{\rho\rho}(\mathbf{r}-\mathbf{r}',t-t')\delta v(\mathbf{r}',t'). \tag{4.41}$$

If we do a Fourier transformation we obtain

$$\delta\rho(\mathbf{k},\omega) = \Pi(\mathbf{k},\omega)\delta v(\mathbf{k},\omega), \tag{4.42}$$

where we defined $\Pi(\mathbf{k},\omega) = \chi_{\rho\rho}(\mathbf{k},\omega)$ in order to avoid confusion with χ_{ij}. The scalar potential can be transformed into a longitudinal vector potential by the gauge transformation given in Eq. (2.29) with $\Lambda(\mathbf{r},t)$ a solution of Eq. (2.31). In Fourier space this means that $\Lambda(\mathbf{k},\omega)$ is given by

$$i\omega\Lambda(\mathbf{k},\omega) = \delta v(\mathbf{k},\omega), \tag{4.43}$$

and the vector potential becomes

$$\delta\mathbf{A}_L(\mathbf{k},\omega) = i\mathbf{k}\Lambda(\mathbf{k},\omega). \tag{4.44}$$

Therefore we find

$$\delta\mathbf{A}_L(\mathbf{k},\omega) = \frac{\mathbf{k}}{\omega}\delta v(\mathbf{k},\omega), \tag{4.45}$$

which is a longitudinal vector field. We further consider the continuity equation

$$\frac{\partial\delta\rho(\mathbf{r},t)}{\partial t} = -\nabla\cdot\delta\mathbf{j}(\mathbf{r},t), \tag{4.46}$$

in Fourier space which gives

$$i\omega\delta\rho(\mathbf{k},\omega) = i\mathbf{k}\cdot\delta\mathbf{j}(\mathbf{k},\omega). \tag{4.47}$$

With this expression we then obtain

$$\begin{aligned}\delta\rho(\mathbf{k},\omega) &= \frac{\mathbf{k}\cdot\delta\mathbf{j}(\mathbf{k},\omega)}{\omega} = \frac{\mathbf{k}\cdot\chi_L(\mathbf{k},\omega)\delta\mathbf{A}_L(\mathbf{k},\omega)}{\omega} \\ &= \frac{|\mathbf{k}|^2}{\omega^2}\chi_L(\mathbf{k},\omega)\delta v(\mathbf{k},\omega).\end{aligned} \tag{4.48}$$

From this relation we see that

$$\chi_L(\mathbf{k},\omega) = \frac{\omega^2}{|\mathbf{k}|^2}\Pi(\mathbf{k},\omega). \tag{4.49}$$

Finally, we give some useful relations to extract the longitudinal and transverse response functions from $\chi_{ij}(\mathbf{k},\omega)$. From Eq. (4.39) we see that

$$\chi_L(\mathbf{k},\omega) = \sum_{ij}\frac{k_i k_j}{|\mathbf{k}|^2}\chi_{ij}(\mathbf{k},\omega). \tag{4.50}$$

Since

$$\mathrm{Tr}\chi_{ij} = \sum_i \chi_{ii}(\mathbf{k},\omega) = \chi_L(\mathbf{k},\omega) + 2\chi_T(\mathbf{k},\omega), \tag{4.51}$$

we have

$$\chi_T(\mathbf{k},\omega) = \frac{1}{2}\sum_{ij}(\delta_{ij} - \frac{k_i k_j}{|\mathbf{k}|^2})\chi_{ij}(\mathbf{k},\omega). \tag{4.52}$$

4.4 TDCDFT for the Homogeneous Electron Gas

As explained in section 2.6 in TDCDFT we introduce the set of Kohn-Sham potentials $\{v_s(\mathbf{r},t), \mathbf{A}_s(\mathbf{r},t)\}$ that reproduces the true induced current density of an interacting system with potentials $\{v(\mathbf{r},t), \mathbf{A}(\mathbf{r},t)\}$ in a noninteracting system. Here and in the remaining of this chapter we choose the gauge such that in the interacting and non-interacting system all perturbations are included in the vector potential, i.e., $\delta v(\mathbf{r},t)$ and $\delta v_s(\mathbf{r},t)$ are equal to zero for all times t. We then have the following expression for the induced current density,

$$\delta j_i(\mathbf{r},t) = \sum_j \int d\mathbf{r}' dt' \chi_{ij,s}(\mathbf{r},t,\mathbf{r}',t') \delta A_{j,s}(\mathbf{r}',t'), \tag{4.53}$$

where

$$\delta \mathbf{A}_s(\mathbf{r},t) = \delta \mathbf{A}(\mathbf{r},t) + \delta \mathbf{A}_H(\mathbf{r},t) + \delta \mathbf{A}_{xc}(\mathbf{r},t). \tag{4.54}$$

In this equation

$$\frac{\partial \delta \mathbf{A}_H(\mathbf{r},t)}{\partial t} = -\nabla \delta v_H(\mathbf{r},t) = -\nabla \int d\mathbf{r}' \frac{\rho(\mathbf{r}',t)}{|\mathbf{r}-\mathbf{r}'|} \tag{4.55}$$

is the longitudinal vector potential corresponding to the dynamic Hartree potential. We further define the exchange-correlation kernel $\mathbf{f}_{xc}$ by

$$\delta A_{xc,i}(\mathbf{r},t) = \sum_j \int d\mathbf{r}' dt' f_{xc,ij}(\mathbf{r},t,\mathbf{r}',t') \delta j_j(\mathbf{r}',t'). \tag{4.56}$$

For the special case of the homogeneous electron gas we obtain in Fourier space the equation

$$\delta j_i(\mathbf{k},\omega) = \sum_j \chi_{ij,s}(\mathbf{k},\omega) \delta A_{j,s}(\mathbf{k},\omega), \tag{4.57}$$

where

$$\delta \mathbf{A}_s(\mathbf{k},\omega) = \delta \mathbf{A}(\mathbf{k},\omega) + \frac{\mathbf{k}}{\omega} \delta v_H(\mathbf{k},\omega) + \delta \mathbf{A}_{xc}(\mathbf{k},\omega), \tag{4.58}$$

and

$$\delta A_{xc,i}(\mathbf{k},\omega) = \sum_j f_{xc,ij}(\mathbf{k},\omega) \delta j_j(\mathbf{k},\omega). \tag{4.59}$$

For any practical application of TDCDFT we need an approximation for $\delta \mathbf{A}_{xc}(\mathbf{k},\omega)$. Let us therefore analyze this term a bit further. If we express $\delta v_H(\mathbf{k},\omega)$ in terms of the current using the continuity equation

$$\delta v_H(\mathbf{k},\omega) = \frac{4\pi \delta \rho(\mathbf{k},\omega)}{|\mathbf{k}|^2} = \frac{4\pi \mathbf{k} \cdot \delta \mathbf{j}(\mathbf{k},\omega)}{\omega |\mathbf{k}|^2}, \tag{4.60}$$

we have

$$\delta\mathbf{A}_{xc}(\mathbf{k},\omega) = \delta\mathbf{A}_s(\mathbf{k},\omega) - \delta\mathbf{A}(\mathbf{k},\omega) - \frac{4\pi\mathbf{k}}{\omega^2|\mathbf{k}|^2}\mathbf{k}\cdot\delta\mathbf{j}(\mathbf{k},\omega). \tag{4.61}$$

From this equation we immediately see that

$$f_{xc,ij}(\mathbf{k},\omega) = \chi^{-1}_{ij,s}(\mathbf{k},\omega) - \chi^{-1}_{ij}(\mathbf{k},\omega) - \frac{4\pi k_i k_j}{\omega^2|\mathbf{k}|^2}. \tag{4.62}$$

From this equation and Eq. (4.40) we see that

$$\begin{aligned} f_{xc,ij}(\mathbf{k},\omega) &= \left[\frac{1}{\chi_{L,s}(\mathbf{k},\omega)} - \frac{1}{\chi_L(\mathbf{k},\omega)} - \frac{4\pi}{\omega^2}\right]\frac{k_i k_j}{|\mathbf{k}|^2} \\ &+ \left[\frac{1}{\chi_{T,s}(\mathbf{k},\omega)} - \frac{1}{\chi_T(\mathbf{k},\omega)}\right](\delta_{ij} - \frac{k_i k_j}{|\mathbf{k}|^2}), \end{aligned} \tag{4.63}$$

where $\chi_{L,s}$ and $\chi_{T,s}$ are the noninteracting longitudinal and transverse response functions of the electron gas. We now define the longitudinal and transverse response kernels by

$$f_{xc,ij}(\mathbf{k},\omega) = \frac{1}{\omega^2}\left[f^h_{xcL}(\mathbf{k},\omega)k_i k_j + f^h_{xcT}(\mathbf{k},\omega)(|\mathbf{k}|^2\delta_{ij} - k_i k_j)\right]. \tag{4.64}$$

These functions are explicitely given by

$$\begin{aligned} f^h_{xcL}(\mathbf{k},\omega) &= \frac{\omega^2}{|\mathbf{k}|^2}\left[\frac{1}{\chi_{L,s}(\mathbf{k},\omega)} - \frac{1}{\chi_L(\mathbf{k},\omega)}\right] - \frac{4\pi}{|\mathbf{k}|^2} \\ &= \frac{1}{\Pi_s(\mathbf{k},\omega)} - \frac{1}{\Pi(\mathbf{k},\omega)} - \frac{4\pi}{|\mathbf{k}|^2}, \end{aligned} \tag{4.65}$$

and

$$f^h_{xcT}(\mathbf{k},\omega) = \frac{\omega^2}{|\mathbf{k}|^2}\left[\frac{1}{\chi_{T,s}(\mathbf{k},\omega)} - \frac{1}{\chi_T(\mathbf{k},\omega)}\right]. \tag{4.66}$$

In these equations Π_s is the Kohn-Sham density-density response function. We see that f^h_{xcL} coincides with the f_{xc} of scalar TDDFT. It was shown by Vignale and Kohn [12, 13] that in the limit $\mathbf{k}\to 0$ the kernels $f^h_{xcL,T}(\mathbf{k},\omega)$ are finite functions of the frequency according to

$$\lim_{\mathbf{k}\to 0} f^h_{xcL,T}(\mathbf{k},\omega) = f^h_{xcL,T}(\omega) \tag{4.67}$$

With this relation we obtain that

$$f^h_{xc,ij}(\mathbf{k},\omega) = \frac{1}{\omega^2}\left[f^h_{xcL}(\omega)k_i k_j + f^h_{xcT}(\omega)(|\mathbf{k}|^2\delta_{ij} - k_i k_j)\right] \tag{4.68}$$

is a good approximation if $|\mathbf{k}| \ll k_F, \omega/v_F$ where k_F is the Fermi momentum and v_F is the Fermi velocity. This result will be important later in the derivation of the Vignale-Kohn expression for the exchange-correlation vector potential.

4.5 The Weakly Inhomogeneous Electron Gas

4.5.1 The Expansion of the Exchange-Correlation Kernel

We now consider the case of the weakly inhomogeneous electron gas with a ground-state density

$$\rho_0(\mathbf{r}) = \rho(1 + 2\gamma \cos(\mathbf{q}\cdot\mathbf{r})), \tag{4.69}$$

and $\gamma \ll 1$. This density is periodic in the direction $\mathbf{a}$,

$$\rho_0(\mathbf{r}+\mathbf{a}) = \rho_0(\mathbf{r}), \tag{4.70}$$

for $\mathbf{q}\cdot\mathbf{a} = 2\pi m$ where m is an integer. The exchange-correlation kernel then has the same periodicity

$$f_{xc,ij}(\mathbf{r}+\mathbf{a}, \mathbf{r}'+\mathbf{a}, \omega) = f_{xc,ij}(\mathbf{r}, \mathbf{r}', \omega). \tag{4.71}$$

We then define the following coefficients

$$f_{xc,ij}(\mathbf{k}+m\mathbf{q}, \mathbf{k}, \omega) \equiv \frac{1}{V}\int d\mathbf{r}\int d\mathbf{r}' f_{xc,ij}(\mathbf{r}, \mathbf{r}', \omega) e^{-i(\mathbf{k}+m\mathbf{q})\cdot\mathbf{r}} e^{i\mathbf{k}\cdot\mathbf{r}'}, \tag{4.72}$$

where V is the volume of the system. Formally the volume is infinite and therefore Eq. (4.72) should be understood in the appropriate limit. If $f_{xc,ij}$ satisfies the periodicity condition Eq. (4.71) then $f_{xc,ij}$ has the expansion

$$f_{xc,ij}(\mathbf{r}, \mathbf{r}', \omega) = \sum_{m=-\infty}^{\infty}\int \frac{d\mathbf{k}}{(2\pi)^3} f_{xc,ij}(\mathbf{k}+m\mathbf{q}, \mathbf{k}, \omega) e^{i(\mathbf{k}+m\mathbf{q})\cdot\mathbf{r}} e^{-i\mathbf{k}\cdot\mathbf{r}'}. \tag{4.73}$$

The proof goes as follows. Let A be the right-hand side of Eq. (4.73). Then by insertion of the definition (4.72) we have

$$\begin{aligned}
A &= \frac{1}{V}\sum_{m=-\infty}^{\infty}\int d\mathbf{x}\int d\mathbf{x}'\int \frac{d\mathbf{k}}{(2\pi)^3} f_{xc,ij}(\mathbf{x}, \mathbf{x}', \omega) e^{-i(\mathbf{k}+m\mathbf{q})\cdot\mathbf{x}} e^{i\mathbf{k}\cdot\mathbf{x}'} e^{i(\mathbf{k}+m\mathbf{q})\cdot\mathbf{r}} e^{-i\mathbf{k}\cdot\mathbf{r}'} \\
&= \frac{1}{V}\sum_{m=-\infty}^{\infty}\int d\mathbf{x}\int d\mathbf{x}' f_{xc,ij}(\mathbf{x}, \mathbf{x}', \omega) e^{-im\mathbf{q}\cdot(\mathbf{x}-\mathbf{r})}\delta(\mathbf{x}'-\mathbf{x}+\mathbf{r}-\mathbf{r}') \\
&= \frac{1}{V}\sum_{m=-\infty}^{\infty}\int d\mathbf{x} f_{xc,ij}(\mathbf{x}, \mathbf{x}+\mathbf{r}'-\mathbf{r}, \omega) e^{-im\mathbf{q}\cdot(\mathbf{x}-\mathbf{r})} \\
&= \frac{1}{V}\sum_{m=-\infty}^{\infty}\int d\mathbf{x} f_{xc,ij}(\mathbf{x}+\mathbf{r}, \mathbf{x}+\mathbf{r}', \omega) e^{-im\mathbf{q}\cdot\mathbf{x}},
\end{aligned} \tag{4.74}$$

where in the last step we made the substitution $\mathbf{x} \to \mathbf{x}+\mathbf{r}$. We can now write $\mathbf{x}$ as

$$\mathbf{x} = x\,\hat{\mathbf{q}} + y\,\mathbf{e}_1 + z\,\mathbf{e}_2, \tag{4.75}$$

where $\hat{\mathbf{q}}$ is a unit vector in the $\mathbf{q}$-direction and $\mathbf{e}_1$ and $\mathbf{e_2}$ are unit vectors which are orthogonal to $\mathbf{q}$ and to each other. Then this coordinate transformation has a Jacobian equal to one. Because of Eq. (4.71) we now have that in Eq. (4.74) we can write

$$f_{xc,ij}(\mathbf{x}+\mathbf{r},\mathbf{x}+\mathbf{r}',\omega) = f_{xc,ij}(x\,\hat{\mathbf{q}}+\mathbf{r},x\,\hat{\mathbf{q}}+\mathbf{r}',\omega). \tag{4.76}$$

Therefore we obtain from Eq. (4.74) by integrating over y and z the relation

$$A = \frac{1}{L}\sum_{m=-\infty}^{\infty}\int dx\, f_{xc,ij}(x\,\hat{\mathbf{q}}+\mathbf{r},x\,\hat{\mathbf{q}}+\mathbf{r}',\omega)e^{-imqx}, \tag{4.77}$$

where $q=|\mathbf{q}|$ and L is the dimension of the system. We now use

$$\sum_{m=-\infty}^{\infty} e^{-imqx} = L_u\sum_{m=-\infty}^{\infty}\delta(x-\frac{2\pi m}{q}), \tag{4.78}$$

where $L_u = 2\pi/q$ is the lenght of the unit cell. We then have

$$\begin{aligned} A &= \frac{L_u}{L}\sum_{m=-\infty}^{\infty} f_{xc,ij}(\mathbf{r}+\frac{2\pi m}{q}\hat{\mathbf{q}}\,,\,\mathbf{r}'+\frac{2\pi m}{q}\hat{\mathbf{q}},\omega) \\ &= f_{xc,ij}(\mathbf{r},\mathbf{r}',\omega)\sum_{m=-\infty}^{\infty}\frac{L_u}{L} = f_{xc,ij}(\mathbf{r},\mathbf{r}',\omega), \end{aligned} \tag{4.79}$$

where we again used the periodicity condition Eq. (4.71). We note that the above expressions must be understood in the appropriate limit. We have thus proved Eq. (4.73).

4.5.2 First Order in the Inhomogeneity and the Ward Identity

Now we are going to study the exchange-correlation kernel to first order in the inhomogeneity parameter γ. We define the density deviation form homogeneity as

$$\delta\rho(\mathbf{r}) = \rho_0(\mathbf{r}) - \rho = 2\gamma\rho\cos(\mathbf{q}\cdot\mathbf{r}). \tag{4.80}$$

Then $f_{xc,ij}(\mathbf{r},\mathbf{r}',\omega)$ can be functionally Taylor-expanded as

$$f_{xc,ij}(\mathbf{r},\mathbf{r}',\omega) = f_{xc,ij}(\rho,\mathbf{r},\mathbf{r}',\omega) + \int d\mathbf{r}'' g_{xc,ij}(\rho,\mathbf{r},\mathbf{r}',\mathbf{r}'',\omega)\delta\rho(\mathbf{r}'') + O(\delta\rho^2) \tag{4.81}$$

$$\begin{aligned} &= f^h_{xc,ij}(\rho,\mathbf{r}-\mathbf{r}',\omega) \\ &+ 2\gamma\rho\int d^3\mathbf{r}'' g^h_{xc,ij}(\rho,\mathbf{r}-\mathbf{r}'',\mathbf{r}'-\mathbf{r}'',\omega)\cos(\mathbf{q}\cdot\mathbf{r}'') + O(\gamma^2), \end{aligned} \tag{4.82}$$

where we defined the function

$$g_{xc,ij}(\mathbf{r},\mathbf{r}',\mathbf{r}'',\omega) = \frac{\delta f_{xc,ij}(\mathbf{r},\mathbf{r}',\omega)}{\delta\rho(\mathbf{r}'')}. \tag{4.83}$$

This can be done since the response functions and hence $f_{xc,ij}(\mathbf{r},\mathbf{r}',\omega)$ are ground-state expectation values and therefore functionals of the ground-state density. We used in Eq. (4.82) that any n-point function F in the homogeneous electron gas is translationally invariant, i.e.,

$$F(\mathbf{r},\ldots,\mathbf{r}_n) = F(\mathbf{r}+\mathbf{a},\ldots,\mathbf{r}_n+\mathbf{a}), \tag{4.84}$$

for any vector $\mathbf{a}$. In particular we can choose $\mathbf{a} = -\mathbf{r}_n$ and therefore

$$F(\mathbf{r},\ldots,\mathbf{r}_n) = F(\mathbf{r}-\mathbf{r}_n,\ldots,\mathbf{r}_{n-1}-\mathbf{r}_n,0). \tag{4.85}$$

We can now write the function $g^h_{xc,ij}$ in a Fourier expansion as

$$g^h_{xc,ij}(\rho,\mathbf{r}-\mathbf{r}'',\mathbf{r}'-\mathbf{r}'',\omega) = \int \frac{d\mathbf{k}}{(2\pi)^3}\frac{d\mathbf{p}}{(2\pi)^3}\, g^h_{xc,ij}(\mathbf{k},\mathbf{p},\omega)e^{i\mathbf{k}\cdot(\mathbf{r}-\mathbf{r}'')}e^{-i\mathbf{p}\cdot(\mathbf{r}'-\mathbf{r}'')}. \tag{4.86}$$

Then we obtain

$$\begin{aligned}
&f_{xc,ij}(\mathbf{r},\mathbf{r}',\omega) = f^h_{xc,ij}(\rho,\mathbf{r}-\mathbf{r}',\omega) + \\
&\gamma\rho\sum_{m=\pm1}\int\frac{d\mathbf{k}}{(2\pi)^3}\frac{d\mathbf{p}}{(2\pi)^3}\int d^3\mathbf{r}'' g^h_{xc,ij}(\mathbf{k},\mathbf{p},\omega)e^{i\mathbf{k}\cdot(\mathbf{r}-\mathbf{r}'')}e^{-i\mathbf{p}\cdot(\mathbf{r}'-\mathbf{r}'')}e^{im\mathbf{q}\cdot\mathbf{r}''} + O(\gamma^2) &(4.87)\\
&= f^h_{xc,ij}(\rho,\mathbf{r}-\mathbf{r}',\omega) + \\
&\gamma\rho\sum_{m=\pm1}\int\frac{d\mathbf{k}}{(2\pi)^3}\frac{d\mathbf{p}}{(2\pi)^3} g^h_{xc,ij}(\mathbf{k},\mathbf{p},\omega)e^{i\mathbf{k}\cdot\mathbf{r}}e^{-i\mathbf{p}\cdot\mathbf{r}'}\delta(\mathbf{p}-\mathbf{k}+m\mathbf{q}) + O(\gamma^2) &(4.88)\\
&= \int\frac{d\mathbf{p}}{(2\pi)^3} f^h_{xc,ij}(\rho,\mathbf{p},\omega)e^{i\mathbf{p}\cdot(\mathbf{r}-\mathbf{r}')} + \\
&\gamma\rho\sum_{m=\pm1}\int\frac{d\mathbf{p}}{(2\pi)^3} g^h_{xc,ij}(\mathbf{p}+m\mathbf{q},\mathbf{p},\omega)e^{i(\mathbf{p}+m\mathbf{q})\cdot\mathbf{r}}e^{-i\mathbf{p}\cdot\mathbf{r}'} + O(\gamma^2). &(4.89)
\end{aligned}$$

Comparing this expression to the expansion in Eq. (4.73) we immediately find that to first order in γ

$$\begin{aligned}
f_{xc,ij}(\mathbf{k},\mathbf{k},\omega) &= f^h_{xc,ij}(\mathbf{k},\omega) &(4.90)\\
f_{xc,ij}(\mathbf{k}\pm\mathbf{q},\mathbf{k},\omega) &= \gamma\rho\, g^h_{xc,ij}(\mathbf{k}\pm\mathbf{q},\mathbf{k},\omega). &(4.91)
\end{aligned}$$

This means that to first order in the inhomogeneity parameter γ we have the following expression for $f_{xc,ij}(\mathbf{r},\mathbf{r}',\omega)$:

$$\begin{aligned} f_{xc,ij}(\mathbf{r},\mathbf{r}',\omega) &= \int \frac{d\mathbf{k}}{(2\pi)^3} f^h_{xc,ij}(\rho,\mathbf{k},\omega) e^{i\mathbf{k}\cdot(\mathbf{r}-\mathbf{r}')} \\ &+ \sum_{m=\pm 1} \int \frac{d\mathbf{k}}{(2\pi)^3} f_{xc,ij}(\mathbf{p}+m\mathbf{q},\mathbf{p},\omega) e^{i(\mathbf{k}+m\mathbf{q})\cdot\mathbf{r}} e^{-i\mathbf{k}\cdot\mathbf{r}'}. \quad (4.92) \end{aligned}$$

This is an important relation that will be used in the remainder of this section. It now remains to find an expression for the expansion coefficients $f_{xc,ij}(\mathbf{k}\pm\mathbf{q},\mathbf{k},\omega)$. The form of these coefficients is fixed by a number of exact relations. If we take the $\mathbf{q}\to 0$ limit of Eq. (4.89) we obtain

$$f_{xc,ij}(\mathbf{r},\mathbf{r}',\omega) = f^h_{xc,ij}(\rho,\mathbf{r}-\mathbf{r}',\omega) + 2\gamma\rho \int \frac{d\mathbf{p}}{(2\pi)^3} g^h_{xc,ij}(\mathbf{p},\mathbf{p},\omega) e^{i\mathbf{p}\cdot(\mathbf{r}-\mathbf{r}')} + O(\gamma^2), \quad (4.93)$$

where

$$g^h_{xc,ij}(\mathbf{p},\mathbf{p},\omega) = \lim_{\mathbf{q}\to 0} g^h_{xc,ij}(\mathbf{p}\pm\mathbf{q},\mathbf{p},\omega). \quad (4.94)$$

Here we write the limit since it is important when $\mathbf{p}=0$. On the other hand in the $\mathbf{q}\to 0$ limit the density change is simply $\delta\rho(\mathbf{r}) = 2\gamma\rho$ and therefore

$$\begin{aligned} f_{xc,ij}(\mathbf{r},\mathbf{r}',\omega) &= f^h_{xc,ij}(\rho+2\gamma\rho,\mathbf{r}-\mathbf{r}',\omega) & (4.95)\\ &= f^h_{xc,ij}(\rho,\mathbf{r}-\mathbf{r}',\omega) + 2\gamma\rho \frac{\partial f^h_{xc,ij}(\rho,\mathbf{r}-\mathbf{r}',\omega)}{\partial\rho} + O(\gamma^2) & (4.96)\\ &= f^h_{xc,ij}(\rho,\mathbf{r}-\mathbf{r}',\omega) + 2\gamma\rho \int \frac{d\mathbf{p}}{(2\pi)^3} \frac{\partial f^h_{xc,ij}(\mathbf{p},\omega)}{\partial\rho} e^{i\mathbf{p}\cdot(\mathbf{r}-\mathbf{r}')} + O(\gamma^2). & (4.97) \end{aligned}$$

Comparing Eq. (4.97) to Eq. (4.93) we see that

$$\lim_{\mathbf{q}\to 0} g^h_{xc,ij}(\mathbf{p}\pm\mathbf{q},\mathbf{p},\omega) = \frac{\partial f^h_{xc,ij}(\mathbf{p},\omega)}{\partial\rho}, \quad (4.98)$$

With Eq. (4.91) this yields

$$\lim_{\mathbf{q}\to 0} f_{xc,ij}(\mathbf{p}\pm\mathbf{q},\mathbf{p},\omega) = \gamma\rho \frac{\partial f^h_{xc,ij}(\mathbf{p},\omega)}{\partial\rho}. \quad (4.99)$$

This relation is referred to by Vignale and Kohn as the Ward identity [12, 13]. It is very important for our later expansion in gradients of the density $\rho_0(\mathbf{r})$ since it allows us to replace the density dependence of the gradient expansion coefficients on ρ by $\rho_0(\mathbf{r})$. We will discuss this in detail later.

4.5.3 The Onsager Relation and the Conservation Laws

When the Onsager symmetry relation (3.83) is inserted in the definition Eq. (4.72) we find

$$f_{xc,ij}(\mathbf{k}+m\mathbf{q},\mathbf{k},\omega) = f_{xc,ji}(-\mathbf{k},-\mathbf{k}-m\mathbf{q},\omega). \tag{4.100}$$

Furthermore, from the constraints set by the zero-force and zero-torque theorems given in Eqs. (3.86) and (3.87) it follows that to first order in γ we have

$$\lim_{\mathbf{k}\to 0} f_{xc,ij}(\mathbf{k}+\mathbf{q},\mathbf{k},\omega) = -\gamma[f^h_{xc,ij}(\mathbf{q},\omega) - \frac{q_i q_j}{\omega^2} f^h_{xcL}(\mathbf{q},\omega=0)] \tag{4.101}$$

$$\begin{aligned}\lim_{\mathbf{k}\to 0}\sum_{j,k}\epsilon_{ljk}\frac{\partial f_{xc,ij}(\mathbf{k},\mathbf{k}+\mathbf{q},\omega)}{\partial k_k} &= -\gamma\sum_{j,k}\epsilon_{ljk}\frac{\partial f^h_{xc,ij}(\mathbf{q},\omega)}{\partial q_k} \\ &\quad +\frac{\gamma}{\omega^2}f^h_{xcL}(\mathbf{q},\omega=0)\sum_j \epsilon_{lji}q_j. \end{aligned}\tag{4.102}$$

The proof goes as follows. We insert expansion (4.73) in Eq. (3.86),

$$\begin{aligned}&\sum_{m=-\infty}^{\infty}\int\frac{d\mathbf{k}}{(2\pi)^3}\int d\mathbf{r}' f_{xc,ij}(\mathbf{k}+m\mathbf{q},\mathbf{k},\omega)e^{i(\mathbf{k}+m\mathbf{q})\cdot\mathbf{r}}e^{-i\mathbf{k}\cdot\mathbf{r}'}(\rho+2\gamma\rho\cos(\mathbf{q}\cdot\mathbf{r}')) = \\ &\frac{\partial_i\partial_j v_{xc,0}(\mathbf{r})}{(i\omega)^2}.\end{aligned}\tag{4.103}$$

On the right-hand side of this expression we can use

$$\begin{aligned} v_{xc,0}(\mathbf{r}) &= v^h_{xc}(\rho)+\int d\mathbf{r}'\frac{\delta v_{xc}(\mathbf{r})}{\delta\rho(\mathbf{r}')}\delta\rho(\mathbf{r}')+O(\delta\rho^2) \\ &= v^h_{xc}(\rho)+2\gamma\rho\int d\mathbf{r}' f^h_{xcL}(\rho,\mathbf{r}-\mathbf{r}',\omega=0)\cos(\mathbf{q}\cdot\mathbf{r}')+O(\gamma^2) \\ &= v^h_{xc}(\rho)+\gamma\rho\int\frac{d\mathbf{k}}{(2\pi)^3}\int d\mathbf{r}' f^h_{xcL}(\rho,\mathbf{k},\omega=0)e^{i\mathbf{k}\cdot(\mathbf{r}-\mathbf{r}')}(e^{i\mathbf{q}\cdot\mathbf{r}'}+e^{-i\mathbf{q}\cdot\mathbf{r}'})+O(\gamma^2) \\ &= v^h_{xc}(\rho)+\gamma\rho\int\frac{d\mathbf{k}}{(2\pi)^3}f^h_{xcL}(\rho,\mathbf{k},\omega=0)e^{i\mathbf{k}\cdot\mathbf{r}}(\delta(\mathbf{k}-\mathbf{q})+\delta(\mathbf{k}+\mathbf{q}))+O(\gamma^2) \\ &= v^h_{xc}(\rho)+\gamma\rho f^h_{xcL}(\rho,\mathbf{q},\omega=0)(e^{i\mathbf{q}\cdot\mathbf{r}}+e^{-i\mathbf{q}\cdot\mathbf{r}})+O(\gamma^2), \end{aligned}\tag{4.104}$$

where we used the inversion symmetry $f^h_{xcL}(-\mathbf{q}) = f^h_{xcL}(\mathbf{q})$. If we insert this equation (4.104) into the right-hand side of Eq. (4.103) and collect on both sides the terms that are of first order in γ we obtain the relation

$$\begin{aligned}&\rho\sum_{m\pm 1}\int\frac{d\mathbf{k}}{(2\pi)^3}\int d\mathbf{r}' f_{xc,ij}(\mathbf{k}+m\mathbf{q},\mathbf{k},\omega)e^{i(\mathbf{k}+m\mathbf{q})\cdot\mathbf{r}}e^{-i\mathbf{k}\cdot\mathbf{r}'} \\ &+\gamma\rho\int\frac{d\mathbf{k}}{(2\pi)^3}\int d\mathbf{r}' f^h_{xc,ij}(\mathbf{k},\omega)e^{i\mathbf{k}\cdot(\mathbf{r}-\mathbf{r}')}(e^{i\mathbf{q}\cdot\mathbf{r}'}+e^{-i\mathbf{q}\cdot\mathbf{r}'}) \\ &= \gamma\rho\frac{q_i q_j}{\omega^2}f^h_{xcL}(\mathbf{q},\omega=0)(e^{i\mathbf{q}\cdot\mathbf{r}}+e^{-i\mathbf{q}\cdot\mathbf{r}}).\end{aligned}\tag{4.105}$$

Carrying out subsequently the $\mathbf{r}'$ and $\mathbf{k}$ integrations on the left-hand side of this expression then yields

$$\begin{aligned}&\rho\sum_{m\pm1} f_{xc,ij}(m\mathbf{q},0,\omega)e^{im\mathbf{q}\cdot\mathbf{r}} + \gamma\rho f^h_{xc,ij}(\mathbf{q},\omega)(e^{i\mathbf{q}\cdot\mathbf{r}}+e^{-i\mathbf{q}\cdot\mathbf{r}})\\ &= \gamma\rho\frac{q_iq_j}{\omega^2}f^h_{xcL}(\mathbf{q},\omega=0)(e^{i\mathbf{q}\cdot\mathbf{r}}+e^{-i\mathbf{q}\cdot\mathbf{r}}).\end{aligned} \tag{4.106}$$

If we compare the exponents on both sides we thus find

$$\lim_{\mathbf{k}\to0} f_{xc,ij}(\mathbf{k}+\mathbf{q},\mathbf{k},\omega) = -\gamma\left[f^h_{xc,ij}(\mathbf{q},\omega) - \frac{q_iq_j}{\omega^2}f^h_{xcL}(\mathbf{q},\omega=0)\right], \tag{4.107}$$

which proves Eq. (4.101).

The other relation given in Eq. (4.102) can be proved similarly. We first note that by taking the derivative of Eq. (4.72) we obtain

$$\begin{aligned}-i\frac{\partial f_{xc,ij}}{\partial k_k}(\mathbf{k}+m\mathbf{q},\mathbf{k},\omega) &= \frac{1}{V}\int d\mathbf{r}\int d\mathbf{r}'\Big\{f_{xc,ij}(\mathbf{r},\mathbf{r}',\omega)(r'_k-r_k)\\ &\times\ e^{-i(\mathbf{k}+m\mathbf{q})\cdot\mathbf{r}}e^{i\mathbf{k}\cdot\mathbf{r}'}\Big\}.\end{aligned} \tag{4.108}$$

The function $(r'_k-r_k)f_{xc,ij}(\mathbf{r},\mathbf{r}',\omega)$ also satisfies the periodicity condition given in Eq. (4.71) and thus has the expansion

$$\begin{aligned}(r'_k-r_k)f_{xc,ij}(\mathbf{r},\mathbf{r}',\omega) &= -i\sum_{m=-\infty}^{\infty}\int\frac{d\mathbf{k}}{(2\pi)^3}\Big\{\frac{\partial f_{xc,ij}}{\partial k_k}(\mathbf{k}+m\mathbf{q},\mathbf{k},\omega)\\ &\times\ e^{i(\mathbf{k}+m\mathbf{q})\cdot\mathbf{r}}e^{-i\mathbf{k}\cdot\mathbf{r}'}\Big\}.\end{aligned} \tag{4.109}$$

Inserting expression (4.109) into Eq. (3.87) then yields

$$\begin{aligned}&-i\sum_{j,k}\epsilon_{ljk}\sum_{m=-\infty}^{\infty}\int\frac{d\mathbf{k}}{(2\pi)^3}\int d\mathbf{r}'\Big\{\frac{\partial f_{xc,ij}}{\partial k_k}(\mathbf{k}+m\mathbf{q},\mathbf{k},\omega)e^{i(\mathbf{k}+m\mathbf{q})\cdot\mathbf{r}}e^{-i\mathbf{k}\cdot\mathbf{r}'}\\ &\times(\rho+2\gamma\rho\cos(\mathbf{q}\cdot\mathbf{r}'))\Big\} = \frac{1}{(i\omega)^2}\sum_j\epsilon_{lji}\partial_j v_{xc,0}(\mathbf{r}).\end{aligned} \tag{4.110}$$

If we now insert expression (4.104) in the right-hand side and collect terms to first order in γ we obtain

$$\begin{aligned}&-i\rho\sum_{j,k}\epsilon_{ljk}\sum_{m\pm1}\int\frac{d\mathbf{k}}{(2\pi)^3}\int d\mathbf{r}'\frac{\partial f_{xc,ij}}{\partial k_k}(\mathbf{k}+m\mathbf{q},\mathbf{k},\omega)e^{i(\mathbf{k}+m\mathbf{q})\cdot\mathbf{r}}e^{-i\mathbf{k}\cdot\mathbf{r}'}\\ &-i\gamma\rho\sum_{j,k}\epsilon_{ljk}\int\frac{d\mathbf{k}}{(2\pi)^3}\int d\mathbf{r}'\frac{\partial f^h_{xc,ij}}{\partial k_k}(\mathbf{k},\omega)e^{i\mathbf{k}\cdot(\mathbf{r}-\mathbf{r}')}(e^{i\mathbf{q}\cdot\mathbf{r}'}+e^{-i\mathbf{q}\cdot\mathbf{r}'})\\ &= -\frac{i\gamma\rho}{\omega^2}f^h_{xcL}(\mathbf{q},\omega=0)(e^{i\mathbf{q}\cdot\mathbf{r}}-e^{-i\mathbf{q}\cdot\mathbf{r}})\sum_j\epsilon_{lji}q_j.\end{aligned} \tag{4.111}$$

Now performing the $\mathbf{r}'$ and $\mathbf{k}$ integrals and using that $\partial f_{xc,ij}(\mathbf{k})/\partial k_k = -\partial f_{xc,ij}(-\mathbf{k})/\partial k_k$ gives

$$- i\rho \sum_{j,k} \epsilon_{ljk} \sum_{m\pm 1} \frac{\partial f_{xc,ij}}{\partial k_k}(m\mathbf{q},0,\omega) e^{im\mathbf{q}\cdot\mathbf{r}} - i\gamma\rho \sum_{j,k} \epsilon_{ljk} \frac{\partial f^h_{xc,ij}}{\partial q_k}(\mathbf{q},\omega)(e^{i\mathbf{q}\cdot\mathbf{r}} - e^{-i\mathbf{q}\cdot\mathbf{r}}) =$$
$$- \frac{i\gamma\rho}{\omega^2} f^h_{xcL}(\mathbf{q},\omega=0)(e^{i\mathbf{q}\cdot\mathbf{r}} - e^{-i\mathbf{q}\cdot\mathbf{r}}) \sum_j \epsilon_{lji} q_j. \tag{4.112}$$

Comparing both sides then yields the equation

$$\lim_{\mathbf{k}\to 0} \sum_{j,k} \epsilon_{ljk} \frac{\partial f_{xc,ij}}{\partial k_k}(\mathbf{k}\pm\mathbf{q},\mathbf{k},\omega) = \pm \gamma \left\{ \frac{1}{\omega^2} f^h_{xcL}(\mathbf{q},\omega=0) \sum_j \epsilon_{lji} q_j \right.$$
$$\left. - \sum_{j,k} \epsilon_{ljk} \frac{\partial f^h_{xc,ij}}{\partial q_k}(\mathbf{q},\omega) \right\}. \tag{4.113}$$

This proves equation (4.102).

It is important to note that the expressions in Eqs. (4.101) and (4.102) are valid for general $\mathbf{q}$. To arrive at the Vignale-Kohn expression for the exchange-correlation kernel we now have to further restrict $f^h_{xc,ij}(\mathbf{q},\omega)$ to have the limiting form of Eq. (4.68), i.e.,

$$f^h_{xc,ij}(\mathbf{q},\omega) = \frac{1}{\omega^2}\left[f^h_{xcL}(\omega) q_i q_j + f^h_{xcT}(\omega)(|\mathbf{q}|^2\delta_{ij} - q_i q_j)\right], \tag{4.114}$$

which is a good approximation when $q \ll k_F$ and $q \ll \omega/v_F$. We see that here the constraints on the Fourier component of the homogeneous electron gas impose contraints on $\mathbf{q}$ for the inhomogeneous electron gas kernel $\mathbf{f}_{xc}(\mathbf{k}\pm\mathbf{q},\mathbf{k},\omega)$. Under these constraints the last term on the right-hand side of Eq. (4.113) becomes

$$\sum_{j,k} \epsilon_{ljk} \frac{\partial f^h_{xc,ij}}{\partial q_k} = \frac{1}{\omega^2}(f^h_{xcL}(\omega) - f^h_{xcT}(\omega)) \sum_j \epsilon_{lji} q_j + \frac{2}{\omega^2} f^h_{xcT}(\omega) \sum_k \epsilon_{lik} q_k$$
$$= \frac{1}{\omega^2}(f^h_{xcL}(\omega) - 3 f^h_{xcT}(\omega)) \sum_j \epsilon_{lji} q_j, \tag{4.115}$$

and then equations (4.101) and (4.102) become

$$\lim_{\mathbf{k}\to 0} f_{xc,ij}(\mathbf{k}+\mathbf{q},\mathbf{k},\omega) = -\frac{\gamma}{\omega^2}[\delta f^h_{xcL}(\omega) q_i q_j + f^h_{xcT}(\omega)(q^2\delta_{ij} - q_i q_j)] \tag{4.116}$$
$$\lim_{\mathbf{k}\to 0} \sum_{j,k} \epsilon_{ljk} \frac{\partial f_{xc,ij}(\mathbf{k},\mathbf{k}+\mathbf{q},\omega)}{\partial k_k} = -\frac{\gamma}{\omega^2}[\delta f^h_{xcL}(\omega) - 3 f^h_{xcT}(\omega)] \sum_k \epsilon_{lki} q_k, \tag{4.117}$$

where we defined the quantity

$$\delta f^h_{xcL}(\omega) = f^h_{xcL}(\omega) - \lim_{\mathbf{k}\to 0} f^h_{xcL}(\mathbf{k}, \omega = 0). \tag{4.118}$$

We have derived all equations that determine $f_{xc,ij}(\mathbf{k}+\mathbf{q}, \mathbf{k}, \omega)$.

4.5.4 Explicit Form of the Exchange-Correlation Kernel to First Order in γ

Let us now summarize the equations that determine $f_{xc,ij}(\mathbf{k}+\mathbf{q}, \mathbf{k}, \omega)$,

$$f_{xc,ij}(\mathbf{k}+m\mathbf{q}, \mathbf{k}, \omega) = f_{xc,ji}(-\mathbf{k}, -\mathbf{k}-m\mathbf{q}, \omega) \tag{4.119}$$

$$\lim_{\mathbf{q}\to 0} f_{xc,ij}(\mathbf{k}+\mathbf{q}, \mathbf{k}, \omega)(\omega) = \gamma\rho \frac{\partial f^h_{xc,ij}(\mathbf{k}, \omega)}{\partial \rho} \tag{4.120}$$

$$= \frac{\gamma\rho}{\omega^2}\left[\frac{\partial f^h_{xcL}(\omega)}{\partial \rho} k_i k_j + \frac{\partial f^h_{xcT}(\omega)}{\partial \rho}(k^2\delta_{ij} - k_i k_j)\right] \tag{4.121}$$

$$\lim_{\mathbf{k}\to 0} f_{xc,ij}(\mathbf{k}+\mathbf{q}, \mathbf{k}, \omega) = -\frac{\gamma}{\omega^2}[\delta f^h_{xcL}(\omega) q_i q_j + f^h_{xcT}(\omega)(q^2\delta_{ij} - q_i q_j)] \tag{4.122}$$

$$\lim_{\mathbf{k}\to 0} \sum_{j,k} \epsilon_{ljk} \frac{\partial f_{xc,ij}(\mathbf{k}, \mathbf{k}+\mathbf{q}, \omega)}{\partial k_k} = -\frac{\gamma}{\omega^2}[\delta f^h_{xcL}(\omega) - 3 f^h_{xcT}(\omega)] \sum_k \epsilon_{lki} q_k. \tag{4.123}$$

In Eq. (4.121) we used again the limiting form of Eq. (4.68) which is a good approximation when $k \ll k_F$ and $k \ll \omega/v_F$. Now Eqs. (4.121), (4.122) and (4.123) immediately tell us that $f_{xc,ij}(\mathbf{k}+\mathbf{q}, \mathbf{k}, \omega)$ is a quadratic function of $\mathbf{k}$ and $\mathbf{q}$ of the form

$$f_{xc,ij}(\mathbf{k}+\mathbf{q}, \mathbf{k}, \omega) = C q_i q_j + D\delta_{ij} q^2 + E k_i k_j + F\delta_{ij} k^2 + \sum_{mn} \gamma^{ij}_{mn} q_m k_n, \tag{4.124}$$

where

$$C = -\frac{\gamma}{\omega^2}(\delta f^h_{xcL}(\omega) - f^h_{xcT}(\omega)) \tag{4.125}$$

$$D = -\frac{\gamma}{\omega^2} f^h_{xcT}(\omega) \tag{4.126}$$

$$E = \frac{\gamma\rho}{\omega^2}\left[\frac{\partial f^h_{xcL}}{\delta\rho}(\omega) - \frac{\partial f^h_{xcT}}{\delta\rho}(\omega)\right] \tag{4.127}$$

$$F = \frac{\gamma\rho}{\omega^2}\frac{\partial f^h_{xcT}}{\delta\rho}(\omega), \tag{4.128}$$

and where γ^{ij}_{nm} are coefficients to be determined. Let us now use the Onsager relation of Eq. (4.119). For that we have to make the substitution $\mathbf{k} \to -\mathbf{k}-\mathbf{q}$ and interchange

the indices i and j. From Eq. (4.124) we then obtain

$$\begin{aligned} f_{xc,ji}(-\mathbf{k},-\mathbf{k}-\mathbf{q},\omega) &= Cq_iq_j + D\delta_{ij}q^2 + E(k_i+q_i)(k_j+q_j) \\ &+ F\delta_{ij}(\mathbf{k}+\mathbf{q})^2 - \sum_{mn}\gamma^{ji}_{mn}q_m(k_n+q_n). \end{aligned} \tag{4.129}$$

Comparing Eq. (4.124) and (4.129) in the limit $\mathbf{k}\to 0$ and using the Onsager relation of Eq. (4.119) then yields the identity

$$\sum_{mn}\gamma^{ji}_{mn}q_mq_n = Eq_iq_j + F\delta_{ij}q^2. \tag{4.130}$$

Since q_iq_j for $i\le j$ are independent functions it follows immediately from this relation that

$$\gamma^{ji}_{mn} = \alpha\delta_{im}\delta_{jn} + \beta\delta_{jm}\delta_{in} + F\delta_{ij}\delta_{mn}, \tag{4.131}$$

where $\alpha+\beta = E$. If we insert this relation back into Eq. (4.124) we obtain the expression

$$\begin{aligned} f_{xc,ij}(\mathbf{k}+\mathbf{q},\mathbf{k},\omega) &= Cq_iq_j + D\delta_{ij}q^2 + Ek_ik_j + F\delta_{ij}\mathbf{k}\cdot(\mathbf{k}+\mathbf{q}) \\ &+ \alpha q_ik_j + (E-\alpha)q_jk_i. \end{aligned} \tag{4.132}$$

The parameter α is then determined by Eq. (4.123). Using Eq. (4.132) we obtain

$$\begin{aligned} -\frac{\gamma}{\omega^2}[\delta f^h_{xcL}(\omega) - 3f^h_{xcT}(\omega)]\sum_k \epsilon_{lki}q_k &= \lim_{\mathbf{k}\to 0}\sum_{j,k}\epsilon_{ljk}\frac{\partial f_{xc,ij}(\mathbf{k},\mathbf{k}+\mathbf{q},\omega)}{\partial k_k} \\ &= \sum_{j,k}\epsilon_{ljk}(F\delta_{ij}q_k + \alpha q_i\delta_{jk} + (E-\alpha)q_j\delta_{ik}) \\ &= (E-\alpha-F)\sum_k\epsilon_{lki}q_k. \end{aligned} \tag{4.133}$$

We therefore find

$$\begin{aligned} \alpha &= E - F + \frac{\gamma}{\omega^2}[\delta f^h_{xcL}(\omega) - 3f^h_{xcT}(\omega)] \\ &= -\frac{\gamma}{\omega^2}\left[3f^h_{xcT}(\omega) - \delta f^h_{xcL}(\omega) + \rho\left(2\frac{\partial f^h_{xcT}(\omega)}{\partial\rho} - \frac{\partial f^h_{xcL}(\omega)}{\partial\rho}\right)\right] \end{aligned} \tag{4.134}$$

$$\begin{aligned} E-\alpha &= F - \frac{\gamma}{\omega^2}[\delta f^h_{xcL}(\omega) - 3f^h_{xcT}(\omega)] \\ &= \frac{\gamma}{\omega^2}\left[\rho\frac{\partial f^h_{xcT}(\omega)}{\partial\rho} + 3f^h_{xcT}(\omega) - \delta f^h_{xcL}(\omega)\right]. \end{aligned} \tag{4.135}$$

When we insert this in Eq. (4.132) and collect our results we obtain the expression derived by Vignale and Kohn for the exchange-correlation kernel [12, 13],

$$\begin{aligned} f_{xc,ij}(\mathbf{k}+\mathbf{q},\mathbf{k},\omega) &= -\frac{\gamma}{\omega^2}\Big\{(\delta f^h_{xcL}(\omega) - f^h_{xcT}(\omega))q_i q_j + f^h_{xcT}(\omega)\delta_{ij}q^2 \\ &\quad -\rho\frac{\partial f^h_{xcT}(\omega)}{\partial\rho}\delta_{ij}\mathbf{k}\cdot(\mathbf{k}+\mathbf{q}) + A(\rho,\omega)(k_i+q_i)k_j \\ &\quad -B(\rho,\omega)k_i(k_j+q_j)\Big\}, \end{aligned} \tag{4.136}$$

where

$$A(\rho,\omega) = \left[\rho(2\frac{\partial f^h_{xcT}(\omega)}{\partial\rho} - \frac{\partial f^h_{xcL}(\omega)}{\partial\rho}) + 3f^h_{xcT}(\omega) - \delta f^h_{xcL}(\omega)\right] \tag{4.137}$$

$$B(\rho,\omega) = \left[\rho\frac{\partial f^h_{xcT}(\omega)}{\partial\rho} + 3f^h_{xcT}(\omega) - \delta f^h_{xcL}(\omega)\right]. \tag{4.138}$$

We have now completely determined the exchange-correlation kernel to first order in γ. All that remains now is to reconstruct the kernel in real space.

4.5.5 Construction of the Vignale-Kohn Functional in Real Space

Having obtained the form of Eq. (4.136) we will now construct the exchange-correlation vector potential in real space. Let the frequency-dependent functions $\delta\mathbf{j}(\mathbf{r},\omega)$ and $\delta\mathbf{A}_{xc}(\mathbf{r},\omega)$ be the first order change in the current density and the exchange-correlation vector potential, respectively. Then

$$\delta A_{xc,i}(\mathbf{r},\omega) = \sum_j \int d\mathbf{r}' f_{xc,ij}(\mathbf{r},\mathbf{r}',\omega)\delta j_j(\mathbf{r}',\omega). \tag{4.139}$$

If we now insert the form of the exchange-correlation kernel given in Eq. (4.92) we obtain the expression

$$\begin{aligned} \delta A_{xc,i}(\mathbf{r},\omega) &= \sum_j \int \frac{d\mathbf{k}}{(2\pi)^3} f^h_{xc,ij}(\mathbf{k},\omega)\delta j_j(\mathbf{k},\omega)e^{i\mathbf{k}\cdot\mathbf{r}} \\ &\quad + \sum_{m=\pm1} e^{im\mathbf{q}\cdot\mathbf{r}} \sum_j \int \frac{d\mathbf{k}}{(2\pi)^3} f_{xc,ij}(\mathbf{k}+m\mathbf{q},\mathbf{k},\omega)\delta j_j(\mathbf{k},\omega)e^{i\mathbf{k}\cdot\mathbf{r}}, \end{aligned} \tag{4.140}$$

where we defined the Fourier transform of the current as

$$\delta j_j(\mathbf{k},\omega) = \int d\mathbf{r}'\delta j_j(\mathbf{r}',\omega)e^{-i\mathbf{k}\cdot\mathbf{r}'}. \tag{4.141}$$

If we now for notational convenience write

$$
\begin{aligned}
f^h_{xc,ij}(\mathbf{k},\omega) &= Pk_ik_j + Q\delta_{ij}k^2 && (4.142)\\
f_{xc,ij}(\mathbf{k}+m\mathbf{q},\mathbf{k},\omega) &= Rq_iq_j + S\delta_{ij}q^2 + T\delta_{ij}\mathbf{k}\cdot(\mathbf{k}+m\mathbf{q}) \\
&+ U(k_i+mq_i)k_j + Vk_i(k_j+mq_j), && (4.143)
\end{aligned}
$$

where

$$
\begin{aligned}
P &= \frac{1}{\omega^2}(f^h_{xcL}(\omega) - f^h_{xcT}(\omega)) && (4.144)\\
Q &= \frac{1}{\omega^2} f^h_{xcT}(\omega) && (4.145)\\
R &= -\frac{\gamma}{\omega^2}(\delta f^h_{xcL}(\omega) - f^h_{xcT}(\omega)) && (4.146)\\
S &= -\frac{\gamma}{\omega^2} f^h_{xcT}(\omega) && (4.147)\\
T &= \frac{\gamma\rho}{\omega^2}\frac{\partial f^h_{xcT}(\omega)}{\partial\rho} && (4.148)\\
U &= -\frac{\gamma}{\omega^2}\left[\rho(2\frac{\partial f^h_{xcT}(\omega)}{\partial\rho} - \frac{\partial f^h_{xcL}(\omega)}{\partial\rho}) + 3f^h_{xcT}(\omega) - \delta f^h_{xcL}(\omega)\right] && (4.149)\\
V &= \frac{\gamma}{\omega^2}\left[\rho\frac{\partial f^h_{xcT}(\omega)}{\partial\rho} + 3f^h_{xcT}(\omega) - \delta f^h_{xcL}(\omega)\right], && (4.150)
\end{aligned}
$$

then the integral in Eq. (4.140) can be rewritten as

$$
\begin{aligned}
\delta A_{xc,i}(\mathbf{r},\omega) &= P\sum_j \int \frac{d\mathbf{k}}{(2\pi)^3} k_ik_j\delta j_j(\mathbf{k},\omega)e^{i\mathbf{k}\cdot\mathbf{r}} + Q\sum_j \delta_{ij}\int \frac{d\mathbf{k}}{(2\pi)^3} k^2\delta j_j(\mathbf{k},\omega)e^{i\mathbf{k}\cdot\mathbf{r}} \\
&+ \sum_{m=\pm1} e^{im\mathbf{q}\cdot\mathbf{r}}\sum_j (Rq_iq_j + Sq^2\delta_{ij})\int \frac{d\mathbf{k}}{(2\pi)^3}\,\delta j_j(\mathbf{k},\omega)e^{i\mathbf{k}\cdot\mathbf{r}} \\
&+ T\sum_{m=\pm1} e^{im\mathbf{q}\cdot\mathbf{r}}\sum_j \delta_{ij}\int \frac{d\mathbf{k}}{(2\pi)^3}\,\mathbf{k}\cdot(\mathbf{k}+m\mathbf{q})\,\delta j_j(\mathbf{k},\omega)e^{i\mathbf{k}\cdot\mathbf{r}} \\
&+ U\sum_{m=\pm1} e^{im\mathbf{q}\cdot\mathbf{r}}\sum_j \int \frac{d\mathbf{k}}{(2\pi)^3}\,(k_i+mq_i)k_j\,\delta j_j(\mathbf{k},\omega)e^{i\mathbf{k}\cdot\mathbf{r}} \\
&+ V\sum_{m=\pm1} e^{im\mathbf{q}\cdot\mathbf{r}}\sum_j \int \frac{d\mathbf{k}}{(2\pi)^3}\,k_i(k_j+mq_j)\,\delta j_j(\mathbf{k},\omega)e^{i\mathbf{k}\cdot\mathbf{r}}. \qquad (4.151)
\end{aligned}
$$

The integrals in this expression are now easily evaluated (they all basically amount to the substitution $k_j \to -i\partial_j$),

$$\int \frac{d\mathbf{k}}{(2\pi)^3} k_i k_j \delta j_j(\mathbf{k},\omega) e^{i\mathbf{k}\cdot\mathbf{r}} = -\partial_i \partial_j \delta j_j(\mathbf{r},\omega) \tag{4.152}$$

$$\int \frac{d\mathbf{k}}{(2\pi)^3} k^2 \delta j_j(\mathbf{k},\omega) e^{i\mathbf{k}\cdot\mathbf{r}} = -\nabla^2 \delta j_j(\mathbf{r},\omega) \tag{4.153}$$

$$\begin{aligned}\sum_{m=\pm 1} e^{im\mathbf{q}\cdot\mathbf{r}} (Rq_i q_j + Sq^2\delta_{ij}) \int \frac{d\mathbf{k}}{(2\pi)^3} \delta j_j(\mathbf{k},\omega) e^{i\mathbf{k}\cdot\mathbf{r}} &= -\frac{1}{\gamma\rho}[R\partial_i\partial_j\rho_0(\mathbf{r}) \\ &+ \delta_{ij} S\nabla^2\rho_0(\mathbf{r})]\delta j_j(\mathbf{r},\omega) \end{aligned} \tag{4.154}$$

$$\begin{aligned}\sum_{m=\pm 1} e^{im\mathbf{q}\cdot\mathbf{r}} \int \frac{d\mathbf{k}}{(2\pi)^3} \mathbf{k}\cdot(\mathbf{k}+m\mathbf{q}) \delta j_j(\mathbf{k},\omega) e^{i\mathbf{k}\cdot\mathbf{r}} &= -\frac{1}{\gamma\rho}[\delta\rho(\mathbf{r})\nabla^2\delta j_j(\mathbf{r},\omega) \\ &+ \nabla\rho_0(\mathbf{r})\cdot\nabla\delta j_j(\mathbf{r},\omega)] \end{aligned} \tag{4.155}$$

$$\begin{aligned}\sum_{m=\pm 1} e^{im\mathbf{q}\cdot\mathbf{r}} \int \frac{d\mathbf{k}}{(2\pi)^3} (k_i+mq_i) k_j \delta j_j(\mathbf{k},\omega) e^{i\mathbf{k}\cdot\mathbf{r}} &= -\frac{1}{\gamma\rho}[\delta\rho(\mathbf{r})\partial_i\partial_j\delta j_j(\mathbf{r},\omega) \\ &+ \partial_i\rho_0(\mathbf{r})\partial_j\delta j_j(\mathbf{r},\omega)] \end{aligned} \tag{4.156}$$

$$\begin{aligned}\sum_{m=\pm 1} e^{im\mathbf{q}\cdot\mathbf{r}} \int \frac{d\mathbf{k}}{(2\pi)^3} k_i (k_j+mq_j) \delta j_j(\mathbf{k},\omega) e^{i\mathbf{k}\cdot\mathbf{r}} &= -\frac{1}{\gamma\rho}[\delta\rho(\mathbf{r})\partial_i\partial_j\delta j_j(\mathbf{r},\omega) \\ &+ \partial_j\rho_0(\mathbf{r})\partial_i\delta j_j(\mathbf{r},\omega)], \end{aligned} \tag{4.157}$$

where we used the definition of $\rho_0(\mathbf{r})$ and $\delta\rho(\mathbf{r})$ as in Eq. (4.80). Our expression for $\delta\mathbf{A}_{xc}(\mathbf{r},\omega)$ therefore becomes in real space,

$$\begin{aligned}\delta A_{xc,i}(\mathbf{r},\omega) &= -\sum_j \Big(P\partial_i\partial_j\delta j_j(\mathbf{r},\omega) + Q\delta_{ij}\nabla^2\delta j_j(\mathbf{r},\omega) + \frac{1}{\gamma\rho}[R\,\partial_i\partial_j\rho_0(\mathbf{r}) \\ &+ \delta_{ij} S\,\nabla^2\rho_0(\mathbf{r})]\,\delta j_j(\mathbf{r},\omega) \\ &+ \delta_{ij}\frac{T}{\gamma\rho}[\delta\rho(\mathbf{r})\nabla^2\delta j_j(\mathbf{r},\omega) + \nabla\rho_0(\mathbf{r})\cdot\nabla\delta j_j(\mathbf{r},\omega)] \\ &+ \frac{U}{\gamma\rho}[\delta\rho(\mathbf{r})\partial_i\partial_j\delta j_j(\mathbf{r},\omega) + \partial_i\rho_0(\mathbf{r})\,\partial_j\delta j_j(\mathbf{r},\omega)] \\ &+ \frac{V}{\gamma\rho}[\delta\rho(\mathbf{r})\partial_i\partial_j\delta j_j(\mathbf{r},\omega) + \partial_j\rho_0(\mathbf{r})\,\partial_i\delta j_j(\mathbf{r},\omega)]\Big). \end{aligned} \tag{4.158}$$

This can be rewritten as

$$\begin{aligned}
\delta A_{xc,i}(\mathbf{r},\omega) &= -\sum_j \Big(P\partial_i\partial_j\delta j_j(\mathbf{r},\omega) + Q\partial_j\partial_j j_i(\mathbf{r},\omega) \\
&+ \frac{1}{\gamma\rho}[R\,\partial_i\partial_j\rho_0(\mathbf{r}) + \delta_{ij}S\,\nabla^2\rho_0(\mathbf{r})]\,\delta j_j(\mathbf{r},\omega) \\
&+ \frac{T}{\gamma\rho}\partial_j[\delta\rho(\mathbf{r})\partial_j\delta j_i(\mathbf{r},\omega)] + \frac{U}{\gamma\rho}\partial_i[\delta\rho(\mathbf{r})\partial_j\delta j_j(\mathbf{r},\omega)] \\
&+ \frac{V}{\gamma\rho}\partial_j[\delta\rho(\mathbf{r})\partial_i\delta j_j(\mathbf{r},\omega)]\Big) \\
&= -\sum_j \partial_j \left\{ \left[Q + \frac{T}{\gamma\rho}\delta\rho(\mathbf{r}) \right] (\partial_i\delta j_j(\mathbf{r},\omega) + \partial_j\delta j_i(\mathbf{r},\omega)) \right. \\
&+ \left. \delta_{ij}\left[P - Q + \frac{1}{\gamma\rho}(U+W)\delta\rho(\mathbf{r}) \right] \nabla\cdot\mathbf{j}(\mathbf{r},\omega) \right\} \\
&- \sum_j \Big(\frac{W}{\gamma\rho}[\partial_j(\delta\rho(\mathbf{r})\partial_i\delta j_j(\mathbf{r},\omega)) - \partial_i(\delta\rho(\mathbf{r})\partial_j\delta j_j(\mathbf{r},\omega))] \\
&+ \frac{1}{\gamma\rho}[R\,\partial_i\partial_j\rho_0(\mathbf{r}) + \delta_{ij}S\,\nabla^2\rho_0(\mathbf{r})]\,\delta j_j(\mathbf{r},\omega)\Big), \qquad (4.159)
\end{aligned}$$

where we defined

$$W = \frac{\gamma}{\omega^2}(3f^h_{xcT}(\omega) - \delta f^h_{xcL}(\omega)), \qquad (4.160)$$

and used that $V = T + W$. Now we use that to first order in γ

$$\begin{aligned}
Q + \frac{T}{\gamma\rho}\delta\rho(\mathbf{r}) &= \frac{1}{\omega^2}\left[f^h_{xcT}(\omega) + \frac{\partial f^h_{xcT}(\omega)}{\partial\rho}\delta\rho(\mathbf{r}) \right] \\
&= \frac{1}{\omega^2} f^h_{xcT}(\rho_0(\mathbf{r}),\omega) \qquad (4.161) \\
P - Q + \frac{1}{\gamma\rho}(U+W)\delta\rho(\mathbf{r}) &= \frac{1}{\omega^2}\left[f^h_{xcL}(\omega) - 2f^h_{xcT}(\omega) \right] \\
&+ \frac{1}{\omega^2}\left[\frac{\partial f^h_{xcL}(\omega)}{\partial\rho} - 2\frac{\partial f^h_{xcT}(\omega)}{\partial\rho} \right]\delta\rho(\mathbf{r}) \\
&= \frac{1}{\omega^2}(f^h_{xcL}(\rho_0(\mathbf{r}),\omega) - 2f^h_{xcT}(\rho_0(\mathbf{r}),\omega). \qquad (4.162)
\end{aligned}$$

We thus see that the Ward identity has allowed us to replace ρ by $\rho_0(\mathbf{r})$ in $f^h_{xcL,T}(\omega)$. This is essential for applying the theory to systems with a general density profile and is a necessary requirement for the existence of a gradient expansion in terms of $\rho_0(\mathbf{r})$.

Our expression for $\delta\mathbf{A}_{xc}(\mathbf{r},\omega)$ now attains the form,

$$\begin{aligned}
\delta A_{xc,i}(\mathbf{r},\omega) &= -\frac{1}{\omega^2}\sum_j \partial_j \Big(f^h_{xcT}(\rho_0,\omega)(\partial_i\delta j_j(\mathbf{r},\omega)+\partial_j\delta j_i(\mathbf{r},\omega)) \\
&+ (f^h_{xcL}(\rho_0,\omega)-2f^h_{xcT}(\rho_0,\omega))\delta_{ij}\nabla\cdot\mathbf{j}(\mathbf{r},\omega)\Big) \\
&- \sum_j \Big(\frac{W}{\gamma\rho}[\partial_j\delta\rho(\mathbf{r})\partial_i\delta j_j(\mathbf{r},\omega)-\partial_i\delta\rho(\mathbf{r})\partial_j\delta j_j(\mathbf{r},\omega)] \\
&+ \frac{1}{\gamma\rho}[R\,\partial_i\partial_j\rho_0(\mathbf{r})+\delta_{ij}S\,\nabla^2\rho_0(\mathbf{r})]\,\delta j_j(\mathbf{r},\omega)\Big). \qquad (4.163)
\end{aligned}$$

We are now going to write the last term in a different form,

$$\begin{aligned}
&\sum_j \frac{1}{\gamma\rho}[R\,\partial_i\partial_j\rho_0(\mathbf{r})+\delta_{ij}S\,\nabla^2\rho_0(\mathbf{r})]\,\delta j_j(\mathbf{r},\omega) \\
&= -\frac{1}{\rho\omega^2}\sum_j[(\delta f^h_{xcL}-f^h_{xcT})\partial_i\partial_j\rho_0+f^h_{xcT}\delta_{ij}\nabla^2\rho_0]\delta j_j(\mathbf{r},\omega) \\
&= -\frac{1}{\rho\omega^2}\sum_j \partial_j[f^h_{xcT}(\omega)(\delta j_i\partial_j\rho_0+\delta j_j\partial_i\rho_0)+(\delta f^h_{xcL}(\omega)-2f^h_{xcT}(\omega))\delta_{ij}(\mathbf{j}\cdot\nabla\rho_0)] \\
&\quad +\frac{1}{\rho\omega^2}\sum_j\{f^h_{xcT}(\omega)(\partial_j\delta j_i\partial_j\rho_0+\partial_j\delta j_j\partial_i\rho_0) \\
&\quad +(\delta f^h_{xcL}(\omega)-2f^h_{xcT}(\omega))\partial_i\delta j_j\partial_j\rho_0\}. \qquad (4.164)
\end{aligned}$$

This brings the equation for $\delta\mathbf{A}_{xc}(\mathbf{r},\omega)$ in the form,

$$\begin{aligned}
\delta A_{xc,i}(\mathbf{r},\omega) = &-\frac{1}{\omega^2}\sum_j \partial_j\Big\{ f^h_{xcT}(\rho_0,\omega)(\partial_i\delta j_j(\mathbf{r},\omega)+\partial_j\delta j_i(\mathbf{r},\omega)) \\
&+(f^h_{xcL}(\rho_0,\omega)-2f^h_{xcT}(\rho_0,\omega))\delta_{ij}\nabla\cdot\delta\mathbf{j}(\mathbf{r},\omega)\Big\} \\
&+\frac{1}{\rho\omega^2}\sum_j \partial_j\Big\{ f^h_{xcT}(\omega)(\delta j_i\partial_j\rho_0+\delta j_j\partial_i\rho_0) \\
&+(\delta f^h_{xcL}(\omega)-2f^h_{xcT}(\omega))\delta_{ij}(\delta\mathbf{j}\cdot\nabla\rho_0)\Big\} \\
&-\frac{1}{\rho\omega^2}\sum_j\Big\{ f^h_{xcT}(\omega)(\partial_j\delta j_i\partial_j\rho_0+\partial_j\delta j_j\partial_i\rho_0) \\
&+(\delta f^h_{xcL}(\omega)-2f^h_{xcT}(\omega))\partial_i\delta j_j\partial_j\rho_0\Big\} \\
&-\frac{1}{\rho\omega^2}\sum_j(3f^h_{xcT}(\omega)-\delta f^h_{xcL})(\partial_j\rho_0\partial_i\delta j_j-\partial_i\rho_0\partial_j\delta j_j). \qquad (4.165)
\end{aligned}$$

Now in the first line of this equation we can add and subtract the term

$$\begin{aligned} -\frac{1}{\omega^2}\partial_i(f^h_{xcL}(\rho_0,\omega=0)\nabla\cdot\delta\mathbf{j}(\mathbf{r},\omega)) &= \frac{1}{i\omega}\partial_i(f^h_{xcL}(\rho_0,\omega=0)\delta\rho(\mathbf{r},\omega)) \\ &= \frac{1}{i\omega}\partial_i\delta v^{ALDA}_{xc}(\mathbf{r},\omega), \end{aligned} \tag{4.166}$$

where we used the continuity equation $\nabla\cdot\delta\mathbf{j}(\mathbf{r},\omega)=i\omega\delta\rho(\mathbf{r},\omega)$ where $\delta\rho(\mathbf{r},\omega)$ is the first order density change due to the applied field and $\delta v^{ALDA}_{xc}(\mathbf{r},\omega)$ the first order change in the ALDA exchange-correlation potential which is given in Eq. (2.26). We can further rearrange the last two lines of Eq. (4.165) to obtain

$$\begin{aligned} \delta A_{xc,i}(\mathbf{r},\omega) = &\frac{1}{i\omega}\partial_i\delta v^{ALDA}_{xc}(\mathbf{r},\omega) \\ &-\frac{1}{\omega^2}\sum_j\partial_j\Big\{f^h_{xcT}(\rho_0,\omega)(\partial_i\delta j_j(\mathbf{r},\omega)+\partial_j\delta j_i(\mathbf{r},\omega)) \\ &+(\delta f^h_{xcL}(\rho_0,\omega)-2f^h_{xcT}(\rho_0,\omega))\delta_{ij}\nabla\cdot\delta\mathbf{j}(\mathbf{r},\omega)\Big\} \\ &+\frac{1}{\rho\omega^2}\sum_j\partial_j\Big\{f^h_{xcT}(\omega)(\delta j_i\partial_j\rho_0+\delta j_j\partial_i\rho_0) \\ &+(\delta f^h_{xcL}(\omega)-2f^h_{xcT}(\omega))\delta_{ij}(\delta\mathbf{j}\cdot\nabla\rho_0)\Big\} \\ &-\frac{1}{\rho\omega^2}\sum_j\partial_j\rho_0\Big\{f^h_{xcT}(\omega)(\partial_i\delta j_j+\partial_j\delta j_i) \\ &+(\delta f^h_{xcL}(\omega)-2f^h_{xcT}(\omega))\delta_{ij}(\nabla\cdot\delta\mathbf{j})\Big\}. \end{aligned} \tag{4.167}$$

The last two lines are proportional to derivatives of $\rho_0(\mathbf{r})$ and therefore of first order in γ. Since $1/\rho = 1/\rho_0(\mathbf{r}) + O(\gamma)$ and $f^h_{xcL,T}(\rho,\omega) = f^h_{xcL,T}(\rho,\omega) + O(\gamma)$ we can replace $\rho \to \rho_0(\mathbf{r})$ in these last two lines and rewrite this expression up to terms of

order γ^2 as

$$\begin{aligned}
\delta A_{xc,i}(\mathbf{r},\omega) &= \frac{1}{i\omega}\partial_i \delta v_{xc}^{ALDA}(\mathbf{r},\omega) \\
&- \frac{1}{\rho_0\omega^2}\sum_j \partial_j \Big\{ \rho_0 f_{xcT}^h(\rho_0,\omega)(\partial_i \delta j_j(\mathbf{r},\omega) + \partial_j \delta j_i(\mathbf{r},\omega)) \\
&+ \rho_0(\delta f_{xcL}^h(\rho_0,\omega) - 2 f_{xcT}^h(\rho_0,\omega))\delta_{ij}\nabla\cdot\delta\mathbf{j}(\mathbf{r},\omega)\Big\} \\
&+ \frac{1}{\rho_0\omega^2}\sum_j \partial_j [f_{xcT}^h(\rho_0,\omega)(\delta j_i \partial_j \rho_0 + \delta j_j \partial_i \rho_0) \\
&+ (\delta f_{xcL}^h(\rho_0,\omega) - 2 f_{xcT}^h(\rho_0,\omega))\delta_{ij}(\delta\mathbf{j}\cdot\nabla\rho_0)] \\
&= \frac{1}{i\omega}\partial_i \delta v_{xc}^{ALDA}(\mathbf{r},\omega) \\
&- \frac{1}{\rho_0\omega^2}\sum_j \partial_j \Big\{ \rho_0^2 f_{xcT}^h(\rho_0,\omega)\Big[\frac{\partial_i\delta j_j}{\rho_0} - \frac{\delta j_j \partial_i\rho_0}{\rho_0^2} + \frac{\partial_j \delta j_i}{\rho_0} - \frac{\delta j_i \partial_j \rho_0}{\rho_0^2}\Big] \\
&+ \rho_0^2((\delta f_{xcL}^h(\rho_0,\omega) - 2 f_{xcT}^h(\rho_0,\omega))\delta_{ij}\Big[\frac{\nabla\cdot\delta\mathbf{j}}{\rho_0} - \frac{\delta\mathbf{j}\cdot\nabla\rho_0}{\rho_0^2}\Big]\Big\} \\
&= \frac{1}{i\omega}\partial_i \delta v_{xc}^{ALDA}(\mathbf{r},\omega) \\
&- \frac{1}{\rho_0\omega^2}\sum_j \partial_j \Big\{ \rho_0^2 f_{xcT}^h(\rho_0,\omega)(\partial_i u_j(\mathbf{r},\omega) + \partial_j u_i(\mathbf{r},\omega)) \\
&+ \rho_0^2(\delta f_{xcL}^h(\rho_0,\omega) - 2 f_{xcT}^h(\rho_0,\omega))\delta_{ij}\nabla\cdot\mathbf{u}(\mathbf{r},\omega)\Big\}, \qquad (4.168)
\end{aligned}$$

where we defined the velocity field as $\mathbf{u}(\mathbf{r},\omega) = \delta\mathbf{j}(\mathbf{r},\omega)/\rho_0(\mathbf{r})$. The latter expression can now finally be rewritten as

$$\delta A_{xc,i}(\mathbf{r},\omega) = \frac{1}{i\omega}\partial_i \delta v_{xc}^{ALDA}(\mathbf{r},\omega) - \frac{1}{i\omega\rho_0(\mathbf{r})}\sum_j \partial_j \sigma_{xc,ij}(\mathbf{r},\omega), \qquad (4.169)$$

where we defined

$$\sigma_{xc,ij}(\mathbf{r},\omega) = \tilde{\eta}_{xc}(\mathbf{r},\omega)\left[\partial_i u_j + \partial_j u_i - \frac{2}{3}\delta_{ij}(\nabla\cdot\mathbf{u})\right] + \tilde{\zeta}_{xc}(\mathbf{r},\omega)\delta_{ij}(\nabla\cdot\mathbf{u}), \qquad (4.170)$$

and we defined the coefficients

$$\tilde{\eta}_{xc}(\mathbf{r},\omega) = -\frac{\rho_0^2(\mathbf{r})}{i\omega} f_{xcT}^h(\rho_0,\omega) \qquad (4.171)$$

$$\tilde{\zeta}_{xc}(\mathbf{r},\omega) = -\frac{\rho_0^2(\mathbf{r})}{i\omega}[f_{xcL}^h(\rho_0,\omega) - \frac{4}{3} f_{xcT}^h(\rho_0,\omega) - f_{xcL}^h(\rho_0,\omega=0)] \qquad (4.172)$$

The equation Eq. (4.169) is the form of the Vignale-Kohn functional as derived by Vignale, Ullrich and Conti [46]. We note that $\sigma_{xc}(\mathbf{r},\omega)$ has the structure of a symmetric viscoelastic stress tensor.

4.6 The Response Coefficients $f^h_{xcL,T}(\rho,\omega)$

The longitudinal and transverse response coefficients of the homogeneous electron gas $f^h_{xcL}(\rho,\omega)$ and $f^h_{xcT}(\rho,\omega)$ still have to be specified. These functions are well studied [14, 15, 47–49]. In Fourier space they are defined as

$$\lim_{\mathbf{k}\to 0} f^h_{xcL,T}(\mathbf{k},\omega) \equiv f^h_{xcL,T}(\omega) = \lim_{\mathbf{k}\to 0} \frac{\omega^2}{k^2}\left(\chi^{-1}_{s,L,T}(\mathbf{k},\omega) - \chi^{-1}_{L,T}(\mathbf{k},\omega)\right) - v_{L,T}(\mathbf{k}), \tag{4.173}$$

where $\chi_{L,T}(\mathbf{k},\omega)$ is the current-current longitudinal (transverse) response function of the homogeneous electron gas, $\chi_{s,L,T}(\mathbf{k},\omega)$ are the equivalent response functions of the noninteracting homogeneous electron gas, $v_L(\mathbf{k}) = 4\pi/k^2$ is the Fourier transform of the Coulomb potential, and $v_T(\mathbf{k}) = 0$. The identity $\lim_{\mathbf{k}\to 0} f^h_{xcL,T}(\mathbf{k},\omega) \equiv f^h_{xcL,T}(\omega)$ was obtained by Vignale and Kohn [13, 50]. Note that $f^h_{xcL}(\mathbf{k},\omega)$ as defined in Eq. (4.173) coincides with $f^h_{xc}(\mathbf{k},\omega)$ from scalar TDDFT and it can thus be related to the local field correction $G(\mathbf{k},\omega)$ according to

$$f^h_{xcL}(\mathbf{k},\omega) = -v_L(\mathbf{k})G(\mathbf{k},\omega). \tag{4.174}$$

The response functions $\chi_{s,L,T}(\mathbf{k},\omega)$ in Eq. (4.173) are well-known functions first calculated by Lindhard [51] and are given by

$$\chi_{s,L}(\mathbf{k},\omega) = \lim_{\eta\to 0^+} \frac{\omega^2}{k^2}\int \frac{d\mathbf{p}}{(2\pi)^3} \frac{f(\epsilon_{\mathbf{p}}) - f(\epsilon_{\mathbf{p}+\mathbf{k}})}{\omega - (\epsilon_{\mathbf{p}+\mathbf{k}} - \epsilon_{\mathbf{p}}) + i\eta} \tag{4.175}$$

and

$$\chi_{s,T}(\mathbf{k},\omega) = \rho_0 + \lim_{\eta\to 0^+} \frac{1}{2}\int \frac{d\mathbf{p}}{(2\pi)^3}\left(k^2 - \frac{(\mathbf{p}\cdot\mathbf{k})^2}{k^2}\right) \frac{f(\epsilon_{\mathbf{p}}) - f(\epsilon_{\mathbf{p}+\mathbf{k}})}{\omega - (\epsilon_{\mathbf{p}+\mathbf{k}} - \epsilon_{\mathbf{p}}) + i\eta}, \tag{4.176}$$

where $\epsilon_k = k^2/2$ is the free particle energy and $f(\epsilon_{\mathbf{p}})$ is the Fermi distribution function. The full response functions $\chi_{L,T}(\mathbf{k},\omega)$ are not known analytically though. There are, however, well-known exact features of $\chi_{L,T}(\mathbf{k},\omega)$ and $G(\mathbf{k},\omega)$ obtained from sum rules and results from second-order perturbative expansions. From these features and the relations (4.173) and (4.174) Gross and Kohn (GK) obtained exact properties of $f^h_{xcL}(\mathbf{k},\omega)$ for the three-dimensional electron gas [45, 52]. We summarize them here

1. As a consequence of the compressibility sum rule we have [53]

$$\lim_{\mathbf{k}\to 0}\lim_{\omega\to 0} f^h_{xcL}(\mathbf{k},\omega) = \frac{d^2\epsilon^h_{xc}(\rho)}{d\rho^2} \equiv f_{L,0}(\rho). \tag{4.177}$$

2. It follows from the third-frequency-moment sum rule that we have the relation [52, 53]

$$\lim_{\mathbf{k}\to 0}\lim_{\omega\to\infty} f^h_{xcL}(\mathbf{k},\omega) = -\frac{4}{5}\rho^{2/3}\frac{d}{d\rho}\left[\frac{\epsilon^h_{xc}(\rho)}{\rho^{2/3}}\right] + 6\rho^{1/3}\frac{d}{d\rho}\left[\frac{\epsilon^h_{xc}(\rho)}{\rho^{1/3}}\right] \equiv f_{L,\infty}(\rho). \tag{4.178}$$

3. According to the best estimates of $\epsilon^h_{xc}(\rho)$ [54, 55] we have for all densities ρ

$$f_{L,0}(\rho) < f_{L,\infty}(\rho) < 0. \tag{4.179}$$

4. The function $f^h_{xcL}(\mathbf{k},\omega)$ is complex-valued and obeys the following symmetry relations,

$$\mathrm{Re}f^h_{xcL}(\mathbf{k},\omega) = \mathrm{Re}f^h_{xcL}(\mathbf{k},-\omega) \tag{4.180}$$

$$\mathrm{Im}f^h_{xcL}(\mathbf{k},\omega) = -\mathrm{Im}f^h_{xcL}(\mathbf{k},-\omega). \tag{4.181}$$

5. Since $f^h_{xcL}(\mathbf{k},\omega)$ is an analytic functions of ω in the upper half of the complex ω-plane and approaches a real function for $\omega\to\infty$ it satisfies the standard Kramers-Krönig relations,

$$\mathrm{Re}f^h_{xcL}(\mathbf{k},\omega) = f^h_{xcL}(\mathbf{k},\infty) + P\int_{-\infty}^{\infty}\frac{d\omega'}{\pi}\frac{\mathrm{Im}f^h_{xcL}(\mathbf{k},\omega')}{\omega'-\omega}, \tag{4.182}$$

$$\mathrm{Im}f^h_{xcL}(\mathbf{k},\omega) = -P\int_{-\infty}^{\infty}\frac{d\omega'}{\pi}\frac{\mathrm{Re}f^h_{xcL}(\mathbf{k},\omega') - f^h_{xcL}(\mathbf{k},\infty)}{\omega'-\omega}, \tag{4.183}$$

where P denotes the principle value of the integral.

6. The imaginary part of $f^h_{xcL}(\mathbf{k},\omega)$ has the following behavior in the limit $\omega\to\infty$,

$$\lim_{\omega\to\infty}\mathrm{Im}f^h_{xcL}(\mathbf{k},\omega) = -\frac{c_L}{\omega^{3/2}}, \tag{4.184}$$

for all $\mathbf{k} < \infty$ [56]. The constant c_L was obtained from a second-order perturbative expansion of the irreducible polarization propagator [56] according to which

$$c_L = \frac{23\pi}{15}. \tag{4.185}$$

7. The result obtained in 6 together with the Kramers-Krönig relations in 5 give the following behavior for the real part of $f^h_{xcL}(\mathbf{k},\omega)$ in the limit $\omega\to\infty$ [45],

$$\lim_{\omega\to\infty}\mathrm{Re}f^h_{xcL}(\mathbf{k},\omega) = f_{L,\infty}(\mathbf{q}) + \frac{c}{\omega^{3/2}}. \tag{4.186}$$

Because $c > 0$ this means that f_∞ is approached from above.

Under some implicit assumptions Gross and Kohn derived an interpolation formula for the imaginary part of $f^h_{xcL}(\mathbf{k},\omega)$ in the limit $\mathbf{k}\to 0$ which satisfies all of the above mentioned exact features [45]. It is given by

$$\mathrm{Im}f^{h,GK}_{xcL}(\rho,\omega)=\frac{a(\rho)\omega}{[1+b(\rho)\omega^2]^{5/4}}, \tag{4.187}$$

where

$$a(\rho) = -c_L\left(\frac{\gamma}{c_L}\right)^{5/3}(f_{L,\infty}(\rho)-f_{L,0}(\rho))^{5/3} \tag{4.188}$$

$$b(\rho) = \left(\frac{\gamma}{c_L}\right)^{4/3}(f_{L,\infty}(\rho)-f_{L,0}(\rho))^{4/3} \tag{4.189}$$

$$\gamma = \frac{\left[\Gamma(\frac{1}{4})\right]^2}{4\sqrt{2\pi}}, \tag{4.190}$$

with $f_0(\rho)$, $f_\infty(\rho)$, and c_L determined by Eqs. (4.177), (4.178), and (4.185), respectively. The real part of $\mathrm{Im}f^h_{xcL}(\omega)$ can subsequently be obtained from Eq. (4.182) evaluated at $\mathbf{k}=0$,

$$\mathrm{Re}f^h_{xcL}(\omega)=f^h_{xcL}(\infty)+P\int_{-\infty}^{\infty}\frac{d\omega'}{\pi}\frac{\mathrm{Im}f^h_{xcL}(\omega')}{\omega'-\omega}. \tag{4.191}$$

The implicit assumptions mentioned above are that the right-hand sides of Eqs. (4.177) and (4.178) do not change upon the interchange of the order of limits on the left-hand sides of these equations. However, it was shown by Conti and Vignale that upon the interchange of the order of limits in Eq. (4.177) the right-hand side acquires an extra term. We will discuss this later in this section.

A different approach to obtain $f^h_{xcL}(\omega)$ as well as $f^h_{xcT}(\omega)$ was given by Conti, Nifosì, and Tosi (CNT) [14]. They calculated $\mathrm{Im}f_{xcL,T}(\omega)$ by direct evaluation of the imaginary parts of the current-current response functions, $\mathrm{Im}\chi_{L,T}(\mathbf{k},\omega)$. CNT used an exact expression for $\mathrm{Im}\chi_{L,T}(\mathbf{k},\omega)$ in terms of four-point response functions which were subsequently approximated by decoupling them into products of two-point response functions. In order to include the effect of plasmons the two-point response functions were then taken to be the RPA response functions. This decoupling scheme only keeps direct contributions and neglects exchange processes. To account for the latter processes CNT introduced a phenomenological factor which reduces the total two-pair spectral weight by a factor of 2 in the high-frequency limit. In the low-frequency limit the factor is close to unity at metallic densities, thereby largely neglecting exchange processes. A distinct feature of the CNT result is a pronounced peak at $\omega=2\omega_{pl}$ in $\mathrm{Im}f_{xcL,T}(\omega)$, where ω_{pl} is the plasmon frequency. Since the

double excitations take up most of the spectral strength and the plasmon excitation is large with respect to single-pair excitations, the spectral strength accumulates around $\omega = 2\omega_{pl}$. The high-frequency behavior of the imaginary part of $f^h_{xcL}(\omega)$ is equal to Eq. (4.184) with $c_L = 23\pi/15$ in accordance with the result obtained by Glick and Long [56]. For the high-frequency behavior of the imaginary part of $f^h_{xcT}(\omega)$ CNT find

$$\lim_{\omega\to\infty} \mathrm{Im} f^h_{xcT}(\mathbf{k},\omega) = -\frac{c_T}{\omega^{3/2}}, \tag{4.192}$$

with $c_T = 16\pi/15$. The real parts of $f_{xcL,T}(\omega)$ can again be obtained from the Kramers-Krönig relation (4.182) where the high-frequency limit of $f^h_{xcL}(\omega)$ is given in Eq. (4.178) and the high-frequency limit of $f^h_{xcT}(\omega)$ is given by [14]

$$\lim_{\mathbf{k}\to 0}\lim_{\omega\to\infty} f^h_{xcT}(\mathbf{k},\omega) = \frac{2}{5}\rho^{2/3}\frac{d}{d\rho}\left[\frac{\epsilon^h_{xc}(\rho)}{\rho^{2/3}}\right] + 2\rho^{1/3}\frac{d}{d\rho}\left[\frac{\epsilon^h_{xc}(\rho)}{\rho^{1/3}}\right] \equiv f_{T,\infty}(\rho). \tag{4.193}$$

The low-frequency limit of $f^h_{xcL}(\omega)$ was obtained from Eq. (4.177). Thereby CNT assume that the order of the limits on the left-hand side of Eq. (4.177) can be interchanged without significantly changing the result on the right-hand side. Since they expect the discontinuity in the limit $(\mathbf{k},\omega) \to (0,0)$ to be small and since its exact value is unknown they prefer to enforce equality of the order of limits. Furthermore, CNT introduced parametrizations for $\mathrm{Im} f_{xcL,T}(\omega)$ that reproduce their numerical results. They are given by

$$\begin{aligned}
\mathrm{Im} f^{h,CNT}_{xcL}(\omega) &= -g_x(\omega)\left\{\Theta(2-\omega)\left[c_0\omega + c_1\frac{\omega-1}{e^{(7/\omega)-5}+1}\right]\right. \\
&\quad \left. +\Theta(\omega-2)\frac{d_0\sqrt{\omega-2}+d_1}{\omega(\omega-\omega_1\sqrt{\omega}-\omega_2)}\right\} \qquad (4.194)\\
\mathrm{Im} f^{h,CNT}_{xcT}(\omega) &= 0.72\mathrm{Im} f^{h,CNT}_{xcL}(\omega). \qquad (4.195)
\end{aligned}$$

In the above expression ω is in units of the plasmon frequency $\omega_{pl} = \sqrt{4\pi\rho}$ and $f^{CNT}_{xcL,T}$ is in units of $2\omega_{pl}/\rho$. The function $g_x(\omega)$ in the parametrizations is the phenomenological factor that accounts for exchange proccesses. It is given by

$$g_x(\omega) = \frac{\beta + 0.5\omega/(2\epsilon_F)}{1+\omega/(2\epsilon_F)}, \tag{4.196}$$

where $\epsilon_F = k_F^2/2$ is the Fermi energy, in which the Fermi momentum k_F is given by $k_F^3 = (3\pi^2\rho)$. The fit parameters $c_0, c_1, d_0, d_1, \omega_1, \omega_2, \beta$ depend on the Wigner-Seitz radius r_s $(4\pi r_s^3/3 = 1/\rho)$ and can be found in the CNT paper (Ref. [14]) for several values of r_s.

Conti and Vignale [49] obtained exact results for $\lim_{\omega\to 0}\lim_{\mathbf{k}\to 0} f_{xcL,T}(\mathbf{k},\omega)$ by comparing the microscopic linear-response equations with the macroscopic viscoelastic

equation of motion. Their evaluations led to the following identities for the three-dimensional electron gas,

$$\lim_{\omega\to 0}\lim_{\mathbf{k}\to 0} f^h_{xcL}(\mathbf{k},\omega) = \frac{1}{\rho^2}\left(K_{xc}+\frac{4}{3}\mu_{xc}\right) \equiv \tilde{f}_{L,0}(\rho) \tag{4.197}$$

$$\lim_{\omega\to 0}\lim_{\mathbf{k}\to 0} f^h_{xcT}(\mathbf{k},\omega) = \frac{\mu_{xc}}{\rho^2} \equiv \tilde{f}_{T,0}(\rho), \tag{4.198}$$

where the tilde in $\tilde{f}_{L,0}(\rho)$ and $\tilde{f}_{T,0}(\rho)$ indicates that these quantities were obtained from taking the reverse order of limits with respect to the order of limits that was used to obtain $f_{L,0}$ in Eq. (4.177). The quantity μ_{xc} is the exchange-correlation part of the shear modulus and K_{xc} is the exchange-correlation part of the bulk modulus which can be expressed as

$$K_{xc} = \rho^2 \frac{d^2\epsilon^h_{xc}(\rho)}{d\rho^2}. \tag{4.199}$$

From Eqs. (4.197) and (4.199) we observe that interchanging the order of limits on the left-hand side of Eq. (4.177) gives an extra term on the right-hand side equal to $4\mu_{xc}/3$. The shear modulus remains finite in the $\omega \to 0$ limit because the $q \to 0$ limit is taken before the $\omega \to 0$ limit. Taking the reverse order of limits would result in a shear modulus equal to zero. In that limit, however, $f^h_{xcT}(\mathbf{k},\omega)$ is no longer related to the shear modulus, but to the diamagnetic susceptibility, which is very small. From the above considerations we see that effectively GK and CNT make the approximation $\mu_{xc} = 0$.

Let us now write Eqs. (4.171) and (4.172) in terms of the homogeneous electron gas density ρ

$$\tilde{\eta}^h_{xc}(\mathbf{r},\omega) = -\frac{\rho^2}{i\omega} f^h_{xcT}(\rho,\omega) \tag{4.200}$$

$$\tilde{\zeta}^h_{xc}(\mathbf{r},\omega) = -\frac{\rho^2}{i\omega}\left[f^h_{xcL}(\rho,\omega) - \frac{4}{3}f^h_{xcT}(\rho,\omega) - \frac{d^2\epsilon^h_{xc}(\rho)}{d\rho^2}\right], \tag{4.201}$$

where we used that

$$f^h_{xcL}(\rho,\omega=0) = \lim_{\mathbf{k}\to 0}\lim_{\omega\to 0} f^h_{xcL}(\rho,\mathbf{k},\omega) = \frac{d^2\epsilon^h_{xc}(\rho)}{d\rho^2}. \tag{4.202}$$

From Eqs. (4.197), (4.198), and (4.199) we observe that the coefficient $\zeta^h_{xc}(\mathbf{r},\omega)$ contains a factor that has the property

$$\lim_{\omega\to 0}\left[f^h_{xcL}(\rho,\omega) - \frac{4}{3}f^h_{xcT}(\rho,\omega) - \frac{d^2\epsilon^h_{xc}(\rho)}{d\rho^2}\right] = 0. \tag{4.203}$$

Conti and Vignale further showed that μ_{xc} can be related to the Landau parameters F_l according to

$$\mu_{xc} = \frac{2\rho\epsilon_F}{5}\frac{F_2/5 - F_1/3}{1 + F_1/3}. \tag{4.204}$$

Qian and Vignale (QV) [15] combined the methods of GK and CNT. They obtained an analytic result for the slope of $\mathrm{Im}f_{xcL,T}(\omega)$ at $\omega = 0$ by evaluating $\mathrm{Im}\chi_{L,T}(\mathbf{k},\omega)$ within perturbation theory in a similar way as CNT. The direct contributions were treated the same, but QV also included their exchange counterparts in the evaluation. The slopes of $\mathrm{Im}f_{xcL,T}(\omega)$ at $\omega = 0$ are then given by

$$\lim_{\omega\to 0}\frac{\mathrm{Im}f^h_{xcL,T}(\omega)}{\omega} = -\frac{k_F S_{L,T}}{(\rho\pi)^2}, \tag{4.205}$$

where

$$\begin{aligned} S_L &= -\frac{1}{45\pi}\left\{5 - (\lambda + 5/\lambda)\tan^{-1}(\lambda) - \frac{2}{\lambda}\sin^{-1}\left(\frac{\lambda}{\sqrt{1+\lambda^2}}\right)\right. \\ &\quad \left. + \frac{2}{\lambda\sqrt{2+\lambda^2}}\left[\frac{\pi}{2} - \tan^{-1}\left(\frac{1}{\lambda\sqrt{2+\lambda^2}}\right)\right]\right\} \qquad (4.206) \\ S_T &= \frac{3}{4}S_L. \qquad (4.207) \end{aligned}$$

Here λ is defined as $\lambda = \sqrt{\pi k_F}$. They then adopted the interpolation scheme of GK for $\mathrm{Im}f_{xcL,T}(\omega)$ but with the coefficients now determined by their analytic result for the slope at $\omega = 0$ in Eq. (4.205) and the correct low-frequency limits given in Eqs. (4.197) and (4.198) as well as the correct high-frequency behavior. Their parametrizations for $\mathrm{Im}f_{xcL,T}(\omega)$ are given by

$$\mathrm{Im}f^{h,QV}_{xcL,T}(\omega) = -\frac{2\omega_{pl}}{\rho}\tilde{\omega}\left\{\frac{a_{L,T}}{(1 + b_{L,T}\tilde{\omega}^2)^{5/4}} + \tilde{\omega}^2\exp\left[-\frac{(|\tilde{\omega}| - \Omega_{L,T})^2}{\Gamma_{L,T}}\right]\right\}, \tag{4.208}$$

where $\tilde{\omega} = \omega/(2\omega_{pl})$. We see that the first term is the GK interpolation formula. The second term arises from the extra constraint given in Eq. (4.205). It models the two-plasmon contribution first identified by CNT. The requirement that this contribution has its maximum value near $\omega = 2\omega_{pl}$ yields the following relation between $\Omega_{L,T}$ and $\Gamma_{L,T}$,

$$\Omega_{L,T} = 1 - \frac{3\Gamma_{L,T}}{2}. \tag{4.209}$$

The parameter $a_{L,T}$ is fixed by the low-frequency result given in Eq. (4.205) and the parameter $b_{L,T}$ is fixed by the high-frequency results given in Eqs. (4.178) and

(4.193). They are given by

$$a_{L,T} = 2\left(\frac{2}{3}\right)^{1/3}\pi^{-2/3}r_s^2 S_{L,T} \tag{4.210}$$

$$b_{L,T} = 16\left(\frac{2^{10}}{3\pi^8}\right)^{1/15} r_s \left(\frac{S_{L,T}}{c_{L,T}}\right)^{4/5}. \tag{4.211}$$

From Eq. (4.191) and an equivalent expression for $f^h_{xcT}(\omega)$ together with Eq. (4.208) we obtain

$$-\frac{2\omega_{pl}}{\rho}\left\{\frac{4\sqrt{2\pi}a_{L,T}}{[\Gamma(1/4)]^2\sqrt{b_{L,T}}} + \frac{1}{2\pi}\left[2\Omega_{L,T}\Gamma_{L,T}\exp\left[-\frac{\Omega^2_{L,T}}{\Gamma_{L,T}}\right]\right.\right.$$
$$\left.\left. + \sqrt{\pi\Gamma_{L,T}}\left(\Gamma_{L,T}+2\Omega^2_{L,T}\right)\left(1+\mathrm{erf}\left[\frac{\Omega_{L,T}}{\sqrt{\Gamma_{L,T}}}\right]\right)\right]\right\} = \tilde{f}_{L,T,0}(\rho) - f_{L,T,\infty}(\rho), \tag{4.212}$$

where the error function is defined by

$$\mathrm{erf}(x) = \frac{2}{\sqrt{\pi}}\int_0^x e^{-y^2}dy. \tag{4.213}$$

The values for μ_{xc} that enter $\tilde{f}_{L,T,0}(\rho)$ can be obtained for some values of r_s either from Eq. (4.204) using the Landau parameters calculated by Yasuhara and Ousaka [57] as was done by Qian and Vignale (QV) [15] or from the direct calculations of μ_{xc} by Nifosì, Conti, and Tosi (NCT) [48]. However, NCT do not expect their values for μ_{xc} to be very accurate as they were obtained from the integration over the whole frequency range of $\mathrm{Im}f_{xcT}(\omega)$ using an equivalent expression of the Kramers-Krönig relation at $\mathbf{k}=0$ given in Eq. (4.191) for the transverse coefficient. A comparison of μ_{xc} obtained with the two calculations mentioned above is given in Table 4.1 up to $r_s = 5$ from which it is clear that the two calculations yield quite different results especially for the higher r_s values.

Let us now evaluate Eqs. (4.171) and (4.172) in the limit $\omega \to 0$. These equations can be rewritten as

$$\tilde{\eta}_{xc}(\mathbf{r},\omega) = -\frac{\rho_0^2(\mathbf{r})}{i\omega}f^h_{xcT}(\rho_0,\omega) \tag{4.214}$$

$$\tilde{\zeta}_{xc}(\mathbf{r},\omega) = -\frac{\rho_0^2(\mathbf{r})}{i\omega}\left[f^h_{xcL}(\rho_0,\omega) - \frac{4}{3}f^h_{xcT}(\rho_0,\omega) - \frac{d^2\epsilon^h_{xc}(\rho_0)}{d\rho^2}\right], \tag{4.215}$$

where we used Eq. (4.202). Using Eq. (4.203) we obtain the following limits,

$$\lim_{\omega\to 0}\omega\tilde{\eta}_{xc}(\mathbf{r},\omega) = i\rho_0^2(\mathbf{r})\tilde{f}_T(\rho) \tag{4.216}$$

$$\lim_{\omega\to 0}\omega\tilde{\zeta}_{xc}(\mathbf{r},\omega) = 0. \tag{4.217}$$

r_s	0.5	1	2	3	4	5
QV	-	0.00738	0.00770	0.00801	0.00837	0.00869
NCT	0.0065	0.0064	0.0052	0.0037	0.0020	0.0002

Table 4.1: μ_{xc} in units of $2\omega_{pl}\rho$

So only the imaginary part of $\omega\tilde{\eta}_{xc}(\mathbf{r},\omega)$ remains finite in this limit and $\omega\tilde{\zeta}_{xc}(\mathbf{r},\omega)$ vanishes identically. In the limit $\omega \to 0$ the VK functional with the CNT parametrization for $f^h_{xcL,T}(\omega)$ obviously reduces to the ALDA, as it was constructed under the assumption $f^h_{xcT}(\rho,0) = 0$ which means that the tensor $\sigma_{xc}(\mathbf{r},\omega)$ given in Eq. (4.170) vanishes in this limit. The static limit of the VK functional with the QV parametrization is not equal to the ALDA since in this parametrization $f^h_{xcT}(\rho,0)$ is nonzero.

Chapter 5

Analysis of the Viscoelastic Coefficients in the Vignale-Kohn Functional: The Cases of One- and Three-Dimensional Polyacetylene

In this chapter we employ the Vignale-Kohn (VK) current functional in the calculation of the linear response properties of polyacetylene for both the one-dimensional infinite chain and the infinite three-dimensional crystal. We test the two existing parametrizations of the longitudinal and transverse exchange-correlation kernels of the homogeneous electron gas that enter the VK functional and show that they lead to very different results. We argue that this is mainly caused by the different values of these kernels in the zero-frequency limit in the two parametrizations. In this limit knowledge of the exchange correlation part of the shear modulus of the homogeneous electron gas becomes very important. It is exactly this quantity that is not known accurately. Furthermore, we show that our results are in good qualitative agreement with results obtained earlier using the Vignale-Kohn functional for polyacetylene oligomers.

5.1 Introduction

Time-dependent density functional theory (TDDFT) developed by Runge and Gross [3] makes it possible to describe the dynamic properties of interacting many-particle systems in an exact manner. [3, 20, 37, 58]. Ghosh and Dhara [4, 5] showed that the Runge-Gross theorems could be extended to systems that are subjected to general time-dependent electromagnetic fields. The method has proven to be an accurate tool in the study of electronic response properties [8, 37, 59]. In this chapter we study infinite systems for which we use time-dependent current-density-functional theory (TDCDFT) [12, 13, 37, 60]. In this approach the electron density of TDDFT is substituted by the electron current density as the fundamental quantity. There are mainly three reasons to use TDCDFT instead of ordinary TDDFT. The first reason is related to the use of periodic boundary conditions which provide an efficient way to describe infinite systems but that artificially remove the effects of density changes at the surface [7]. For example, when a system is perturbed by an electric field there will be a macroscopic response of the system and there will be a current flowing through the interior with a nonzero average given by $\mathbf{j}(t) = (1/V)\int_V \mathbf{j}(\mathbf{r},t)d\mathbf{r}$, which is the spatial average of the current density $\mathbf{j}(\mathbf{r},t)$ over an arbitrary volume V. This macroscopic current is directly related through the continuity equation to a density change at the outer surface of the system but does not correspond to a density change in the bulk of the system. The density change at the surface of the system leads to a macroscopic screening field in the bulk of the system. When using periodic boundary conditions this phenomenon cannot be described with a functional of the bulk density alone [7] but it can be described by a functional of the current density in the bulk. Some of these difficulties can be circumvented by use of an expression which relates the density-density response function to the trace of the current-current response function [8–10]. However, for anisotropic materials this relation only provides enough information to extract the trace of the dielectric tensor and not its individual components. Second, in TDDFT only the response caused by longitudinal vector potentials can be accounted for since only purely longitudinal vector potentials can be gauge transformed to scalar potentials. The scalar potential is the natural conjugate variable of the density in the meaning of a Legendre transform [20]. However, when we consider transverse vector potentials the natural Legendre conjugate is the current density [61]. Third, to describe nonlocal exchange-correlation (xc) effects in large systems [9, 62, 63] it can be more convenient and more efficient to use a local functional of the current density instead of a nonlocal functional of the density [64–66]. Within TDDFT one would need an exchange-correlation functional that is completely nonlocal to be able to take into account the charges that are

induced at the surface of the system caused by the external field and which produce a counteracting field [7, 67]. Instead, by applying a local functional of the current density we can still take into account nonlocal effects that are induced in the system by an external field.

TDDFT has mainly been used within the adiabatic local density approximation (ALDA) in which the exchange-correlation scalar potential $v_{xc}(\mathbf{r},t)$ is just a local functional of the density. In this chapter we use another method that goes beyond the ALDA in which we employ an exchange-correlation vector potential, $\mathbf{A}_{xc}(\mathbf{r},t)$, which we approximate as a local functional of the current density using the expression derived by Vignale and Kohn [12,13]. They were the first to derive an expression for $\mathbf{A}_{xc}(\mathbf{r},t)$ that goes beyond the ALDA by formulating a local gradient expansion in terms of the current density. By studying the weakly inhomogeneous electron gas they found a dynamical exchange-correlation functional in terms of the current density that is nonlocal in time but still local in space. By applying this functional in an approximated fashion as a polarization functional we have observed that the Vignale-Kohn (VK) functional holds great promise since the dielectric functions of several semiconductors were much improved [68]. However, to obtain results in good agreement with experiment an empirical prefactor had to be used to reduce the intensity of the spectra. Later van Faassen *et al.* [64, 65] showed that the inclusion of the VK functional in TDDFT calculations provides greatly improved polarizabilities for π-conjugated polymers.

The evaluation of the VK expression for $\mathbf{A}_{xc}(\mathbf{r},t)$ requires knowledge of some properties of the homogeneous electron gas, i.e., the exchange correlation energy $\epsilon^h_{xc}(\rho)$ and the longitudinal and transverse exchange-correlation kernels, $f^h_{xcL}(\rho,\omega) \equiv \lim_{\mathbf{k}\to 0} f^h_{xcL}(\rho,\mathbf{k},\omega)$ and $f^h_{xcT}(\rho,\omega) \equiv \lim_{\mathbf{k}\to 0} f^h_{xcT}(\rho,\mathbf{k},\omega)$, respectively, where ρ is the electron density of the electron gas. Knowledge of the first is already required in the ALDA and can be obtained from the accurate results of Monte Carlo calculations [55, 69]. The exchange-correlation kernels, on the other hand, are not known accurately. Gross and Kohn (GK) [45, 52] proposed an interpolation formula for $\mathrm{Im} f^h_{xcL}(\rho,\omega)$ in which the coefficients were obtained from sum rule arguments and exact results from second-order perturbation theory that fix the low- and high-frequency limits of the interpolation formula. The real part can then be obtained from the Kramers-Krönig relations. In the limit $\omega \to \infty$ their interpolation formula reduces to the exact result obtained by Glick and Long [56] However, the low-frequency behavior of their interpolation formula is only determined by global sum rules. Moreover, the real part corresponding to $\mathrm{Im} f^h_{xcL}(\rho,\omega)$ given by their interpolation formula reduces to the wrong value in the limit $\omega \to 0$. The reason is that GK implicitly assume that $\lim_{\omega\to 0}\lim_{\mathbf{k}\to 0} f^h_{xcL}(\rho,\mathbf{k},\omega) = \lim_{\mathbf{k}\to 0}\lim_{\omega\to 0} f^h_{xcL}(\rho,\mathbf{k},\omega)$. It was later shown

by Conti and Vignale that this assumption is incorrect by an explicit calculation of $\lim_{\omega\to 0}\lim_{\mathbf{k}\to 0} f^h_{xcL,T}(\rho,\mathbf{k},\omega)$ [49]. Gross and Kohn do not give an expression for $\mathrm{Im}f^h_{xcT}(\rho,\omega)$ which renders their method inadequate for evaluation of the VK functional. Conti, Nifosì, and Tosi (CNT) [14] chose a different route and calculated $\mathrm{Im}f^h_{xcL,T}(\rho,\omega)$ directly by means of an approximate decoupling of an exact four-point response function. Their results show more structure than those of GK, in particular near twice the plasmon frequency ω_{pl}, where the contribution from two-plasmon excitations is the strongest. In addition CNT introduced parametrizations of their numerical results which makes it applicable in the VK approach. However, the real part corresponding to $\mathrm{Im}f^h_{xcL,T}(\rho,\omega)$ given by their parametrizations reduce to the wrong values in the limit $\omega \to 0$. The reason is that, like GK, they use the approximation $\lim_{\omega\to 0}\lim_{\mathbf{k}\to 0} f^h_{xcL,T}(\rho,\mathbf{k},\omega) = \lim_{\mathbf{k}\to 0}\lim_{\omega\to 0} f^h_{xcL,T}(\rho,\mathbf{k},\omega)$. Qian and Vignale (QV) [15] combined the interpolation scheme of GK with the results obtained from the CNT calculations. First they obtained an exact result for the slope of the imaginary part of $\mathrm{Im}f^h_{xcL,T}(\rho,\omega)$ at $\omega = 0$. Then they adopt the GK interpolation formula in which they need one more parameter to satisfy this new constraint. This extra parameter in their scheme is the width of a Gaussian peak around $\omega = 2\omega_{pl}$ that accounts for the two-plasmon contributions found by CNT. The coefficients in their interpolation formula are chosen such to reproduce the correct behavior in the limit $\omega \to \infty$ as well as the correct behavior in the limit $\omega \to 0$. The low-frequency behavior is now determined by the exact result they found for the slope of $\mathrm{Im}f^h_{xcL,T}(\rho,\omega)$ at $\omega = 0$ and the exact result obtained by Conti and Vignale for the $\lim_{\omega\to 0}\lim_{\mathbf{k}\to 0} f^h_{xcL,T}(\rho,\mathbf{k},\omega)$ [49].

One of the aims of this chapter is to give a comparison between the CNT and QV parametrizations of $f^h_{xcL,T}(\rho,\omega)$. More specifically we will test their influence in the application of the VK functional to the calculation of linear response properties of polyacetylene. We will show that the result strongly depends on the values of $f^h_{xcT}(\rho,\omega)$ in the limit $\omega \to 0$. In order to show this we will also evaluate the CNT and the QV parametrization in the static limit. We use polyacetylene as a test case and calculate the polarizability per unit chain length of the infinite chain (1D) and the dielectric function of crystalline polyacetylene (3D). The reason for looking at polyacetylene is to be able to connect to the work of van Faassen *et al.* [64–66] in which it was one of the π-conjugated polymers studied for which a great improvement of the polarizability was found by introducing the VK functional. We will show that in the case of the infinite polymer (1D and 3D) we obtain qualitatively similar results. The polyacetylene crystal has the so-called herring-bone structure with two polymer chains per unit cell. There exist two different configurations of polyacetylene belonging to the space groups $P2_1/a$ and $P2_1/n$. The former has an inphase arrangement of the

two chains with respect to the dimerized backbone and the latter has an antiphase arrangement. It was found that the total energy for $P2_1/a$ is slightly lower than that for $P2_1/n$ and the former can therefore be considered to be more stable [70]. In this chapter we will consider polyacetylene belonging to the space group $P2_1/a$ only and therefore we will drop the specification of the space group in the remainder.

In other works calculations have been performed to obtain the absorption spectra of 1D and 3D polyacetylene by solving the Bethe-Salpeter equation (BSE), which is an accurate and well-established method. The absorption spectrum of the 1D infinite polyacetylene chain has been calculated by Rohlfing and Louie [71]. They found two bound exciton states at excitation energies 1.7 and 1.8 eV of which only the former shows a sharp peak in the absorption spectrum, the latter has no oscillator strength for optical transitions. Puschnig and Ambrosch-Draxl [72] also performed calculations on the 1D chain as well as on the 3D crystal. Starting from a ground-state DFT calculation they obtained the absorption spectrum by solving the BSE. They rigidly shifted upwards the conduction bands found from their DFT calculation in order to obtain quasiparticle energies from the Kohn-Sham energies. In the 1D case they shifted the conduction bands such as to obtain the same energy gap as Rohlfing and Louie. Subsequently solving the BSE they find a bound exciton state with nonzero oscillator strength at excitation energy 1.55 eV. In the 3D case they find the lowest exciton state to have a binding energy of 0.05 eV but it has almost no oscillator strength for optical transitions. The main feature of the absorption spectrum they found is a broad peak at 0.5 eV above the energy gap. Recent BSE calculations by Tiago *et al.* [73] on the 3D crystal show a peak at 1.7 eV. There is also experimental data available from measurements on highly oriented polyacetylene films. The polyacetylene films are oriented by stretching. The absorption spectrum measured by Leising [74] shows a broad peak at about 1.7 eV. We have to be careful, however, when comparing to experiment since the polymer crystals often suffer from substantial static and dynamic disorder [75] and it is not clear to what extent these effects influence the results.

The outline of this chapter is as follows. In Sec. 5.2 we start by giving a description of the theory we use. It consists of an outline of TDCDFT and the way in which we apply it in the regime of linear response as well as an introduction to the VK functional where we discuss some of its aspects and discuss the parametrizations of the exchange-correlation kernels of the homogeneous electron gas $f^h_{xcL,T}(\rho,\omega)$ that enter the VK functional. In Sec. 5.3 we then give the main aspects of the implementation. The computational details of the calculations are the subject of Sec. 5.4. We have tested our method on polyacetylene (1D and 3D), the results of which can be found in Sec. 5.5. Finally we draw conclusions from our findings in Sec. 5.6.

5.2 Theory

5.2.1 TDCDFT

It was shown by Runge and Gross [3] that, for a given initial state, there is a one-to-one correspondence between the time-dependent density $\rho(\mathbf{r},t)$ and the time-dependent external scalar potential $v(\mathbf{r},t)$ up to a purely time-dependent function $c(t)$. Ghosh and Dhara [4, 5] extended the Runge-Gross proof to systems subjected to general time-dependent electromagnetic fields by proving that, for a given initial state, there exists a one-to-one correspondence up to a gauge transformation between the time-dependent current density and the set of potentials $\{v(\mathbf{r},t), \mathbf{A}(\mathbf{r},t)\}$, in which $\mathbf{A}(\mathbf{r},t)$ is the time-dependent external vector potential (see also Refs. [6, 37]). The latter theory has the advantages that were already mentioned in the Introduction. Ghosh and Dhara further provide a practical scheme for calculating time-dependent densities and current densities. Here an interacting many-particle system in an external electromagnetic field is replaced by an auxiliary non-interacting many-particle system in an effective field desribed by the set of Kohn-Sham potentials $\{v_s(\mathbf{r},t), \mathbf{A}_s(\mathbf{r},t)\}$. This set of potentials has the property that it produces the exact time-dependent current density and the exact time-dependent density for a given initial state. If the initial state is the ground state, it is already determined by the ground-state density on the basis of the Hohenberg-Kohn theorem [1]. This time-dependent Kohn-Sham theory was later strengthened by a generalization of the Runge-Gross theorem by Vignale who showed that under some assumptions such a set of potentials indeed exists and is unique [6]. In the Kohn-Sham scheme the time-dependent single-particle wave functions are solutions of the following equation

$$i\frac{\partial}{\partial t}\phi_n(\mathbf{r},t) = \left(\frac{1}{2}\left[\hat{\mathbf{p}} + \mathbf{A}_s(\mathbf{r},t)\right]^2 + v_s(\mathbf{r},t)\right)\phi_n(\mathbf{r},t), \tag{5.1}$$

where $\hat{\mathbf{p}} = -i\nabla$ is the momentum operator. The time-dependent Kohn-Sham potentials are uniquely determined (apart from an arbitrary gauge transformation) by the exact time-dependent density and current density. These exact particle densities can be obtained from the solutions of Eq. (5.1) for $\phi_n(\mathbf{r},t)$:

$$\rho(\mathbf{r},t) = \sum_n f_n \phi_n^*(\mathbf{r},t)\phi_n(\mathbf{r},t) \tag{5.2}$$

and

$$\mathbf{j}(\mathbf{r},t) = \sum_n f_n \mathrm{Re}[-i\phi_n^*(\mathbf{r},t)\nabla\phi_n(\mathbf{r},t)] + \rho(\mathbf{r},t)\mathbf{A}_s(\mathbf{r},t), \tag{5.3}$$

where f_n are the occupation numbers of the Kohn-Sham wave functions and we assume that our initial state is nondegenerate and is described by a single Slater determinant.

The first and second terms on the right-hand side of Eq. (5.3) correspond to the paramagnetic and diamagnetic current, respectively. The current density defined in Eq. (5.3) is the physical gauge-invariant current density. The Kohn-Sham potentials of Eq. (5.1) consist of the externally applied potentials and potentials arising from the Hartree and exchange-correlation contributions of the density and current density. We have chosen our gauge for the potentials according to Kootstra *et al.* [76,77] where for the use of periodic boundary conditions it is essential that the macroscopic part of the external field is contained in the vector potential. The scalar potential is lattice periodic and therefore cannot contain any components that represent a macroscopic field. We split the Kohn-Sham potentials into the following contributions:

$$\mathbf{A}_s(\mathbf{r},t) = \mathbf{A}_{mac}(\mathbf{r},t) + \mathbf{A}_{xc}(\mathbf{r},t), \tag{5.4}$$

$$v_s(\mathbf{r},t) = v_{H,mic}(\mathbf{r},t) + v_{xc,mic}(\mathbf{r},t). \tag{5.5}$$

Here $v_{H,mic}(\mathbf{r},t)$ is the microscopic part of the Hartree potential and $v_{xc,mic}(\mathbf{r},t)$ is the microscopic part of the exchange-correlation potential. The term $\mathbf{A}_{mac}(\mathbf{r},t)$ denotes the macroscopic vector potential,

$$\mathbf{A}_{mac}(\mathbf{r},t) = \mathbf{A}_{ext}(\mathbf{r},t) + \mathbf{A}_{ind}(\mathbf{r},t), \tag{5.6}$$

where $\mathbf{A}_{ext}(\mathbf{r},t)$ is the external vector potential and $\mathbf{A}_{ind}(\mathbf{r},t)$ is the induced macroscopic vector potential. The latter potential accounts for the long-range contribution of the Hartree potential of the surface charge as well as the retarded contribution of the induced transverse current density. We can safely ignore the microscopic part, because its electric field contribution is already a factor ω^2/c^2 smaller than that of the microscopic Hartree potential [76,78,79]. The gauge is chosen such that the external field is incorporated into $\mathbf{A}_{mac}(\mathbf{r},t)$. Finally, $\mathbf{A}_{xc}(\mathbf{r},t)$ is the exchange-correlation vector potential. In practice approximations are required for the set of exchange-correlation potentials $\{v_{xc}(\mathbf{r},t), \mathbf{A}_{xc}(\mathbf{r},t)\}$.

5.2.2 Linear Response

To study the linear response properties of systems, which are initially in the ground state and perturbed by a time-dependent electromagnetic field, it is convenient to work in the frequency domain. To do this we use a Fourier transformation defined by

$$\tilde{\mathbf{j}}(\mathbf{r},\omega) = \int \mathbf{j}(\mathbf{r},t) e^{i\omega t} d\omega. \tag{5.7}$$

For notational convenience we will drop the tilde on $\tilde{\mathbf{j}}(\mathbf{r},\omega)$ in the following and assume that it is clear from the frequency dependence that we are dealing with a different quantity. We use similar transforms for other quantities.

A time-dependent electric field $\mathbf{E}_{ext}(\omega)$ applied to a solid will induce a macroscopic polarization $\mathbf{P}_{mac}(\omega)$ which can be obtained from the induced current density by

$$\mathbf{P}_{mac}(\omega) = \frac{-i}{\omega V}\int_V \delta\mathbf{j}(\mathbf{r},\omega)d\mathbf{r}. \tag{5.8}$$

and which will be proportional to the macroscopic field $\mathbf{E}_{mac}(\omega)$, i.e., the applied field plus the average induced field within the solid. The constant of proportionality is the electric susceptibity $\chi_e(\omega)$,

$$\mathbf{P}_{mac}(\omega) = \chi_e(\omega)\cdot\mathbf{E}_{mac}(\omega). \tag{5.9}$$

Unlike $\mathbf{P}_{mac}(\omega)$ and $\mathbf{E}_{mac}(\omega)$, the susceptibility $\chi(\omega)$ is independent of the size and shape and is therefore a bulk property of the system. The induced current density can, in principle, be calculated from the true current-current response function $\chi_{\mathbf{jj}}(\mathbf{r},\mathbf{r}',\omega)$ of the system according to

$$\delta\mathbf{j}(\mathbf{r},\omega) = \frac{-i}{\omega}\int \chi_{\mathbf{jj}}(\mathbf{r},\mathbf{r}',\omega)\cdot\mathbf{E}_{mac}(\mathbf{r}',\omega)d\mathbf{r}'. \tag{5.10}$$

From Eqs. (5.8)-(5.10) it follows that

$$\chi_e(\omega) = \frac{-1}{\omega^2}\frac{1}{V}\int d\mathbf{r}\int d\mathbf{r}'\chi_{\mathbf{jj}}(\mathbf{r},\mathbf{r}',\omega). \tag{5.11}$$

The direct evaluation of the current-current response function is, however, unpractical. In our method we therefore adopt a Kohn-Sham formulation, in which the response to an external electric field of an interacting system is calculated as the response of an auxiliary noninteracting system to an effective field described by the set of Kohn-Sham potentials $\{v_s(\mathbf{r},\omega),\mathbf{A}_s(\mathbf{r},\omega)\}$. We choose the field $\mathbf{E}_{mac}(\mathbf{r},\omega)$ to be given and its relation to $\mathbf{A}_{mac}(\mathbf{r},\omega)$ is given by $\mathbf{A}_{mac}(\mathbf{r},\omega) = \mathbf{E}_{mac}(\mathbf{r},\omega)/i\omega$. We leave the relation between $\mathbf{E}_{mac}(\mathbf{r},\omega)$ and $\mathbf{E}_{ext}(\omega)$ unspecified as this depends on the sample size and shape and requires knowledge of $\chi_e(\omega)$. The set of Kohn-Sham potentials $\{v_s(\mathbf{r},\omega),\mathbf{A}_s(\mathbf{r},\omega)\}$ have the property that they produce the exact current density of the interacting system in the noninteracting Kohn-Sham system. From the exact current density we can calculate the exact density according to the continuity equation,

$$i\omega\delta\rho(\mathbf{r},\omega) = \nabla\cdot\delta\mathbf{j}(\mathbf{r},\omega). \tag{5.12}$$

The set of Kohn-Sham potentials $\{v_s(\mathbf{r},\omega),\mathbf{A}_s(\mathbf{r},\omega)\}$ is a functional of the induced current density and therefore it has to be solved in a self-consistent manner.

Within the linear response regime the effective perturbing field in the Kohn-Sham Hamiltonian of Eq. (5.1) is given by

$$\delta\hat{H}_s(\mathbf{r},t) = \frac{1}{2}[\hat{\mathbf{p}}\cdot\delta\mathbf{A}_s(\mathbf{r},t) + \delta\mathbf{A}_s(\mathbf{r},t)\cdot\hat{\mathbf{p}}] + \delta v_s(\mathbf{r},t)., \tag{5.13}$$

in which the exchange-correlation contribution is given by

$$\delta\hat{H}_{xc}(\mathbf{r},t) = \frac{1}{2}[\hat{\mathbf{p}}\cdot\delta\mathbf{A}_{xc}(\mathbf{r},t) + \delta\mathbf{A}_{xc}(\mathbf{r},t)\cdot\hat{\mathbf{p}}] + \delta v_{xc,mic}^{ALDA}(\mathbf{r},t). \tag{5.14}$$

This defines the gauge we use for the exchange-correlation potentials, namely that all the contributions from the ALDA are contained in the scalar potential and all the contributions beyond the ALDA are contained in the vector potential. This definition is compatible with the gauge set in Eqs. (5.4) and (5.5), in which the scalar potential only contains components that represent microscopic fields. To first order the perturbation in Eq. (5.13) leads to the following expressions within the Kohn-Sham scheme for the induced density,

$$\delta\rho(\mathbf{r},\omega) = \int d\mathbf{r}' \left\{\chi_{s,\rho\mathbf{j}_p}(\mathbf{r},\mathbf{r}',\omega)\cdot\delta\mathbf{A}_s(\mathbf{r}',\omega) + \chi_{s,\rho\rho}(\mathbf{r},\mathbf{r}',\omega)\delta v_s(\mathbf{r}',\omega)\right\} \tag{5.15}$$

and the induced current density,

$$\begin{aligned}\delta\mathbf{j}(\mathbf{r},\omega) \quad = \quad & \int d\mathbf{r}' \left\{[\chi_{s,\mathbf{j}_p\mathbf{j}_p}(\mathbf{r},\mathbf{r}',\omega) + \rho_0(\mathbf{r})\delta(\mathbf{r}-\mathbf{r}')]\cdot\delta\mathbf{A}_s(\mathbf{r}',\omega)\right. \\ & \left. + \chi_{s,\mathbf{j}_p\rho}(\mathbf{r},\mathbf{r}',\omega)\delta v_s(\mathbf{r}',\omega)\right\}. \end{aligned} \tag{5.16}$$

The Kohn-Sham response functions $\chi_{s,ab}$ are properties of the ground state. They are given by

$$\chi_{s,ab}(\mathbf{r},\mathbf{r}',\omega) = \lim_{\eta\to 0^+}\sum_{n,n'}(f_n - f_{n'})\frac{[\phi_n^*(\mathbf{r})\tilde{a}\phi_{n'}(\mathbf{r})]\,[\phi_{n'}^*(\mathbf{r}')\tilde{b}\phi_n(\mathbf{r}')]}{\omega - (\epsilon_{n'}-\epsilon_n) + i\eta}. \tag{5.17}$$

in which $\tilde{a}$ and $\tilde{b}$ can be either $\tilde{\rho} = 1$ or $\tilde{\mathbf{j}}_p = -i(\nabla - \nabla^\dagger)/2$, where the dagger on the nabla operator indicates that it acts on terms to the left of it. We use a tilde instead of a hat in the auxiliary operators $\tilde{\rho}$ and $\tilde{\mathbf{j}}_p$ in order to differentiate them from the density operator and paramagnetic current-density operator. In Eq. (5.17) ϵ_n are the eigenvalues of the Kohn-Sham orbitals $\phi_n(\mathbf{r})$ of the unperturbed system. The positive infinitesimal η in Eq. (5.17) ensures the causality of the response function.

In principle the scalar potential could have been gauge transformed into a vector potential [50,80] and $\delta\rho(\mathbf{r},\omega)$ could have been expressed in terms of $\delta\mathbf{j}(\mathbf{r},\omega)$ by means of the continuity equation, Eq. (5.12). For the implementation it is, however, convenient to include both the induced density and the scalar potential in our formalism.

If we neglect the small Landau diamagnetic part, which only is important in the evaluation of magnetic properties, we can use the approximate conductivity sum rule [10],

$$\left[\chi_{s,\mathbf{j}_p\mathbf{j}_p}(\mathbf{r},\mathbf{r}',0)\right]_{ij} + \rho_0(\mathbf{r})\delta_{ij}\delta(\mathbf{r}-\mathbf{r}') = 0. \tag{5.18}$$

This sum rule can be used to relate the diamagnetic contribution to the induced current density $\delta\mathbf{j}_d(\mathbf{r},\omega) = -\rho_0(\mathbf{r})\delta\mathbf{A}_s(\mathbf{r},\omega)/c$ to the static Kohn-Sham current-current response function $\chi_{s,\mathbf{j}_p\mathbf{j}_p}(\mathbf{r},\mathbf{r}',0)$. With this approximation we now get for the induced current density

$$\begin{aligned}\delta\mathbf{j}(\mathbf{r},\omega) &= \int d\mathbf{r}' \left\{ \left(\chi_{s,\mathbf{j}_p\mathbf{j}_p}(\mathbf{r},\mathbf{r}',\omega) - \chi_{s,\mathbf{j}_p\mathbf{j}_p}(\mathbf{r},\mathbf{r}',0)\right)\cdot\delta\mathbf{A}_s(\mathbf{r}',\omega) \right. \\ &\quad \left. +\chi_{s,\mathbf{j}_p\rho}(\mathbf{r},\mathbf{r}',\omega)\delta v_s(\mathbf{r}',\omega)\right\}, \end{aligned} \tag{5.19}$$

This provides an efficient way to deal with the incompleteness of the basis set in the $\omega \to 0$ limit in actual applications. In Eq. (5.19) the Kohn-Sham potentials are given, to first order, by

$$\delta\mathbf{A}_s(\mathbf{r},\omega) = \delta\mathbf{A}_{mac}(\mathbf{r},\omega) + \delta\mathbf{A}_{xc}(\mathbf{r},\omega), \tag{5.20}$$

$$\delta v_s(\mathbf{r},\omega) = \delta v_{H,mic}(\mathbf{r},\omega) + \delta v_{xc,mic}(\mathbf{r},\omega). \tag{5.21}$$

In our gauge the use of the ALDA is equivalent to $\delta v_{xc,mic}(\mathbf{r},\omega) = \delta v^{ALDA}_{xc,mic}(\mathbf{r},\omega)$ and $\delta\mathbf{A}_{xc}(\mathbf{r},\omega) = 0$, in which case the Kohn-Sham vector potential becomes equal to $\delta\mathbf{A}_{mac}(\mathbf{r},\omega)$. In the following we will go beyond the ALDA and give an expression for $\delta\mathbf{A}_{xc}(\mathbf{r},\omega)$ using the spin-restricted expressions of Vignale and Kohn [12, 13, 46].

5.2.3 The Vignale-Kohn Functional

In this section we will present a brief summary of the derivation of the Vignale-Kohn expression for the exchange-correlation vector potential. The general expression for the exchange-correlation vector potential to first order is

$$\delta\mathbf{A}_{xc}(\mathbf{r},\omega) = \int d\mathbf{r}'\mathbf{f}_{xc}(\mathbf{r},\mathbf{r}',\omega)\cdot\delta\mathbf{j}(\mathbf{r}',\omega), \tag{5.22}$$

which defines the tensor kernel $\mathbf{f}_{xc}(\mathbf{r},\mathbf{r}',\omega)$. Here we chose the gauge in the true interacting system and in the noninteracting Kohn-Sham system such that all perturbations are included in the vector potential. Vignale and Kohn derived an approximation for this exchange-correlation kernel [12, 13]. To obtain this approximation they studied a periodically modulated electron gas with wave vector $\mathbf{q}$, i.e.,

$$\rho_0(\mathbf{r}) = \rho(1 + 2\gamma\cos(\mathbf{q}\cdot\mathbf{r})), \tag{5.23}$$

where ρ is the density of the homogeneous electron gas and $\gamma \ll 1$, and performed an expansion of the exchange-correlation kernel

$$\mathbf{f}_{xc}(\mathbf{k}+m\mathbf{q},\mathbf{k},\omega) = \frac{1}{V}\int d\mathbf{r}\int d\mathbf{r}'\,\mathbf{f}_{xc}(\mathbf{r},\mathbf{r}',\omega)e^{-i(\mathbf{k}+m\mathbf{q})\cdot\mathbf{r}}e^{i\mathbf{k}\cdot\mathbf{r}'}, \tag{5.24}$$

to second order in $\mathbf{k}$ and $\mathbf{q}$ and to first order in γ. In Eq. (5.24) V is the volume of the system and m is an integer for which to first order in γ only the values for $|m| \leq 1$ are needed. This expansion was shown to be analytic for small $\mathbf{k}$ and $\mathbf{q}$ and to be valid under the constraints $k, q \ll k_F, \omega/v_F$, where k_F and v_F are the Fermi momentum and the Fermi velocity, respectively. The coefficients in this expansion are completely determined in terms of the density ρ and the coefficients $f^h_{xcL}(\rho,\omega)$ and $f^h_{xcT}(\rho,\omega)$ of the exchange-correlation kernel of the homogeneous electron gas by the Onsager symmetry relation, the zero-force and zero-torque theorems and a Ward identity [12, 13]. The VK expression for $\delta\mathbf{A}_{xc}(\mathbf{r},\omega)$ is then obtained from

$$\delta\mathbf{A}_{xc}(\mathbf{r},\omega) = \sum_{m=0,\pm1} \int \frac{d\mathbf{k}}{(2\pi)^3}\, \mathbf{f}_{xc}(\mathbf{k}+m\mathbf{q},\mathbf{k},\omega) e^{i(\mathbf{k}+m\mathbf{q})\cdot\mathbf{r}} \delta\mathbf{j}(\mathbf{k},\omega), \tag{5.25}$$

by inserting the expansion for $\mathbf{f}_{xc}$ in Eq. (5.25) and using Eq. (5.23). Since this expression contains first- and second-order powers of $\mathbf{k}$ we obtain first- and second-order derivatives of the current density in real space. Similarly first- and second-order powers of $\mathbf{q}$ lead to first- and second-order derivatives of $\rho_0(\mathbf{r})$ in real space. The constraint $q \ll k_F, \omega/v_F$ implies in real space that

$$\frac{|\nabla\rho_0(\mathbf{r})|}{\rho_0(\mathbf{r})} \ll k_F, \omega/v_F, \tag{5.26}$$

where $k_F = v_F = (3\pi^2\rho)^{1/3}$.

From analysis of Eq. (5.25) and as a consequence of a Ward identity ρ can be replaced by $\rho_0(\mathbf{r})$ in the coefficients $f^h_{xcL}(\rho,\omega)$ and $f^h_{xcT}(\rho,\omega)$. This will only affect terms of order γ^2 which were already neglected in the derivation. By doing this we obtain a functional we can apply to general systems, although if applied to systems with large density variations we may go outside the range of validity of the VK derivation. It was shown by Vignale, Ullrich and Conti that the VK expression for $\delta\mathbf{A}_{xc}(\mathbf{r},\omega)$ could be written in the following form [46, 49],

$$i\omega\delta A_{xc,i}(\mathbf{r},\omega) = \partial_i \delta v^{ALDA}_{xc}(\mathbf{r},\omega) - \frac{1}{\rho_0(\mathbf{r})} \sum_j \partial_j \sigma_{xc,ij}(\mathbf{r},\omega), \tag{5.27}$$

where $v^{ALDA}_{xc}(\mathbf{r},\omega)$ is the ALDA exchange-correlation scalar potential and $\sigma_{xc}(\mathbf{r},\omega)$ is a tensor field which has the structure of a symmetric viscoelastic stress tensor,

$$\sigma_{xc,ij} = \tilde{\eta}_{xc}\left(\partial_j u_i + \partial_i u_j - \frac{2}{3}\delta_{ij}\sum_k \partial_k u_k\right) + \tilde{\zeta}\delta_{ij}\sum_k \partial_k u_k, \tag{5.28}$$

in which the velocity field $\mathbf{u}(\mathbf{r},\omega)$ is given by

$$\mathbf{u}(\mathbf{r},\omega) = \frac{\delta\mathbf{j}(\mathbf{r},\omega)}{\rho_0(\mathbf{r})}. \tag{5.29}$$

The coefficients $\tilde{\eta}_{xc}(\mathbf{r},\omega)$ and $\tilde{\zeta}_{xc}(\mathbf{r},\omega)$ are determined by the transverse and longitudinal response coefficients $f^h_{xcT}(\rho_0(\mathbf{r}),\omega)$ and $f^h_{xcL}(\rho_0(\mathbf{r}),\omega)$ of the homogeneous electron gas evaluated at the density $\rho_0(\mathbf{r})$,

$$\tilde{\eta}_{xc}(\mathbf{r},\omega) = \frac{i}{\omega}\rho_0^2(\mathbf{r}) f^h_{xcT}(\rho_0(\mathbf{r}),\omega), \tag{5.30}$$

and

$$\tilde{\zeta}_{xc}(\mathbf{r},\omega) = \frac{i}{\omega}\rho_0^2(\mathbf{r}) \left(f^h_{xcL}(\rho_0(\mathbf{r}),\omega) - \frac{4}{3} f^h_{xcT}(\rho_0(\mathbf{r}),\omega) - \frac{d^2\epsilon^h_{xc}}{d\rho^2}(\rho_0(\mathbf{r})) \right), \tag{5.31}$$

where ϵ^h_{xc} is the exchange-correlation energy per unit volume of the homogeneous electron gas. The quantities $\tilde{\eta}_{xc}(\mathbf{r},\omega)$ and $\tilde{\zeta}_{xc}(\mathbf{r},\omega)$ can be interpreted as viscoelastic coefficients [46,49]. The parameter $\tilde{\zeta}_{xc}(\mathbf{r},\omega)$ contains a factor for which one can prove the exact relation [46, 49]

$$\lim_{\omega\to 0} \left(f^h_{xcL}(\rho_0(\mathbf{r}),\omega) - \frac{4}{3} f^h_{xcT}(\rho_0(\mathbf{r}),\omega) - \frac{d^2\epsilon^h_{xc}}{d\rho^2}(\rho_0(\mathbf{r})) \right) = 0. \tag{5.32}$$

From Eq. (5.27) we can now derive an expression for the exchange-correlation kernel in real space for which we obtain

$$\begin{aligned} f_{xc,ij}(\mathbf{r},\mathbf{r}',\omega) &= \frac{1}{i\omega}\frac{1}{\rho_0(\mathbf{r})\rho_0(\mathbf{r}')} \left(\partial_j\partial'_i + \delta_{ij}\sum_k \partial_k\partial'_k - \frac{2}{3}\partial_i\partial'_j \right) [\delta(\mathbf{r}-\mathbf{r}')\tilde{\eta}_{xc}(\mathbf{r},\omega)] \\ &+ \frac{1}{i\omega}\frac{1}{\rho_0(\mathbf{r})\rho_0(\mathbf{r}')}\partial_i\partial'_j[\delta(\mathbf{r}-\mathbf{r}')\tilde{\zeta}_{xc}(\mathbf{r},\omega)] \\ &+ \frac{1}{\omega^2}\partial_i\partial'_j \left[\delta(\mathbf{r}-\mathbf{r}')\frac{d^2\epsilon^h_{xc}}{d\rho^2}(\rho_0(\mathbf{r})) \right]. \end{aligned} \tag{5.33}$$

Note that $f_{xc,ij}$ satisfies the Onsager symmetry relation [13], i.e.,

$$f_{xc,ij}(\mathbf{r},\mathbf{r}',\omega) = f_{xc,ji}(\mathbf{r}',\mathbf{r},\omega), \tag{5.34}$$

and it is clear from Eq. (5.33) that $\mathbf{f}_{xc}$ is local in space but nonlocal in time.

We note that after an appropriate gauge transformation the first term on the right-hand side of Eq. (5.27) is simply the ALDA scalar potential. Therefore, it is the second term on the right-hand side of Eq. (5.27) that allows us to go beyond the ALDA. In practice we consider the contribution of the ALDA within the scalar potential in accordance with the gauge we specified in the previous sections.

5.2.4 The Response Coefficients

The longitudinal and transverse response kernels of the electron gas $f^h_{xcL}(\rho,\omega)$ and $f^h_{xcT}(\rho,\omega)$ still have to be specified. These functions are well studied [14, 15, 47–49].

In Fourier space they are defined as

$$\lim_{\mathbf{k}\to 0} f^h_{xcL,T}(\mathbf{k},\omega) \equiv f^h_{xcL,T}(\omega) = \lim_{\mathbf{k}\to 0} \frac{\omega^2}{k^2}\left(\chi^{-1}_{s,L,T}(\mathbf{k},\omega) - \chi^{-1}_{L,T}(\mathbf{k},\omega)\right) - v_{L,T}(\mathbf{k}), \tag{5.35}$$

where $\chi_{L,T}(\mathbf{k},\omega)$ are the current-current longitudinal and transverse response functions of the homogeneous electron gas, $\chi_{s,L,T}(\mathbf{k},\omega)$ are the equivalent response functions of the noninteracting homogeneous electron gas, $v_L(\mathbf{k}) = 4\pi/k^2$ is the Fourier transform of the Coulomb potential, and $v_T(\mathbf{k}) = 0$. The identity $\lim_{\mathbf{k}\to 0} f^h_{xcL,T}(\mathbf{k},\omega) \equiv f^h_{xcL,T}(\omega)$ was obtained by Vignale and Kohn [13, 50]. Note that $f^h_{xcL}(\mathbf{k},\omega)$ as defined in Eq. (5.35) coincides with $f^h_{xc}(\mathbf{k},\omega)$ from scalar TDDFT and it can thus be related to the local field correction $G(\mathbf{k},\omega)$ according to

$$f^h_{xcL}(\mathbf{k},\omega) = -v_L(\mathbf{k})G(\mathbf{k},\omega). \tag{5.36}$$

Since $f^h_{xcL,T}(\mathbf{k},\omega)$ are analytic functions of ω in the upper half of the complex ω-plane and approach real functions $f^h_{xcL,T}(\mathbf{k},\infty)$ for $\omega\to\infty$ they satisfy the standard Kramers-Krönig relations,

$$\mathrm{Re}f^h_{xcL,T}(\mathbf{k},\omega) = f^h_{xcL,T}(\mathbf{k},\infty) + P\int_{-\infty}^{\infty}\frac{d\omega'}{\pi}\frac{\mathrm{Im}f^h_{xcL,T}(\mathbf{k},\omega')}{\omega'-\omega}, \tag{5.37}$$

$$\mathrm{Im}f^h_{xcL,T}(\mathbf{k},\omega) = -P\int_{-\infty}^{\infty}\frac{d\omega'}{\pi}\frac{\mathrm{Re}f^h_{xcL,T}(\mathbf{k},\omega') - f^h_{xcL,T}(\mathbf{k},\infty)}{\omega'-\omega}, \tag{5.38}$$

where P denotes the principle value of the integral. The response functions $\chi_{s,L,T}(\mathbf{k},\omega)$ in Eq. (5.35) are well-known functions first calculated by Lindhard [51] and are given by

$$\chi_{s,L}(\mathbf{k},\omega) = \lim_{\eta\to 0^+}\frac{\omega^2}{k^2}\int\frac{d\mathbf{p}}{(2\pi)^3}\frac{f(\epsilon_{\mathbf{p}}) - f(\epsilon_{\mathbf{p}+\mathbf{k}})}{\omega - (\epsilon_{\mathbf{p}+\mathbf{k}} - \epsilon_{\mathbf{p}}) + i\eta} \tag{5.39}$$

and

$$\chi_{s,T}(\mathbf{k},\omega) = \rho + \lim_{\eta\to 0^+}\frac{1}{2}\int\frac{d\mathbf{p}}{(2\pi)^3}\left(p^2 - \frac{(\mathbf{p}\cdot\mathbf{k})^2}{k^2}\right)\frac{f(\epsilon_{\mathbf{p}}) - f(\epsilon_{\mathbf{p}+\mathbf{k}})}{\omega - (\epsilon_{\mathbf{p}+\mathbf{k}} - \epsilon_{\mathbf{p}}) + i\eta}, \tag{5.40}$$

where $\epsilon_{\mathbf{p}} = p^2/2$ is the free particle energy and $f(\epsilon_{\mathbf{p}})$ is the Fermi distribution function. The full response functions $\chi_{L,T}(\mathbf{k},\omega)$ are not known analytically though. There are, however, well-known exact features of $\chi_{L,T}(\mathbf{k},\omega)$ and $G(\mathbf{k},\omega)$ in the limit $\mathbf{k}\to 0$ obtained from sum rules and results from second-order perturbative expansions. From these features and the relations (5.35) and (5.36) Gross and Kohn (GK) obtained exact properties of $f^h_{xcL}(\mathbf{k}=0,\omega) \equiv f^h_{xcL}(\omega)$ in the low- and high-frequency limits [45, 52]. Furthermore, they introduced an interpolation formula for $\mathrm{Im}f^h_{xcL}(\omega)$ which reduces to the exact high-frequency limit for $\omega\to\infty$ obtained from second-order perturbative

expansions by Glick and Long [56] and vanishes linearly in the limit $\omega \to 0$. The low-frequency behavior was determined from the $\omega \to 0$ limit of the $\mathbf{k} \to 0$ limit of Eq. (5.37) resulting in the following sum rule,

$$f^h_{xcL}(0) - f^h_{xcL}(\infty) = P \int_{-\infty}^{\infty} \frac{d\omega}{\pi} \frac{\mathrm{Im} f^h_{xcL}(\omega)}{\omega}, \tag{5.41}$$

where $f^h_{xcL}(0)$ was obtained from the compressibility sum rule [53]

$$\lim_{\mathbf{k}\to 0} \lim_{\omega \to 0} f^h_{xcL}(\mathbf{k}, \omega) = \frac{K_{xc}}{\rho^2}, \tag{5.42}$$

where K_{xc} is the exchange-correlation part of the bulk modulus given by

$$K_{xc} = \rho^2 \frac{d^2 \epsilon^h_{xc}(\rho)}{d\rho^2}, \tag{5.43}$$

and $f^h_{xcL}(\infty)$ was obtained from the third-frequency-moment sum rule [52,53], However, the compressibility sum rule contains $\lim_{\mathbf{k}\to 0} \lim_{\omega\to 0} f^h_{xcL}(\mathbf{k}, \omega)$, which is not the same as $\lim_{\omega\to 0} \lim_{\mathbf{k}\to 0} f^h_{xcL}(\mathbf{k}, \omega)$ entering Eq. (5.41) as was implicitly assumed by GK. This difference was first pointed out by Conti and Vignale [49] and will be briefly discussed below. The real part of $\mathrm{Im} f^h_{xcL}(\omega)$ can subsequently be obtained from Eq. (5.37) evaluated at $\mathbf{k} = 0$.

A different approach to obtain $f^h_{xcL}(\omega)$ as well as $f^h_{xcT}(\omega)$ was given by Conti, Nifosì, and Tosi (CNT) [14]. They calculated $\mathrm{Im} f^h_{xcL,T}(\omega)$ by direct evaluation of the imaginary parts of the current-current response functions, $\mathrm{Im}\chi_{L,T}(\mathbf{k}, \omega)$. CNT used an exact expression for $\mathrm{Im}\chi_{L,T}(\mathbf{k}, \omega)$ in terms of four-point response functions which were subsequently approximated by decoupling them into products of two-point response functions. In order to include the effect of plasmons the two-point response functions were then taken to be the RPA response functions. This decoupling scheme only keeps direct contributions and neglects exchange processes. To account for the latter processes CNT introduced a phenomenological factor which reduces the total two-pair spectral weight by a factor of 2 in the high-frequency limit. In the low-frequency limit the factor is close to unity for metallic densities, thereby largely neglecting exchange processes. A distinct feature of the CNT result is a pronounced peak at $\omega = 2\omega_{pl}$ in $\mathrm{Im} f^h_{xcL,T}(\omega)$, where ω_{pl} is the plasmon frequency. Since the double excitations take up most of the spectral strength and the plasmon excitation is large with respect to single-pair excitations, the spectral strength accumulates around $\omega = 2\omega_{pl}$. The high-frequency behavior of $\mathrm{Im} f^h_{xcL}(\omega)$ obtained by CNT coincides with the result of Glick and Long [56], and the high-frequency behavior of $\mathrm{Im} f^h_{xcT}(\omega)$ given by CNT is new. Furthermore, CNT introduced parametrizations for $\mathrm{Im} f^h_{xcL,T}(\omega)$

that reproduce their numerical results. The real parts can again be obtained from the Kramers-Krönig relation (5.37) where the high-frequency limits of $f^h_{xcL,T}(\omega)$ were obtained from third-frequency-moment sum rules [49,52,53]. However, like GK, CNT obtained the value for $f^h_{xcL}(\omega)$ in the limit $\omega \to 0$ by invoking the compressibility sum rule, thereby interchanging the order of the limits. Since they expect the discontinuity in the limit $(\mathbf{k}, \omega) \to (0, 0)$ to be small and since the exact value of this discontinuity is unknown they prefer to enforce equality of the order of limits. We note that, within the accuracy of their model, they found $f^h_{xcT}(\omega = 0)$ to be indistinguishable from zero in their calculations.

Shortly after Conti and Vignale [49] obtained exact expressions for $\lim_{\omega\to 0} \lim_{\mathbf{k}\to 0} f^h_{xcL,T}(\mathbf{k}, \omega)$ by comparing the microscopic linear-response equations with the macroscopic viscoelastic equation of motion. Their evaluations led to the following identities for the three-dimensional electron gas,

$$\lim_{\omega\to 0} \lim_{\mathbf{k}\to 0} f^h_{xcL}(\mathbf{k}, \omega) \equiv f^h_{xcL}(0) = \frac{1}{\rho^2}\left(K_{xc} + \frac{4}{3}\mu_{xc}\right) \tag{5.44}$$

$$\lim_{\omega\to 0} \lim_{\mathbf{k}\to 0} f^h_{xcT}(\mathbf{k}, \omega) \equiv f^h_{xcT}(0) = \frac{\mu_{xc}}{\rho^2}, \tag{5.45}$$

where μ_{xc} is the exchange-correlation part of the shear modulus. [From the above identities together with Eq. (5.43) follows immediately Eq. (5.32)]. The shear modulus remains finite in the $\omega \to 0$ limit because the $\mathbf{k} \to 0$ limit is taken before the $\omega \to 0$ limit. Taking the reverse order of limits would result in a shear modulus equal to zero. In that limit, however, $f^h_{xcT}(\mathbf{k}, \omega)$ is no longer related to the shear modulus, but to the diamagnetic susceptibility, which is very small. Conti and Vignale further show that μ_{xc} can be related to the Landau parameters F_l according to

$$\mu_{xc} = \frac{2\rho\epsilon_F}{5}\frac{F_2/5 - F_1/3}{1 + F_1/3}, \tag{5.46}$$

where $\epsilon_F = k_F^2/2$ is the Fermi energy. Comparing Eqs. (5.42) and (5.44) it becomes immediately clear that interchanging the order of the limits for $\lim_{\omega\to 0} \lim_{\mathbf{k}\to 0} f^h_{xcL,T}(\mathbf{k}, \omega)$ is equivalent to the approximation $\mu_{xc} = 0$, and from Eq. (5.45) we see that this means $f^h_{xcT}(0) = 0$ as observed in the calculations of CNT. In a subsequent paper Nifosì, Conti, and Tosi (NCT) [48] use the correct expressions for $f^h_{xcL,T}(0)$ given by Eqs. (5.44) and (5.45) and their calculations then show a non-vanishing $f^h_{xcT}(0)$. However, they do not expect their values for $f^h_{xcT}(0)$ to be very accurate as they are obtained from the integration over the whole frequency range of $\mathrm{Im} f^h_{xcT}(\mathbf{k} = 0, \omega)$ in Eq. (5.37).

Qian and Vignale (QV) [15] combined the methods of GK and CNT. They obtained an analytic result for the slope of $\mathrm{Im} f^h_{xcL,T}(\omega)$ at $\omega = 0$ by evaluating $\mathrm{Im}\chi_{L,T}(\mathbf{k}, \omega)$

within perturbation theory in a similar way as CNT. The direct contributions were treated the same, but QV also included their exchange counterparts in the evaluation. They adopted the interpolation scheme of GK for $\mathrm{Im}f^h_{xcL,T}(\omega)$ in which they need one more parameter to satisfy the new constraint on the slope of $\mathrm{Im}f^h_{xcL,T}(\omega)$ at $\omega = 0$. This extra parameter in their scheme is the width of a Gaussian peak around $\omega = 2\omega_{pl}$ that accounts for the two-plasmon contributions found by CNT. The coefficients in their interpolation formula are now determined by their analytic result for the slope at $\omega = 0$ and the correct low-frequency limits, Eqs. (5.44) and (5.45), as well as the correct high-frequency behavior. The values for μ_{xc} were obtained from the Landau parameters calculated by Yasuhara and Ousaka [57] for some values of of the Wigner-Seitz radius r_s ($4\pi r_s^3/3 = 1/\rho$). Their model shows a peak around $\omega = 2\omega_{pl}$ that is less pronounced than CNT's.

From Eqs. (5.30)-(5.32) we can now determine the behavior of $\tilde{\eta}_{xc}(\mathbf{r},\omega)$ and $\tilde{\zeta}_{xc}(\mathbf{r},\omega)$ in the limit $\omega \to 0$. We obtain

$$\lim_{\omega\to 0} \omega\tilde{\eta}_{xc}(\mathbf{r},\omega) = i\rho_0^2(\mathbf{r}) f^h_{xcT}(\rho_0(\mathbf{r}),0) \tag{5.47}$$

and

$$\lim_{\omega\to 0} \omega\tilde{\zeta}_{xc}(\mathbf{r},\omega) = 0. \tag{5.48}$$

So only the imaginary part of $\omega\tilde{\eta}_{xc}(\mathbf{r},\omega)$ remains finite in this limit and $\omega\tilde{\zeta}_{xc}(\mathbf{r},\omega)$ vanishes identically. In this limit the VK functional with the CNT parametrization for $f^h_{xcL,T}(\omega)$ obviously reduces to the ALDA, as it was constructed under the assumption $f^h_{xcT}(\rho,0) = 0$ which means that the tensor $\sigma_{xc}(\mathbf{r},\omega)$ given in Eq. (5.28) vanishes in this limit. The static limit of the VK functional with the QV parametrization for $f^h_{xcL,T}(\omega)$, which we will denote by QV0, is not equal to the ALDA since in this parametrization $f^h_{xcT}(\rho,0)$ is nonzero.

To summarize, the various parametrizations of $f^h_{xcL,T}(\rho,\omega)$ presented above are denoted by CNT and QV for the completely frequency-dependent parametrizations, given in Refs. [14] and [15], respectively, whereas NCT and QV0 are frequency-independent parametrizations. NCT takes its values for $f^h_{xcT}(\rho,0)$ from Ref. [48] and QV0 is simply the static limit of the QV parametrization. These four parametrizations will be used in our calculations.

5.3 Implementation

We will show that we can write $\delta\mathbf{A}_{xc}(\mathbf{r},\omega)$ as expressed in Eqs. (5.27)-(5.29) in a more convenient way,

$$\delta\mathbf{A}_{xc}(\mathbf{r},\omega) = -\frac{i}{\omega}\nabla[\delta v_{xc}^{ALDA}(\mathbf{r},\omega) + \delta u_{xc}(\mathbf{r},\omega)] + \delta\mathbf{a}_{xc}(\mathbf{r},\omega) + \nabla\times\delta\mathbf{b}_{xc}(\mathbf{r},\omega). \tag{5.49}$$

Here $\delta u_{xc}(\mathbf{r},\omega)$ is a scalar field, $\delta\mathbf{a}_{xc}(\mathbf{r},\omega)$ is a polar vector field, and $\delta\mathbf{b}_{xc}(\mathbf{r},\omega)$ is an axial vector field. There is much freedom in choosing the contributions $\delta u_{xc}(\mathbf{r},\omega)$, $\delta\mathbf{a}_{xc}(\mathbf{r},\omega)$ and $\delta\mathbf{b}_{xc}(\mathbf{r},\omega)$, and we choose a form that involves only the local values of $\delta\mathbf{j}(\mathbf{r},\omega)$, $\nabla\cdot\delta\mathbf{j}(\mathbf{r},\omega) = i\omega\delta\rho(\mathbf{r},\omega)$ and $\nabla\times\delta\mathbf{j}(\mathbf{r},\omega) = \delta\mathbf{m}(\mathbf{r},\omega)$ (For a detailed derivation see the Appendix)

$$\delta u_{xc} = -i\omega\frac{\frac{4}{3}\tilde{\eta}_{xc}+\tilde{\zeta}_{xc}}{\rho_0^2}\delta\rho + \left(\frac{\frac{4}{3}\tilde{\eta}_{xc}+\tilde{\zeta}_{xc}}{\rho_0^2}\frac{\nabla\rho_0}{\rho_0} - 2\frac{\nabla\tilde{\eta}_{xc}}{\rho_0^2}\right)\cdot\delta\mathbf{j}, \tag{5.50}$$

$$\begin{aligned} i\omega\delta\mathbf{a}_{xc} = &-i\omega\left(\frac{\frac{4}{3}\tilde{\eta}_{xc}+\tilde{\zeta}_{xc}}{\rho_0^2}\frac{\nabla\rho_0}{\rho_0} - 2\frac{\nabla\tilde{\eta}_{xc}}{\rho_0^2}\right)\delta\rho + \frac{\tilde{\eta}_{xc}}{\rho_0^2}\frac{\nabla\rho_0}{\rho_0}\times\delta\mathbf{m} \\ &+\left(\frac{\frac{1}{3}\tilde{\eta}_{xc}+\tilde{\zeta}_{xc}}{\rho_0^2}\frac{\nabla\rho_0\otimes\nabla\rho_0}{\rho_0^2} - 2\frac{\nabla\tilde{\eta}_{xc}\otimes\nabla\rho_0+\nabla\rho_0\otimes\nabla\tilde{\eta}_{xc}}{\rho_0^3}\right)\cdot\delta\mathbf{j} \\ &+\left(2\frac{\nabla\otimes\nabla\tilde{\eta}_{xc}}{\rho_0^2} + \frac{\tilde{\eta}_{xc}}{\rho_0^2}\frac{|\nabla\rho_0|^2}{\rho_0^2}\mathbf{I}\right)\cdot\delta\mathbf{j}, \end{aligned} \tag{5.51}$$

$$i\omega\delta\mathbf{b}_{xc} = \frac{\tilde{\eta}_{xc}}{\rho_0^2}\delta\mathbf{m} - \frac{\tilde{\eta}_{xc}}{\rho_0^2}\frac{\nabla\rho_0}{\rho_0}\times\delta\mathbf{j}. \tag{5.52}$$

The functions $\delta\rho(\mathbf{r},\omega)$, $\delta\mathbf{j}(\mathbf{r},\omega)$, and $\delta\mathbf{m}(\mathbf{r},\omega)$ can all be obtained by using at most first-order derivatives of the orbitals. The induced density $\delta\rho(\mathbf{r},\omega)$ and the induced current density $\delta\mathbf{j}(\mathbf{r},\omega)$ are defined in Eqs. (5.15) and (5.19), respectively. Furthermore, we have have the following expression for the curl of the induced current density $\delta\mathbf{m}(\mathbf{r},\omega)$,

$$\begin{aligned} \delta\mathbf{m}(\mathbf{r},\omega) \;=\; &\int d\mathbf{r}'\left\{\left(\chi_{s,\mathbf{mj}_p}(\mathbf{r},\mathbf{r}',\omega)-\chi_{s,\mathbf{mj}_p}(\mathbf{r},\mathbf{r}',0)\right)\cdot\delta\mathbf{A}_s(\mathbf{r}',\omega)\right. \\ &\left.+\chi_{s,\mathbf{m}\rho}(\mathbf{r},\mathbf{r}',\omega)\delta v_s(\mathbf{r}',\omega)\right\}, \end{aligned} \tag{5.53}$$

where the Kohn-Sham response $\chi_{s,ab}$ functions are given in Eq. (5.17), in which $\tilde{a}$ now has to be substituted by $\tilde{\mathbf{m}} = -i(\nabla^\dagger\times\nabla)$. Here the dagger on the nabla operator again indicates that it acts on terms to the left of it.

We are now able to write Eqs. (5.50), (5.51) and (5.52) in the following compact and elegant matrix vector product

$$\begin{pmatrix} \delta u_{xc} \\ i\omega\delta\mathbf{a}_{xc} \\ i\omega\delta\mathbf{b}_{xc} \end{pmatrix} = \begin{pmatrix} y_{\rho\rho} & y_{\rho\mathbf{j}} & 0 \\ y_{\mathbf{j}\rho} & y_{\mathbf{jj}} & y_{\mathbf{jm}} \\ 0 & y_{\mathbf{mj}} & y_{\mathbf{mm}} \end{pmatrix}\begin{pmatrix} \delta\rho \\ i\delta\mathbf{j}/\omega \\ i\delta\mathbf{m}/\omega \end{pmatrix} \tag{5.54}$$

The matrix entries are given as

$$y_{\rho\rho} = -i\omega\frac{\frac{4}{3}\tilde{\eta}_{xc}+\tilde{\zeta}_{xc}}{\rho_0^2}, \tag{5.55}$$

$$y_{\rho\mathbf{j}} = y^T_{\mathbf{j}\rho} = -i\omega\left(\frac{\frac{4}{3}\tilde{\eta}_{xc}+\tilde{\zeta}_{xc}}{\rho_0^2}-2\frac{\tilde{\eta}'_{xc}}{\rho_0}\right)\frac{\nabla\rho_0}{\rho_0}, \tag{5.56}$$

$$\begin{aligned} y_{\mathbf{jj}} &= -i\omega\left(\frac{\frac{1}{3}\tilde{\eta}_{xc}+\tilde{\zeta}_{xc}}{\rho_0^2}-4\frac{\tilde{\eta}'_{xc}}{\rho_0}+2\tilde{\eta}''_{xc}\right)\frac{\nabla\rho_0\otimes\nabla\rho_0}{\rho_0^2} \\ &\quad -i\omega\left(2\frac{\tilde{\eta}'_{xc}}{\rho_0}\frac{\nabla\otimes\nabla\rho_0}{\rho_0}+\frac{\tilde{\eta}_{xc}}{\rho_0^2}\frac{|\nabla\rho_0|^2}{\rho_0^2}\mathbf{I}\right), \end{aligned} \tag{5.57}$$

$$y_{\mathbf{jm}} = y^T_{\mathbf{mj}} = -i\omega\frac{\tilde{\eta}_{xc}}{\rho_0^2}\left[\frac{\nabla\rho_0}{\rho_0}\times\right], \tag{5.58}$$

$$y_{\mathbf{mm}} = -i\omega\frac{\tilde{\eta}_{xc}}{\rho_0^2}\mathbf{I}, \tag{5.59}$$

in which we define the antisymmetric 3×3 matrix $[\nabla\rho_0/\rho_0\times]_{ij} = -\sum_k \epsilon_{ijk}(\partial_k\rho_0)/\rho_0$ and where $\tilde{\eta}'_{xc}(\mathbf{r},\omega)$ and $\tilde{\eta}''_{xc}(\mathbf{r},\omega)$ are the first- and second-order derivatives of $\tilde{\eta}_{xc}(\mathbf{r},\omega)$ with respect to the ground-state density. The matrix in Eq. (5.54) is a local function of the ground-state density and its first- and second-order gradients and has additional ω dependence through the coefficients $\tilde{\eta}_{xc}(\mathbf{r},\omega)$ and $\tilde{\zeta}_{xc}(\mathbf{r},\omega)$.

The exchange-correlation contribution to the perturbation given in Eq. (5.14) can now be written as

$$\delta\hat{H}_{xc}(\mathbf{r},t) = \delta v_{xc}^{ALDA}(\mathbf{r},t)+\delta u_{xc}(\mathbf{r},t)+\tilde{\mathbf{j}}_p\cdot\delta\mathbf{a}_{xc}(\mathbf{r},t)+\tilde{\mathbf{m}}\cdot\delta\mathbf{b}_{xc}(\mathbf{r},t), \tag{5.60}$$

Using Eq. (5.60) the self-consistent linear-response equations can be written in the following form

$$\begin{pmatrix}\delta\rho\\ i\delta\mathbf{j}/\omega\\ i\delta\mathbf{m}/\omega\end{pmatrix} = \begin{pmatrix}\chi_{s,\rho\rho} & -i\chi_{s,\rho\mathbf{j}_p}/\omega & -i\chi_{s,\rho\mathbf{m}}/\omega\\ i\chi_{s,\mathbf{j}_p\rho}/\omega & \Delta\chi_{s,\mathbf{jj}}/\omega^2 & \Delta\chi_{s,\mathbf{jm}}/\omega^2\\ i\chi_{s,\mathbf{m}\rho}/\omega & \Delta\chi_{s,\mathbf{mj}}/\omega^2 & \Delta\chi_{s,\mathbf{mm}}/\omega^2\end{pmatrix}\begin{pmatrix}\delta v_{Hxc,mic}^{ALDA}+\delta u_{xc}\\ i\omega(\delta\mathbf{A}_{mac}+\delta\mathbf{a}_{xc})\\ i\omega\delta\mathbf{b}_{xc}\end{pmatrix} \tag{5.61}$$

where $\delta v_{Hxc,mic}^{ALDA} = \delta v_{H,mic}+\delta v_{xc,mic}^{ALDA}$. This relation has been written in such a way that all matrix elements are real and finite for nonmetals in the limit $\omega\to0$ as follows

from the following explicit expressions for the various response kernels:

$$\chi_{s,\rho\rho}(\mathbf{r},\mathbf{r}',\omega) = \sum_{n,n'} w_{nn'}(\omega)(\phi_n^*(\mathbf{r})\phi_{n'}(\mathbf{r})\phi_{n'}^*(\mathbf{r}')\phi_n(\mathbf{r}')) \tag{5.62}$$

$$-\frac{i}{\omega}\chi_{s,\rho\mathbf{a}}(\mathbf{r},\mathbf{r}',\omega) = \sum_{n,n'} w_{nn'}(\omega)\left(\phi_n^*(\mathbf{r})\phi_{n'}(\mathbf{r})\frac{i\phi_{n'}^*(\mathbf{r}')\hat{\mathbf{a}}\phi_n(\mathbf{r}')}{\epsilon_n-\epsilon_{n'}}\right) \tag{5.63}$$

$$\frac{i}{\omega}\chi_{s,\mathbf{a}\rho}(\mathbf{r},\mathbf{r}',\omega) = \sum_{n,n'} w_{nn'}(\omega)\left(\frac{i\phi_n^*(\mathbf{r}')\hat{\mathbf{a}}\phi_{n'}(\mathbf{r}')}{\epsilon_{n'}-\epsilon_n}(\mathbf{r}')\phi_{n'}^*(\mathbf{r})\phi_n(\mathbf{r})\right) \tag{5.64}$$

$$\begin{aligned}\frac{1}{\omega^2}\Delta\chi_{s,\mathbf{ab}}(\mathbf{r},\mathbf{r}',\omega) &= \frac{1}{\omega^2}(\chi_{s,\mathbf{ab}}(\omega)-\chi_{s,\mathbf{ab}}(\omega=0)) \\ &= \sum_{n,n'} w_{nn'}(\omega)\left(\frac{i\phi_n^*(\mathbf{r})\hat{\mathbf{a}}\phi_{n'}(\mathbf{r})}{\epsilon_{n'}-\epsilon_n}\frac{i\phi_{n'}^*(\mathbf{r}')\hat{\mathbf{b}}\phi_n(\mathbf{r}')}{\epsilon_n-\epsilon_{n'}}\right),\end{aligned} \tag{5.65}$$

where $\hat{\mathbf{a}}$ and $\hat{\mathbf{b}}$ can be either $\tilde{\mathbf{j}}_p$ or $\tilde{\mathbf{m}}$. We have defined

$$w_{nn'}(\omega) = \frac{(f_n-f_{n'})(\epsilon_n-\epsilon_{n'})}{(\epsilon_n-\epsilon_{n'})^2-(\omega+i\eta)^2} \tag{5.66}$$

as the frequency-dependent transition weights. In the periodic systems we study here n is a multi-index composed of the band index and the Bloch vector. The transition weights are included in the now ω-dependent quadrature scheme of the Brillouin zone in order to handle the singular denominator analytically as in Kootstra *et al.* [76, 77].

5.4 Computational Details

The implementation was done in the ADF-BAND program [76, 81–83] and we performed our calculations with this modified version. We made use of Slater-type orbitals (STO) in combination with frozen cores and a hybrid valence basis set consisting of the numerical solutions of a free-atom Herman-Skillman program [84] that solves the radial Kohn-Sham equations. The spatial resolution of this basis is equivalent to a STO triple-zeta basis set augmented with two polarization functions. This valence basis set was made orthogonal to the core states. The Herman-Skillman program also provides us with the free-atom effective potential. The Hartree potential was evaluated using an auxiliary basis set of STO functions to fit the deformation density in the ground-state calculation and the induced density in the response calculation. We used the VK exchange-correlation kernel of Eq. (5.33) to calculate the polarizability per unit chain length of an infinite polyacetylene chain and the macroscopic dielectric function of an infinite polyacetylene crystal. They are both semiconducting materials. In the 1D case we use the geometry given in Fig. 1 of Ref. [64]. For the

crystal we use the experimental structural parameters given in Table II of Ref. [70] with the exception that we put β equal to 90 deg. We used Eqs. (5.8) and (5.9) to obtain $\chi_e(\omega)$ from which the macroscopic dielectric function can directly be obtained through $\epsilon(\omega) = 1 + 4\pi\chi_e(\omega)$. To obtain the polarizability per unit chain length of the 1D polyacetylene chain we used $\mathbf{E}_{mac}(\omega) = \mathbf{E}_{ext}(\omega)$ which is justified in the 1D case for a nonconducting system. This will be discussed in the next chapter. For the evaluation of the **p**-space integrals we used a numerical integration scheme with 23 (1D) and 110 (3D) symmetry-unique sample points in the irreducible wedge of the Brillouin zone which was constructed by adopting a Lehmann-Taut tetrahedron scheme [85]. Since in the 3D calculation the dispersion in the direction of the chain is larger than perpendicular to the chain, the sampling in the direction of the chain was 11 times denser than in the direction perpendicular to it, thereby limiting the total number of **p**-points. We checked the convergence with respect to the number of conduction bands used and found that ten conduction bands are sufficient. This number was used in all our calculations. We made use of the Vosko-Wilk-Nusair parametrization [55] of the LDA exchange-correlation potential which was also used to construct the ALDA exchange-correlation kernel. As mentioned above the values of $f^h_{xcL,T}(\rho,\omega)$ were obtained from the parametrizations given in Refs. [14, 15] denoted by CNT and QV, respectively, and the values of $f^h_{xcL,T}(\rho,0)$ were taken from Refs. [15, 48] denoted by QV0 and NCT, respectively. However, $f^h_{xcL,T}(\rho,0)$ are known only at specific values of the Wigner-Seitz radius r_s ($4\pi r_s^3/3 = 1/\rho$). We used a cubic spline interpolation to obtain values for $f^h_{xcL,T}(\rho,0)$ at arbitrary r_s in which the behavior for small r_s was taken to be quadratic similar to exchange-only behavior. A plot of $f^h_{xcT}(\rho,0)$ from NCT and QV0 can be found in Fig. 5.1.

5.5 Results

In Figs. 5.2 and 5.3 we show the effect of the VK exchange-correlation kernel $\mathbf{f}_{xc}(\mathbf{r},\mathbf{r}',\omega)$ given in Eq. (5.33) on the polarizability per unit chain length of 1D polyacetylene and on the macroscopic dielectric function of 3D polyacetylene, respectively. The various results correspond to different approximations of $f^h_{xcL,T}(\rho,\omega)$ that enter $\mathbf{f}_{xc}(\mathbf{r},\mathbf{r}',\omega)$. We compare our results obtained with the VK functional with our ALDA results, in which the exchange-correlation vector potential is neglected. It clearly shows in Figs. 5.2 and 5.3 that the CNT and QV parametrizations of $f^h_{xcL,T}(\rho,\omega)$ give drastically different results. Whereas the CNT spectra are relatively close to the ALDA spectra, the QV spectra differ strongly from them. Let us first take a look at the absorption spectrum in the 1D case. We see that the CNT spectrum has roughly the same structure as the ALDA spectrum with the exception that it shows absorption at energies

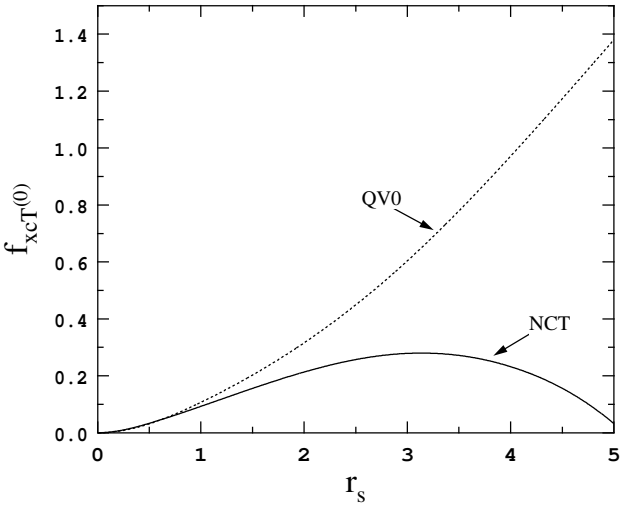

Figure 5.1: $f^h_{xcT}(\rho, 0)$ in a.u. for values of r_s up to $r_s = 5$. Continuous curve: NCT; dashed curve: QV0. The meanings of the abbrevations are explained in the text.

below the Kohn-Sham gap. This is caused by the fact that we now consider complex values of $f^h_{xcL,T}(\rho, \omega)$. The main peak in the QV spectrum on the other hand is shifted by about 2.5 eV to higher frequency with respect to the ALDA spectrum and shows a much smoother structure. An accompanying effect of the shift is that the absorption intensity of the peak in the QV spectrum is much smaller than in the ALDA spectrum because the absorption intensity scales inversely with the square of the frequency at which the absorption occurs. Other effects may also have contributed to this lowering of intensity. Close to the QV spectrum lies the QV0 spectrum which shows that approximating the QV parametrization by its static limit is a good approximation in this case. This is not surprising because within the range of frequencies where the absorption has significant intensity and in the range of r_s values that are relevant for polyacetylene, which we checked to be $r_s \lesssim 2$, the coefficients $f^h_{xcL,T}(\rho, \omega)$ do not change much with respect to their values in the static limit. Like the QV0 spectrum, the NCT spectrum is obtained from values of $f^h_{xcL,T}(\rho, \omega)$ evaluated in their static limit. The only difference between the two approximations is the set of μ_{xc} values that is used. The NCT values are slightly lower than those of QV (in the relevant range of r_s values for polyacetylene). We observe that this difference leads to an NCT spectrum that lies a bit lower in energy than the QV0 spectrum. In fact, we see that the approximations for $f^h_{xcL,T}(\rho, \omega)$ that have nonzero values for μ_{xc} (NCT,QV,QV0),

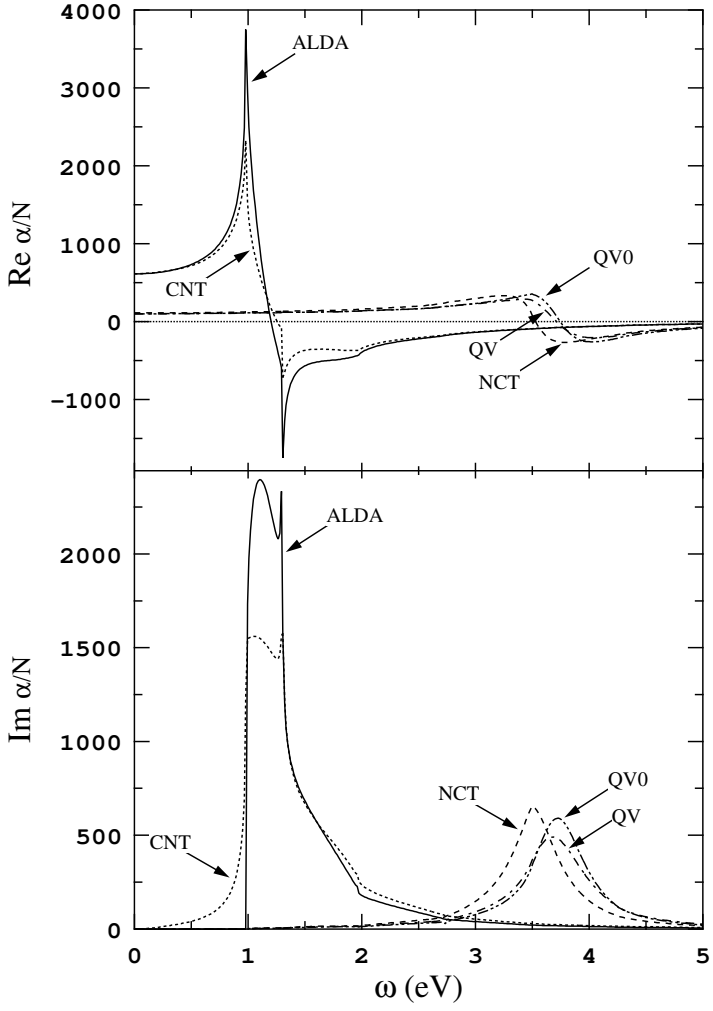

Figure 5.2: The real and imaginary parts of the polarizability per unit length of an infinite polyacetylene chain in a.u.. Dashed curve: CNT; long-dashed curve: NCT; dot-dashed curve: QV; double-dot-dashed curve: QV0; continuous curve: ALDA. The meanings of the abbrevations are explained in the text.

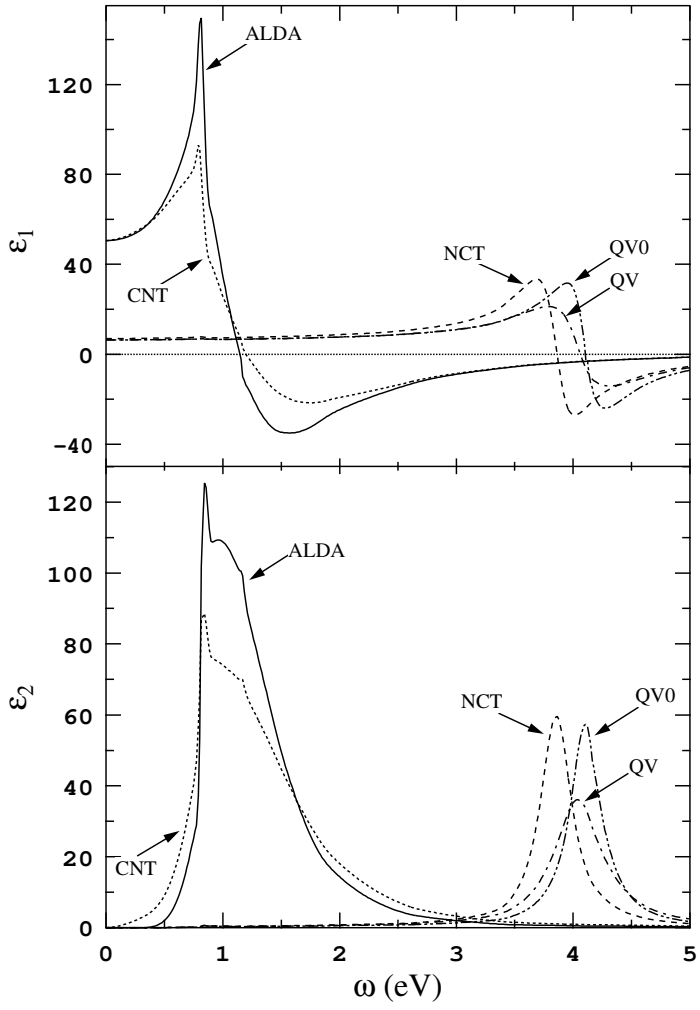

Figure 5.3: The real and imaginary parts of the dielectric function of crystalline polyacetylene. Dashed curve: CNT; long-dashed curve: NCT; dot-dashed curve: QV; double-dot-dashed curve: QV0; continuous curve: ALDA. The meanings of the abbrevations are explained in the text.

related to $f^h_{xcT}(\rho,0)$ by Eq. (5.45), lead to peaks in the absorption spectra that are shifted with respect to the ALDA spectrum. The influence of the frequency dependence of $f^h_{xcL,T}(\rho,\omega)$ for $\omega > 0$ on the position and the shape of the peak is only small as we can see by comparing the CNT spectrum with the ALDA spectrum and the QV spectrum with the QV0 spectrum. These considerations imply a large dependance on the values of μ_{xc} and a relatively small dependance on the behavior of $f^h_{xcL,T}(\rho,\omega)$ for $\omega > 0$ for the position and the shape of the spectrum in the 1D case. We note that the CNT-behavior of $f^h_{xcL,T}(\rho,\omega)$ for $\omega > 0$ does have influence on the intensity of the absorption as can be seen by comparing the CNT spectrum with the ALDA spectrum, but relative to the effect of μ_{xc} on the spectrum it seems to be small. Looking at the absorption spectrum in the 3D case we observe the same qualitative features as in the 1D spectrum. The difference between the QV and QV0 spectrum is somewhat larger, however, than in the 1D case. Still the contribution from μ_{xc} to the spectra seems to be the most important. Unfortunately, not much is known about the precise values of μ_{xc}. As mentioned above, NCT do not deem their values of μ_{xc} to be very accurate and it is not clear how accurate the values are of the Landau parameters calculated by Yasuhara and Ousaka [57] which were used by QV to obtain values for μ_{xc}. These calculations of the Landau parameters are the only recent calculations done for the three-dimensional electron gas.

We will now compare our results for the infinite polyacetylene chain with the results obtained by van Faassen *et al.* for polyacetylene oligomers. They showed that the static polarizability per unit chain length of these oligomers is largely reduced by including the VK functional in their calculations [64, 65] with respect to the ALDA results, which substantially overestimate this quantity. Their results reproduce those of MP2 calculations. The absolute and relative reduction is increased with increasing chain length leading to a reduction of about a factor of 3 for the longest oligomers that they calculated. Their VK results were obtained using the values for μ_{xc} from NCT. It is, however, difficult to obtain a quantitative comparison with their findings since this requires extrapolation of their results to infinite chain length, something that is not straightforward. From our NCT results in the real part in Fig. 5.2 we see the same effect as observed by van Faassen *et al.*, a large reduction of about a factor of 6 of our static polarizability per unit chain length with respect to the ALDA values. Our NCT result in the static limit should be an upper limit for the static polarizability per unit chain length of the polyacetylene oligomers of increasing chain length obtained by van Faassen *et al.*. They furthermore showed that by including the VK functional in their calculations the oscillator strengths of low-lying excitations decrease and those of higher-lying excitations increase with respect to the oscillator strengths obtained in the ALDA when the length of the chain is increased [66]. We observe similar

features in our absorption spectrum where the intensity of the absorption, which is proportional to the oscillator strength, in the NCT spectrum is reduced at low excitation energies and is increased at higher excitation energies with respect to the ALDA spectrum. However, when comparing the NCT spectra with results obtained from accurate calculations and experiment we see that the peak is shifted to too high energy. As mentioned in the Introduction, Rohlfing and Louie [71] performed BSE calculations on 1D polyacetylene and found the position of the peak in the absorption spectrum at 1.7 eV. Furthermore, the experimental results from measurements on 3D polyacetylene by Leising [74] also show the peak in the absorption spectrum at 1.7 eV. These results indicate that the peaks in the ALDA and CNT spectra appear at too low energy and the peaks in the NCT, QV, and QV0 spectra appear at too high energy. As was mentioned above, there seems to be a strong dependence of the shift of the peak position with respect to that in the ALDA spectrum on the parameter μ_{xc}. Actually, we can show that by steadily increasing the values for μ_{xc} from zero upwards (in the r_s-range relevant for polyacetylene) the peak smoothly "walks" away from the ALDA result to higher frequency. The two sets of values for μ_{xc} that are available, those calculated by NCT and QV, differ substantially for $r_s \gtrsim 2$. Because of the uncertainty in the theoretical values of μ_{xc} we choose to fit the position of the peak to the BSE result, which we find more reliable than the experimental result for reasons mentioned in the Introduction, for 1D polyacetylene with μ_{xc} as fitting parameter. We test this idea in a simple static scheme like the NCT and QV0 approximation. With this scheme and with μ_{xc} equal to 7.5×10^{-4} for $r_s \geq 1$. we can reproduce the position of the peak for 1D polyacetylene as found in the BSE spectrum. The behavior for small r_s was again taken to be quadratic. We note that there are probably other choices possible for μ_{xc} as a function of r_s that give the same result for the peak position. Using these values for μ_{xc} in the calculation of the absorption spectrum in the 3D case we find the peak at 1.8 eV compared to 1.7 eV in experiment. The results of these calculations of the absorption spectra can be found in Figs. 5.4 and 5.5. The real parts of the spectra are not reported but we note that the static values are not reduced to such a great extent with respect to the ALDA values as we found from the NCT, QV, and QV0 calculations. The static values are now reduced to 386 in the 1D case and 26.4 in the 3D case. The position of the peak in the absorption spectrum now being the same as the BSE result (1D) and almost the same as in experiment (3D) we can now compare the shape of the spectra. In the case of 1D polyacetylene Rohlfing and Louie found a sharp peak in their absorption spectrum. This is clearly not reproduced in our spectrum as we find a very broad peak. In the case of 3D polyacetylene Puschnig and Ambrosch-Draxl [72] find by solving the BSE a peak with a full-width at half-maximum of 0.3 eV and a

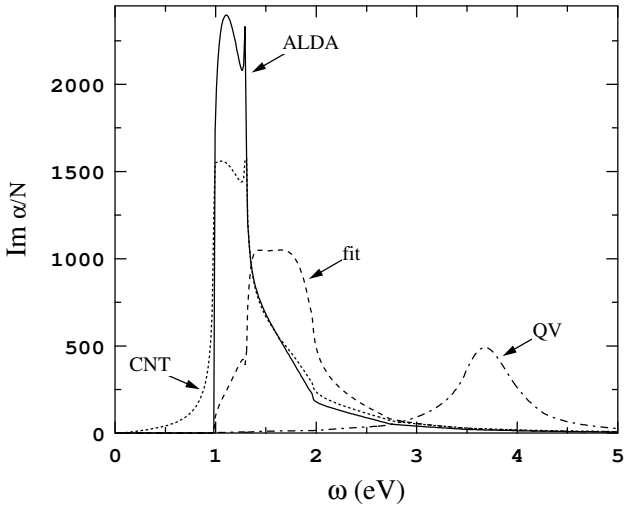

Figure 5.4: The imaginary part of the polarizability per unit length of an infinite polyacetylene chain in a.u.. Dashed curve: CNT; dot-dashed curve: QV; continuous curve: ALDA; long-dashed curve: fit. The meanings of the abbrevations are explained in the text.

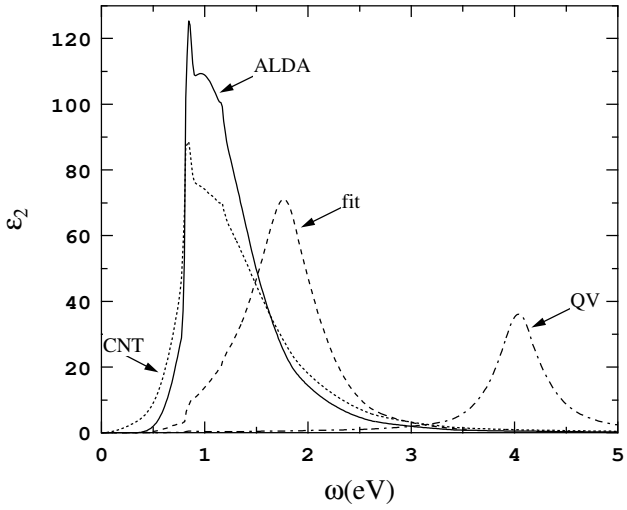

Figure 5.5: The imaginary part of the dielectric function of crystalline polyacetylene. Dashed curve: CNT; dot-dashed curve: QV; continuous curve: ALDA; long-dashed curve: fit. The meanings of the abbrevations are explained in the text.

maximum of 180. Tiago *et al.* [73] find, also from BSE calculations, a peak at 1.7 eV with a full-width at half-maximum of 0.14 eV and a maximum of 350. Leising finds a peak at 1.7 eV with a full-width at half-maximum of 0.5 eV and a maximum of 30. We find a peak with a full-width at half-maximum of 0.7 eV and a maximum of 71. With respect to the BSE results, the width of the peak in our absorption spectrum is too large and its height too small, the total intensity of the spectra are, however, comparable. In general we find that the peaks in the 1D and 3D absorption spectra are too broad. This can either be caused by a wrong choice of the μ_{xc} dependence on r_s, the wrong ω dependence of $f^h_{xcL,T}(\rho,\omega)$ (none in this case), or flaws in the VK functional itself. We note that including the ω dependence of $f^h_{xcL,T}(\rho,\omega)$ in the calculations through either the CNT or the QV parametrization will not solve this problem as it does not alter the width of the peaks, it mainly reduces their height (see Figs. 5.2 and 5.3).

5.6 Conclusions

In this chapter we used the current density as the natural fundamental quantity in which to formulate TDDFT for extended systems. So-called time-dependent current density functional theory (TDCDFT) may provide an elegant way to account for contributions of nonlocal exchange-correlation effects. We introduced an efficient way to include the Vignale-Kohn current functional for the induced exchange-correlation vector potential into our self-consistent calculation scheme. In order to evaluate the Vignale-Kohn functional one has to have knowledge of the exchange-correlation kernels of the homogeneous electron gas $f^h_{xcL,T}(\rho,\omega)$ as a function of the denstity and as a function of the frequency. There exist two frequency-dependent parametrizations of $f^h_{xcL,T}(\rho,\omega)$, one by Conti, Nifosì, and Tosi (CNT) [14] and the other by Qian and Vignale (QV) [15]. We tested the effect of these parametrizations within the Vignale-Kohn functional on the calculation of linear response properties of polyacetylene, namely the polarizability per unit chain length of an infinite polyacetylene chain (1D) and the dielectric function of crystalline polyacetylene (3D). We showed that the two frequency-dependent parametrizations lead to very different results. Furthermore, we showed that the effect on the results caused by the frequency dependence of $f^h_{xcL,T}(\rho,\omega)$ is small with respect to the effect caused by the values of the transverse exchange-correlation kernel $f^h_{xcT}(\rho,\omega)$ in the limit $\omega \to 0$ by inspecting the two frequency-dependent parametrizations in their static limit. They correspond to the ALDA and QV0 for CNT and QV, respectively. It can be shown that the values for $f^h_{xcT}(\rho,\omega)$ in the limit $\omega \to 0$ are related to the exchange-correlation part of the shear modulus μ_{xc} [49].

The results we obtain are in good qualitative agreement with the Vignale-Kohn results obtained for polyacetylene oligomers [64–66]. They are, however, very different from the results of calculations done on polyacetylene by solving the BSE. One of the main causes of this discrepancy is the lack of accurate values that are available for μ_{xc}. This is an important quantity as the positions of the peak in the absorption spectra depend strongly on it. When restoring this difference by fitting the peak position to BSE results with μ_{xc} as a parameter we are able to obtain spectra that show the peaks at the right position but these peaks are too broad. This can be caused by our specific choice of μ_{xc} or by the wrong description of the frequency dependence of $f^h_{xcL,T}(\rho,\omega)$. It may even be a problem inherent to the Vignale-Kohn functional itself. But in order to be able to assess the merits of the Vignale-Kohn functional it is important to first obtain accurate values for μ_{xc} either by first-principle calculations or by some empirical fitting scheme.

Appendix: Derivation of the Exchange-Correlation Vector Potential

The exchange-correlation vector potential as written in Eq. (5.27) and in particular the $\partial_j(\tilde{\eta}_{xc}\partial_j u_i)$ term cannot easily be evaluated as such. Consider therefore the following vector identity:

$$\left[\nabla\times[\tilde{\eta}_{xc}(\nabla\times\mathbf{u})]\right]_i = \sum_j\left[\partial_j(\tilde{\eta}_{xc}\partial_i u_j) - \partial_j(\tilde{\eta}_{xc}\partial_j u_i)\right]. \tag{5.67}$$

Let us work out the first term on the righthand side a bit further,

$$\partial_j(\tilde{\eta}_{xc}\partial_i u_j) = \partial_i[\tilde{\eta}_{xc}\partial_j u_j + (\partial_j\tilde{\eta}_{xc})u_j] - (\partial_i\partial_j\tilde{\eta}_{xc})u_j - (\partial_i\tilde{\eta}_{xc})(\partial_j u_j), \tag{5.68}$$

so that we can combine the two results, Eqs. (5.67) and (5.68), to arrive at the following expression

$$\begin{aligned}\sum_j\partial_j\sigma_{xc,ij} &= \{-\nabla\times[\tilde{\eta}_{xc}(\nabla\times\mathbf{u})]\}_i \\ &\quad+\sum_j\left[2\partial_j(\tilde{\eta}_{xc}\partial_i u_j) - \frac{2}{3}\partial_i(\tilde{\eta}_{xc}\partial_j u_j) + \partial_i(\tilde{\zeta}_{xc}\partial_j u_j)\right] \qquad (5.69)\\ &= \{-\nabla\times[\tilde{\eta}_{xc}(\nabla\times\mathbf{u})]\}_i + \sum_j\partial_i\left[\left(\frac{4}{3}\tilde{\eta}_{xc}+\tilde{\zeta}_{xc}\right)\partial_j u_j + 2(\partial_j\tilde{\eta}_{xc})u_j\right] \\ &\quad-2\sum_j\left[(\partial_i\partial_j\tilde{\eta}_{xc})u_j + (\partial_i\tilde{\eta}_{xc})\partial_j u_j\right]. \qquad (5.70)\end{aligned}$$

Using the nabla operator, we arrive at the following result for the exchange-correlation vector potential field,

$$\begin{aligned}
-\frac{1}{\rho_0}\nabla\cdot\sigma_{xc} &= -\nabla\left[\frac{1}{\rho_0}\left(\frac{4}{3}\tilde{\eta}_{xc}+\tilde{\zeta}_{xc}\right)(\nabla\cdot\mathbf{u})+2\frac{1}{\rho_0}\nabla\tilde{\eta}_{xc}\cdot\mathbf{u}\right] \\
&\quad +\nabla\times\left(\frac{1}{\rho_0}\tilde{\eta}_{xc}(\nabla\times\mathbf{u})\right)-\frac{\nabla\rho_0}{\rho_0^2}\left[\left(\frac{4}{3}\tilde{\eta}_{xc}+\tilde{\zeta}_{xc}\right)(\nabla\cdot\mathbf{u})+2\nabla\tilde{\eta}_{xc}\cdot\mathbf{u}\right] \\
&\quad +\tilde{\eta}_{xc}\frac{\nabla\rho_0}{\rho_0^2}\times(\nabla\times\mathbf{u})+\frac{2}{\rho_0}\left[\nabla\otimes\nabla\tilde{\eta}_{xc}\cdot\mathbf{u}+\nabla\tilde{\eta}_{xc}(\nabla\cdot\mathbf{u})\right]. \qquad (5.71)
\end{aligned}$$

We obtain

$$-\frac{1}{\rho_0}\nabla\cdot\sigma_{xc}\doteq i\omega\delta\mathbf{A}_{xc}=\nabla[\delta v_{xc}^{ALDA}+\delta u_{xc}]+i\omega\delta\mathbf{a}_{xc}+i\omega\nabla\times\delta\mathbf{b}_{xc}, \qquad (5.72)$$

where δu_{xc}, $\delta\mathbf{a}_{xc}$, and $\delta\mathbf{b}_{xc}$ are given in Eqs. (5.50)-(5.52)

Chapter 6

A Physical Model for the Longitudinal Polarizabilities of Polymer Chains

The aim of this chapter is to provide a physical model to relate the polarizability per unit cell of oligomers to that of their corresponding infinite polymer chains. For this we propose an extrapolation method for the polarizability per unit cell of oligomers by fitting them to a physical model describing the dielectric properties of polymer chains. This physical model is based on the concept of a dielectric needle in which we assume a polymer chain to be well described by a cylindrically shaped nonconducting rod with a radius much smaller than its length. With this model we study in which way the polarizability per unit cell approaches the limit of the infinite chain. We show that within this model the macroscopic contribution of the induced electric field to the macroscopic electric field vanishes in the limit of an infinite polymer chain, i.e., there is no macroscopic screening. The macroscopic electric field becomes equal to the external electric field in this limit. We show that this identification leads to a relation between the polarizability per unit cell and the electric susceptibility of the infinite polymer chain. We test our dielectric needle model on the polarizability per unit cell of oligomers of the hydrogen chain and polyacetylene obtained earlier using time-dependent current-density-functional theory in the adiabatic local-density approximation and with the Vignale-Kohn functional. We also perform calculations using the same theory on truly infinite polymer chains by employing periodic boundary conditions. We show that by extrapolating the oligomer results according to our

dielectric needle model we get good agreement with our results from calculations on the corresponding infinite polymer chains.

6.1 Introduction

In several studies physical properties of infinite polymer chains have been obtained by calculating the desired property for a series of oligomers of increasing length and subsequently extrapolating these results to the infinite polymer limit. In the case of polyacetylene Kirtman *et al.* found that the equilibrium geometry, energy per monomer unit (C_2H_2), and isomerization energies had converged at a chain length of three or four monomer units [86]. Other properties such as the ionization potential, band gaps and band widths of the infinite chain were shown to converge less rapidly, but it was demonstrated that one could obtain them by extrapolating the results of calculations on small chains up to a length of four units. However, the convergence of the static longitudinal linear polarizability per unit cell, $\alpha_{zz}(N)/N$, of polymers with increasing chain length has been found to be very slow in general (see, for example, Refs. [64, 65, 87–90]). Here $\alpha_{zz}(N)$ is the longitudinal linear polarizability of a polymer chain containing N monomer units where its axis is parallel to the applied field, which is chosen to be in the z direction. A consequence of this slow convergence with increasing chain length is that it is very difficult to obtain an accurate value for the polarizability per unit cell of the infinite polymer chain by extrapolation of the results from calculations on oligomer chains because, in general, the correct form of the extrapolation function is not known.

The aim of this chapter is to provide a relation between the polarizability per unit cell of oligomers and their corresponding infinite polymer chains based on a physical model. The reason we need a physical model is twofold. First, we need it to relate the susceptibility of our infinite polymer chain calculated using periodic boundary conditions to the polarizability per unit cell, which is defined only for finite systems, in the limit to infinite length of the chain. Second, we need a model to establish in which way the polarizability per unit converges to the infinite polymer limit. Most extrapolation methods currently available lack a physical basis, rendering them inadequate to make the connection between the polarizability per unit cell of oligomers with that of the infinite polymer chain. They are mainly concerned with achieving high stability and efficiency. These methods assume a linear behavior of the polarizability as a function of the number of units yielding a finite value for the polarizability per unit for the infinite polymer chain. However, the way in which this limit is approached is highly sensitive to the chosen fit form. Moreover, the exact behavior is unknown. For this reason some studies have been performed that do have

a physical basis and thus are able to provide this information. Such studies are those by Rojo and Mahan [91] and Tretiak *et al.* [92]. They both studied the dependence of the polarizability on the chain length using tight-binding model Hamiltonians, being respectively a Hubbard and a Pariser-Parr-Pople Hamiltonian. Recently, Kudin *et al.* studied a model of a one-dimensional stack of equally spaced and identical localized polarizable charge distributions that are considered pointlike with respect to the distance between nearest neighbors [90]. Their analysis led to the conclusion that the static longitudinal linear polarizability per unit cell, $\alpha_{zz}(N)/N$, has the form of a power series, at least to second order, in $1/N$.

In this chapter we present a physical model that has at its basis a continuous charge distribution in contrast to the work of Kudin *et al.* [90], namely a dielectric needle. Moreover, by using this model we will establish a connection between the polarizability per unit cell of oligomers and that of the infinite polymer chain, something that could not be achieved in the discrete model. In this model we assume a polymer chain to be well described by a cylindrically shaped nonconducting rod with a radius much smaller than its length. With this model we can explain the linear behavior in the number of unit cells of the polarizability and we can also obtain information on the way the limit of the average polarizability per unit to the infinite polymer chain is approached.

We will show that we arrive at the same conclusion as Kudin *et al.* for the form of $\alpha_{zz}(N)/N$. The aim of this chapter is, therefore, to obtain an extrapolation model that is physically motivated rather than one that is necessarily more stable or more efficient than other methods.

In the previous chapter we evaluated the response of an infinite polyacetylene chain to a macroscopic electric field using time-dependent current-density-functional theory (TDCDFT) [93]. The exchange-correlation effects were treated in the adiabatic local-density approximation (ALDA) as well as with the Vignale-Kohn (VK) functional [12, 13]. One of the results was that the static longitudinal linear polarizability per unit cell was greatly decreased upon going from the ALDA to the VK functional. The same result was already observed by van Faassen *et al.* for polyacetylene oligomers as well as for other π-conjugated oligomers [64,65]. Their VK results for these oligomers greatly improved those obtained within the ALDA, obtaining results at the MP2 level (where available). Also for two σ-conjugated polymers and one nonconjugated polymer they found a reduction of the static polarizability, although not as large as for the π-conjugated systems. In this chapter we want to evaluate if our results for infinite polymers are in keeping with results obtained by van Faassen *et al.* for oligomers. This means that we have to find a reliable way to extrapolate the oligomer results for the polarizability per unit cell of oligomer chains to the infinite polymer chain. We define

$\bar{\alpha}_{zz}(\infty)$ as the $N \to \infty$ limit of $\bar{\alpha}_{zz}(N) = \alpha_{zz}(N)/N$, the polarizability divided by the number of monomer units. We will refer to this approach as the average approach because there is also an alternative approach that is used in literature to obtain $\bar{\alpha}_{zz}(\infty)$. In this, so-called difference approach, one evaluates the $N \to \infty$ limit of $\alpha_{zz}(N) - \alpha_{zz}(N-1)$, the difference in polarizability between two oligomers which differ by one monomer unit. With the currently used fit functions, the difference approach is often used since it has the advantage of faster convergence with increasing chain length. The reason for this is believed to be that the effects of the ends of the polymer chain are removed from consideration in this approach. It is not guaranteed that the difference approach leads to the same asymptotic value for the polarizability per unit cell as the average approach, as is often tacitly assumed. For example, an oscillatory behavior in $\alpha_{zz}(N)/N$ can lead to a different asymptotic value in the two approaches. Only if end effects decay fast enough for polymer chains of increasing length, such that they leave no contributions in the case of an infinite polymer chain, will the difference approach lead to the same asymptotic value as the average approach. We investigate if this is the case within our physical model, and we will show that within our model both approaches lead to the same asymptotic value, albeit that the asymptotic value is approached very slowly as has also been stressed by Kudin *et al.* [90] Moreover, we will show that for the model we used the results obtained in the average approach can readily be transformed to those of the difference approach. An advantage of the average approach is that numerical errors are reduced for larger polymer chains because they are divided by N. This is not the case for the difference approach, and these errors may lead to numerical instabilities in the extrapolation procedure. Several extrapolation methods have been proposed so far and a summary is given in the next section.

An altogether different approach to obtain properties of infinite systems is to make use of their translational symmetry and employ periodic boundary condtions. In this way one can directly evaluate the properties of the infinite polymer chain and one avoids the problem of needing to find a good extrapolation method. However, when using periodic boundary conditions the effects of density changes at the end points are artificially removed. As a consequence the dipole moment and the polarizability of such systems become ill defined. Instead, we will show that it is more natural to evaluate the polarization with the dimension of a dipole moment per unit length. This is still a well-defined property for infinite quasi-one-dimensional systems. The polarization is related to the average electric field instead of the external electric field through the electric susceptibility. We will show that it is possible to obtain a relation between the susceptibility of the infinite polymer chain and the polarizability per unit cell of oligomers in the limit of $N \to \infty$ by adopting a physical model describing the

dielectric properties of polymer chains. The physical model we use approximates a polymer chain by a so-called dielectric needle, a nonconducting cylinder with a length much bigger than its radius, having a uniform and isotropic susceptibility. Within this model we can directly obtain the polarizability per unit cell of infinite polymer chains by calculating its susceptibility from a periodic boundary calculation. Furthermore, our dielectric needle model provides us with a means to extrapolate the results for the polarizability per unit cell of oligomer chains to infinite length. The results that we obtain from this extrapolation procedure can then be compared to the results obtained from the periodic boundary calculations. This tells us something about the quality of our model. We have done this comparison for two kinds of polymers: the hydrogen chain and *trans*-polyacetylene. Finally, we will give our results for $\bar{\alpha}_{zz}(\infty)$ of a number of infinite polymer chains.

The outline of this chapter is as follows. In Sec. 6.2 we give a description of the theory we will need. It consists of an overview of extrapolation methods that are already available in the literature, an account of the properties of quasi-one-dimensional dielectric media, and an explanation of the dielectric needle model that we use to describe polymers. In Sec. 6.3 we give the computational details of our calculations on infinite polymer chains using periodic boundary conditions and of our extrapolation method. The results obtained from these calculations are discussed in Sec. 6.4. Finally, we draw conclusions from our findings in Sec. 6.5.

6.2 Theory

6.2.1 Extrapolation Methods

Several extrapolation procedures of the polarizabilities per unit cell of oligomers have been proposed. The first was by Kirtman, who proposed a least squares fit of $\alpha_{zz}(N)/N$ to a power series in $1/N$ according to [87]

$$\alpha_{zz}(N)/N = \sum_{n=0}^{N} c_n N^{-n}, \tag{6.1}$$

where c_n are constants. Kirtman had already used this scheme successfully to obtain the extrapolated values for the properties of polyacetylene chains mentioned in the Introduction. Similarly, Hurst *et al.* used the same polynomial expansion to fit log $\alpha_{zz}(N)/N$. [88] In order to emphasize the decaying behavior of the difference between the polarizability per unit cell of the infinite polymer chain and that of oligomer chains of increasing length. Champagne *et al.* proposed a fitting function which has

an exponential decreasing behavior according to [89]

$$\alpha_{zz}(N) - \alpha_{zz}(N-1) = a - be^{-cN}, \tag{6.2}$$

where a, b, and c are constants. The obtained values for $\bar{\alpha}_{zz}(\infty)$ are found to be smaller using this exponential fitting function in comparison with the polynomial fitting function. This is consistent with the faster decay caused by the exponential in Eq. (6.2). We can solve Eq. (6.2) for $\alpha_{zz}(N)$, which results in

$$\alpha_{zz}(N) = \alpha_{zz}(k-1) + a(N-k+1) - b\frac{e^{-kc} - e^{-c(N+1)}}{1-e^{-c}}, \tag{6.3}$$

where k is the number of unit cells of the smallest oligomer that is taken into account in the fitting procedure. We can rewrite Eq. (6.3) as

$$\frac{\alpha_{zz}(N)}{N} = a + \frac{d}{N} + \frac{f}{N}e^{-cN}, \tag{6.4}$$

where d and f are new constants combining the constants appearing in Eq. (6.3). A different fitting function that could be used is the so-called logistic equation, which was proposed in Ref. [94] for the extrapolation of the first hyperpolarizability. Other fitting procedures that have been proposed deal with Padé approximants or are based on purely mathematical approaches [95, 96]. The problem with these fitting methods is that they are not derived from a physical model for the polymer chains. In this sense these extrapolation functions are arbitrary. As mentioned in the Introduction there are some works in the literature that are based on physical models such as those by Rojo and Mahan [91], Tretiak *et al.* [92], and recently by Kudin *et al.* [90] From the analysis in the work by Kudin *et al.* it was shown that $\alpha_{zz}(N)/N$ has the form of a power series in $1/N$ as given in Eq. (6.1), at least to second order in $1/N$. This means that they confirm the scheme proposed by Kirtman at least up to second order in $1/N$ and the scheme proposed by Champagne *et al.* up to first order in $1/N$.

6.2.2 Infinite Quasi-one-dimensional Dielectric Media

A direct manner to obtain properties of infinite quasi-one-dimensional dielectric media is to make use of their translational symmetry and employ periodic boundary conditions. Other works in which infinite quasi-one-dimensional systems are studied are, for example, Refs. [97, 98], in which coupled-perturbed Hartree-Fock is used. However, when using periodic boundary conditions the effects of density changes at the end points are artificially removed. Let us now evaluate the consequences this has for the evaluation of the polarizability.

In a finite system the polarizability tensor $\boldsymbol{\alpha}(\mathbf{r},\tau)$ can be obtained from the relation between the induced electric dipole moment $\Delta\boldsymbol{\mu}(t)$ and the external electric field $\mathbf{E}_{ext}(\mathbf{r},t)$ according to

$$\Delta\boldsymbol{\mu}(t) = \int_{t_0}^{t}\int_{\mathcal{V}} \boldsymbol{\alpha}(\mathbf{r},t-t')\cdot\mathbf{E}_{ext}(\mathbf{r},t')d\mathbf{r}dt', \tag{6.5}$$

where the space integral is over the volume of the entire system, $\mathcal{V}$. The induced dipole moment is defined by

$$\Delta\boldsymbol{\mu}(t) = -\int_{\mathcal{V}} \mathbf{r}\delta\rho(\mathbf{r},t)d\mathbf{r}, \tag{6.6}$$

in which $\delta\rho(\mathbf{r},t)$ is the induced density. It becomes immediately clear that for an infinite quasi-one-dimensional system described with periodic boundary conditions $\Delta\boldsymbol{\mu}(t)$ becomes ill defined. This means that the polarizability tensor in infinite systems is ill defined as well. However, we can also derive an expression for $\Delta\boldsymbol{\mu}(t)$ in terms of the current density $\delta\mathbf{j}(\mathbf{r},t)$. Starting from Eq. (6.6) and using the continuity equation, $-\partial_t\delta\rho(\mathbf{r},t) = \nabla\cdot\delta\mathbf{j}(\mathbf{r},t)$, we obtain

$$\Delta\boldsymbol{\mu}(t) = -\int_{t_0}^{t}\int_{\mathcal{V}} \delta\mathbf{j}(\mathbf{r},t')d\mathbf{r}dt' + \int_{t_0}^{t}\int_{\mathcal{S}} \mathbf{r}\,\delta\mathbf{j}(\mathbf{r},t)\cdot\mathbf{n}\,d\mathcal{S}dt', \tag{6.7}$$

where $\mathcal{S}$ is the surface of the system. Since in finite systems there are no currents flowing across $\mathcal{S}$, the surface integral vanishes.

We are considering an infinite quasi-one-dimensional system, therefore we have the assumption that the induced current density is lattice periodic. We can now define the polarization as an induced dipole moment per unit length $\Delta\bar{\boldsymbol{\mu}}(t)$ according to

$$\Delta\bar{\boldsymbol{\mu}}(t) = -\frac{1}{L}\int_{t_0}^{t}\int_{L}\int_{S} \delta\mathbf{j}(\mathbf{r}_\perp,z,t')dSdzdt', \tag{6.8}$$

where L is the length of a unit cell of a quasi-one-dimensional system with its axis in the z direction, S is the surface that cuts the system parallel to the xy plane, and $\mathbf{r}_\perp = (x,y)$. In this way effects caused by the end points are implicitly accounted for. For example, when an infinite quasi-one-dimensional system is perturbed by an electric field there will be a current flowing through the interior with a nonzero average along its axis given by $\mathbf{j}(t) = (1/\Lambda)\int_\Lambda\int_S \mathbf{j}(\mathbf{r}_\perp,z,t)dSdz$, which is the average current over an arbitrary length Λ. This current is directly related through the continuity equation to a density change at the end points of the system. It is therefore not necessary to consider end effects explicitly. So the induced dipole moment per unit length $\Delta\bar{\boldsymbol{\mu}}(t)$ is a well-defined quantity also for infinite quasi-one-dimensional systems.

The induced current, and therefore $\Delta\bar{\boldsymbol{\mu}}(t)$, depends not only on the external electric field but also on the field that is induced inside the one-dimensional dielectric medium caused by this external field. It is therefore more natural to relate $\Delta\bar{\boldsymbol{\mu}}(t)$ to the average electric field. We define the average electric field $\bar{\mathbf{E}}(\mathbf{r}_\perp, t)$ as an average over the length of a unit cell of the external electric field plus the induced electric field:

$$\bar{\mathbf{E}}(\mathbf{r}_\perp, t) = \frac{1}{L}\int_L \left[\mathbf{E}_{ext}(\mathbf{r}_\perp, z, t) + \mathbf{E}_{ind}(\mathbf{r}_\perp, z, t)\right] dz. \tag{6.9}$$

We can now define the induced dipole moment per unit length $\Delta\bar{\boldsymbol{\mu}}(t)$ as the response to an average electric field rather than an external field according to

$$\Delta\bar{\boldsymbol{\mu}}(t) = \int_{t_0}^{t}\int_S \boldsymbol{\chi}(\mathbf{r}_\perp, t-t')\cdot\bar{\mathbf{E}}(\mathbf{r}_\perp, t')dSdt', \tag{6.10}$$

which defines the electric susceptibility $\boldsymbol{\chi}(\mathbf{r}_\perp, \tau)$ as the constant of proportionality.

In this chapter we would like to obtain a relation between the polarizability per unit cell and the susceptibility of infinite polymer chains, or in other words to establish the following relation

$$\Delta\bar{\boldsymbol{\mu}}(t) = \lim_{N\to\infty}\frac{\Delta\boldsymbol{\mu}(N,t)}{NL}, \tag{6.11}$$

where we made explicit that $\Delta\boldsymbol{\mu}(N,t)$ is the induced dipole moment for the oligomer containing N monomer units. To obtain this relation we adopt a physical model for polymer chains, namely, that of a dielectric needle. The main reason that we adopt this model is that, in contrast to real polymer chains, we can evaluate the polarizability of the dielectric needle in the limit of infinite length in an analytic way. This is the subject of the next section.

6.2.3 The Dielectric Needle

We consider a dielectric needle model. A similar model was considered by Fixman [99]. We define the polarization to first order, $\mathbf{P}(\mathbf{r},\omega)$, as

$$\mathbf{P}(\mathbf{r},\omega) = -\frac{i}{\omega}\delta\mathbf{j}(\mathbf{r},\omega), \tag{6.12}$$

where the Fourier transform is defined as

$$\mathbf{j}(\mathbf{r},\omega) = \int \mathbf{j}(\mathbf{r},t)e^{i\omega t}dt. \tag{6.13}$$

Similar transforms are used for other quantities. The macroscopic polarization $\mathbf{P}_{mac}(\mathbf{r},\omega)$ is defined as the average of $\mathbf{P}(\mathbf{r},\omega)$ over a volume element according to

$$\mathbf{P}_{mac}(\mathbf{r},\omega) = \frac{1}{V_r}\int_{V_r}\mathbf{P}(\mathbf{r}',\omega)d\mathbf{r}' = -\frac{i}{\omega V_r}\int_{V_r}\delta\mathbf{j}(\mathbf{r}',\omega)d\mathbf{r}', \tag{6.14}$$

where V_r is a volume element surrounding the point $\mathbf{r}$ with a size that is small compared to the wavelength of the perturbing field but large enough to contain a large number of bulk unit cells. In analogy to Eq. (6.9) we now define a macroscopic electric field $\mathbf{E}_{mac}(\mathbf{r},\omega)$ as the spatial average over V_r of the external electric field plus the induced electric field,

$$\mathbf{E}_{mac}(\mathbf{r},\omega) = \frac{1}{V_r}\int_{V_r}\left[\mathbf{E}_{ext}(\mathbf{r}',\omega)+\mathbf{E}_{ind}(\mathbf{r}',\omega)\right]d\mathbf{r}'. \tag{6.15}$$

Note that Eq. (6.15) is only well-defined in a three-dimensional dielectricum, as V_r is ill defined in one- and two-dimensional systems, whereas Eq. (6.9) is well-defined in (quasi-)one-dimensional dielectric media. We now consider a cylinder having radius $\mathcal{R}$ and length $\mathcal{L}$. We assume that this rodlike system is not conducting, that it has a uniform and isotropic electric susceptibility $\chi_e(\omega)$. We can now write the macroscopic polarization $\mathbf{P}_{mac}(\mathbf{r},\omega)$ as

$$\mathbf{P}_{mac}(\mathbf{r},\omega) = \chi_e(\omega)\cdot\left[\mathbf{E}_{ext}(\mathbf{r},\omega)+\mathbf{E}_{ind}(\mathbf{r},\omega)\right], \tag{6.16}$$

with $\chi_e(\omega)$ as a constant of proportionality. Of course, higher order susceptibilities could be included in Eq. (6.16) to go beyond the linear response regime we discuss here. The induced electric field can be obtained from

$$\mathbf{E}_{ind}(\mathbf{r},\omega) = -\nabla\int_{Cylinder}\frac{\mathbf{P}_{mac}(\mathbf{r}',\omega)\cdot(\mathbf{r}-\mathbf{r}')}{|\mathbf{r}-\mathbf{r}'|^3}\,d\mathbf{r}'. \tag{6.17}$$

For reasons of simplicity we will assume that the rod is indeed needlelike, i.e., the ratio $\mathcal{R}/\mathcal{L}$ is small, and that it is placed in a uniform external field $\mathbf{E}_{ext}(\omega)$ oriented parallel to the axis of the cylinder. In this case we can safely assume that the electric field is not dependent on the distance to the cylinder axis and that both the polarization and the induced field are parallel to this axis. We get for the induced field at the axis in cylindrical coordinates,

$$E_{ind}(z,\omega) = -\frac{\partial}{\partial z}\int_{-\mathcal{L}/2}^{\mathcal{L}/2}\int_0^{\mathcal{R}}\frac{P_{mac}(z',\omega)(z-z')}{\left[(z-z')^2+(r')^2\right]^{3/2}}2\pi r'\,dr'\,dz'. \tag{6.18}$$

Performing the integration and the differentiation we obtain

$$E_{ind}(z,\omega) = -4\pi P_{mac}(z,\omega) + 2\pi\int_{-\mathcal{L}/2}^{\mathcal{L}/2}P_{mac}(z',\omega)\frac{\mathcal{R}^2}{\left[(z-z')^2+\mathcal{R}^2\right]^{3/2}}dz'. \tag{6.19}$$

Inserting Eq. (6.16) and introducing the dimensionless coordinates $\zeta = z/\mathcal{L}$ and $\xi = \mathcal{R}/\mathcal{L}$ results in

$$p(\zeta,\omega) = \beta(\omega)\int_{-1/2}^{1/2}p(\zeta',\omega)K(\zeta-\zeta')d\zeta' + \gamma(\omega), \tag{6.20}$$

in which $p(\zeta,\omega) = P_{mac}(\mathcal{L}\zeta,\omega)$ and where we defined

$$K(\zeta) = \frac{\xi^2}{(\zeta^2+\xi^2)^{3/2}}, \tag{6.21}$$

$$\beta(\omega) = \frac{2\pi\chi_e(\omega)}{1+4\pi\chi_e(\omega)}, \tag{6.22}$$

$$\gamma(\omega) = \frac{\chi_e(\omega)E_{ext}(\omega)}{1+4\pi\chi_e(\omega)}. \tag{6.23}$$

The expression in Eq. (6.20) is a standard Fredholm equation of the second kind. Unless $\beta(\omega)$ happens to be a characteristic value of the integral kernel, this equation has a unique solution. If $p(\zeta,\omega)$ can be expanded in a Taylor series for $|\zeta| < 1/2$, the integral in Eq. (6.20) is equal to $2p(\zeta,\omega)$ in the limit $\xi \to 0$ under certain assumptions. We show this in Appendix A. One then immediately obtains the following relation for a dielectric rod of infinite length, i.e., in the limit $\xi \to 0$:

$$\lim_{\xi\to 0} p(\zeta,\omega) = \chi_e(\omega)E_{ext}(\omega). \tag{6.24}$$

So in the case of the infinite dielectric needle, the polarization is uniform. Moreover, we have shown that in the case of an infinite dielectric rod the induced field vanishes and the macroscopic field is equal to the external field for any (finite) radius. This means that the effects caused by the charge buildup at the ends of a dielectric rod decay when the length of the rod is increased. As a result end effects do not lead to macroscopic screening in the infinite dielectric needle. For large $\chi_e(\omega)$ the factor $\beta(\omega)$ in the integral equation of Eq. (6.20) approaches the characteristic value and the Fredholm equation becomes singular. Therefore we can expect a singular behavior for large $\chi_e(\omega)$ in combination with small ξ.

We now assume that the result we obtained within the model for the infinite dielectric needle, namely, that the average induced field vanishes, is also valid in the case of real polymer chains of infinite length. We then obtain from Eqs. (6.9) and (6.10) for a polymer chain of infinite length

$$\Delta\bar{\mu}(\omega) = E_{ext}(\omega)\int_S \chi_{zz}(\mathbf{r}_\perp,\omega)dS. \tag{6.25}$$

This enables us to define $\bar{\alpha}_\infty(\omega)$ as the polarizability per unit for a polymer chain of infinite length as

$$\bar{\alpha}_\infty(\omega) = L\frac{\Delta\bar{\mu}(\omega)}{E_{ext}(\omega)} = L\int_S \chi_{zz}(\mathbf{r}_\perp,\omega)dS. \tag{6.26}$$

In the case of a dielectric needle of infinite length this equation becomes

$$\bar{\alpha}_\infty(\omega) = \pi\mathcal{R}^2 L\chi_e(\omega). \tag{6.27}$$

We now want to compare this result for the truly infinite dielectric needle with that of a finite dielectric needle in the limit to infinite length. For a dielectric needle of finite length we obtain the following relation from Eqs. (6.7) and (6.14):

$$\Delta\mu(\omega) = \pi\mathcal{R}^2\mathcal{L}\int_{-1/2}^{1/2} p(\zeta,\omega)d\zeta. \tag{6.28}$$

Inserting Eq. (6.5) and dividing both sides by N we obtain ($\mathcal{L} = LN$),

$$\frac{\alpha_{zz}(N,\omega)}{N} = \frac{\pi\mathcal{R}^2 L}{E_{ext}(\omega)}\int_{-1/2}^{1/2} p(\zeta,\omega)d\zeta, \tag{6.29}$$

where we defined

$$\alpha_{zz}(N,\omega) = \int_{NV} \alpha(\mathbf{r},\omega)d\mathbf{r}, \tag{6.30}$$

in which V is the volume of a unit cell. We can evaluate analytically the polarizability per unit of a dielectric needle of infinite length by taking the limit $N \to \infty$ in Eq. (6.29). We obtain

$$\bar{\alpha}_{zz}(\infty,\omega) \equiv \lim_{N\to\infty}\frac{\alpha_{zz}(N,\omega)}{N} = \pi\mathcal{R}^2 L\chi_e(\omega), \tag{6.31}$$

where we used the result of Eq. (6.24). We see that in the case of a dielectric needle we can obtain $\bar{\alpha}_{zz}(\infty,\omega)$ directly from the susceptibility $\chi_e(\omega)$. Comparing this result to Eq. (6.27) we have

$$\bar{\alpha}_{\infty}(\omega) = \bar{\alpha}_{zz}(\infty,\omega). \tag{6.32}$$

In the remainder of this chapter we show that this result also holds for real polymer chains, which means that we can obtain $\bar{\alpha}_{zz}(\infty,\omega)$ for real polymers from

$$\bar{\alpha}_{zz}(\infty,\omega) \equiv \lim_{N\to\infty}\frac{\alpha_{zz}(N,\omega)}{N} = L\int_S \chi_{zz}(\mathbf{r}_\perp,\omega)dS. \tag{6.33}$$

This is our main result. The integral in Eq. (6.33) can be evaluated by applying periodic boundary conditions so that there is no need for an extrapolation procedure to obtain $\bar{\alpha}_{zz}(\infty,\omega)$. The validity to apply the results obtained with the dielectric needle model to real polymer chains can be checked explicitly. This is done by fitting the polarizabilities per unit cell of finite oligomer chains to the dielectric needle model using Eq. (6.29), in which the only fitting parameters are the radius $\mathcal{R}$ and the susceptibility $\chi_e(\omega)$. The best-fit values for $\mathcal{R}$ and $\chi_e(\omega)$ can then be used to obtain $\bar{\alpha}_{zz}(\infty,\omega)$ from Eq. (6.31). Comparing this result for the extrapolated value at infinite length to that obtained with a periodic boundary calculation will give a direct estimate of the quality of the dielectric needle model for real systems.

The above procedure can be extended to the non-linear response regime. As mentioned above this means one has to include higher order susceptibilities in the expression for the macroscopic polarization, Eq. (6.16). One is then able to study the dependence of hyperpolarizabilities on the chain length. It would be interesting to know, for example, if the induced field would still vanish in the limit of the infinite dielectric needle when these hyperpolarizabilities are considered and how these hyperpolarizabilities approach the infinite limit. To the best of our knowledge, the only work that has gone beyond the linear-response regime using a physical model is that by Rojo and Mahan [91]. They used a Hubbard model to study the dependence of the second hyperpolarizability on the chain length.

6.2.4 Approximate Solution of the Fredholm Equation

In this section we want to discuss an iterative solution of Eq. (6.20) to give some insight into our model. We follow the same line of reasoning as Gusmão [100] for his treatment of Love's integral equation [101–103], which is very similar to our integral equation, the difference being that the power of the denominator in the kernel is 1 instead of 3/2. We are interested in the limit that ξ is very small. In that case the kernel is sharply peaked. The main contribution to the integral over the kernel therefore comes from the region $\zeta \approx \zeta'$ and as a first approximation we may therefore replace ζ' by ζ in the argument of p under the integral sign. This yields the following equation for the approximate solution $p_0(\zeta)$.

$$p_0(\zeta) = \beta p_0(\zeta) \int_{-1/2}^{1/2} K(\zeta - \zeta') d\zeta' + \gamma, \tag{6.34}$$

where we suppressed the ω dependence for notational convenience and will continue to do so in the following. The solution $p_0(\zeta)$ is given by

$$p_0(\zeta) = \gamma \left[1 - \beta \left(\frac{(\zeta + 1/2)}{\sqrt{(\zeta + 1/2)^2 + \xi^2}} - \frac{(\zeta - 1/2)}{\sqrt{(\zeta - 1/2)^2 + \xi^2}} \right) \right]^{-1} \tag{6.35}$$

We see that for $\xi \to 0$ and $|\zeta| < 1/2$ we have $p_0 = \chi E_{ext}$. Moreover, at the end points we have

$$p_0(\pm 1/2) = \frac{\gamma}{1 - \beta \frac{1}{\sqrt{1+\xi^2}}}. \tag{6.36}$$

To give an impression what $p_0(\zeta)/E_{ext}$ looks like we plot its solution for $\xi = 0.01$ and $\chi_e = 1$ in Fig. 6.1 together with the exact solution, $p(\zeta)/E_{ext}$, from Eq. (6.20). We see that in the middle of the dielectric needle $p(\zeta)/E_{ext}$ and $p_0(\zeta)/E_{ext}$ are close to uniform and rapidly decrease close to the end points. This behavior is enhanced

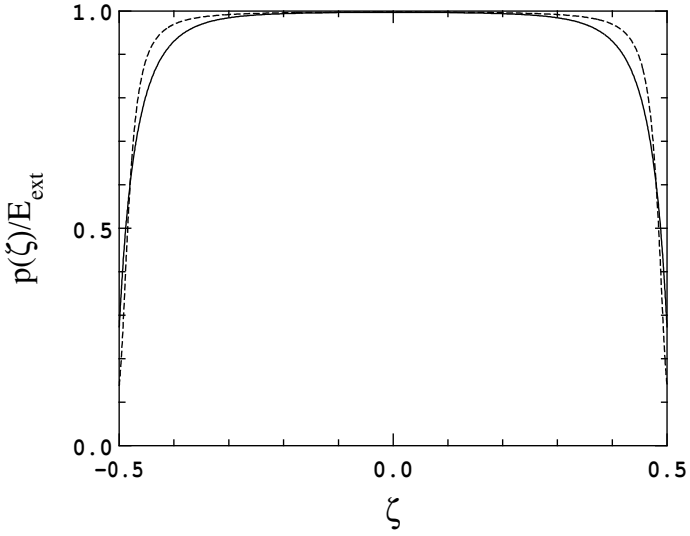

Figure 6.1: The static polarization divided by the external field along a dielectric needle for $\chi_e = 1$ and $\xi = 0.01$. Continuous curve: exact solution $p(\zeta)$; Dashed curve: approximate solution $p_0(\zeta)$.

for smaller values of ξ and smaller values of χ_e. The region in which $p_0(\zeta)/E_{ext}$ is close to uniform is somewhat larger than that for the exact solution and $p_0(\zeta)/E_{ext}$ falls off faster than the exact solution near the end points. Furthermore, we observe that in the center of the dielectric needle $p(\zeta)/E_{ext}$ as well as $p_0(\zeta)/E_{ext}$ are equal to $\chi_e(= 1)$.

Let us now obtain the average polarization of $p_0(\zeta)$ over the length of the dielectric needle. We define the average polarization of $p(\zeta)$ by

$$\bar{p} = \int_{-1/2}^{1/2} p(\zeta) d\zeta. \tag{6.37}$$

We have a similar expression for $\bar{p}_0$. As is shown in Appendix B we obtain for $\bar{p}_0$ to first order in ξ,

$$\bar{p}_0^{[1]} = \chi_e E_{ext} + 2\gamma\xi h(\beta, 0), \tag{6.38}$$

where $h(\beta, 0)$ is a constant given in Eq. (6.58). Similarly we can obtain $\bar{p}_0$ up to higher orders of ξ. To order ξ^4 we obtain the following form for $\bar{p}_0$,

$$\bar{p}_0 = \chi_e E_{ext} + A\xi + B\xi^2 + C\xi^3 + D\xi^4 + E\xi^4 \ln\xi + O(\xi^5). \tag{6.39}$$

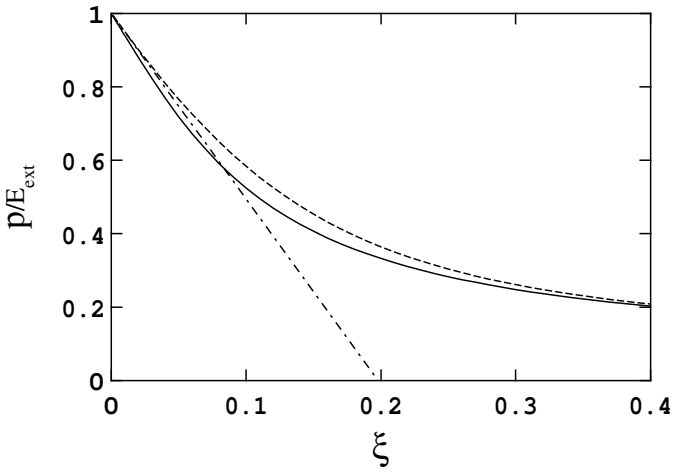

Figure 6.2: The average static polarization divided by the external field of a dielectric needle against ξ, the ratio of the radius and the length of the dielectric needle, for $\chi_e = 1$. Continuous curve: exact solution $\bar{p}$; Dashed curve: approximate solution $\bar{p}_0$; Dot-dashed curve: $\bar{p}_0^{[1]}$.

So we find that $\bar{p}_0$ to third order in ξ behaves like a polynomial, but the logarithmic term shows that the correct form of $\bar{p}_0$ is more complicated. Similar nonanalytic terms involving logarithms that we find for $\bar{p}_0$ in Eq. (6.39) were obtained by Gusmão [100] in his treatment of Love's integral equation. In Fig. (6.2) we plot $\bar{p}_0^{[1]}/E_{ext}$ together with $\bar{p}_0/E_{ext}$ and the exact solution $\bar{p}/E_{ext}$. We observe that $\bar{p}_0/E_{ext}$ is a reasonable approximation for $\bar{p}/E_{ext}$ for small ξ and becomes better for larger ξ. Furthermore, we see that $\bar{p}_0^{[1]}/E_{ext}$ is still a reasonable approximation for the exact solution $\bar{p}/E_{ext}$ for $\xi < 0.1$. We also see that in the limit $\xi \to 0$ the exact solution and the approximate solution $\bar{p}_0/E_{ext}$ go to $\chi_e(= 1)$, which indicates that the assumptions made in deriving Eq. (6.24) were justified and that indeed the macroscopic part of the induced electric field vanishes in the limit $\xi \to 0$. We note that for the exact and the approximate solution this limit is approached linearly (albeit with different slopes). We thereby confirm the $1/N$ convergence of $\alpha_{zz}(N)/N$ to its asymptotic value found by Kudin *et al* [90]. The results obtained for $\alpha_{zz}(N,\omega)/N$ can easily be transformed to obtain the corresponding results for $\alpha_{zz}(N,\omega) - \alpha_{zz}(N-1,\omega)$ by applying a transformation similar to the inverse of the one we performed on Eq. (6.2). This transformation shows that within our model the difference approach converges to the same asymptotic value as the average approach. However, we see from the approximate solution in Eq. (6.39)

that $\alpha_{zz}(N,\omega) - \alpha_{zz}(N-1,\omega)$ approaches its asymptotic value as $1/N^2$ instead of $1/N$. We also see from Eq. (6.39) that successive elimination of higher order terms in $1/N$, for example, using the Romberg interpolation, will eventually fail due to the nonanalytic behavior of $\bar{p}_0$ in $\xi = 0$.

6.3 Computational Details

6.3.1 Periodic Boundary Calculations

The calculations were done in a modified version of the ADF-BAND program [76, 81–83]. We made use of Slater-type orbitals (STO) in combination with frozen cores and a hybrid valence basis set consisting of the numerical solutions of a free-atom Herman-Skillman program [84] that solves the radial Kohn-Sham equations. The spatial resolution of this basis is equivalent to a STO triple-zeta basis set augmented with two polarization functions, which was the basis used in Ref. [64, 65] for the oligomer calculations. This valence basis set was made orthogonal to the core states. The Herman-Skillman program also provides us with the free-atom effective potential. The Hartree potential was evaluated using an auxiliary basis set of STO functions to fit the deformation density in the ground-state calculation and the induced density in the response calculation. For the evaluation of the **k**-space integrals we used a numerical integration scheme with 101 symmetry-unique sample points in the irreducible wedge of the Brillouin zone which was constructed by adopting a Lehmann-Taut tetrahedron scheme [85]. We made use of the Vosko-Wilk-Nusair parametrization [55] of the local-density approximation (LDA) exchange-correlation potential which was also used to construct the ALDA exchange-correlation kernel. In the VK calculations we need the static transverse exchange-correlation kernel, $f_{xcT}(\rho_0, \omega = 0)$. They were obtained from Ref. [48], because these values were also used by van Faassen *et al.* . However, $f_{xcT}(\rho_0, \omega = 0)$ is known only at specific values of the Wigner-Seitz radius r_s ($4\pi r_s^3/3 = 1/\rho_0$). We used a cubic spline interpolation to obtain values of $f_{xcT}(\rho_0, \omega = 0)$ at arbitrary r_s in which the behavior for small r_s was taken to be quadratic, similar to exchange-only behavior. The integral of $\chi_{zz}(\mathbf{r}_\perp, \omega)$ over the surface S in Eq. (6.33) is solved numerically with the integration scheme in Ref. [81]. We performed periodic boundary calculations on the following infinite polymer chains: the hydrogen chain (H), polyacetylene (PA), polyyne (PY), polymethineimine (PMI), polydiacetylene (PDA), polybutatriene (PBT), polythiophene (PT), polyethylene (PE), polysilane (PSi), and polysilene (PSi2). The geometries of these polymer chains were taken from Refs. [64, 65]. We have checked that the results were converged with respect to all parameters involved in the calculations. To

be consistent we used a basis set and a numerical integration scheme in our periodic boundary calculations that were equivalent to those used in the oligomer calculations.

6.3.2 Extrapolation

The longitudinal linear polarizabilities per unit cell, $\alpha_{zz}(N)/N$, of several finite hydrogen chains and polyacetylene chains were obtained from Ref. [64,104]. To fit these results for $\alpha_{zz}(N)/N$ to our dielectric needle model we used the Levenberg-Marquardt method, a standard nonlinear least-squares algorithm. As mentioned above the fit parameters were the radius $\mathcal{R}$ and the electric susceptibility χ_e. The Fredholm equation in Eq. (6.20) was solved numerically using a Gauss-Legendre quadrature.

6.4 Results

In Figs. 6.3 and 6.4 we show the static longitudinal polarizabilities per unit cell, $\alpha_{zz}(N)/N$, of several hydrogen chain oligomers and polyacetylene oligomers, respectively, as obtained by van Faassen *et al.* [64] using TDCDFT with the VK functional together with the fits of these values to our dielectric needle model. We see that in the case of the hydrogen chain the fit in which all oligomer results were taken into account is very close to the oligomer results for $N \geq 6$. For this reason and because the dielectric needle model is probably not such a good approximation for the smallest oligomers, we also did a fit in which all oligomer results were taken into account except those for the five smallest oligomer chains. The result is a fit that lies on top of the first one. In the case of polyacetylene the situation is somewhat different. Here it does make a difference whether or not we discard the results of the five smallest oligomers in our fitting scheme. If we do so the fit is much improved for the longer oligomer chains. The fit is then again very close to the oligomer results (for $N \geq 6$). There are two reasons for the fact that in the case of polyacetylene the two fits are different while in the case of the hydrogen chain they are on top of each other. First, in the case of polyacetylene we have a smaller number of results for the longer oligomers than we have for the hydrogen chain, meaning that the small oligomers have a relatively larger weight in the fit. Second, the ratio of the length and width of a polyacetylene monomer is smaller than that of a hydrogen chain monomer, which is mainly caused by the hydrogen atoms that are bound almost perpendicular to the direction of the polyacetylene chain. We also applied our fitting procedure to the oligomer results of van Faassen *et al.* [64] using TDCDFT within the ALDA. The results are shown in Figs. 6.5 and 6.6. Here we only show the results for the fits in which the five smallest oligomers have been discarded. Again, the fit is in very good

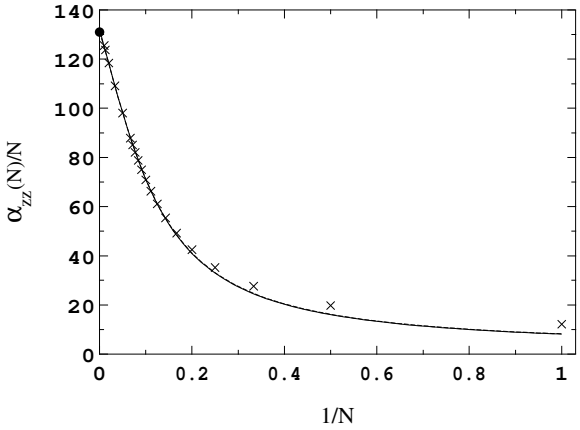

Figure 6.3: The polarizability per unit cell $\alpha_{zz}(N)/N$ of the hydrogen chain obtained with TDCDFT using the VK functional. Crosses: Oligomer results from Ref. [64]; dashed curve: least-squares fit of the oligomer results to our dielectric needle model; continuous curve: least-squares fit of the oligomer results to our dielectric needle model where the results of the smallest five oligomers were discarded; Dot: Infinite chain result from a periodic boundary calculation.

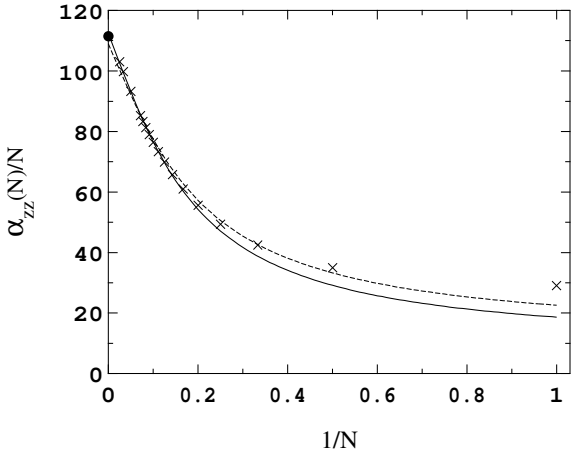

Figure 6.4: The polarizability per unit cell $\alpha_{zz}(N)/N$ of polyacetylene obtained with TDCDFT using the VK functional. Crosses: Oligomer results from Ref. [64]; dashed curve: least-squares fit of the oligomer results to our dielectric needle model; continuous curve: least-squares fit of the oligomer results to our dielectric needle model where the results of the smallest five oligomers were discarded; Dot: Infinite chain result from a periodic boundary calculation.

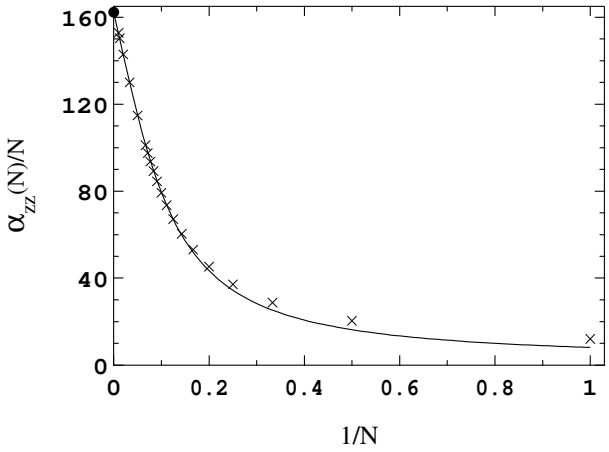

Figure 6.5: The polarizability per unit cell $\alpha_{zz}(N)/N$ of the hydrogen chain obtained with TDCDFT using the ALDA. Crosses: Oligomer results from Ref. [64]; dashed curve: least-squares fit of the oligomer results to our dielectric needle model where the results of the smallest five oligomers were discarded; Dot: Infinite chain result from a periodic boundary calculation.

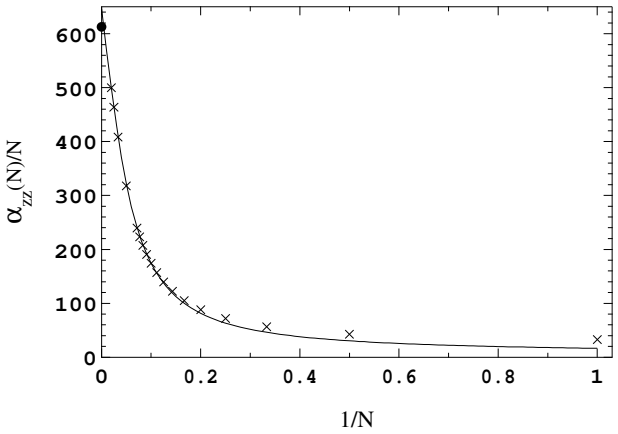

Figure 6.6: The polarizability per unit cell $\alpha_{zz}(N)/N$ of polyacetylene obtained with TDCDFT using the ALDA. Crosses: Oligomer results from Ref. [64]; dashed curve: least-squares fit of the oligomer results to our dielectric needle model where the results of the smallest five oligomers were discarded; Dot: Infinite chain result from a periodic boundary calculation.

Polymer(functional)	$\bar{\alpha}_{zz}(\infty)$			
	PBC	Dielectric Needle	Polynomial	Exponential
H(VK)	131.01	132.16	133.45	132.40
PA(VK)	111.48	112.44	114.94	113.24
H(ALDA)	162.28	162.26	164.42	162.60
PA(ALDA)	612.78	646.21	668.53	656.77

Table 6.1: The polarizabilities per unit cell of the infinite polymer chain, $\bar{\alpha}_{zz}(\infty)$, obtained from a calculation using periodic boundary conditions (PBC) and from a fit of the oligomer results to our dielectric needle model, to a polynomial as proposed in Ref. [87], and to an exponential function as proposed in Ref. [89]. The results are for the infinite hydrogen chain (H) and the infinite polyacetylene chain (PA) both calculated using TDCDFT within the ALDA as well as with the VK functional.

agreement with the oligomer results.

From the fitting procedure of the oligomer results to our dielectric needle model we obtain the best-fit values of our fit parameters, the radius and the electric susceptibility. With these best-fit values we obtain directly $\bar{\alpha}_{zz}(\infty)$ for the infinite polymer chains from Eq. (6.31). The results are given in Table 6.1. We see that the results obtained with both methods are nearly the same, the difference being below 1% with the exception of the infinite polyacetylene chain calculated within the ALDA. There we see a difference of about 5%. Along with these results we also listed the results for $\bar{\alpha}_{zz}(\infty)$ in Table 6.1 those we obtained using the extrapolation methods of Kirtman and Champagne *et al.* as given in Eqs. (6.1) and (6.2), respectively. For the extrapolation method of Kirtman we fitted $\alpha_{zz}(N)/N$ to a third-order polynomial in $1/N$. Instead of fitting $\alpha_{zz}(N)/N$, Champagne *et al.* fitted $\alpha_{zz}(N)-\alpha_{zz}(N-1)$ to an exponential function. However, we do not always have the polarizabilities of polymer chains differing in one monomer unit available. Therefore we fit to Eq. (6.4), which is the same as fitting to Eq. (6.2) as was shown above. From Table 6.1 we see that, although the results obtained with the extrapolation according to our dielectric needle model lie closest to the results obtained from periodic boundary calculations, the differences between the three methods are small. This is not surprising if we compare the extrapolation formulas of Kirtman and Champagne *et al.* in Eqs. (6.1) and (6.4), respectively, to our approximate solution $\bar{p}_0(\omega)$ given in Eq. (6.39). We see that up to third order in the $1/N$ we have the same form as Kirtman and up to first order in $1/N$ we have almost the same form as Champagne *et al.* since the exponential in Eq. (6.4) goes to zero fastly for large N, assuming the constant c is positive. As

Polymer(functional)	$\xi_u = \mathcal{R}/L$	χ_e
H(VK)	0.304	4.98
PA(VK)	0.623	0.907
H(ALDA)	0.300	6.29
PA(ALDA)	0.501	8.06

Table 6.2: The ratios, $\xi_u = \mathcal{R}/L$, of the radius and the length of a unit cell and the electric susceptibility χ_e of the hydrogen chain (H) and polyacetylene (PA) obtained from a fit of the oligomer results to our dielectric needle model. The results are calculated using TDCDFT within the ALDA as well as with the VK functional.

expected the results obtained with the extrapolation formula of Champagne *et al.* lie lower than those obtained with Kirtman's formula. In Table 6.2 we show our best-fit values for the radius $\mathcal{R}$ and the electric susceptibility χ_e. We do not give the radius as such but the ratio $\xi_u = \mathcal{R}/L$ of the radius and the length of a unit cell because it shows in a better way that the best-fit values for the radius are realistic. Now that we have shown that the polarizabilities per unit cell of infinite polymer chains, $\bar{\alpha}_{zz}(\infty)$, from periodic boundary calculations are in keeping with the extrapolated values of $\alpha_{zz}(N)/N$ obtained by van Faassen *et al.* ,we present the $\bar{\alpha}_{zz}(\infty)$ for several kinds of polymers obtained from our periodic boundary calculations in Table 6.3. We use TDCDFT within the ALDA as well as with the VK functional. We see that the VK values are greatly reduced for all polymers with respect to the ALDA results. Especially for the π-conjugated systems (PA, PY, PMI, PDA, PBT, PT and PSi2), this reduction is substantial.

6.5 Conclusions

In this chapter we presented a physical model for the longitudinal polarizabilities of polymer chains that describes their dielectric properties. We showed that within this model we can relate the polarizability per unit cell $\alpha_{zz}(N,\omega)/N$ of oligomers to that of the their corresponding infinite polymer chains. The physical model we use is that of a dielectric needle in which we assume a polymer chain to be well described by a cylindrically shaped nonconducting rod with a radius much smaller than its length. We showed that within this model the macroscopic contribution of the induced electric field to the macroscopic electric field vanishes in the limit of $N \to \infty$, i.e., there is no macroscopic screening. This identification leads to a relation between $\alpha_{zz}(N,\omega)/N$ in the limit $N \to \infty$ and the electric susceptibility of the infinite polymer chain. This

means that we can obtain the polarizability per unit cell of the infinite polymer chain, $\bar{\alpha}_{zz}(\infty,\omega)$, directly from a periodic boundary calculation. Moreover, by studying an approximate solution of our model and from the information contained in Fig. (6.2) we conclude that the leading terms in an expansion of $\alpha_{zz}(N,\omega)/N$ is $\bar{\alpha}_{zz}(\infty,\omega)+a/N$, but that higher-order terms become nonanalytic. This means that end effects, which ultimately vanish in the infinite polymer chain, decrease only slowly with increasing chain length. The dielectric needle also provides us with a procedure to extrapolate the results of $\alpha_{zz}(N,\omega)/N$ of oligomer chains to infinite length. Comparing this result for the extrapolated value at infinite length to that obtained with a periodic boundary calculation gives a direct estimate of the validity of using the dielectric needle model. We have tested our extrapolation method on the static longitudinal polarizabilities per unit cell, $\alpha_{zz}(N,\omega=0)/N$, of oligomers of the hydrogen chain and of polyacetylene that were obtained by van Faassen *et al.* [64] using time-dependent current-density-functional theory in the adiabatic local-density approximation and with the Vignale-Kohn functional. At the same time we performed calculations using the same theory on truly infinite polymer chains by employing periodic boundary conditions. We showed that by extrapolating the oligomer results according to our dielectric needle model we get good agreement with our results from calculations on infinite polymer

Polymer	Monomer unit	$\bar{\alpha}_{zz}(\infty)$	
		ALDA	VK
H	H_2	162.28	131.01
PA	C_2H_2	612.78	111.48
PY	C_2	315.73	143.28
PMI	CNH	352.91	79.70
PDA	C_4H_2	771.46	194.49
PBT	C_4H_2	6017.24	245.07
PT	$C_8S_2H_4$	1162.06	329.63
PE	C_2H_4	36.28	31.67
PSi	Si_2H_4	209.49	101.62
PSi2	Si_2H_2	6263.73	390.09

Table 6.3: Polarizabilities per unit cell for various polymer chains of infinite length, $\bar{\alpha}_{zz}(\infty)$, obtained from TDCDFT calculations using periodic boundary conditions within the ALDA and with the VK functional. H: hydrogen chain, PA: polyacetylene, PY: polyyne, PMI: polymethineimine, PDA: polydiacetylene, PBT: polybutatriene, PT: polythiophene, PE: polyethylene, PSi: polysilane and PSi2: polysilene.

chains using periodic boundary conditions. This shows that our dielectric needle model is a good approximation to describe the dielectric properties of long polymer chains. Furthermore, it shows that our results for the infinite polymer chains of the hydrogen chain and polyacetylene, both from ALDA and VK calculations, are in keeping with the oligomer results of van Faassen *et al.*

Appendix A: Infinite Limit of the Dielectric Needle

We define for $|\zeta| < \frac{1}{2}$,

$$I(\zeta,\xi) = \int_{-1/2}^{1/2} p(\zeta',\xi) \frac{\xi^2}{[(\zeta-\zeta')^2+\xi^2]^{3/2}} d\zeta'. \tag{6.40}$$

We now show that we have the following equality

$$\lim_{\xi\to 0} I(\zeta,\xi) = 2p(\zeta,0), \tag{6.41}$$

under the assumption that $p(\zeta',\xi)$ can be expanded in a Taylor series around $\zeta' = \zeta$ for $|\zeta| < 1/2$. It is easy to see that we have

$$I(\zeta,\xi) = \int_{-1/2}^{1/2} p(\zeta',\xi) \frac{\partial^2}{\partial\zeta'^2} \sqrt{(\zeta-\zeta')^2+\xi^2} d\zeta'. \tag{6.42}$$

Inserting the Taylor expansion of $p(\zeta',\xi)$ and assuming that we can integrate term by term, we obtain

$$I(\zeta) = \sum_{n=0}^{\infty} I_n(\zeta,\xi), \tag{6.43}$$

where

$$I_n(\zeta,\xi) = \frac{1}{n!} p^{(n)}(\zeta,\xi) \int_{-1/2}^{1/2} (\zeta'-\zeta)^n \frac{\partial^2}{\partial\zeta'^2} \sqrt{(\zeta-\zeta')^2+\xi^2} d\zeta', \tag{6.44}$$

in which $p^{(n)}(\zeta,\xi)$ is the n-th order derivative of $p(\zeta',\xi)$ with respect to ζ' at ζ. Changing variables according to $\zeta'-\zeta = x$ and performing integration by parts twice we have

$$\begin{aligned} I_n(\zeta,\xi) &= \frac{1}{n!} p^{(n)}(\zeta,\xi) \left\{ \left[x^n \frac{\partial}{\partial x} \sqrt{x^2+\xi^2} - n x^{n-1} \sqrt{x^2+\xi^2} \right]_{-1/2-\zeta}^{1/2-\zeta} + \right. \\ &\left. n(n-1) \int_{-1/2-\zeta}^{1/2-\zeta} x^{n-2} \sqrt{x^2+\xi^2} dx \right\}. \end{aligned} \tag{6.45}$$

Note that $1/2-\zeta \geq 0$ and $-1/2-\zeta \leq 0$. In the following we assume that we can interchange the limit of $\xi \to 0$ with the integrals and that the n-th order derivatives of $p(\zeta', \xi)$ are finite in the limit $\xi \to 0$. For $n = 0$ we then have

$$\lim_{\xi \to 0} I_0(\zeta, \xi) = p^{(0)}(\zeta, 0) \left[\frac{\partial}{\partial x} |x| \right]_{-\zeta-1/2}^{\zeta-1/2} = 2p(\zeta, 0). \tag{6.46}$$

For $n = 1$ we have

$$\lim_{\xi \to 0} I_1(\zeta, \xi) = p^{(1)}(\zeta, 0) \left[x \frac{\partial}{\partial x} |x| - |x| \right]_{-\zeta-1/2}^{\zeta-1/2} = 0. \tag{6.47}$$

For $n \geq 2$ we have

$$\begin{aligned} \lim_{\xi \to 0} I_n(\zeta, \xi) &= \frac{1}{n!} p^{(n)}(\zeta, 0) \left\{ \left[x^n \frac{\partial}{\partial x} |x| - n x^{n-1} |x| \right]_{-1/2-\zeta}^{1/2-\zeta} + \right. \\ &\quad \left. n(n-1) \left[\int_{-1/2-\zeta}^{0} -x^{n-1} dx + \int_{0}^{1/2-\zeta} x^{n-1} dx \right] \right\} \\ &= \sum_{n=2}^{\infty} \frac{1}{n!} p^{(n)}(\zeta, 0) \left\{ \left[-x^n + n x^n - (n-1) x^n \right]_{-1/2-\zeta}^{0} \right. \\ &+ \left. \left[x^n - n x^n + (n-1) x^n \right]_{0}^{1/2-\zeta} \right\} = 0. \end{aligned} \tag{6.48}$$

Combining the results for all n gives Eq. (6.41).

Appendix B: Asymptotic Expansion of $\bar{p}_0$

To obtain $\bar{p}_0$ from Eq. (6.35) we have to solve

$$\bar{p}_0 = 2\gamma \int_0^{1/2} d\zeta \left[1 - \beta \left(\frac{(\zeta + 1/2)}{\sqrt{(\zeta + 1/2)^2 + \xi^2}} - \frac{(\zeta - 1/2)}{\sqrt{(\zeta - 1/2)^2 + \xi^2}} \right) \right]^{-1}, \tag{6.49}$$

where we used the fact that the integrand is even. We will evaluate this integral in the limit of small ξ. For the first term in the denominator of this expression we can write to first order in ξ

$$\frac{(\zeta + 1/2)}{\sqrt{(\zeta + 1/2)^2 + \xi^2}} = 1 + O(\xi^2). \tag{6.50}$$

We thus obtain

$$\bar{p}_0 = 2\gamma \int_0^{1/2} d\zeta \left[1 - \beta \left(1 - \frac{(\zeta - 1/2)}{\sqrt{(\zeta - 1/2)^2 + \xi^2}} \right) \right]^{-1} + O(\xi^2). \tag{6.51}$$

We now make the substitution $\xi x = 1/2 - \zeta$. Then $\bar{p}(\zeta)$ attains the form

$$\bar{p}_0 = 2\gamma\xi \int_0^{1/(2\xi)} dx \left[1 - \beta\left(1 + \frac{x}{\sqrt{x^2+1}}\right)\right]^{-1} + O(\xi^2). \tag{6.52}$$

The large x behavior of the integrand to first order in $1/x$ is given by

$$\frac{1}{1 - \beta\left(1 + \frac{x}{\sqrt{x^2+1}}\right)} = \frac{1}{1-2\beta} + O\left(\frac{1}{x^2}\right). \tag{6.53}$$

We can therefore add and subtract the limiting values of the integrand for $\bar{p}_0(x)$ and write

$$\begin{aligned} \bar{p}_0 &= 2\gamma\xi \int_0^{1/(2\xi)} \frac{1}{1-2\beta} dx + 2\gamma\xi h(\beta,\xi) + O(\xi^2) && (6.54)\\ &= \frac{\gamma}{(1-2\beta)} + 2\gamma\xi h(\beta,\xi) + O(\xi^2), && (6.55) \end{aligned}$$

where we defined

$$h(\beta,\xi) = \int_0^{1/(2\xi)} \left[\frac{1}{1 - \beta\left(1 + \frac{x}{\sqrt{x^2+1}}\right)} - \frac{1}{1-2\beta}\right] dx. \tag{6.56}$$

We can expand $h(\beta,\xi)$ in a Taylor expansion around $\xi = 0$ according to

$$h(\beta,\xi) = h(\beta,0) + h'(\beta,0)\xi + O(\xi^2), \tag{6.57}$$

where the coefficients $h^{(n)}(\beta,0)$ can be shown to be finite. The coefficient $h(\beta,0)$ is given by

$$h(\beta,0) = -\frac{\beta}{1-2\beta} - \frac{2\beta^2}{(1-2\beta)^{3/2}}\left[\arctan\left(\sqrt{1-2\beta}\right) + \arctan\left(\frac{\beta}{\sqrt{1-2\beta}}\right)\right]. \tag{6.58}$$

Inserting the expansion for $h(\beta,\xi)$ given in Eq. (6.57) into Eq. (6.55) gives Eq. (6.38).

Chapter 7

Analysis of the Vignale-Kohn Current Functional in the Calculation of the Optical Spectra of Semiconductors

In this chapter we investigate the Vignale-Kohn current functional when applied to the calculation of optical spectra of semiconductors. We discuss our results for silicon. We found qualitatively similar results for other semiconductors. These results show that there are serious limitations to the general applicability of the Vignale-Kohn functional. We show that the constraints on the degree of nonuniformity of the ground-state density and on the degree of the spatial variation of the external potential under which the Vignale-Kohn functional was derived are almost all violated. We argue that the Vignale-Kohn functional is not suited to use in the calculation of optical spectra of semiconductors since the functional was derived for a weakly inhomogeneous electron gas in the region above the particle-hole continuum whereas the systems we study are strongly inhomogeneous and the absorption spectrum is closely related to the particle-hole continuum.

7.1 Introduction

Time-dependent density functional theory (TDDFT) developed by Runge and Gross [3] makes it possible to describe the dynamic properties of interacting many-particle

systems in an exact manner [3, 20, 37, 45]. Ghosh and Dhara [4, 5] showed that the Runge-Gross theorem could be extended to systems that are subjected to general time-dependent electromagnetic fields (see also Ref. [6]). The method has proven to be an accurate tool in the study of electronic response properties [8, 37, 59]. TDDFT has mainly been used within the adiabatic local density approximation (ALDA) in which the exchange-correlation scalar potential $v_{xc}(\mathbf{r}, t)$ is just a local functional of the density. In this chapter we investigate a method that goes beyond the ALDA in which we employ an exchange-correlation vector potential, $\mathbf{A}_{xc}(\mathbf{r}, t)$, the longitudinal part of which can be related to $v_{xc}(\mathbf{r}, t)$ by a gauge transformation. We approximate the exchange-correlation vector potential as a local functional of the current density using the expression derived by Vignale and Kohn [12,13]. By studying a weakly inhomogeneous electron gas they found a dynamical exchange-correlation vector potential as a functional of the current density that is nonlocal in time but still local in space. It was later shown by Vignale, Ullrich, and Conti [46] that the exchange-correlation vector potential obtained by Vignale and Kohn could be recast in terms of a viscoelastic stress tensor, making the formalism physically more transparent. The Vignale-Kohn (VK) functional was derived under the constraints $k, q \ll k_F, \omega/v_F$, where k is the length of the wave vector of the external perturbation, q is the length of the wave vector of the inhomogeneity of the ground-state density and k_F and v_F are the local Fermi wave vector and velocity, respectively. The constraint $q \ll k_F, \omega/v_F$ means that formally the application of the VK functional is only justified if the ground-state density is slowly varying and the constraint $k \ll k_F, \omega/v_F$ means we are formally allowed to use the VK functional if the induced current density is slowly varying. Furthermore, the constraint $k \ll \omega/v_F$ implies the region above the particle-hole continuum of the homogeneous electron gas.

The VK functional was first applied by Ullrich and Vignale to study the line widths of collective modes in two dimensional quantum strips and the line widths of intersubband plasmons in quantum wells [50, 80, 105, 106]. These phenomena occur in the region above the particle-hole regime. They obtain a quantitative agreement with the experimentally observed linewidths of the intersubband plasmons. We then applied the VK functional in an approximated fashion as a polarization functional and we observed that the dielectric functions of several semiconductors were much improved [68]. However, to obtain results in good agreement with experiment an empirical prefactor had to be used. Later van Faassen *et al.* [64, 65] showed that the inclusion of the VK functional in TDDFT calculations yields greatly improved polarizabilities for π-conjugated polymers, obtaining results that are comparable with MP2 values. These results were indications that the VK formalism is a very promising one, even when it is applied to describe phenomena related to the particle-hole regime in

systems of which the ground-state density nor the induced current density is slowly varying. However, more recent results show that there are serious limitations to the general applicability of the VK functional. It was observed by van Faassen and de Boeij that the excitation energies of $n \rightarrow \pi^*$ transitions in π-conjugated polymers and a benchmark set of molecules are greatly overestimated [66, 107]. A similar overestimation was found by Ullrich and Burke for the excitation energies of $s \rightarrow p$ transitions in atoms [108]. Finally, in a recent article we showed that the peak that appears in the optical spectra of 1D- and 3D-polyacetylene, which is a π-conjugated polymer, shows a large shift to higher frequency with respect to the peak that appears in the spectra obtained within the ALDA. Furthermore, the height of this peak is largely reduced. However, to obtain agreement with optical spectra from BSE calculations on 3D-polyacetylene [72, 73] the height of the peak should increase and its width should decrease with respect to the peak in the ALDA spectrum. These results raise the question whether or not it is justified to apply the VK functional in the calculation of phenomena related to the particle-hole regime like optical spectra and excitation energies. In this chapter we will try to answer this question. To do so we will study some limiting behavior of the VK functional and we will evaluate the VK functional when applied in the calculation of the optical spectra of silicon.

The outline of this chapter is as follows. In Sec. 7.2 we give an overview of the theory we use, it consists of an account of linear response theory within time-dependent current-density-functional theory (TDCDFT), an introduction to the VK functional, an analysis of the limiting behavior of the response kernels of the electron gas which enter the VK functional and a short summary of the parametrizations available for these kernels. The computational details are discussed in Sec. 7.3. We present and discuss our result obtained for the optical spectrum of silicon in Sec. 7.4. Finally, we draw conclusions from our findings in Sec. 7.5.

7.2 Theory

7.2.1 TDCDFT Linear Response Equations

A frequency-dependent electric field $\mathbf{E}_{ext}(\omega)$ applied to a solid will induce a macroscopic polarization $\mathbf{P}_{mac}(\omega)$ which can be obtained from the induced current density by

$$\mathbf{P}_{mac}(\omega) = \frac{-i}{\omega V} \int_V \delta\mathbf{j}(\mathbf{r}, \omega) d\mathbf{r}, \tag{7.1}$$

and which will be proportional to the macroscopic field $\mathbf{E}_{mac}(\omega)$, i.e., the applied field plus the average induced field within the solid. The constant of proportionality is the

electric susceptibity $\chi_e(\omega)$,

$$\mathbf{P}_{mac}(\omega) = \chi_e(\omega) \cdot \mathbf{E}_{mac}(\omega). \tag{7.2}$$

Unlike $\mathbf{P}_{mac}(\omega)$ and $\mathbf{E}_{mac}(\omega)$, the susceptibility $\chi(\omega)$ is independent of the size and shape and is therefore a bulk property of the system. The induced current density can, in principle, be calculated from the true current-current response function $\chi_{\mathbf{jj}}(\mathbf{r}, \mathbf{r}', \omega)$ of the system according to

$$\delta\mathbf{j}(\mathbf{r}, \omega) = \frac{-i}{\omega} \int \chi_{\mathbf{jj}}(\mathbf{r}, \mathbf{r}', \omega) d\mathbf{r}' \cdot \mathbf{E}_{mac}(\omega). \tag{7.3}$$

From Eqs. (7.1)-(7.3) it follows that

$$\chi_e(\omega) = \frac{-1}{\omega^2} \frac{1}{V} \int d\mathbf{r} \int d\mathbf{r}' \chi_{\mathbf{jj}}(\mathbf{r}, \mathbf{r}', \omega). \tag{7.4}$$

The direct evaluation of the current-current response function is, however, unpractical. In our method we therefore adopt a Kohn-Sham formulation, in which the response to an external electric field of an interacting system is calculated as the response of an auxiliary noninteracting system to an effective field described by the set of Kohn-Sham potentials $\{\delta v_s(\mathbf{r}, \omega), \delta\mathbf{A}_s(\mathbf{r}, \omega)\}$. We choose the field $\mathbf{E}_{mac}(\omega)$ to be given and its relation to $\mathbf{A}_{mac}(\omega)$ is given by $\mathbf{A}_{mac}(\omega) = \mathbf{E}_{mac}(\omega)/i\omega$. We leave the relation between $\mathbf{E}_{mac}(\omega)$ and $\mathbf{E}_{ext}(\omega)$ unspecified as this depends on the sample size and shape and requires knowledge of $\chi_e(\omega)$. The Kohn-Sham vector potential has the property that it produces the exact current density in the Kohn-Sham system. From the exact current density we can calculate the exact density according to the continuity equation,

$$\nabla \cdot \delta\mathbf{j}(\mathbf{r}, \omega) = i\omega\delta\rho(\mathbf{r}, \omega). \tag{7.5}$$

The effective field is a functional of the induced current density and it has to be solved in a self-consistent manner. To first order we have the following expressions within the Kohn-Sham scheme for the induced density,

$$\delta\rho(\mathbf{r}, \omega) = \int \left\{\chi_{s,\rho\mathbf{j}_p}(\mathbf{r}, \mathbf{r}', \omega) \cdot \delta\mathbf{A}_s(\mathbf{r}', \omega) + \chi_{s,\rho\rho}(\mathbf{r}, \mathbf{r}', \omega)\delta v_s(\mathbf{r}', \omega)\right\} d\mathbf{r}', \tag{7.6}$$

and the induced current density,

$$\begin{aligned} \delta\mathbf{j}(\mathbf{r}, \omega) &= \int \left\{[\chi_{s,\mathbf{j}_p\mathbf{j}_p}(\mathbf{r}, \mathbf{r}', \omega) + \rho_0(\mathbf{r})\delta(\mathbf{r} - \mathbf{r}')] \cdot \delta\mathbf{A}_s(\mathbf{r}', \omega)\right. \\ &+ \left. \chi_{s,\mathbf{j}_p\rho}(\mathbf{r}, \mathbf{r}', \omega)\delta v_s(\mathbf{r}', \omega)\right\} d\mathbf{r}'. \end{aligned} \tag{7.7}$$

Here the $\chi_{s,ab}$ are the Kohn-Sham response kernels which are properties of the ground state. They are given by

$$\chi_{s,ab}(\mathbf{r},\mathbf{r}',\omega) = \lim_{\eta\to 0^+} \sum_{n,n'} (f_n - f_{n'}) \frac{[\phi_n^*(\mathbf{r})\tilde{a}\phi_{n'}(\mathbf{r})]\,[\phi_{n'}^*(\mathbf{r}')\tilde{b}\phi_n(\mathbf{r}')]}{\omega - (\epsilon_{n'} - \epsilon_n) + i\eta}, \tag{7.8}$$

in which $\tilde{a}$ and $\tilde{b}$ can be either $\tilde{\rho} = 1$ or $\tilde{\mathbf{j}}_p = -i(\nabla - \nabla^\dagger)/2$, where the dagger on the nabla operator indicates that the operator acts on terms to the left of it. We use a tilde instead of a hat in the auxiliary operators $\tilde{\rho}$ and $\tilde{\mathbf{j}}_p$ in order to differentiate them from the density operator and paramagnetic current-density operator. In Eq. (7.8) ϵ_n are the eigenvalues of the Kohn-Sham orbitals $\phi_n(\mathbf{r})$ of the unperturbed system. The positive infinitesimal η in Eq. (7.8) ensures the causality of the response function.

In principle the scalar potential could have been gauge transformed into a vector potential [50,80] and $\delta\rho(\mathbf{r},\omega)$ could have been expressed in terms of $\delta\mathbf{j}(\mathbf{r},\omega)$ by means of the continuity equation, Eq. (7.5). For the implementation it is, however, convenient to include both the induced density and the scalar potential in our formalism.

If we neglect the small Landau diamagnetic part, which only is important in the evaluation of magnetic properties, we can use the approximate conductivity sum rule [10],

$$\left[\chi_{s,\mathbf{j}_p\mathbf{j}_p}(\mathbf{r},\mathbf{r}',0)\right]_{ij} + \rho_0(\mathbf{r})\delta_{ij}\delta(\mathbf{r}-\mathbf{r}') = 0. \tag{7.9}$$

This sum rule can be used to relate the diamagnetic contribution to the induced current density $\delta\mathbf{j}_d(\mathbf{r},\omega) = -\rho_0(\mathbf{r})\delta\mathbf{A}_s(\mathbf{r},\omega)$ to the static Kohn-Sham current-current response function $\chi_{s,\mathbf{j}_p\mathbf{j}_p}(\mathbf{r},\mathbf{r}',0)$. With this approximation we now get for the induced current density,

$$\begin{aligned} \delta\mathbf{j}(\mathbf{r},\omega) &= \int \Big\{ \big(\chi_{s,\mathbf{j}_p\mathbf{j}_p}(\mathbf{r},\mathbf{r}',\omega) - \chi_{s,\mathbf{j}\mathbf{j}}(\mathbf{r},\mathbf{r}',0)\big)\cdot\delta\mathbf{A}_s(\mathbf{r}',\omega) \\ &+ \chi_{s,\mathbf{j}_p\rho}(\mathbf{r},\mathbf{r}',\omega)\delta v_s(\mathbf{r}',\omega)\Big\}\, d\mathbf{r}'. \end{aligned} \tag{7.10}$$

This provides an efficient way to deal with the incompleteness of the basis set in the $\omega \to 0$ limit in actual applications. In Eq. (7.10) the Kohn-Sham potentials are given, to first order, by

$$\delta\mathbf{A}_s(\mathbf{r},\omega) = \delta\mathbf{A}_{mac}(\omega) + \delta\mathbf{A}_{xc}(\mathbf{r},\omega), \tag{7.11}$$

$$\delta v_s(\mathbf{r},\omega) = \delta v_{H,mic}(\mathbf{r},\omega) + \delta v_{xc,mic}(\mathbf{r},\omega). \tag{7.12}$$

where we chose the gauge such that all components that represent a macroscopic field are included in the vector potential since we choose the scalar potential to be lattice periodic [76]. In the above expression $\delta v_{H,mic}(\mathbf{r},\omega)$ is the microscopic part

of the Hartree potential and $\delta v_{xc,mic}(\mathbf{r},\omega)$ is the microscopic part of the exchange-correlation scalar potential. The macroscopic vector potential $\delta\mathbf{A}_{mac}(\omega)$ consists of the external plus the induced vector potential. The latter potential accounts for the long-range contribution of the Hartree potential of the surface charge as well as the retarded contribution of the induced transverse current density. We can safely ignore the microscopic part, because its electric field contribution is already a factor ω^2/c^2 smaller than that of the microscopic Hartree potential [76,78,79]. The gauge is chosen such that the external field is incorporated into $\mathbf{A}_{mac}(\omega)$. Finally, $\delta\mathbf{A}_{xc}(\mathbf{r},\omega)$ is the exchange-correlation vector potential. In practice approximations are required for the exchange-correlation potentials $\delta v_{xc}(\mathbf{r},\omega)$ and $\delta\mathbf{A}_{xc}(\mathbf{r},\omega)$.

In the next section we will discuss the expression that Vignale and Kohn derived for $\delta\mathbf{A}_{xc}(\mathbf{r},\omega)$. In this derivation they chose the gauge such that $\delta v_{xc}(\mathbf{r},\omega)$ vanishes for all frequencies ω. It turns out that a part of their final expression for $\delta\mathbf{A}_{xc}(\mathbf{r},\omega)$ is equal to the gradient of the ALDA exchange-correlation scalar potential. This part can then be gauge transformed into $\delta v_{xc,mic}(\mathbf{r},\omega)$.

7.2.2 The Vignale-Kohn Functional

The general expression for the exchange-correlation vector potential to first order is

$$\delta\mathbf{A}_{xc}(\mathbf{r},\omega) = \int d\mathbf{r}'\,\mathbf{f}_{xc}(\mathbf{r},\mathbf{r}',\omega)\cdot\delta\mathbf{j}(\mathbf{r}',\omega), \tag{7.13}$$

which defines the tensor kernel $\mathbf{f}_{xc}(\mathbf{r},\mathbf{r}',\omega)$. Vignale and Kohn derived an approximation for this exchange-correlation kernel [12,13]. For this they studied a periodically modulated electron gas with wave vector $\mathbf{q}$, i.e.,

$$\rho_0(\mathbf{r}) = \rho[1+2\gamma\cos(\mathbf{q}\cdot\mathbf{r})], \tag{7.14}$$

where ρ is the density of the homogeneous electron gas and $\gamma \ll 1$, and performed an expansion of the exchange-correlation kernel

$$\mathbf{f}_{xc}(\mathbf{k}+m\mathbf{q},\mathbf{k},\omega) = \frac{1}{V}\int d\mathbf{r}\int d\mathbf{r}'\,\mathbf{f}_{xc}(\mathbf{r},\mathbf{r}',\omega)e^{-i(\mathbf{k}+m\mathbf{q})\cdot\mathbf{r}}e^{i\mathbf{k}\cdot\mathbf{r}'}, \tag{7.15}$$

to second order in $\mathbf{k}$ and $\mathbf{q}$ and to first order in γ. In Eq. (7.15) V is the volume of the system and m is an integer for which to first order in γ only the values for $|m| \leq 1$ are needed. This expansion was shown to be analytic for small $\mathbf{k}$ and $\mathbf{q}$ and to be valid under the constraints $k, q \ll k_F, \omega/v_F$, where k_F and v_F are the local Fermi momentum and the Fermi velocity, respectively. The coefficients in this expansion are completely determined in terms of the density ρ and the coefficients $f^h_{xcL}(\rho,\omega)$ and $f^h_{xcT}(\rho,\omega)$ of the exchange-correlation kernel of the homogeneous electron gas by

the Onsager symmetry relation, the zero-force and zero-torque theorems and a Ward identity [12, 13]. The VK expression for $\delta\mathbf{A}_{xc}(\mathbf{r},\omega)$ is then obtained from

$$\delta\mathbf{A}_{xc}(\mathbf{r},\omega) = \sum_{m=0,\pm1} \int \frac{d\mathbf{k}}{(2\pi)^3}\, \mathbf{f}_{xc}(\mathbf{k}+m\mathbf{q},\mathbf{k},\omega) e^{i(\mathbf{k}+m\mathbf{q})\cdot\mathbf{r}} \delta\mathbf{j}(\mathbf{k},\omega), \tag{7.16}$$

by inserting the expansion for $\mathbf{f}_{xc}$ in Eq. (7.16) and using Eq. (7.14). Since this expression contains first- and second-order powers of $\mathbf{k}$ we obtain first- and second-order derivatives of the current density in real space. Similarly first- and second-order powers of $\mathbf{q}$ lead to first- and second-order derivatives of $\rho_0(\mathbf{r})$ in real space. From analysis of Eq. (7.16) and as a consequence of a Ward identity ρ can be replaced by $\rho_0(\mathbf{r})$ in the coefficients $f^h_{xcL}(\rho,\omega)$ and $f^h_{xcT}(\rho,\omega)$. This will only affect terms of order γ^2 which were already neglected in the derivation. By doing this we obtain a functional we can apply to general systems, although if applied to systems with large density variations we may go outside the range of validity of the VK derivation. It was shown by Vignale, Ullrich and Conti that the VK expression for $\delta\mathbf{A}_{xc}(\mathbf{r},\omega)$ could be written in the form of a viscoelastic field [46, 49]

$$i\omega\delta A_{xc,i}(\mathbf{r},\omega) = \partial_i \delta v^{ALDA}_{xc}(\mathbf{r},\omega) - \frac{1}{\rho_0(\mathbf{r})}\sum_j \partial_j \sigma_{xc,ij}(\mathbf{r},\omega), \tag{7.17}$$

where $v^{ALDA}_{xc}(\mathbf{r},\omega)$ is the ALDA exchange-correlation scalar potential and $\sigma_{xc}(\mathbf{r},\omega)$ is a tensor field which has the structure of a symmetric viscoelastic stress tensor,

$$\sigma_{xc,ij} = \tilde{\eta}_{xc}\left(\partial_j u_i + \partial_i u_j - \frac{2}{3}\delta_{ij}\sum_k \partial_k u_k\right) + \tilde{\zeta}\delta_{ij}\sum_k \partial_k u_k, \tag{7.18}$$

in which the velocity field $\mathbf{u}(\mathbf{r},\omega)$ is given by

$$\mathbf{u}(\mathbf{r},\omega) = \frac{\delta\mathbf{j}(\mathbf{r},\omega)}{\rho_0(\mathbf{r})}. \tag{7.19}$$

The coefficients $\tilde{\eta}_{xc}(\mathbf{r},\omega)$ and $\tilde{\zeta}_{xc}(\mathbf{r},\omega)$ are determined by the transverse and longitudinal response coefficients $f^h_{xcT}(\rho_0(\mathbf{r}),\omega)$ and $f^h_{xcL}(\rho_0(\mathbf{r}),\omega)$ of the homogeneous electron gas evaluated at the density $\rho_0(\mathbf{r})$,

$$\tilde{\eta}_{xc}(\mathbf{r},\omega) = \frac{i}{\omega}\rho_0^2(\mathbf{r}) f^h_{xcT}(\rho_0(\mathbf{r}),\omega), \tag{7.20}$$

and

$$\tilde{\zeta}_{xc}(\mathbf{r},\omega) = \frac{i}{\omega}\rho_0^2(\mathbf{r})\left(f^h_{xcL}(\rho_0(\mathbf{r}),\omega) - \frac{4}{3}f^h_{xcT}(\rho_0(\mathbf{r}),\omega) - \frac{d^2\epsilon^h_{xc}}{d\rho^2}(\rho_0(\mathbf{r}))\right), \tag{7.21}$$

where ϵ_{xc}^h is the exchange-correlation energy per unit volume of the homogeneous electron gas. The quantities $\tilde{\eta}_{xc}(\mathbf{r},\omega)$ and $\tilde{\zeta}_{xc}(\mathbf{r},\omega)$ can be interpreted as viscoelastic coefficients [46,49]. The parameter $\tilde{\zeta}_{xc}(\mathbf{r},\omega)$ contains a factor for which one can prove the exact relation [46, 49]

$$\lim_{\omega\to 0}\left(f_{xcL}^h(\rho_0(\mathbf{r}),\omega)-\frac{4}{3}f_{xcT}^h(\rho_0(\mathbf{r}),\omega)-\frac{d^2\epsilon_{xc}^h}{d\rho^2}(\rho_0(\mathbf{r}))\right)=0. \tag{7.22}$$

However, as mentioned before the expression in Eq. (7.17) is valid only under the constraints $k, q \ll k_F, \omega/v_F$. From Eq. (7.14) we see that the constraint $q \ll k_F, \omega/v_F$ implies in real space that

$$\frac{|\nabla\rho_0(\mathbf{r})|}{\rho_0(\mathbf{r})} \lesssim 2\gamma q \ll k_F, \omega/v_F. \tag{7.23}$$

To obtain an expression for the constraint $k \ll k_F, \omega/v_F$ in real space we start from the expression of the current density for the homogeneous electron gas,

$$\delta\mathbf{j}(\mathbf{r},\omega)=\int d\mathbf{r}'\chi_{\mathbf{jj}}(\mathbf{r}-\mathbf{r}',\omega)\cdot\delta\mathbf{A}(\mathbf{r}',\omega). \tag{7.24}$$

It is convenient to do a Fourier transformation with respect to $(\mathbf{r}-\mathbf{r}')$. We obtain

$$\delta\mathbf{j}(\mathbf{r},\omega)=\int\frac{d\mathbf{k}}{(2\pi)^3}e^{i\mathbf{k}\cdot\mathbf{r}}\chi_{\mathbf{jj}}(\mathbf{k},\omega)\cdot\delta\mathbf{A}(\mathbf{k},\omega), \tag{7.25}$$

where the Fourier transform and its inverse are given by

$$f(\mathbf{k}) = \int d\mathbf{r}e^{-i\mathbf{k}\cdot\mathbf{r}}f(\mathbf{r}) \tag{7.26}$$

$$f(\mathbf{r}) = \int\frac{d\mathbf{k}}{(2\pi)^3}e^{i\mathbf{k}\cdot\mathbf{r}}f(\mathbf{k}). \tag{7.27}$$

We can define the longitudinal and transverse parts of $\chi_{\mathbf{jj}}(\mathbf{k},\omega)$ denoted by $\chi_L(\mathbf{k},\omega)$ and $\chi_T(\mathbf{k},\omega)$, respectively, according to

$$\chi_{\mathbf{jj},mn}(\mathbf{k},\omega)=\chi_L(\mathbf{k},\omega)\frac{k_mk_n}{k^2}+\chi_T(\mathbf{k},\omega)\left(\delta_{mn}-\frac{k_mk_n}{k^2}\right). \tag{7.28}$$

It then follows that we have the following expressions,

$$\nabla\cdot\delta\mathbf{j}(\mathbf{r},\omega) = \int\frac{d\mathbf{k}}{(2\pi)^3}ie^{i\mathbf{k}\cdot\mathbf{r}}\chi_L(\mathbf{k},\omega)\mathbf{k}\cdot\delta\mathbf{A}(\mathbf{k},\omega) \tag{7.29}$$

$$\nabla\times\delta\mathbf{j}(\mathbf{r},\omega) = \int\frac{d\mathbf{k}}{(2\pi)^3}ie^{i\mathbf{k}\cdot\mathbf{r}}\chi_T(\mathbf{k},\omega)\mathbf{k}\times\delta\mathbf{A}(\mathbf{k},\omega). \tag{7.30}$$

We now consider a vector potential that is consistent with the slowly varying external perturbation considered in the derivation of the VK functional, i.e., $\delta\mathbf{A}(\mathbf{k},\omega) = \delta(\mathbf{k}-\mathbf{k}_0)(\mathbf{A}_L(\mathbf{k},\omega)+\mathbf{A}_T(\mathbf{k},\omega))$ with $|\mathbf{k}_0| \ll k_F, \omega/v_F$ and $\mathbf{A}_{L,T}(\mathbf{k},\omega)$ the longitudinal and transverse part of the vector potential, respectively. We then obtain

$$|\nabla\cdot\delta\mathbf{j}(\mathbf{r},\omega)| = \frac{1}{(2\pi)^3}|\mathbf{k}_0||\delta\mathbf{j}_L(\mathbf{r},\omega)| < |\mathbf{k}_0||\delta\mathbf{j}(\mathbf{r},\omega)| \tag{7.31}$$

$$|\nabla\times\delta\mathbf{j}(\mathbf{r},\omega)| = \frac{1}{(2\pi)^3}|\mathbf{k}_0||\delta\mathbf{j}_T(\mathbf{r},\omega)| < |\mathbf{k}_0||\delta\mathbf{j}(\mathbf{r},\omega)|, \tag{7.32}$$

where $\mathbf{j}_{L,T}(\mathbf{k},\omega)$ are the longitudinal and transverse parts of the current density, respectively. We thus see that the condition $k \ll k_F, \omega/v_F$ implies that

$$\frac{|\nabla\cdot\delta\mathbf{j}(\mathbf{r},\omega)|}{|\delta\mathbf{j}(\mathbf{r},\omega)|} \ll k_F, \omega/v_F \tag{7.33}$$

$$\frac{|\nabla\times\delta\mathbf{j}(\mathbf{r},\omega)|}{|\delta\mathbf{j}(\mathbf{r},\omega)|} \ll k_F, \omega/v_F. \tag{7.34}$$

Therefore, Eq. (7.33) is a measure for the degree in which the longitudinal part of the current density satisfies the constraint $k_L \ll k_F, \omega/v_F$ and Eq. (7.34) is a measure for the degree in which the transverse part of the current density satisfies the constraint $k_T \ll k_F, \omega/v_F$, where $k_{L,T}$ are the lengths of the longitudinal and transverse parts of $\mathbf{k}$, respectively.

7.2.3 Limiting behavior of $f^h_{xcL,T}$

In the VK functional enter the longitudinal and transverse response kernels of the homogeneous electron gas $f^h_{xcL,T}(\omega)$. These are obtained from $f^h_{xcL,T}(\mathbf{k},\omega)$ in the limit $\mathbf{k}\to 0$. Let us now evaluate these kernels in the limit $\omega\to 0$. From a viscoelastic analysis by Conti and Vignale [49] we know that we have the following relations in that limit,

$$\lim_{\omega\to 0}\lim_{\mathbf{k}\to 0} f^h_{xcL}(\mathbf{k},\omega) = \frac{1}{\rho^2}\left(K_{xc}+\frac{4}{3}\mu_{xc}\right) \tag{7.35}$$

$$= \frac{d^2\epsilon^h_{xc}(\rho)}{d\rho^2}+\frac{4}{3}\frac{\mu_{xc}}{\rho^2} \tag{7.36}$$

$$\lim_{\omega\to 0}\lim_{\mathbf{k}\to 0} f^h_{xcT}(\mathbf{k},\omega) = \frac{\mu_{xc}}{\rho^2}, \tag{7.37}$$

where K_{xc} and μ_{xc} are the exchange-correlation parts of the bulk modulus and shear modulus, respectively. The order of limits in Eqs. (7.35) and (7.37) guarantees that the evaluation of $f^h_{xcL,T}(\mathbf{k},\omega)$ in $(\mathbf{k}=0,\omega=0)$ is in the region above the particle-hole continuum. We see that if the limit $\mathbf{k}\to 0$ is taken before the limit $\omega\to 0$

there remains a finite contribution from $f^h_{xcL}(\mathbf{k},\omega)$ as well as $f^h_{xcT}(\mathbf{k},\omega)$. The order in which the limits are taken in Eqs. (7.35) and (7.37) is important, because taking the reverse order of limits leads to the following expressions

$$\lim_{\mathbf{k}\to 0}\lim_{\omega\to 0} f^h_{xcL}(\mathbf{k},\omega) = \frac{d^2\epsilon^h_{xc}(\rho)}{d\rho^2} \tag{7.38}$$

$$\lim_{\mathbf{k}\to 0}\lim_{\omega\to 0} f^h_{xcT}(\mathbf{k},\omega) = \lim_{\mathbf{k}\to 0}\lim_{\omega\to 0}\frac{\omega^2}{k^2}\left(\frac{1}{\chi_{T,s}(\mathbf{k},\omega)}-\frac{1}{\chi_T(\mathbf{k},\omega)}\right)=0. \tag{7.39}$$

The first expression is obtained from the compressibility sum rule [53]. The second expression vanishes because in the limit $\omega\to 0$ both $\chi_{T,s}(\mathbf{k},\omega)$ and $\chi_T(\mathbf{k},\omega)$ have finite values. That $\chi_{T,s}(\mathbf{k},\omega)$ has a finite value in the limit $\omega\to 0$ follows from evaluation of the Lindhard function in that limit. Furthermore, we know from the Landau theory that [10]

$$\lim_{\mathbf{k}\to 0}\chi_T(\mathbf{k},\omega=0)=-\rho, \tag{7.40}$$

from which it is clear that $\chi_T(\mathbf{k},\omega)$ is finite in the limit $\omega\to 0$. The order of limits in Eqs. (7.38) and (7.39) guarantees that the evaluation of $f^h_{xcL,T}(\mathbf{k},\omega)$ in $(\mathbf{k}=0,\omega=0)$ is within the particle-hole continuum. From a comparison of Eqs. (7.36) and (7.37) and Eqs. (7.38) and (7.39) we see that in the limit $(\mathbf{k},\omega)\to(0,0)$ the exchange-correlation kernels $f^h_{xcL,T}(\mathbf{k},\omega)$ have a discontinuity that is proportional to μ_{xc}. Although the precise value of μ_{xc} is unknown, it is much smaller than K_{xc}. However, it turns out that it has a big influence on the optical spectra of one-dimensional and three-dimensional polyacetylene calculated with the VK functional [93]. In fact, surprisingly, the influence on the optical spectra of the terms in the VK functional involving the transverse kernel $f^h_{xcT}(\omega)$ is much bigger than the terms involving the longitudinal kernel $f_{xcL}(\omega)$. These terms are responsible for a large shift of the peak that appears in the optical spectra of 1D- and 3D-polyacetylene to higher frequency with respect to the peak in the ALDA spectra. Furthermore, they cause a large reduction of the height of this peak. However, if one makes the approximation $\mu_{xc}=0$ which effectively is the same as using Eqs. (7.38) and (7.39) instead of Eqs. (7.36) and (7.37) we obtain results close to the results obtained within the ALDA. The reason is that within this approximation the VK functional reduces to the ALDA in the limit $\omega\to 0$ as can be seen from Eqs. (7.17)-(7.22) and the values of $f^h_{xcL,T}(\omega)$ do not change much from their value at $\omega=0$ for $\omega\ll\omega_{pl}$ where ω_{pl} is the plasmon frequency. This is typically the frequency range that we are interested in. From the above considerations it seems that the VK functional gives too much weight to the transverse kernel $f_{xcT}(\omega)$ when it is applied to the calculation of the optical spectra of systems with inhomogeneous ground-state densities. Furthermore, since the optical spectrum of a system is closely related to its particle-hole continuum and in view

of the discontinuity of $f^h_{xcL,T}(\mathbf{k},\omega)$ in $(0,0)$ it is desirable to employ a functional in which the kernels $f^h_{xcL,T}(\mathbf{k},\omega)$ are evaluated in the particle-hole continuum instead of in the region above the particle-hole continuum. However, one should consider a finite $\mathbf{k}$ throughout the derivation of such a functional since taking the limit $\mathbf{k}\to 0$ at any stage in the derivation has the consequence that $f^h_{xcL,T}(\mathbf{k},\omega)$ have to be evaluated in the region above the particle-hole continuum. The exception to the above statement is when the limit $\omega\to 0$ is taken before the limit $\mathbf{k}\to 0$ as is effectively done to obtain the ALDA for example.

7.2.4 Parametrizations for $f^h_{xcL,T}$

In previous chapters we discussed extensively the parametrizations that are available for $f^h_{xcL,T}(\rho_0(\mathbf{r}),\omega)$. Here we will give a brief summary. Gross and Kohn (GK) obtained exact properties of $f^h_{xcL}(\mathbf{k}=0,\omega)\equiv f^h_{xcL}(\omega)$ in the low- and high-frequency limits [45, 52]. Furthermore, they introduced an interpolation formula for $\mathrm{Im}f^h_{xcL}(\omega)$ which reduces to the exact high-frequency limit for $\omega\to\infty$ obtained from second-order perturbative expansions by Glick and Long [56] and vanishes linearly in the limit $\omega\to 0$. The real part of $f^h_{xcL}(\omega)$ can subsequently be obtained from the Kramers-Krönig dispersion relations. However, in deriving this interpolation formula they implicitly made the assumption

$$\lim_{\omega\to 0}\lim_{\mathbf{k}\to 0} f^h_{xcL}(\mathbf{k},\omega)=\lim_{\mathbf{k}\to 0}\lim_{\omega\to 0} f^h_{xcL}(\mathbf{k},\omega)=\frac{d^2\epsilon^h_{xc}(\rho)}{d\rho^2}, \tag{7.41}$$

which from the previous section we know to be wrong. A different approach to obtain $f^h_{xcL}(\omega)$ as well as $f^h_{xcT}(\omega)$ was given by Conti, Nifosì, and Tosi (CNT) [14]. They calculated $\mathrm{Im}f^h_{xcL,T}(\omega)$ by direct evaluation of the imaginary parts of the current-current response functions, $\mathrm{Im}\chi_{L,T}(\mathbf{k},\omega)$. CNT used an exact expression for $\mathrm{Im}\chi_{L,T}(\mathbf{k},\omega)$ in terms of four-point response functions which were subsequently approximated by decoupling them into products of two-point response functions. In order to include the effect of plasmons the two-point response functions were then taken to be the RPA response functions. This decoupling scheme only keeps direct contributions and neglects exchange processes. To account for the latter processes CNT introduced a phenomenological factor which reduces the total two-pair spectral weight by a factor of 2 in the high-frequency limit. In the low-frequency limit the factor is close to unity for metallic densities, thereby largely neglecting exchange processes. A distinct feature of the CNT result is a pronounced peak at $\omega=2\omega_{pl}$ in $\mathrm{Im}f^h_{xcL,T}(\omega)$, where ω_{pl} is the plasmon frequency. The high-frequency behavior of $\mathrm{Im}f^h_{xcL}(\omega)$ obtained by CNT coincides with the result of Glick and Long [56], and the high-frequency behavior of $\mathrm{Im}f^h_{xcT}(\omega)$ given by CNT is new. Furthermore, CNT introduced parametrizations for

$\mathrm{Im}f^h_{xcL,T}(\omega)$ that reproduce their numerical results. The real parts can again be obtained from the Kramers-Krönig dispersion relations where the high-frequency limits of $f^h_{xcL,T}(\omega)$ were obtained from third-frequency-moment sum rules [49, 52, 53]. Like GK, CNT made the approximation (7.41) because they preferred to enforce continuity in the limit $(\mathbf{k},\omega)\to(0,0)$ since they expect the discontinuity in this limit to be small and since the exact value of this discontinuity is unknown.

Qian and Vignale (QV) [15] combined the methods of GK and CNT. They obtained an analytic result for the slope of $\mathrm{Im}f^h_{xcT}(\omega)$ at $\omega=0$ by evaluating $\mathrm{Im}\chi_{L,T}(\mathbf{k},\omega)$ within perturbation theory in a similar way as CNT. The direct contributions were treated the same, but QV also included their exchange counterparts in the evaluation. They adopted the interpolation scheme of GK for $\mathrm{Im}f^h_{xcT}(\omega)$ in which they need one more parameter to satisfy the new constraint on the slope of $\mathrm{Im}f^h_{xcL,T}(\omega)$ at $\omega=0$. This extra parameter in their scheme is the width of a Gaussian peak around $\omega=2\omega_{pl}$ that accounts for the two-plasmon contributions found by CNT. The coefficients in their interpolation formula are now determined by their analytic result for the slope at $\omega=0$ and the correct low-frequency limits, Eqs. (7.36) and (7.37), as well as the correct high-frequency behavior. The values for μ_{xc} were obtained from the Landau parameters calculated by Yasuhara and Ousaka [57] for some values of of the Wigner-Seitz radius r_s ($4\pi r_s^3/3=1/\rho$). Their model shows a peak around $\omega=2\omega_{pl}$ that is less pronounced than CNT's.

Since the CNT parametrization for $f^h_{xcL,T}(\omega)$ is based on the approximation given in Eq. (7.41) the VK functional with this parametrization reduces to the ALDA in the limit $\omega\to 0$. The static limit of the VK functional with the QV parametrization for $f^h_{xcL,T}(\omega)$, is not equal to the ALDA since in this parametrization $f^h_{xcT}(\omega=0)$ is nonzero. The approximation in Eq. (7.41) can easily be included in the QV interpolation formula as it effectively amounts to the approximation $\mu_{xc}=0$. We will denote this approximated form of the QV parametrization for $f^h_{xcL,T}(\omega)$ by QVA.

7.3 Computational Details

The implementation was done in the ADF-BAND program [76, 81–83] and we performed our calculations with this modified version. We made use of Slater-type orbitals (STO) in combination with frozen cores and a hybrid valence basis set consisting of the numerical solutions of a free-atom Herman-Skillman program [84] that solves the radial Kohn-Sham equations. The spatial resolution of this basis is equivalent to a STO triple-zeta basis set augmented with two polarization functions. This valence basis set was made orthogonal to the core states. The Herman-Skillman program also provides us with the free-atom effective potential. The Hartree potential was

evaluated using an auxiliary basis set of STO functions to fit the deformation density in the ground-state calculation and the induced density in the response calculation. We used the VK functional to calculate the dielectric function of silicon. We used Eqs. (7.1) and (7.2) to obtain $\chi_e(\omega)$ from which the macroscopic dielectric function can directly be obtained through $\epsilon(\omega) = 1 + 4\pi\chi_e(\omega)$. For the evaluation of the **k**-space integrals we used a numerical integration scheme with 369 symmetry-unique sample points in the irreducible wedge of the Brillouin zone which was constructed by adopting a Lehmann-Taut tetrahedron scheme [85]. We checked the convergence with respect to the number of conduction bands used and found that ten conduction bands are sufficient. This number was used in all our calculations. We made use of the Vosko-Wilk-Nusair parametrization [55] of the LDA exchange-correlation potential which was also used to construct the ALDA exchange-correlation kernel. As mentioned above the values of $f^h_{xcL,T}(\rho,\omega)$ were obtained from the parametrizations given in Refs. [14, 15] denoted by CNT and QV, respectively. However, $f^h_{xcL,T}(\rho,0)$ are known only at specific values of the Wigner-Seitz radius r_s. We used a cubic spline interpolation to obtain values of $f^h_{xcL,T}(\rho,0)$ at arbitrary r_s in which the behavior for small r_s was taken to be quadratic similar to exchange-only behavior.

7.4 Results

As a typical example for the optical spectra obtained with TDCDFT using the VK functional we report the imaginary part of dielectric function of silicon in Fig. 7.1. We also performed calculations on several other semiconductors and insulators, namely GaAs, GaP, and diamond and found qualitatively similar results. The various results correspond to different approximations of $f^h_{xcL,T}(\rho,\omega)$ that enter the VK expression for $\delta\mathbf{A}_{xc}(\mathbf{r},\omega)$. We compare our results obtained with the VK functional with our ALDA results, and with results obtained from experiment [109]. In order to facilitate comparison we have used a scissors operator in our calculations to coincide the calculated optical gap with that found in experiment. The scissors operator shifts upwards the energies of the unoccupied Kohn-Sham orbitals and changes the matrix elements of the current operator. The spectra obtained with the QV interpolation formula for $f^h_{xcL,T}(\rho,\omega)$ collapse. The spectra obtained with the CNT and QVA parametrizations, however, are close to the ALDA spectrum. They even show some improvement over the ALDA spectrum because the height of the second peak is better reproduced. As mentioned before the CNT and QVA spectra are close to the ALDA spectrum because the VK functional with the CNT or QVA parametrization for $f^h_{xcL,T}(\rho,\omega)$ reduces to the ALDA in the limit $\omega \to 0$ and the fact that the values of $f^h_{xcL,T}(\omega)$ in these parametrizations do not change much from their value at $\omega = 0$ for $\omega \ll \omega_{pl}$

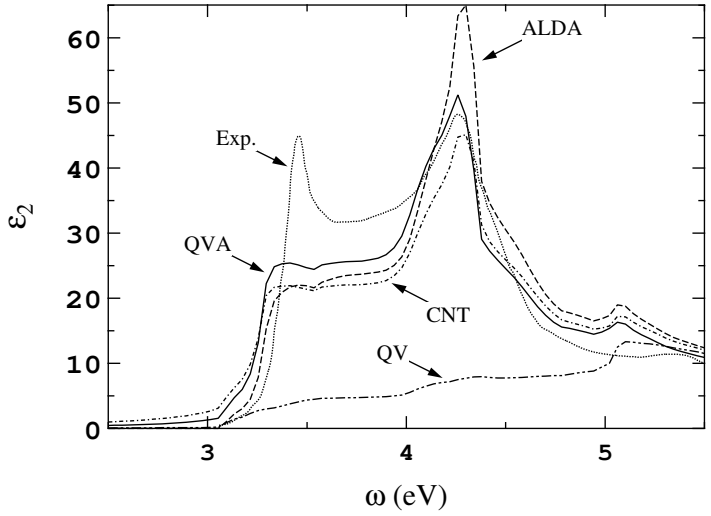

Figure 7.1: The imaginary part of the dielectric function of silicon. Dashed curve: ALDA; Dot-dashed curve: CNT; Double dot-dashed curve: QV; Continuous curve: QVA; Dotted curve: Experimental results from Ref. [109];. The meanings of the abbrevations are explained in the text.

where ω_{pl} is the plasmon frequency. From a comparison between the QV and QVA spectra we can conclude that the transverse kernel $f^h_{xcT}(\rho,\omega)$ has a large unwanted effect on the shape of the spectrum. Since $f^h_{xcT}(\rho,\omega)$ is much smaller than $f^h_{xcL}(\rho,\omega)$ for $\omega \ll \omega_{pl}$ but has a much larger effect on the shape of the spectra, $f^h_{xcT}(\rho,\omega)$ must couple with terms in the VK functional that are large. Therefore, it is the combination of nonzero values for $f^h_{xcT}(\rho,\omega=0)$ and the fact that this transverse part of the exchange-correlation kernel of the homogeneous electron gas couples with large terms that causes the optical spectra to collapse.

Finally, to give an impression of the degree that the constraints given in (7.23) - (7.34) are violated when the Vignale-Kohn functional is applied to the calculation of optical absorption spectra of real systems we show in Fig. 7.2 the results we obtain for silicon at $\omega = 3$ eV using the QV parametrization. Note the logarithmic scale that is used. The results do not depend much on the frequency for $\omega \ll \omega_{pl}$ nor on the parametrization used. We can roughly make the following conclusions based on

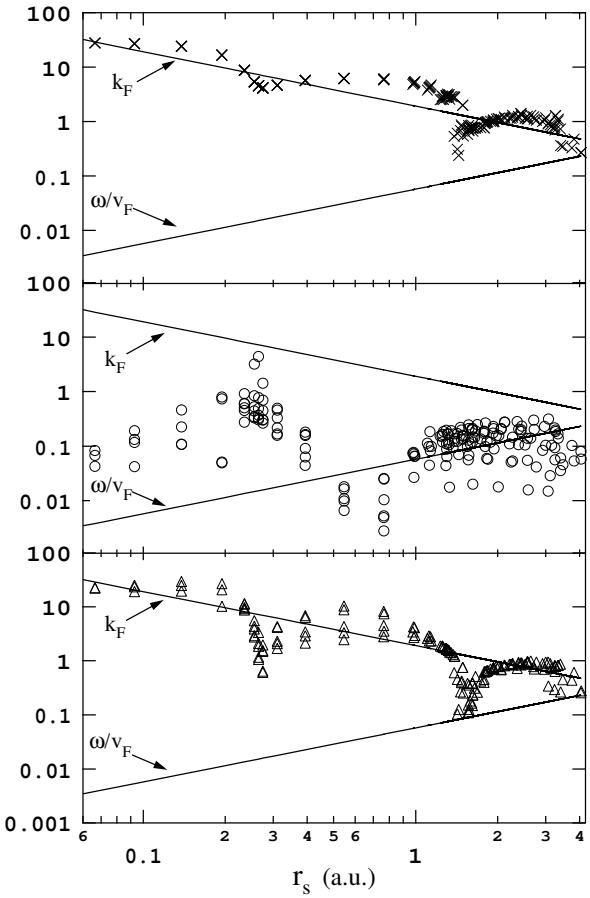

Figure 7.2: Test of the constraints (7.23)-(7.34) at $\omega = 3$ eV for silicon. Top line in each panel: k_F; Bottom line in each panel: ω/v_F; Crosses: $\nabla\rho_0(\mathbf{r})/\rho_0(\mathbf{r})$; Circles: $|\nabla \cdot \delta\mathbf{j}(\mathbf{r},\omega)|/|\delta\mathbf{j}(\mathbf{r},\omega)|$; Triangles: $|\nabla \times \delta\mathbf{j}(\mathbf{r},\omega)|/|\delta\mathbf{j}(\mathbf{r},\omega)|$.

Fig. 7.2,

$$\frac{|\nabla\rho_0(\mathbf{r})|}{\rho_0(\mathbf{r})} \simeq \frac{|\nabla \times \delta\mathbf{j}(\mathbf{r},\omega)|}{|\delta\mathbf{j}(\mathbf{r},\omega))|} \gtrsim k_F \quad \gg \quad \frac{\omega}{v_F} \tag{7.42}$$

$$k_F \gg \frac{|\nabla \cdot \delta\mathbf{j}(\mathbf{r},\omega))|}{|\delta\mathbf{j}(\mathbf{r},\omega))|} \quad \gtrsim \quad \frac{\omega}{v_F} \tag{7.43}$$

We observe that all the constraints except one are violated and in particular the constraints $k, q \ll \omega/v_F$. From these considerations it is therefore not surprising that

the results we obtain for the optical spectra of silicon and other materials are not in agreement with experiment.

7.5 Conclusions

In this chapter we applied the Vignale-Kohn current functional to the calculation of the optical spectra of semiconductors. We discussed our results for silicon which is a typical case. We showed that the optical spectrum collapses if we use the QV parametrization for the longitudinal and transverse exchange-correlation kernels $f_{xcL,T}(\omega) = \lim_{\mathbf{k}\to 0} f_{xcL,T}(\mathbf{k},\omega)$. We discussed possible reasons for this failure. We showed that the constraints on the degree of nonuniformity of the ground-state density, i.e., $q \ll k_F, \omega/v_F$, and on the degree of the spatial variation of the external potential, i.e., $k \ll k_F, \omega/v_F$, under which the Vignale-Kohn functional was derived are almost all violated. Furthermore, since the Vignale-Kohn functional was derived for a weakly inhomogeneous electron gas in the region above the particle-hole continuum we argued that it is not suited to use in the calculation of optical spectra which are closely related to the particle-hole continuum especially because the longitudinal and transverse exchange-correlation kernels $f_{xcL,T}(\mathbf{k},\omega)$ have a discontinuity in $(\mathbf{k} = 0, \omega = 0)$. We showed that the optical spectrum is close to that obtained within the ALDA if we use the CNT or QVA parametrizations for $f_{xcL,T}(\omega)$ that use the approximation $\mu_{xc} = 0$ which effectively is the same as the approximation that $f_{xcL,T}(\mathbf{k},\omega)$ is continuous in $(\mathbf{k} = 0, \omega = 0)$. This is a consequence of the fact that in this approximation the Vignale-Kohn functional reduces to the ALDA in the limit $\omega \to 0$ and the values of the coefficients $f_{xcL,T}(\omega)$ are close to $f_{xcL,T}(\omega = 0)$ for $\omega \ll \omega_{pl}$ and should not be explained as if the CNT and QVA parametrizations are more accurate than the QV parametrization. The constraints $k, q \ll k_F, \omega/v_F$ are as much violated for the CNT and QVA parametrizations as for the QV parametrization.

Chapter 8

Performance of the Vignale-Kohn Functional in the Linear Response of Metals

Recently the linear response of metallic solids has been formulated within the time-dependent current-density-functional approach [110]. The implementation, which originally used only the adiabatic local density approximation for the exchange-correlation kernel is extended in order to include also the Vignale-Kohn current functional. Within this approximation the exchange-correlation kernel $\mathbf{f}_{xc}(\mathbf{r}, \mathbf{r}', \omega)$ is ω dependent, thus relaxation effects due to electron-electron scattering can now be taken into account and some deficiencies of the ALDA, as the absence of the low-frequency Drude-like tail in absorption spectra, can be cured. We strictly follow the formulation given in chapter 5 of the linear response of semiconductors by using the Vignale-Kohn functional [113]. The self-consistent equations for the inter- and intra-band contributions to the induced density and induced current density, which in the long-wavelength limit are completely decoupled within the ALDA, now become coupled. We present our results calculated for the optical properties of the noble metals Cu, Ag, and Au and we compare them with measurements found in literature. In the case of Au we treat the dominant scalar relativistic effects using the zeroth-order regular approximation in the ground-state density-functional-theory calculations, as well as in the time-dependent response calculations.

8.1 Introduction

Recently the time-dependent current-density-functional theory (TDCDFT) formulation has been extended for the response of non-metallic crystals [76, 77] to treat metals [110]. In these systems one should not only consider the interband contribution to the response, involving transitions from (partially) occupied to (partially) unoccupied bands as in non-metals, but also the intraband contribution due to transitions within the same band, more specifically, from just below the Fermi level to just above this level. The latter processes are responsible for the collective plasmon response typical for simple metallic systems [10]. We considered the linear response of the system to a general perturbation with wave vector $\mathbf{g}$ and frequency ω. We found that inter- and intraband processes behave differently for small $\mathbf{g}$ and that the self-consistent-field equations for the inter- and intraband contributions to the response decouple in the optical limit (vanishing $\mathbf{g}$ but finite ω) when we make use of the adiabatic local density approximation (ALDA). In this approximation the exchange-correlation scalar potential $v_{xc}(\mathbf{r}, t)$ is just a local functional of the density. Within the ALDA this method yields good results for the dielectric and the electron energy loss functions of several transition metals. However the adiabatic approximation fails in describing the low-frequency Drude-like absorption, which is missing in all the calculated absorption spectra. This absorption is due to relaxation processes such as electron-electron and electron-phonon scattering. The description of the electron-phonon interaction requires the use of a multicomponent density-functional approach [111,112]. The electron-electron scattering can be described within our method by using more advanced exchange-correlation functionals where a frequency-dependent exchange-correlation kernel $f_{xc}(\mathbf{r}, \mathbf{r}', \omega)$ is used.

In this chapter we go beyond the ALDA and we employ an exchange-correlation vector potential, $\mathbf{A}_{xc}(\mathbf{r}, t)$, which we approximate as a local functional of the current density using the expression derived by Vignale and Kohn [12, 13]. The evaluation of the VK expression requires knowledge of some properties of the homogeneous electron gas, i.e., the exchange correlation energy $\epsilon^h_{xc}(\rho)$ and the longitudinal and transverse exchange-correlation kernels, $f^h_{xcL}(\rho, \omega)$ and $f^h_{xcT}(\rho, \omega)$, respectively, where ρ is the electron density of the electron gas. Knowledge of the first is already required in the ALDA and can be obtained from the accurate results of Monte Carlo calculations [55, 69]. The exchange-correlation kernels, on the other hand, are not known accurately. There are two works in which parametrizations are given for both $f^h_{xcL}(\rho, \omega)$ and $f^h_{xcT}(\rho, \omega)$. One is by Conti, Nifosì and Tosi (CNT) [14] and the other is by Qian and Vignale (QV) [15]. An important difference between the parametrizations of CNT and QV occurs in the $\omega \to 0$ limit of $f^h_{xcT}(\rho, \omega)$. Whereas $f^h_{xcT}(\rho, \omega)$ of CNT

vanishes in that limit, the QV parametrization does not, i.e., it has a small but finite value. The fact that $f^h_{xcT}(\rho,\omega)$ vanishes in the $\omega \to 0$ limit in the case of the CNT parametrization has the important consequence that the VK expression for $\delta\mathbf{A}_{xc}(\mathbf{r},\omega)$ reduces to that of the ALDA in that limit. The value of $f^h_{xcT}(\rho,\omega=0)$ is related to μ_{xc}, the exchange-correlation part of the shear modulus, a quantity that is known only approximately. In previous chapters we showed that it is this difference in behavior of the two parametrizations in the zero-frequency limit that leads to very different absorption spectra of infinite polymer chains and bulk semiconductors [93,113]. Whereas spectra obtained with the CNT parametrization are relatively close to spectra obtained within the ALDA, spectra obtained with the QV parametrization are very different from the ALDA results and from the experiments. Since QV give an expression for their parametrization in which $f^h_{xcL,T}(\rho,0)$ enter, their parametrization can easily be adapted for the case $f^h_{xcT}(\rho,0)=0$. With the resulting parametrization we obtained absorption spectra for silicon that are again close to the spectra obtained with the CNT parametrization and those obtained within the ALDA [93,113]. In view of the obtained results mentioned above and the fact that we are mainly interested in the frequency dependence of the VK functional in order to describe relaxation effects due to electron-electron scattering we choose to enforce continuity with the ALDA in the limit $\omega \to 0$ by setting $f^h_{xcT}(\rho,0)=0$ also in the QV parametrization. Furthermore, we will show that only in the case that $f^h_{xcT}(\rho,0)=0$ the VK functional leads to optical spectra with the correct ω dependence in the limit of $\omega \to 0$. The outline of this chapter is as follows. In section 8.2 we start by giving a description of the theory we use. We first give an outline of TDCDFT and its application in the linear response regime. Then we introduce the self-consistent set of equations which describe the linear response of metallic crystals. Furthermore, we introduce the VK functional and discuss the parametrizations of the exchange-correlation kernels of the homogeneous electron gas $f^h_{xcL,T}(\rho,\omega)$ that enter the VK functional. At the end of the section we give the main equations we use to treat the dominant scalar relativistic effects within the zeroth order regular approximation (ZORA). We will use the ZORA to describe the scalar relativistic effects in Au. We report the main aspects of the implementation in section 8.3. In section 8.4 we show our results for the dielectric and electron energy loss functions of the crystals of Cu, Ag, and Au, and we compare them with the best available experimental data [114–120]. Finally, we give our conclusions in section 8.5.

8.2 Theory

8.2.1 Time-Dependent Current-Density-Functional Theory

It was shown by Runge and Gross [3] that, for a given initial state, there is a one-to-one correspondence between the time-dependent density $\rho(\mathbf{r},t)$ and the time-dependent external scalar potential $v(\mathbf{r},t)$ up to a purely time-dependent function $c(t)$. Ghosh and Dhara [4, 5] extended the Runge-Gross proof to systems subjected to general time-dependent electromagnetic fields by proving that, for a given initial state, there exists a one-to-one correspondence up to a gauge transformation between the time-dependent current density and the set of potentials $\{v(\mathbf{r},t), \mathbf{A}(\mathbf{r},t)\}$, in which $\mathbf{A}(\mathbf{r},t)$ is the time-dependent external vector potential (see also Refs. [6, 37]). Ghosh and Dhara further provide a practical scheme for calculating time-dependent densities and current densities. Here an interacting many-particle system in an external electromagnetic field is replaced by an auxiliary non-interacting many-particle system in an effective field desribed by the set of Kohn-Sham potentials $\{v_s(\mathbf{r},t), \mathbf{A}_s(\mathbf{r},t)\}$ [2]. This set of potentials has the property that, for a given initial state, it produces the exact time-dependent current density and the exact time-dependent density. If the initial state is the ground state, it is already determined by the ground-state density on the basis of the Hohenberg-Kohn theorem [1]. This time-dependent Kohn-Sham theory was later strengthened by a generalization of the Runge-Gross theorem by Vignale who showed that under some assumptions such a set of potentials indeed exists and is unique [6]. In the Kohn-Sham scheme the time-dependent single-particle wave functions are solutions of the following equation,

$$i\frac{\partial}{\partial t}\phi_n(\mathbf{r},t) = \left(\frac{1}{2}\left[\hat{\mathbf{p}} + \mathbf{A}_s(\mathbf{r},t)\right]^2 + v_s(\mathbf{r},t)\right)\phi_n(\mathbf{r},t). \tag{8.1}$$

Given the initial state, the time-dependent potentials $v_s(\mathbf{r},t)$ and $\mathbf{A}_s(\mathbf{r},t)$ produce the exact time-dependent density and current density,

$$\rho(\mathbf{r},t) = \sum_n f_n \phi_n^*(\mathbf{r},t)\phi_n(\mathbf{r},t), \tag{8.2}$$

$$\mathbf{j}(\mathbf{r},t) = \sum_n f_n \mathrm{Re}[-i\phi_n^*(\mathbf{r},t)\nabla\phi_n(\mathbf{r},t)] + \rho(\mathbf{r},t)\mathbf{A}_s(\mathbf{r},t) \tag{8.3}$$

where f_n are the occupation numbers given by the Fermi-Dirac distribution function at zero temperature, i.e., $f_n = f(\epsilon_n) = 2$ for $\epsilon_n \leq \epsilon_F$ and 0 otherwise, with ϵ_n the ground-state orbital energies and ϵ_F the Fermi energy. Here we assumed that our initial state is nondegenerate and is described by a single Slater determinant. The first and second terms on the right-hand side of Eq. (8.3) correspond to the paramagnetic

and diamagnetic current, respectively. Both the density and the current density are gauge invariant.

In this chapter we treat the dynamic linear response of a metallic solid to a macroscopic field within TDCDFT. A time-dependent electric field $\mathbf{E}_{ext}(\mathbf{r},t)$ applied to a solid at a time $t=t_0$ will induce a macroscopic polarization $\mathbf{P}_{mac}(\mathbf{r},t)$, which can be obtained from the induced current density by

$$\mathbf{P}_{mac}(\mathbf{r},t)=\frac{-1}{V}\int_{t_0}^{t}\int_{V}\delta\mathbf{j}(\mathbf{r}',t')d\mathbf{r}'dt'. \tag{8.4}$$

This polarization is proportional to the macroscopic field $\mathbf{E}_{mac}(\mathbf{r},t)$, comprising both the external and the average induced field within the solid,

$$\mathbf{P}_{mac}(\mathbf{r},t)=\int_{t_0}^{t}\chi_e(t-t')\cdot\mathbf{E}_{mac}(\mathbf{r}',t)'dt'. \tag{8.5}$$

Here the constant of proportionality $\chi_e(t-t')$ is the electric susceptibity, which, unlike $\mathbf{P}_{mac}(\mathbf{r},t)$ and $\mathbf{E}_{mac}(\mathbf{r},t)$, is a bulk property of the system since it is independent of its shape and size.

8.2.2 Linear Response

The first-order perturbation of the ground state is governed by the perturbation Hamiltonian $\delta\hat{H}_s$ containing all terms linear in the field,

$$\delta\hat{H}_s(\mathbf{r},t)=\frac{1}{2}[\hat{\mathbf{p}}\cdot\delta\mathbf{A}_s(\mathbf{r},t)+\delta\mathbf{A}_s(\mathbf{r},t)\cdot\hat{\mathbf{p}}]+\delta v_s(\mathbf{r},t), \tag{8.6}$$

where $\hat{\mathbf{p}}=-i\nabla$ is the momentum operator. We choose the gauge to be the microscopic Coulomb gauge of Kootstra *et al.* [76] in which the Kohn-Sham scalar and vector potentials are given by,

$$\delta v_s(\mathbf{r},t) = \delta v_{H,mic}(\mathbf{r},t)+\delta v_{xc,mic}(\mathbf{r},t), \tag{8.7}$$

$$\delta\mathbf{A}_s(\mathbf{r},t) = \delta\mathbf{A}_{mac}(\mathbf{r},t)+\delta\mathbf{A}_{xc}(\mathbf{r},t). \tag{8.8}$$

Here $\delta v_{H,mic}(\mathbf{r},t)$ is the microscopic part of the Hartree potential and $\delta v_{xc,mic}(\mathbf{r},t)$ is the microscopic part of the exchange-correlation potential. The term $\delta\mathbf{A}_{mac}(\mathbf{r},t)$ denotes the macroscopic vector potential,

$$\delta\mathbf{A}_{mac}(\mathbf{r},t)=\delta\mathbf{A}_{ext}(\mathbf{r},t)+\delta\mathbf{A}_{ind}(\mathbf{r},t), \tag{8.9}$$

where $\delta\mathbf{A}_{ext}(\mathbf{r},t)$ is the external vector potential and $\delta\mathbf{A}_{ind}(\mathbf{r},t)$ is the induced macroscopic vector potential. The latter potential accounts for the long-range contribution

of the Hartree potential of the surface charge as well as the retarded contribution of the induced transverse current density. We can neglect the microscopic part of the vector potential which is consistent with the Breit approximation used in the ground-state calculation [76,78,79]. We choose the field $\mathbf{E}_{mac}(\mathbf{r},t)$ to be fixed and its relation to $\delta\mathbf{A}_{mac}(\mathbf{r},t)$ is given by $\partial_t\delta\mathbf{A}_{mac}(\mathbf{r},t) = -\mathbf{E}_{mac}(\mathbf{r},t)$. We leave the relation between $\mathbf{E}_{mac}(\mathbf{r},t)$ and $\mathbf{E}_{ext}(t)$ unspecified as this depends on the sample size and shape and requires knowledge of χ_e. Finally, $\delta\mathbf{A}_{xc}(\mathbf{r},t)$ is the exchange-correlation vector potential. In practice approximations are required for the exchange-correlation potentials $\delta v_{xc}(\mathbf{r},t)$ and $\delta\mathbf{A}_{xc}(\mathbf{r},t)$.

In a recent work [110] $\delta v_{xc}^{ALDA}(\mathbf{r},t)$ was used for the exchange-correlation scalar potential and the exchange-correlation vector potential was neglected. In this case the Kohn-Sham vector potential is completely determined by the macroscopic electric field which is kept fixed. We then only need to solve the equation for the induced density self consistently, and afterwards the induced current density can be calculated. Approximations beyond the ALDA imply a self-consistent solution of the equations for both the induced density and induced current density, which will be coupled.

To study the linear response properties of systems, which are initially in the ground state and perturbed by a time-dependent electromagnetic field, it is convenient to work in the frequency domain. To do this we use a Fourier transformation defined by

$$\delta\tilde{\mathbf{A}}_s(\mathbf{r},\omega) = \int \delta\mathbf{A}_s(\mathbf{r},t)e^{i\omega t}d\omega. \tag{8.10}$$

For notational convenience we will drop the tilde on $\delta\tilde{\mathbf{A}}(\mathbf{r},\omega)$ in the following and assume that it is clear from the frequency dependence that we are dealing with a different quantity. We consider a general perturbation characterized by the wave vector $\mathbf{g}$ and frequency ω according to

$$\delta\mathbf{A}_s(\mathbf{r},\omega) = e^{i\mathbf{g}\cdot\mathbf{r}}\delta\mathbf{A}_{\mathbf{g},s}(\mathbf{r},\omega), \tag{8.11}$$

where $\delta\mathbf{A}_{\mathbf{g},s}(\mathbf{r},\omega)$ is lattice periodic, i.e.,

$$\delta\mathbf{A}_{\mathbf{g},s}(\mathbf{r},\omega) = \delta\mathbf{A}_{\mathbf{g},s}(\mathbf{r}+\mathbf{R},\omega), \tag{8.12}$$

with $\mathbf{R}$ a Bravais lattice vector. We choose the perturbation to be real and therefore we have

$$\delta\mathbf{A}_{\mathbf{g},s}(\mathbf{r},\omega) = \delta\mathbf{A}^*_{-\mathbf{g},s}(\mathbf{r},-\omega), \tag{8.13}$$

We have similar expressions for the scalar potential.

We are interested in the linear response of the system for vanishing $\mathbf{g}$ but finite ω, which is the regime describing optical properties. An essential point of our formulation

is that inter- and intraband processes behave differently for small $\mathbf{g}$. It can be shown that within the linear response regime the induced density and induced current density can be written as [110]

$$\delta\rho(\mathbf{r},\omega) = e^{i\mathbf{g}\cdot\mathbf{r}}\delta\rho_{\mathbf{g}}(\mathbf{r},\omega) \tag{8.14}$$

$$\delta\mathbf{j}(\mathbf{r},\omega) = e^{i\mathbf{g}\cdot\mathbf{r}}\delta\mathbf{j}_{\mathbf{g}}(\mathbf{r},\omega), \tag{8.15}$$

where $\delta\rho_{\mathbf{g}}(\mathbf{r},\omega)$ and $\delta\mathbf{j}_{\mathbf{g}}(\mathbf{r},\omega)$ are lattice periodic. In order to show that inter- and intraband processes behave differently for small $\mathbf{g}$ we split $\delta\rho_{\mathbf{g}}(\mathbf{r},\omega)$ and $\delta\mathbf{j}_{\mathbf{g}}(\mathbf{r},\omega)$ into their contributions from inter- and intraband processes and evaluate these contributions separately. We therefore write

$$\delta\rho_{\mathbf{g}}(\mathbf{r},\omega) = \delta\rho_{\mathbf{g}}^{inter}(\mathbf{r},\omega) + \delta\rho_{\mathbf{g}}^{intra}(\mathbf{r},\omega) \tag{8.16}$$

$$\delta\mathbf{j}_{\mathbf{g}}(\mathbf{r},\omega) = \delta\mathbf{j}_{\mathbf{g}}^{inter}(\mathbf{r},\omega) + \delta\mathbf{j}_{\mathbf{g}}^{intra}(\mathbf{r},\omega). \tag{8.17}$$

For finite $\mathbf{g}$ the lattice periodic density $\delta\rho_{\mathbf{g}}(\mathbf{r},\omega)$ and lattice periodic current density $\delta\mathbf{j}_{\mathbf{g}}(\mathbf{r},\omega)$ can be written in terms of the lattice periodic potentials and Kohn-Sham response functions. We give these expressions in the following concise form,

$$\begin{pmatrix} \delta\rho_{\mathbf{g}}^{inter} \\ i\delta\mathbf{j}_{\mathbf{g}}^{inter}/\omega \end{pmatrix} = \begin{pmatrix} \chi_{\rho\rho,\mathbf{g}}^{inter} & -i\chi_{\rho\mathbf{j}_p,\mathbf{g}}^{inter}/\omega \\ i\chi_{\mathbf{j}_p\rho,\mathbf{g}}^{inter}/\omega & \Delta\chi_{\mathbf{j}_p\mathbf{j}_p,\mathbf{g}}^{inter}/\omega^2 \end{pmatrix} \cdot \begin{pmatrix} \delta v_{\mathbf{g},s} \\ i\omega\delta\mathbf{A}_{\mathbf{g},s} \end{pmatrix}, \tag{8.18}$$

for the interband contributions, and

$$i\omega \begin{pmatrix} \omega/g\,\delta\rho_{\mathbf{g}}^{intra} \\ \delta\mathbf{j}_{\mathbf{g}}^{intra} \end{pmatrix} = \begin{pmatrix} \omega^2/g^2\,\chi_{\rho\rho,\mathbf{g}}^{intra} & \omega/g\,\chi_{\rho\mathbf{j}_p,\mathbf{g}}^{intra} \\ \omega/g\,\chi_{\mathbf{j}_p\rho,\mathbf{g}}^{intra} & \Delta\chi_{\mathbf{j}_p\mathbf{j}_p,\mathbf{g}}^{intra} \end{pmatrix} \cdot \begin{pmatrix} ig\delta v_{\mathbf{g},s} \\ i\omega\delta\mathbf{A}_{\mathbf{g},s} \end{pmatrix}, \tag{8.19}$$

for the intraband part. We note that the matrix vector products in the above expressions include an integration over a real-space coordinate. Furthermore we defined

$$\Delta\chi_{\mathbf{j}_p\mathbf{j}_p,\mathbf{g}} = \chi_{\mathbf{j}_p\mathbf{j}_p,\mathbf{g}}(\mathbf{r},\mathbf{r}',\omega) - \chi_{\mathbf{j}_p\mathbf{j}_p,\mathbf{g}}(\mathbf{r},\mathbf{r}',\omega=0), \tag{8.20}$$

where the Kohn-Sham response function $\chi_{\mathbf{j}_p\mathbf{j}_p,\mathbf{g}}(\omega)$ at $\omega = 0$ enters our expressions because we have made use of the conductivity sum rule given by

$$\left[\chi_{\mathbf{j}_p\mathbf{j}_p}(\mathbf{r},\mathbf{r}',0)\right]_{ij} + \rho_0(\mathbf{r})\delta_{ij}\delta(\mathbf{r}-\mathbf{r}') = 0, \tag{8.21}$$

which is convenient in practical applications. However, this means that we neglect the small Landau diamagnetic contribution for the transverse component of the induced current density [10]. We note that the terms appearing on the left-hand sides of Eqs.

(8.18) and (8.19) are all of order 1. The Kohn-Sham response functions that enter the above expressions are given by

$$\begin{aligned}\chi_{ab,\mathbf{g}}(\mathbf{r},\mathbf{r}',\omega) &= \frac{1}{N_k}\lim_{\eta\to 0^+}\sum_{\mathbf{k}}\sum_{n,n'}\frac{(f_{n\mathbf{k}}-f_{n'\mathbf{k}+\mathbf{g}})}{1+\delta_{n,n'}} \\ &\times \frac{[\phi^*_{n\mathbf{k}}(\mathbf{r})\tilde{a}_{\mathbf{g}}\phi_{n'\mathbf{k}+\mathbf{g}}(\mathbf{r})]\,[\phi^*_{n'\mathbf{k}+\mathbf{g}}(\mathbf{r}')\tilde{b}_{-\mathbf{g}}\phi_{n\mathbf{k}}(\mathbf{r}')]}{\omega-(\epsilon_{n'\mathbf{k}+\mathbf{g}}-\epsilon_{n\mathbf{k}})+i\eta}. \end{aligned} \tag{8.22}$$

in which $\tilde{a}_{\mathbf{g}}$ and $\tilde{b}_{\mathbf{g}}$ can be either $\tilde{\rho}_{\mathbf{g}} = e^{-i\mathbf{g}\cdot\mathbf{r}}$ or $\tilde{\mathbf{j}}_{p,\mathbf{g}} = -i(e^{-i\mathbf{g}\cdot\mathbf{r}}\nabla - \nabla^\dagger e^{-i\mathbf{g}\cdot\mathbf{r}})/2$, where the dagger on the nabla operator indicates that it acts on terms to the left of it. In Eq. (8.22) ϵ_n are the eigenvalues of the Kohn-Sham orbitals ϕ_n of the unperturbed system. The positive infinitesimal η in Eq. (8.22) ensures the causality of the response function. The Bloch functions are normalized on the Wigner-Seitz cell with volume V_{WS}, and the number of $\mathbf{k}$-points in the summation is $N_k = V_{BvK}/V_{WS}$, in which V_{BvK} is the volume of the Born-von Kármán cell. The intraband (interband) contribution to the response functions is given by the terms with $n = n'$ ($n \neq n'$) in the summation over n and n'. In the intraband case the factor $1/(1+\delta_{n,n'})$ corrects for the double counting.

The various interband contributions to the response functions given in Eq. (8.18) have the following ω dependence [110],

$$\begin{aligned}\chi^{inter}_{\rho\rho,\mathbf{g}} &\propto 1, \\ \chi^{inter}_{\rho\mathbf{j}_p,\mathbf{g}}, \chi^{inter}_{\mathbf{j}_p\rho,\mathbf{g}} &\propto \omega, \\ \Delta\chi^{inter}_{\mathbf{j}_p\mathbf{j}_p,\mathbf{g}} &\propto \omega^2, \end{aligned} \tag{8.23}$$

whereas the intraband response functions given in Eq. (8.19) have the following ω and g dependence at small $\mathbf{g}$ but finite ω [110],

$$\begin{aligned}\chi^{intra}_{\rho\rho,\mathbf{g}} &\propto g^2/\omega^2, \\ \chi^{intra}_{\rho\mathbf{j}_p,\mathbf{g}}, \chi^{intra}_{\mathbf{j}_p\rho,\mathbf{g}} &\propto g/\omega, \\ \Delta\chi^{intra}_{\mathbf{j}_p\mathbf{j}_p,\mathbf{g}} &\propto 1, \end{aligned} \tag{8.24}$$

where $g = |\mathbf{g}|$. Therefore the terms that enter the matrices in Eqs. (8.18) and (8.19) are all of order 1. This means that according to Eq. (8.19) in the limit $\mathbf{g} \to 0$ the Kohn-Sham scalar potential does not contribute to the intraband contribution to the induced density and current density. Only the Kohn-Sham vector potential contributes to the intraband contribution to the induced density and current density. Since the Kohn-Sham vector potential itself depends on the total induced current density, i.e., the sum of the inter- and intraband contributions, the set of self-consistent equations for

the inter- and intraband contributions to the density and current density are coupled. From the induced current density obtained from this self-consistent scheme we can obtain the electric susceptibility χ_e from Eqs. (8.4) and (8.5) which within the linear response regime can be rewritten as

$$\mathbf{P}_{mac}(\omega) = \frac{-i}{\omega V} \int_V \delta\mathbf{j}(\mathbf{r},\omega) d\mathbf{r}, \tag{8.25}$$

and

$$\mathbf{P}_{mac}(\omega) = \chi_e(\omega) \cdot \mathbf{E}_{mac}(\omega). \tag{8.26}$$

8.2.3 The Vignale-Kohn Functional

The general expression for the exchange-correlation vector potential is to first order

$$\delta\mathbf{A}_{xc}(\mathbf{r},\omega) = \int \mathbf{f}_{xc}(\mathbf{r},\mathbf{r}',\omega) \cdot \delta\mathbf{j}(\mathbf{r}',\omega) d\mathbf{r}'. \tag{8.27}$$

This expression defines the tensor kernel $\mathbf{f}_{xc}(\mathbf{r},\mathbf{r}',\omega)$. Vignale and Kohn derived an approximation for $\delta\mathbf{A}_{xc}(\mathbf{r},\omega)$ [12, 13] by studying a periodically modulated electron gas with wave vector $\mathbf{q}$ under the influence of an external perturbation with wave vector $\mathbf{k}$. This expression was proved to be valid if $k, q \ll k_F, \omega/v_F$, where k_F and v_F are the Fermi momentum and the Fermi velocity respectively. By construction the VK functional obeys several exact constraints. The VK functional satisfies the zero-force and zero-torque constraints which state that the exchange-correlation potentials cannot exert a net force or a net torque on the system. Furthermore, it obeys the requirement of generalized translational invariance which states that a rigid translation of the current density implies a rigid translation of the exchange-correlation potentials. Finally, it satisfies the Onsager symmetry relation which restricts the form of exchange-correlation kernel $\mathbf{f}_{xc}(\mathbf{r},\mathbf{r}',\omega)$. Vignale, Ullrich and Conti showed that the complicated VK-expression for $\delta\mathbf{A}_{xc}(\mathbf{r},\omega)$ could be written in the following physically transparent form [46]

$$i\omega\delta A_{xc,i}(\mathbf{r},\omega) = \partial_i \delta v_{xc}^{ALDA}(\mathbf{r},\omega) - \frac{1}{\rho_0(\mathbf{r})} \sum_j \partial_j \sigma_{xc,ij}(\mathbf{r},\omega), \tag{8.28}$$

where the first term on the right-hand side is just the linearization of the ALDA exchange-correlation scalar potential. Using a gauge transform this longitidinal part of $\delta\mathbf{A}_{xc}(\mathbf{r},\omega)$ can be included in the scalar potential. The second term is the divergence of a tensor field $\sigma_{xc}(\mathbf{r},\omega)$ which has the structure of a symmetric viscoelastic stress tensor,

$$\sigma_{xc,ij} = \tilde{\eta}_{xc} \left(\partial_j u_i + \partial_i u_j - \frac{2}{3}\delta_{ij} \sum_k \partial_k u_k \right) + \tilde{\zeta}\delta_{ij} \sum_k \partial_k u_k \tag{8.29}$$

in which the velocity field $\mathbf{u}(\mathbf{r},\omega)$ is given by

$$\mathbf{u}(\mathbf{r},\omega) = \frac{\delta\mathbf{j}(\mathbf{r},\omega)}{\rho_0(\mathbf{r})}. \tag{8.30}$$

The coefficients $\tilde{\eta}_{xc}(\mathbf{r},\omega)$ and $\tilde{\zeta}_{xc}(\mathbf{r},\omega)$ are determined by the longitudinal and transverse response coefficients of the homogeneous electron gas evaluated at the density $\rho_0(\mathbf{r})$,

$$\tilde{\eta}_{xc}(\mathbf{r},\omega) = \frac{i}{\omega}\rho_0^2(\mathbf{r}) f^h_{xcT}(\rho_0(\mathbf{r}),\omega), \tag{8.31}$$

and

$$\tilde{\zeta}_{xc}(\mathbf{r},\omega) = \frac{i}{\omega}\rho_0^2(\mathbf{r}) \left(f^h_{xcL}(\rho_0(\mathbf{r}),\omega) - \frac{4}{3} f^h_{xcT}(\rho_0(\mathbf{r}),\omega) - \frac{d^2\epsilon^h_{xc}}{d\rho^2}(\rho_0(\mathbf{r})) \right), \tag{8.32}$$

where $\epsilon^h_{xc}(\rho)$ is the exchange-correlation energy per unit volume of the homogeneous electron gas. The quantities $\tilde{\eta}_{xc}(\mathbf{r},\omega)$ and $\tilde{\zeta}_{xc}(\mathbf{r},\omega)$ can be interpreted as viscoelastic coefficients [46, 49]. The coefficients $f^h_{xcL,T}(\omega)$ are defined by the identity [13, 50]

$$f^h_{xcL,T}(\omega) \equiv \lim_{\mathbf{k}\to 0} f^h_{xcL,T}(\mathbf{k},\omega) \tag{8.33}$$

Unfortunately the longitudinal and transverse exchange-correlation kernels are not known accurately. However, they have been extensively studied and some exact features are well known [14, 15, 47–49]. In particular Conti and Vignale [49] obtained the exact results for $\lim_{\omega\to 0}\lim_{\mathbf{k}\to 0} f^h_{xcL,T}(q,\omega)$ by comparing the microscopic linear-response equations with the macroscopic viscoelastic equation of motion. Their evaluations led to the following identities for the three-dimensional electron gas,

$$\lim_{\omega\to 0}\lim_{\mathbf{k}\to 0} f^h_{xcL}(\mathbf{k},\omega) = \frac{1}{\rho^2}\left(K_{xc} + \frac{4}{3}\mu_{xc}\right) \tag{8.34}$$

$$\lim_{\omega\to 0}\lim_{\mathbf{k}\to 0} f^h_{xcT}(\mathbf{k},\omega) = \frac{\mu_{xc}}{\rho^2}, \tag{8.35}$$

where K_{xc} and μ_{xc} are the exchange-correlation parts of the bulk and shear modulus, respectively, which are real quantities. Since $K_{xc} = \rho^2(d^2\epsilon^h_{xc}(\rho)/d\rho^2)$ we see from Eqs. (8.34) and (8.35) that the parameter $\tilde{\zeta}_{xc}(\mathbf{r},\omega)$ contains a factor for which one can prove the exact relation [46, 49]

$$\lim_{\omega\to 0}\left(f^h_{xcL}(\rho(\mathbf{r}),\omega) - \frac{4}{3} f^h_{xcT}(\rho(\mathbf{r}),\omega) - \frac{d^2\epsilon^h_{xc}}{d\rho^2}(\rho(\mathbf{r})) \right) = 0. \tag{8.36}$$

From the above relations we can determine the behavior of the coefficients $\tilde{\eta}_{xc}(\mathbf{r},\omega)$

and $\tilde{\zeta}_{xc}(\mathbf{r},\omega)$ in the limit $\omega \to 0$. We obtain

$$\lim_{\omega\to 0} \frac{-i\omega\tilde{\zeta}_{xc}(\mathbf{r},\omega)}{\rho_0^2(\mathbf{r})} = 0 \tag{8.37}$$

$$\lim_{\omega\to 0} \frac{-i\omega\tilde{\eta}_{xc}(\mathbf{r},\omega)}{\rho_0^2(\mathbf{r})} = f_{xcT}(\rho_0(\mathbf{r}),0). \tag{8.38}$$

We see that only if $\mu_{xc} = 0$ the VK expression (8.28) reduces to the ALDA in the limit $\omega \to 0$, otherwise it does not. The exchange-correlation part of the shear modulus can be related to the Landau parameters F_l as [49],

$$\mu_{xc} = \frac{2\rho\epsilon_F}{5}\frac{F_2/5 - F_1/3}{1 + F_1/3}. \tag{8.39}$$

The bulk modulus $K_{xc} = \rho^2(d^2\epsilon_{xc}^h(\rho)/d\rho^2)$ can be obtained from accurate results of Monte Carlo calculations [55,69]. The shear modulus μ_{xc}, however, is not accurately known. Values for μ_{xc} can be obtained from the calculations performed by Nifosì, Conti, and Tosi [48] or from Eq. (8.39) using the Landau parameters calculated by Yasuhara and Ousaka [15, 49, 57]. Even though the results may not be accurate, it is clear from these calculations that μ_{xc} is much smaller than K_{xc}. Surprisingly, however, it turns out that μ_{xc} has a much bigger influence than K_{xc} on the optical spectra of infinite polymer chains and bulk semiconductors leading to a collapse of these spectra [93, 113]. If we make the approximation $\mu_{xc} = 0$ we obtain results close to the results obtained within the ALDA, since in this approximation the VK expression, Eq. (8.28), reduces to the ALDA in the limit $\omega \to 0$ and the values of the coefficients $f_{xcL,T}^h(\omega)$ are close to $f_{xcL,T}^h(0)$ for $\omega \ll \omega_{pl}$ which is the range of frequencies that were interested in.

Finally, let us briefly discuss the two parametrizations that exist for $f_{xcL,T}^h(\omega)$ and that we will use in this chapter. Conti, Nifosì and Tosi (CNT) [14] calculated $\mathrm{Im} f_{xcL,T}^h(\omega)$ directly by means of an approximate decoupling of an exact four-point response function. CNT then introduced parametrizations for $\mathrm{Im} f_{xcL,T}^h(\omega)$ that reproduce their numerical results. The real part can then be obtained from the Kramers-Krönig dispersion relations. Their results have the correct behavior in the limit $\omega \to \infty$, the high-frequency limit of $f_{xcL}^h(\omega)$ being equal to that obtained by Glick and Long [56]. The real parts of $f_{xcL,T}^h(\omega)$ can be obtained from the Kramers-Krönig dispersion relations where the high-frequency limits of $f_{xcL,T}^h(\omega)$ were obtained from third-frequency-moment sum rules [45,49,52,53]. However, their results do not reduce to the exact results in the limit $\omega \to 0$ given in Eqs. (8.34) and (8.35) because they invoke the compressibility sum rule,

$$\lim_{\mathbf{k}\to 0}\lim_{\omega\to 0} f_{xcL}^h(q,\omega) = \frac{K_{xc}}{\rho^2}, \tag{8.40}$$

thereby interchanging the order of the limits with respect to the exact result (8.34). This is equivalent to the approximation $\mu_{xc} = 0$. Because of the uncertainty in the precise values of μ_{xc}, the fact that it is small compared to K_{xc} and the appeal of a theory that reduces to the ALDA in the limit $\omega \to 0$ CNT prefer to enforce equality of the order of limits [14]. A distinct feature of the CNT result is a pronounced peak around $\omega = 2\omega_{pl}$ in $\mathrm{Im}f^h_{xcL,T}(\omega)$, where ω_{pl} is the plasmon frequency.

An alternative parametrization was given by Qian and Vignale [15]. First they obtained an exact result for the slope of the imaginary part of $\mathrm{Im}f^h_{xcL,T}(\omega)$ at $\omega = 0$. Then they adopt an interpolation formula first introduced by Gross and Kohn [45] to model $\mathrm{Im}f^h_{xcL,T}(\omega)$. To satisfy the constraint on the slope of $\mathrm{Im}f^h_{xcL,T}(\omega)$ at $\omega = 0$ they need one more parameter. This extra parameter in their scheme is the width of a Gaussian peak around $\omega = 2\omega_{pl}$ that accounts for the two-plasmon contributions found by CNT. The coefficients in their interpolation formula are then chosen such to reproduce the correct behavior in the limit $\omega \to \infty$ as well as the correct behavior in the limit $\omega \to 0$ determined by their result for the slope of $\mathrm{Im}f^h_{xcL,T}(\omega)$ at $\omega = 0$ and Eqs. (8.34) and (8.35). Their model shows a peak that is less pronounced than CNT's. Since QV give an expression for their parametrization in which $f^h_{xcL,T}(0)$ enter explicitly, their parametrization can easily be adapted for the case $f^h_{xcT}(0)$=0. For reasons mentioned in the Introduction we, like CNT, prefer to use a theory that reduces to the ALDA in the limit $\omega \to 0$. This means that we will use the QV parametrization only with $\mu_{xc} = f^h_{xcT}(0) = 0$. We will denote this approximation by QVA.

8.2.4 Relativistic Corrections

In the case of Au we include scalar relativistic effects in our formulation by using the zeroth-order regular approximation (ZORA) [121–123] along the same line as described in Refs. [124–127]. We use the the ground-state ZORA equation,

$$\left[\hat{\mathbf{g}} \cdot \frac{K(\mathbf{r})}{2}\hat{\mathbf{g}} + v_{s,0}(\mathbf{r})\right] \phi_{i\mathbf{g}}(\mathbf{r}) = \epsilon_{i\mathbf{g}}\phi_{i\mathbf{g}}(\mathbf{r}), \tag{8.41}$$

to get the orbitals and the orbital energies needed in Eq. (8.22) to calculate the response functions. Here $v_{s,0}(\mathbf{r})$ is the self-consistent Kohn-Sham potential of the ground state and the factor $K(\mathbf{r})$ is given by

$$K(\mathbf{r}) = \frac{2c^2}{2c^2 - v_{s,0}(\mathbf{r})}, \tag{8.42}$$

where c is the velocity of light. The time-dependent Hamiltonian including scalar relativistic effects within the ZORA is given by

$$\hat{H}^{ZORA}(t) = \hat{\pi} \cdot \frac{K(\mathbf{r})}{2}\hat{\pi} + v_s(\mathbf{r}, t), \tag{8.43}$$

where

$$\hat{\pi} = \hat{\mathbf{p}} + \mathbf{A}_s(\mathbf{r}, t). \tag{8.44}$$

The scalar relativistic induced current density within the ZORA can now be obtained from the nonrelativistic current density in Eq. (8.15) by the substitution of the auxiliary operator $\tilde{\mathbf{j}}_{p,\mathbf{g}}$ with the auxiliary operator

$$\tilde{\mathbf{j}}^{ZORA}_{p,\mathbf{g}} = \frac{-i}{2}(e^{-i\mathbf{g}\cdot\mathbf{r}}K(\mathbf{r})\nabla - \nabla^{\dagger}K(\mathbf{r})e^{-i\mathbf{g}\cdot\mathbf{r}}) \tag{8.45}$$

in the response functions given in Eq. (8.22).

As we will show in the next section, in our implementation we will need the curl of the induced current density,

$$\delta\mathbf{m}(\mathbf{r}, \omega) = \nabla \times \delta\mathbf{j}(\mathbf{r}, \omega). \tag{8.46}$$

In a similar way as for $\delta\mathbf{j}$ we can write

$$\delta\mathbf{m}(\mathbf{r}, \omega) = e^{i\mathbf{g}\cdot\mathbf{r}}\delta\mathbf{m}_{\mathbf{g}}(\mathbf{r}, \omega). \tag{8.47}$$

An expression for $\delta\mathbf{m}_{\mathbf{g}}(\mathbf{r}, \omega)$ can be obtained from Eq. (8.17) by taking the curl on either side which amounts to the substitution of $\tilde{\mathbf{m}}_{\mathbf{g}} = -i(\nabla^{\dagger}e^{-i\mathbf{g}\cdot\mathbf{r}} \times \nabla)$ for $\tilde{a}_{\mathbf{g}}$ in the Kohn-Sham response functions given in Eq. (8.22). In the case that we consider scalar relativistic effects within the ZORA we can do a similar evaluation to obtain the auxiliary operator $\tilde{\mathbf{m}}^{ZORA}_{\mathbf{g}}$. It is given by

$$\begin{aligned} \tilde{\mathbf{m}}^{ZORA}_{\mathbf{g}} &= -i(\nabla^{\dagger}e^{-i\mathbf{g}\cdot\mathbf{r}}K(\mathbf{r}) \times \nabla) \\ &- \frac{i}{2}\left(e^{-i\mathbf{g}\cdot\mathbf{r}}[\nabla K(\mathbf{r})] \times \nabla + \nabla^{\dagger} \times [\nabla K(\mathbf{r})]e^{-i\mathbf{g}\cdot\mathbf{r}}\right). \end{aligned} \tag{8.48}$$

For the materials discussed in this chapter $K(\mathbf{r}) \approx 1$ and $\nabla v_{s,0}(\mathbf{r}) \ll 2c^2$ everywhere except close to the nuclei. The term $\nabla K(\mathbf{r}) = K^2(\mathbf{r})\nabla v_{s,0}(\mathbf{r})/(2c^2)$ is thus smaller than one everywhere, except in a small volume around the nuclei which, however, has a negligible contribution to the integrals in which it appears. Therefore we will neglect the second term on the right-hand side of Eq. (8.48).

8.3 Implementation

As shown in Ref. [93] we can write $\delta\mathbf{A}_{xc}(\mathbf{r},\omega)$ as expressed in Eqs. (8.28)-(8.30) in a more convenient way,

$$\delta\mathbf{A}_{xc}(\mathbf{r},\omega) = -\frac{i}{\omega}\nabla[\delta v_{xc}^{ALDA}(\mathbf{r},\omega) + \delta u_{xc}(\mathbf{r},\omega)] + \delta\mathbf{a}_{xc}(\mathbf{r},\omega) + \nabla\times\delta\mathbf{b}_{xc}(\mathbf{r},\omega). \quad (8.49)$$

where $\delta u_{xc}(\mathbf{r},\omega)$ is a scalar field, $\delta\mathbf{a}_{xc}(\mathbf{r},\omega)$ is a polar vector field, $\delta\mathbf{b}_{xc}(\mathbf{r},\omega)$ is an axial vector field. These fields can be written in the following compact matrix vector product [93]

$$\begin{pmatrix} \delta u_{xc} \\ i\omega\delta\mathbf{a}_{xc} \\ i\omega\delta\mathbf{b}_{xc} \end{pmatrix} = \begin{pmatrix} y_{\rho\rho} & y_{\rho\mathbf{j}} & 0 \\ y_{\mathbf{j}\rho} & y_{\mathbf{jj}} & y_{\mathbf{jm}} \\ 0 & y_{\mathbf{mj}} & y_{\mathbf{mm}} \end{pmatrix} \cdot \begin{pmatrix} \delta\rho \\ i\delta\mathbf{j}/\omega \\ i\delta\mathbf{m}/\omega \end{pmatrix}. \quad (8.50)$$

The matrix entries are given as

$$y_{\rho\rho} = -i\omega\frac{\frac{4}{3}\tilde{\eta}_{xc} + \tilde{\zeta}_{xc}}{\rho_0^2}, \quad (8.51)$$

$$y_{\rho\mathbf{j}} = y_{\mathbf{j}\rho}^T = -i\omega\left(\frac{\frac{4}{3}\tilde{\eta}_{xc} + \tilde{\zeta}_{xc}}{\rho_0^2} - 2\frac{\tilde{\eta}'_{xc}}{\rho_0}\right)\frac{\nabla\rho_0}{\rho_0}, \quad (8.52)$$

$$\begin{aligned} y_{\mathbf{jj}} &= -i\omega\left(\frac{\frac{1}{3}\tilde{\eta}_{xc} + \tilde{\zeta}_{xc}}{\rho_0^2} - 4\frac{\tilde{\eta}'_{xc}}{\rho_0} + 2\tilde{\eta}''_{xc}\right)\frac{\nabla\rho_0\otimes\nabla\rho_0}{\rho_0^2} \\ &\quad -i\omega\left(2\frac{\tilde{\eta}'_{xc}}{\rho_0}\frac{\nabla\otimes\nabla\rho_0}{\rho_0} + \frac{\tilde{\eta}_{xc}}{\rho_0^2}\frac{|\nabla\rho_0|^2}{\rho_0^2}\mathbf{I}\right), \end{aligned} \quad (8.53)$$

$$y_{\mathbf{jm}} = y_{\mathbf{mj}}^T = -i\omega\frac{\tilde{\eta}_{xc}}{\rho_0^2}\left[\frac{\nabla\rho_0}{\rho_0}\times\right], \quad (8.54)$$

$$y_{\mathbf{mm}} = -i\omega\frac{\tilde{\eta}_{xc}}{\rho_0^2}\mathbf{I}, \quad (8.55)$$

in which we define the antisymmetric 3×3 matrix $[\nabla\rho_0/\rho_0\times]_{ij} = -\sum_k \epsilon_{ijk}(\partial_k\rho_0)/\rho_0$ and where $\tilde{\eta}'_{xc}(\mathbf{r},\omega)$ and $\tilde{\eta}''_{xc}(\mathbf{r},\omega)$ are the first- and second-order derivatives of $\tilde{\eta}_{xc}(\mathbf{r},\omega)$ with respect to the ground-state density. The matrix in Eq. (8.50) is a local function of the ground-state density and its first- and second-order gradients and has additional ω dependence through the coefficients $\tilde{\eta}_{xc}(\mathbf{r},\omega)$ and $\tilde{\zeta}_{xc}(\mathbf{r},\omega)$.

Using Eq. (8.49) the exchange-correlation contribution to the perturbation given in Eq. (8.6) can now be rewritten within our linear response formulation as

$$\begin{aligned} \delta\hat{H}_{xc}(\mathbf{r},\omega) &= \tilde{\rho}_{-\mathbf{g}}\left[\delta v_{xc,\mathbf{g}}^{ALDA}(\mathbf{r},\omega) + \delta u_{xc,\mathbf{g}}(\mathbf{r},\omega)\right] \\ &+ \tilde{\mathbf{j}}_{p,-\mathbf{g}}\cdot\delta\mathbf{a}_{xc,\mathbf{g}}(\mathbf{r},\omega) + \tilde{\mathbf{m}}_{-\mathbf{g}}\cdot\delta\mathbf{b}_{xc,\mathbf{g}}(\mathbf{r},\omega). \end{aligned} \quad (8.56)$$

In the case of Au where we include scalar relativistic effects within the ZORA one should read $\tilde{\mathbf{j}}^{ZORA}_{p,-\mathbf{g}}$ and $\tilde{\mathbf{m}}^{ZORA}_{-\mathbf{g}}$ instead of $\tilde{\mathbf{j}}_{p,-\mathbf{g}}$ and $\tilde{\mathbf{m}}_{-\mathbf{g}}$ in Eq. (8.56). Using Eq. (8.56) the self-consistent linear-response equations (8.18) and (8.19) can be written in the following form

$$\begin{pmatrix} \delta\rho^{inter}_{\mathbf{g}} \\ i\delta\mathbf{j}^{inter}_{\mathbf{g}}/\omega \\ i\delta\mathbf{m}^{inter}_{\mathbf{g}}/\omega \end{pmatrix} = \begin{pmatrix} \chi^{inter}_{\rho\rho\mathbf{g}} & -i\chi^{inter}_{\rho\mathbf{j}_p\mathbf{g}}/\omega & -i\chi^{inter}_{\rho\mathbf{mg}}/\omega \\ i\chi^{inter}_{\mathbf{j}_p\rho\mathbf{g}}/\omega & \Delta\chi^{inter}_{\mathbf{j}_p\mathbf{j}_p\mathbf{g}}/\omega^2 & \Delta\chi^{inter}_{\mathbf{j}_p\mathbf{mg}}/\omega^2 \\ i\chi^{inter}_{\mathbf{m}\rho\mathbf{g}}/\omega & \Delta\chi^{inter}_{\mathbf{mj}_p\mathbf{g}}/\omega^2 & \Delta\chi^{inter}_{\mathbf{mmg}}/\omega^2 \end{pmatrix} \cdot \begin{pmatrix} \delta v_{\mathbf{g},H,mic} + \delta v^{ALDA}_{\mathbf{g},xc,mic} + \delta u_{\mathbf{g},xc} \\ i\omega(\delta\mathbf{A}_{\mathbf{g},mac} + \delta\mathbf{a}_{\mathbf{g},xc}) \\ i\omega\delta\mathbf{b}_{\mathbf{g},xc} \end{pmatrix}, \tag{8.57}$$

for the interband parts, and as

$$i\omega \begin{pmatrix} \omega/g\delta\rho^{intra}_{\mathbf{g}} \\ \delta\mathbf{j}^{intra}_{\mathbf{g}} \\ \delta\mathbf{m}^{intra}_{\mathbf{g}} \end{pmatrix} = \begin{pmatrix} \omega^2/g^2\chi^{intra}_{\rho\rho\mathbf{g}} & \omega/g\chi^{intra}_{\rho\mathbf{j}_p\mathbf{g}} & \omega/g\chi^{intra}_{\rho\mathbf{mg}} \\ \omega/g\chi^{intra}_{\mathbf{j}_p\rho\mathbf{g}} & \Delta\chi^{intra}_{\mathbf{j}_p\mathbf{j}_p\mathbf{g}} & \Delta\chi^{intra}_{\mathbf{j}_p\mathbf{mg}} \\ \omega/g\chi^{intra}_{\mathbf{m}\rho\mathbf{g}} & \Delta\chi^{intra}_{\mathbf{mj}_p\mathbf{g}} & \Delta\chi^{intra}_{\mathbf{mmg}} \end{pmatrix} \cdot \begin{pmatrix} ig(\delta v_{\mathbf{g}H,mic} + \delta v^{ALDA}_{\mathbf{g},xc,mic} + \delta u_{\mathbf{g},xc}) \\ i\omega(\delta\mathbf{A}_{\mathbf{g},mac} + \delta\mathbf{a}_{\mathbf{g},xc}) \\ i\omega\delta\mathbf{b}_{\mathbf{g},xc} \end{pmatrix}, \tag{8.58}$$

for the intraband contributions, with $\Delta\chi_{\mathbf{abg}} = (\chi_{\mathbf{ab}}(\omega) - \chi_{\mathbf{ab}}(\omega = 0))$. The matrix vector products in the above expressions again include an integration over a real-space coordinate. The above relations have been written in such a way that all matrix elements are real and finite in the limit $(\mathbf{g}, \omega) \to (0, 0)$. The explicit expressions for the Kohn-Sham response functions have been given in Refs. [93, 110]. In the limit of vanishing $\mathbf{g}$ the set of equations (8.57) reduces to that one used in the case of nonmetallic crystalline systems [93] for which we need to consider only fully occupied bands and fully unoccupied bands. In this limit the term $ig(\delta v_{\mathbf{g}H,mic} + \delta v^{ALDA}_{\mathbf{g},xc,mic} + \delta u_{\mathbf{g},xc})$ on the right-hand side of Eqs (8.58) vanishes [110]. Therefore in the optical limit $\mathbf{g} \to 0$ the intraband parts of the density, the current density and the curl of current density only have contributions from the macroscopic vector potential and the terms $\delta\mathbf{a}_{\mathbf{g},xc}$ and $\delta\mathbf{b}_{\mathbf{g},xc}$ that enter the VK expression for the exchange-correlation vector potential. Once the two sets of Eqs. (8.57) and (8.58) are solved we can calculate the macroscopic dielectric function as

$$\epsilon(\omega) = 1 + 4\pi\chi_e(\omega), \tag{8.59}$$

where $\chi_e(\omega)$ is the electric susceptibility, and the electron energy loss function as

$$\frac{2\pi}{k^2V}S(\mathbf{g}, \omega) = -\mathrm{Im}\frac{1}{\hat{\mathbf{g}} \cdot \epsilon(\mathbf{g}, \omega) \cdot \hat{\mathbf{g}}}, \tag{8.60}$$

where $S(\mathbf{g},\omega)$ is the dynamical structure factor. The above expression is valid for general $\mathbf{g}$. Here we evaluate it in the optical limit $\mathbf{g} \to 0$. In a recent work [110] it was shown that within the ALDA the intraband contribution to the dielectric function is real when evaluated in the optical limit. Therefore there is no intraband contribution to the absorption spectrum within this approximation. By using the Vignale-Kohn functional it is no longer possible to separate inter- and intraband contributions to the dielectric function. Inter- and intraband processes are coupled through the exchange-correlation potentials $\delta\mathbf{a}_{\mathbf{g},xc}$ and $\delta\mathbf{b}_{\mathbf{g},xc}$ which are complex vectors, and give rise to the Drude-like tail on the low-frequency range of the absorption spectrum.

8.4 Results

We calculated the macroscopic dielectric functions $\epsilon(\omega)$ and the electron energy loss functions $-\mathrm{Im}\left\{\epsilon(\omega)\right\}^{-1}$ in the spectral range 0-10 eV for the isotropic crystals of copper, silver, and gold in an fcc lattice. We used the experimental lattice constants 3.61 Å for Cu, 4.09 Å for Ag, and 4.08 Å for Au. All calculations were performed using a modified version of the ADF-BAND program [76, 81–83, 110]. We made use of a hybrid valence basis set consisting of Slater-type orbitals (STO) in combination with the numerical solutions of a free-atom Herman-Skillman program [84]. Cores were kept frozen up to 3p for Cu, 4p for Ag, and 4f for Au. The spatial resolution of this basis is equivalent to a STO triple-zeta basis set augmented with two polarization functions [128]. The Herman-Skillman program also provides us with the free-atom Kohn-Sham potential. The crystal potential was evaluated using an auxiliary basis set of STO functions to fit the deformation density in the ground-state calculation and the induced density in the response calculation. For the evaluation of the $\mathbf{k}$-space integrals we used a numerical integration scheme with 175 symmetry-unique sample points in the irreducible wedge of the Brillouin zone, which was constructed by adopting a Lehmann-Taut tetrahedron scheme [85, 129]. In all our ground-state calculations we used the local density approximation (LDA) for the exchange-correlation functional. In the response calculations we employed the Vignale-Kohn functional as well as the ALDA for comparison. All results shown here were obtained using the Vosko-Wilk-Nusair parametrization [55] of the LDA exchange-correlation potential, which was also used to derive the ALDA exchange-correlation kernel, and both the QVA and CNT parametrizations for the longitudinal and transverse kernels $f^h_{xcL,T}(\omega)$ which enter the VK expression for the exchange-correlation vector potential. In Figs. 8.1-8.3 the real and imaginary parts of the dielectric functions of Cu, Ag, and Au are reported. The results obtained using the VK functional with the QVA and CNT parametrizations for $f^h_{xcL,T}(\omega)$ are in close agreement. The main difference is the

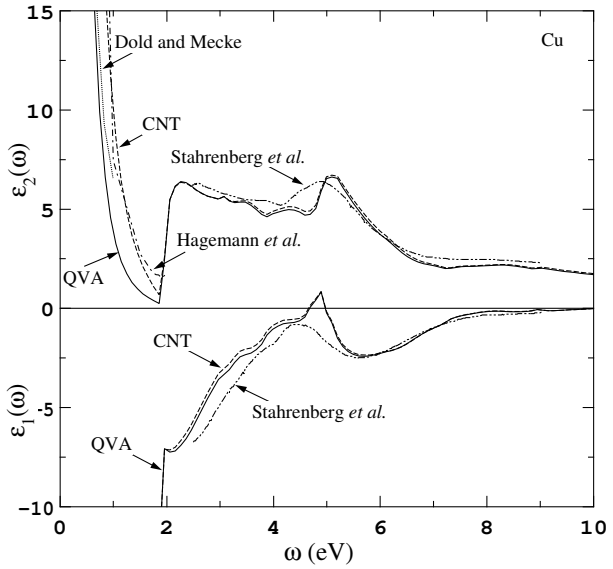

Figure 8.1: The calculated and measured real $[\epsilon_1(\omega)]$ and imaginary $[\epsilon_2(\omega)]$ parts of the dielectric function of Cu. The experimental results are taken from Refs. [114–116].

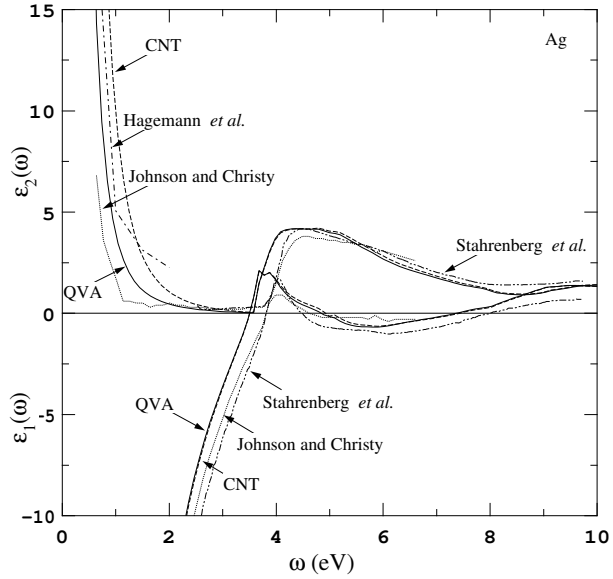

Figure 8.2: The calculated and measured real $[\epsilon_1(\omega)]$ and imaginary $[\epsilon_2(\omega)]$ parts of the dielectric function of Ag. The experimental results are taken from Refs. [114,116,117].

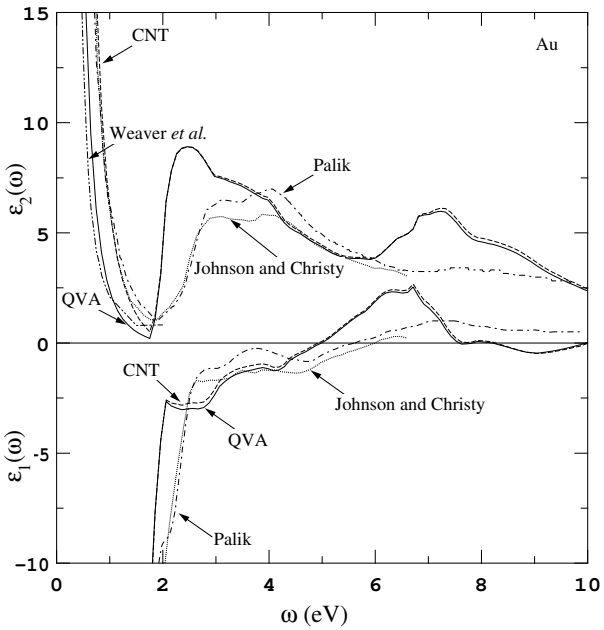

Figure 8.3: The calculated and measured real $[\epsilon_1(\omega)]$ and imaginary $[\epsilon_2(\omega)]$ parts of the dielectric functions of Au. The experimental results are taken from Refs. [117–119]. The theoretical curves are the results of scalar relativistic calculations.

Drude-like tail in the absorption spectra where the two results are roughly 0.25 eV apart. For convenience we do not report the ALDA results [110, 126] since they are almost identical to the VK results with the important exception that the Drude-like tail in its absorption spectrum is absent since the ALDA is a local function in time and therefore cannot describe relaxation processes. When the VK functional is employed we obtain a Drude-like tail in the low-frequency range. This absorption is due to relaxation processes of which the part due to electron-electron scattering can be described by using an exchange-correlation functional that is nonlocal in time. In the appendix we analyze the low-frequency behavior of the dielectric function within our method. There we show that in the case we apply the Vignale-Kohn functional with $\mu_{xc} = 0$ then for frequencies bigger than a characteristic frequency ω_1, which we define in the appendix, the real part of the dielectric function diverges as ω^{-2}, whereas the imaginary part should decay as ω^{-3}. For frequencies below ω_1, the real part of the dielectric function is finite whereas the imaginary part diverges as ω^{-1}. If on the other hand we apply the Vignale-Kohn functional with $\mu_{xc} \neq 0$ we obtain

the same low-frequency behavior as we found above for the case $\mu_{xc} = 0$ with the important difference that for frequencies below a characteristic frequency $\omega_0 < \omega_1$, which we define in the appendix, the imaginary part of the dielectric function will go to zero as ω. Therefore, instead of a Drude-like tail we observe a low-frequency peak in our calculated absorption spectra around ω_1.

The low-frequency behavior we obtain with the Vignale-Kohn functional with $\mu_{xc} = 0$ is in agreement with the description of the intraband contribution to the dielectric function within the classical Drude model. Within this simple model the real and imaginary parts of the dielectric functions, $\epsilon_1(\omega)$ and $\epsilon_2(\omega)$, respectively, are given by,

$$\epsilon_1^D(\omega) = 1 - \frac{\omega_p^2\tau^2}{1+\omega^2\tau^2}, \tag{8.61}$$

$$\epsilon_2^D(\omega) = \frac{\omega_p^2\tau}{\omega(1+\omega^2\tau^2)}, \tag{8.62}$$

with ω_p the plasma frequency and the τ the relaxation time. The latter is in general frequency-dependent [130–133]. For $\omega\tau \gg 1$, which is true for the near infrared, Eqs. (8.61) and (8.62) become,

$$\epsilon_1^D(\omega) = 1 - \frac{\omega_p^2}{\omega^2}, \tag{8.63}$$

$$\epsilon_2^D(\omega) = \frac{\omega_p^2}{\omega^3\tau}. \tag{8.64}$$

The real part of the dielectric function scales as ω^{-2}, whereas the imaginary part scales as ω^{-3} for a frequency-independent τ, in agreement with our calculations. For $\omega\tau \ll 1$, the Drude equations reduce to,

$$\epsilon_1^D(\omega) = 1 - \omega_p^2\tau^2, \tag{8.65}$$

$$\epsilon_2^D(\omega) = \frac{\omega_p^2\tau}{\omega}. \tag{8.66}$$

Again we find a qualitative agreement between the Drude description and our model: a finite real part and an imaginary part which diverges as ω^{-1}. We note that in our calculations we only take into account relaxation processes due to electron-electron scattering whereas the Drude model also describes relaxation processes due to other phenomena such as electron-phonon scattering. However, the analysis given above does not depend on the precise value of τ.

Our results are also in good agreement with the experimental results although the spectra obtained for gold show some discrepancies with respect to the experimental

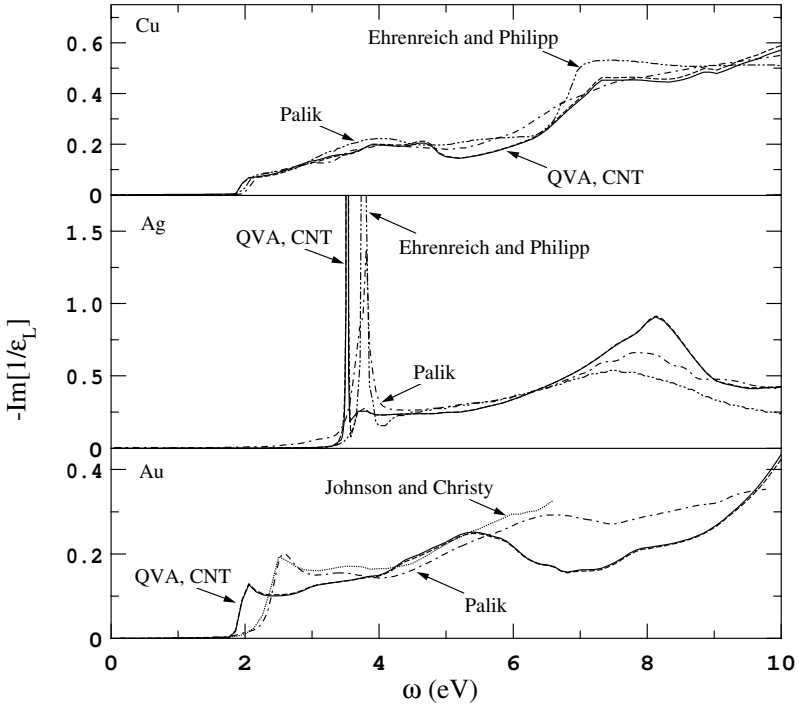

Figure 8.4: Electron-energy loss spectra of Cu, Ag, and Au. The experimental results are taken from Refs. [117, 118, 120]. The calculated results reported for Au refer to scalar relativistic calculations. Since the QVA and CNT spectra are very close to each other we only use one arrow in each panel to indicate both spectra. The QVA spectra and the CNT spectra are denoted by the continuous and dashed curve, respectively.

results, especially the first peak in the absorption spectrum is not well described. The Drude-like tails in the absorption spectra seem to be well described for all the three materials. However, since we only consider relaxation processes due to electron-electron scattering and not those due to electron-phonon scattering our results should be below those obtained with experiment. We therefore expect that the results we obtain for the Drude-like tail using the VK functional with the QVA parametrization are the closest to the exact Drude-like tail due to electron-electron scattering only. In Fig. 8.4 we show the electron energy loss spectra (EELS) of Cu, Ag, and Au. The EELS of Cu and Ag are already well-described within the ALDA [110]. Again the results obtained using the VK functional with the two parametrizations are in close

agreement with each other and with the results obtained within the ALDA which we do not show for convenience. There is one notable discrepancy though. The ALDA fails to reproduce the sharp plasmon peak at about 3.8 eV in the EELS of silver [118, 120] since within this approximation the plasmon peak is simply a delta function. In the EELS obtained with the VK functional one obtains a plasmon peak with finite width. The appearance of this peak is due to the fact that now the imaginary part of the dielectric function is small but nonvanishing at the frequency where the real part crosses the zero axis. This feature is well-described by the VK functional with the QVA and CNT parametrizations for $f^h_{xcL,T}(\omega)$. Also for Au the VK performs very similar to the ALDA and we obtain a reasonable agreement with the experimental results. We note that for Au we have obtained the experimental electron energy-loss spectra from optical measurements.

8.5 Conclusions

In this chapter we have included the Vignale-Kohn expression for the exchange-correlation vector potential in our formulation of the linear response of metals within the time-dependent current-density approach. This functional is nonlocal in time and therefore relaxation effects due to electron-electron scattering could be taken into account. The evaluation of the VK functional requires the knowledge of the exchange-correlation kernels of the homogeneous electron gas $f^h_{xcL,T}(\rho,\omega)$ as a function of the density and the frequency. We have used the two existing parametrizations for $f^h_{xcL,T}(\rho,\omega)$ by Conti, Nifosì and Tosi (CNT) and by Qian and Vignale (QV). In the optical limit $\mathbf{g} \to 0$ the two sets of self consistent equations describing the inter- and intraband contributions to the response are coupled when the Vignale-Kohn expression for the exchange-correlation vector potential is included. We have calculated the dielectric and electron energy loss functions of copper, silver, and gold and we have compared them with the best available measurements reported in literature and with our results from calculations within the adiabatic local density approximation. The VK functional yields results which are in good agreement with the experimental results. The real parts of the dielectric functions and the regions in the absorption spectra where the interband processes are dominant are similarly described by the two approximations and are close to previous results obtained within the ALDA. In addition the VK functional reproduces the low-frequency Drude-like tails in the absorption spectra, which were absent in the previous ALDA calculations. The electron energy loss spectra obtained with the VK functional are close to the spectra obtained within the ALDA with a notable difference in the case of silver: whereas the first sharp plasmon peak found in the experimental EELS was absent in the ALDA spectrum,

this feature is well described in the spectrum obtained with the VK functional.

Appendix: Low-Frequency Behavior of the Dielectric Function.

We define two vectors $\mathbf{P}$ and $\mathbf{F}$ as

$$\mathbf{P} = \begin{pmatrix} \delta\rho \\ i\delta\mathbf{j}/\omega \\ i\delta\mathbf{m}/\omega \end{pmatrix}, \tag{8.67}$$

containing the densities, in which the inter- and intraband contributions are added, i.e., $\delta\rho = \delta\rho^{inter} + \delta\rho^{intra}$ and similarly for $\delta\mathbf{j}$ and $\delta\mathbf{m}$, and where we defined

$$\mathbf{F} = \begin{pmatrix} 0 \\ i\omega\delta\mathbf{A}_{mac} \\ 0 \end{pmatrix} + \begin{pmatrix} \delta v^{ALDA}_{Hxc,mic} \\ 0 \\ 0 \end{pmatrix} + \begin{pmatrix} \delta u_{xc} \\ i\omega\delta\mathbf{a}_{xc} \\ i\omega\delta\mathbf{b}_{xc} \end{pmatrix}, \tag{8.68}$$

which contains all first order contributions to the perturbing potentials. Here the perturbation $\mathbf{F}$ is decomposed into three terms: $\mathbf{F}_{mac}$ containing only the macroscopic field, $\mathbf{F}_a$ containing the adiabatic parts given by the microscopic Hartree potential and the ALDA exchange-correlation potential $\delta v^{ALDA}_{Hxc,mic} = \delta v_{H,mic} + \delta v^{ALDA}_{xc,mic}$, and $\mathbf{F}_d$ containing the dynamic part of the exchange-correlation vector potential. From Eqs. (8.57) and (8.58) it becomes clear that we can write

$$\mathbf{P} = \left(X^{inter} + \frac{1}{\omega^2} Q^\dagger \cdot X^{intra} \cdot Q \right) \cdot \mathbf{F}, \tag{8.69}$$

where

$$Q = \begin{pmatrix} iq & 0 & 0 \\ 0 & 1 & 0 \\ 0 & 0 & 1 \end{pmatrix}, \tag{8.70}$$

and X^{inter} and X^{intra} are the matrices of the inter- and intraband Kohn-Sham response functions given in Eqs. (8.57) and (8.58). In the linear response regime we can write $\mathbf{F}_a = Y_a \cdot \mathbf{P}$ for the adiabatic part of the potential vector, and $\mathbf{F}_d = Y_d \cdot \mathbf{P}$ for the dynamic part. Here the matrix Y_d is the matrix that enters Eq. (8.50) and Y_a is defined as

$$Y_a = \begin{pmatrix} y_a & 0 & 0 \\ 0 & 0 & 0 \\ 0 & 0 & 0 \end{pmatrix}, \tag{8.71}$$

with the frequency independent kernel y_a defined by the relation $y_a\delta\rho = \delta v^{ALDA}_{Hxc,mic}$. The total perturbing potential is then given by

$$\mathbf{F} = \mathbf{F}_{mac} + (Y_a + Y_d)\cdot\mathbf{P}. \tag{8.72}$$

The low-frequency behavior of the matrix Y_d is determined by the low-frequency behavior of the viscoelastic coefficients $\tilde{\eta}_{xc}(\mathbf{r},\omega)$ and $\tilde{\zeta}_{xc}(\mathbf{r},\omega)$ which in turn is determined by the low-frequency behavior of $f_{xcL,T}(\omega)$. Since $f_{xcL,T}(\omega) = f^*_{xcL,T}(-\omega)$ and considering the results obtained in Eqs. (8.37) and (8.38) we can write the following expressions for the low-frequency behavior of $\tilde{\eta}_{xc}(\mathbf{r},\omega)$ and $\tilde{\zeta}_{xc}(\mathbf{r},\omega)$,

$$\frac{-i\omega\tilde{\zeta}_{xc}}{\rho_0^2(\mathbf{r})} = i\omega A + \omega^2 B + O(\omega^3), \tag{8.73}$$

$$\frac{-i\omega\tilde{\eta}_{xc}}{\rho_0^2(\mathbf{r})} = \frac{\mu_{xc}}{\rho_0^2(\mathbf{r})} + i\omega C + \omega^2 D + O(\omega^3), \tag{8.74}$$

where A, B, C, and D are real. Furthermore, from the work of Qian and Vignale [15] we know the exact result for the slope of the imaginary parts of $f^h_{xcL,T}(\omega)$ in the limit $\omega \to 0$, which they show to be finite. This means that in the above expressions A and C are finite. Using Eqs. (8.73) and (8.74), we can write the following low-frequency expansion for Y_d,

$$Y_d = \sum_p (i\omega)^p Y_{d,p}, \tag{8.75}$$

where all $Y_{d,p}$ are real and $Y_{d,0} \propto \mu_{xc}$. It now becomes clear that we can obtain $\mathbf{P}$ by solving Eqs. (8.69) and (8.72) in a self-consistent manner. We have carefully formulated these response equations such that a regular solution can be found for $\lim_{\mathbf{g}\to\mathbf{0}} \mathbf{P}(\mathbf{g}) = \mathbf{P}$, with $\mathbf{P}$ the solution of Eq. (8.69) at $\mathbf{g} = \mathbf{0}$. In this limit we can write the following low-frequency expression for Eq. (8.69),

$$\left[\omega^2 I - \left(\omega^2 \sum_p (i\omega)^p X^{inter}_p + \tilde{X}^{intra}\right)\cdot\left(Y_a + \sum_p (i\omega)^p Y_{d,p}\right)\right]\cdot\mathbf{P} = \left(\omega^2 \sum_p (i\omega)^p X^{inter}_p + \tilde{X}^{intra}\right)\cdot\mathbf{F}_{mac}, \tag{8.76}$$

where, since $X^{inter}(\omega) = X^{inter*}(-\omega)$, we have used the series expansion $X^{inter} = \sum_p (i\omega)^p X^{inter}_p$. Here the matrices X^{inter}_{2p+1} vanish if ω is below the interband absorption edge, and the matrix $\tilde{X}^{intra}$ is frequency independent and defined as

$$\tilde{X}^{intra} = \lim_{q\to 0} Q^\dagger \cdot X^{intra}\cdot Q = \begin{pmatrix} 0 & 0 & 0 \\ 0 & \Delta\chi^{intra}_{\rho\mathbf{jj}} & \Delta\chi^{intra}_{\rho\mathbf{jm}} \\ 0 & \Delta\chi^{intra}_{\rho\mathbf{mj}} & \Delta\chi^{intra}_{\rho\mathbf{mm}} \end{pmatrix}. \tag{8.77}$$

All matrices are real-valued. Note that due to their matrix structure the product $\tilde{X}^{intra} \cdot Y_a$ vanishes. From Eq. (8.76) it immediately becomes clear that the low-frequency behavior of the solution is largely determined by $\tilde{X}^{intra}$ and the low-frequency coefficients of Y_d. Since $\mathbf{P}(\omega) = \mathbf{P}^*(-\omega)$, we can use the series expansion $\mathbf{P} = \sum_{n=n_0}^{\infty} (i\omega)^n \mathbf{P}_n$, where we assume that the expansion truncates at a certain value n_0 since we are interested in the low-frequency behavior of $\mathbf{P}$. We can then write Eq. (8.76) as

$$\left(\sum_{p=0}^{\infty} (i\omega)^p X_p \right) \left(\sum_{n=n_0}^{\infty} (i\omega)^n \mathbf{P}_n \right) = \sum_{m=0}^{\infty} (i\omega)^m \mathbf{F}_m, \tag{8.78}$$

with

$$X_p = -\delta_{p,2} I + X_{p-2}^{inter} \cdot Y_a - \tilde{X}^{intra} \cdot Y_{d,p} + \sum_{s=0}^{p-2} X_{p-s-2}^{inter} \cdot Y_{d,s}, \tag{8.79}$$

$$\mathbf{F}_m = \left(-X_{m-2}^{inter} + \delta_{m,0} \tilde{X}^{intra} \right) \cdot \mathbf{F}_{mac}. \tag{8.80}$$

Note that the odd-indexed potential coefficients vanish, $\mathbf{F}_{2m+1} = \mathbf{0}$. We mention the first two matrix and vector elements in particular,

$$X_0 = -\tilde{X}^{intra} \cdot Y_{d,0}, \qquad \mathbf{F}_0 = \tilde{X}^{intra} \cdot \mathbf{F}_{mac}, \tag{8.81}$$

$$X_1 = -\tilde{X}^{intra} \cdot Y_{d,1}, \qquad \mathbf{F}_1 = \mathbf{0}. \tag{8.82}$$

By equating all orders in Eq. (8.78) separately, we obtain the general structure of the m^{th}-order of the low-frequency expansion of the response equation, which is given by the relation

$$\sum_{n=n_0}^{m} X_{m-n} \mathbf{P}_n = \mathbf{F}_m, \tag{8.83}$$

with $\mathbf{F}_{m<m_0} = \mathbf{0}$, in which we need to choose $n_0 \leq m_0$ such that there is a unique solution. The dimension of the matrices and vectors is d. This infinite set of equations can be written in the following triangular block matrix form

$$\begin{bmatrix} X_0 & 0 & 0 & \cdots \\ X_1 & X_0 & 0 & \ddots \\ X_2 & X_1 & X_0 & \ddots \\ \vdots & \ddots & \ddots & \ddots \end{bmatrix} \begin{bmatrix} \mathbf{P}_{n_0} \\ \vdots \\ \mathbf{P}_{m_0-1} \\ \hline \mathbf{P}_{m_0} \\ \vdots \end{bmatrix} = \begin{bmatrix} \mathbf{0} \\ \vdots \\ \mathbf{0} \\ \hline \mathbf{F}_{m_0} \\ \vdots \end{bmatrix},$$

from which it becomes clear that there is a unique solution if X_0 is invertible, with $n_0 = m_0$ and $\mathbf{P}_{n<n_0} = 0$, generated by

$$\mathbf{P}_n = X_0^{-1}(\mathbf{F}_n - \sum_{m=m_0}^{n-1} X_{n-m} P_m).$$

If on the other hand X_0 is singular as in our case, we proceed to find a solution by constructing the singular value decomposition $X_0 = VDU^\dagger$ with the diagonal matrix D containing singular values $d_1 \cdots d_s = 0$ and $d_{i>s} \neq 0$ with $s > 0$, and the unitary matrices U and V build from the right and left singular vectors spanning the domain, null space and range of X_0. We can multiply each line from the left by $V^\dagger$, and thus remove the first s rows from each diagonal block of the triangular matrix. These rows become replaced by the first s rows of the line below yielding again a triangular form,

$$\begin{bmatrix} \begin{bmatrix} 0 \\ \tilde{D}U^\dagger \end{bmatrix} & 0 & 0 & \cdots \\ V^\dagger X_1 & \begin{bmatrix} 0 \\ \tilde{D}U^\dagger \end{bmatrix} & 0 & \ddots \\ V^\dagger X_2 & V^\dagger X_1 & \begin{bmatrix} 0 \\ \tilde{D}U^\dagger \end{bmatrix} & \ddots \\ \vdots & \ddots & \ddots & \ddots \end{bmatrix} \begin{bmatrix} \mathbf{P}_{n_0} \\ \vdots \\ \mathbf{P}_{m_0-1} \\ \hline \mathbf{P}_{m_0} \\ \vdots \end{bmatrix} = \begin{bmatrix} \mathbf{0} \\ \vdots \\ \mathbf{0} \\ \hline V^\dagger \mathbf{F}_{m_0} \\ \vdots \end{bmatrix}$$

Here $\tilde{D}$ is the matrix D with the first s rows removed. The first s lines of the equation can be removed as these are trivially satisfied. We can do this by defining new blocks

$$[X'_n]_{i,j} = \begin{cases} [V^\dagger X_n]_{i+s,j} & i \leq d-s \\ [V^\dagger X_{n+1}]_{i+s-d,j} & i > d-s \end{cases}, \tag{8.84}$$

and similarly new vectors

$$[\mathbf{F}'_n]_i = \begin{cases} [V^\dagger \mathbf{F}_n]_{i+s} & i \leq d-s \\ [V^\dagger \mathbf{F}_{n+1}]_{i+s-d} & i > d-s \end{cases}, \tag{8.85}$$

such that we retrieve the original structure, however, in general, with a nonzero vector $\mathbf{F}'_{m_0-1}$. Therefore we have to set $m'_0 = m_0 - 1$. If $\mathbf{F}_{m_0}$ is in the range of X_0 then $\mathbf{F}'_{m_0-1}$ will still be zero and we can set $m'_0 = m_0$. By iterating this procedure k times, until we have found a diagonal block $X_0^{\prime\cdots\prime}$ that is invertible, we have constructed a unique solution that truncates from below at $n_0 \geq m_0 - k$ with $\mathbf{P}_{n<n_0} = \mathbf{0}$.

We will now discuss three separate cases, being the adiabatic approximation, in which Y_d is set to zero, the dynamic exchange-correlation case with vanishing static

limit and hence $Y_{d,0} = 0$, but $Y_{d,1} \neq 0$, and the dynamic case with finite static value $Y_{d,0} \neq 0$. In the simplest case (the adiabatic approximation) we have $X_0 = X_1 = X_{2n+1} = 0$, and $\mathbf{F}_{2n+1} = \mathbf{0}$. From Eq. (8.83) it immediately follows that in this case the equations for even and odd indexed $\mathbf{P}$ decouple, with the partial result $\mathbf{P}_{2n+1} = \mathbf{0}$. The singular value decompositions for the first two iterations become trivial, $V = U = I$ and $D = 0$, and we obtain $n_0 = -2$ with the unique even-indexed solutions given by

$$\mathbf{P}_{2n} = X_2^{-1}(\mathbf{F}_{2n+2} - \sum_{m=-1}^{n-1} X_{2(n-m+1)} P_{2m}). \tag{8.86}$$

where we assumed that X_2 is invertible. The susceptibility is therefore purely real valued and is diverging like ω^{-2}. In the dynamic case with vanishing static limit for Y_d, we have $X_0 = 0$, X_1 singular, $\mathbf{F}_0 \neq \mathbf{0}$ but in the range of X_1 (provided that $Y_{d,1}$ is invertible) and again $\mathbf{F}_{2n+1} = \mathbf{0}$. The first iteration is again trivial, with $V = U = I$ and $D = 0$. In the second iteration we can remove the singularity of the new diagonal block $X_0' = X_1$, by applying the SVD again. However, if indeed $\mathbf{F}_{-1}' = \mathbf{F}_0$ is in the range of X_1 (which is the case if $Y_{d,1}$ is invertible), then we do not have to decrease m_0 further and we obtain $n_0 = -1$, otherwise we do, and find $n_0 = -2$. Assuming that the second iteration yields an invertible diagonal block, we have found the solution which truncates at $n_0 = -1(-2)$. We can thus conclude that the susceptibility acquires an imaginary part that diverges like ω^{-1}, and a real value that is finite, unless the first order dynamic exchange-correlation kernel $Y_{d,1}$ is singular. In the dynamic case with finite static limit an extra complication arises. In the first iteration the multiplication from the left with $V^\dagger$ reduces not only the diagonal blocks X_0, but removes also rows from the subdiagonal blocks. This is due to the fact that $X_{0(1)}$ is of the form $\tilde{X}^{intra} \cdot Y_{d,0(1)}$ in which $\tilde{X}^{intra}$ is singular as is clear from its matrix structure. If the ranges of X_0 and X_1 coincide (which is the case if $Y_{d,0(1)}$ is invertible), then an equal amount of rows is removed in the diagonal and subdiagonal blocks, and also in the vector $\mathbf{F}_0$ if $Y_{d,0(1)}$ is invertible. As always $\mathbf{F}_{2n+1} = \mathbf{0}$. One can check readily that in both iterations we do not need to decrease m_0, and we find a solution with $n_0 = 0$, assuming that after the second step an invertible diagonal block is generated. In this case the susceptibility is real and finite in the low frequency range. If on the other hand (one of) the matrices $Y_{d,0(1)}$ is singular a divergent ω dependence may still result.

The analysis given above forms the basis for understanding the solution at finite frequency. Retaining only the lowest order terms of the interband response function in Eq. (8.76) it becomes clear that we can consider the contribution of $Y_{d,0(1)}$ as small

perturbations if $\omega \gg \omega_{0(1)}$, where

$$\omega_0 = \sqrt{|| X_2^{-1} X_0 ||} \tag{8.87}$$

$$\omega_1 = || X_2^{-1} X_1 ||, \tag{8.88}$$

are two characteristic frequencies defined in terms of the X-matrices given in Eq. (8.79). Here $|| A ||= \max_i |\lambda_i|$ indicates the spectral norm of the matrix A, being equal to its largest eigenvalue. Including the first-order correction to the adiabatic solution gives

$$\mathbf{P} \approx \big(-\frac{1}{\omega^2} X_2^{-1} - \frac{1}{\omega^4} X_2^{-1}(i\omega X_1 + X_0) X_2^{-1} \big)(\omega^2 X^{inter} + \tilde{X}^{intra}) \mathbf{F}_{mac}, \tag{8.89}$$

and leads to an imaginary part of the susceptibility that decays as $1/\omega^3$ for $\omega < \omega_p$ since then $\omega^2 \; || \; X^{inter} \; || < || \; \tilde{X}^{intra} \; ||$, where it is understood that we consider the frequency range below the optical gap. For $\omega \lesssim \omega_{0(1)}$ the contributions of $Y_{d,0(1)}$ become dominant and determine the solutions as in the analysis given above. Going from high to low frequency we expect a transition from the adiabatic to the dynamic case at around $\max(\omega_0, \omega_1)$, and, if $\omega_0 < \omega_1$, from the dynamic behavior with vanishing static limit to the case with finite static limit around ω_0. The results of this analysis are summarized in the following,

$$\chi_e(\omega) \propto \begin{cases} \alpha_1 + i\omega\beta_2 & \omega < \omega_0 \\ \alpha_1' + i\beta_2'/\omega & \omega_0 < \omega < \omega_1 \\ \alpha_1''/\omega^2 + i\beta_2''/\omega^3 & \omega > \omega_0, \omega_1 \end{cases} \tag{8.90}$$

As a special case we have $\omega_0 = 0$ if $\mu_{xc} = 0$.

Chapter 9

A Nonlocal Current-Density Functional

In this chapter we relieve the constraint on the length of the wave vector of the perturbation that limits the formal range of applicability of the local Vignale-Kohn current-density functional by introducing a nonlocal functional of the current density with a similar viscoelastic structure as the Vignale-Kohn functional. This nonlocal functional is constructed such that it satisfies the same conservation laws and symmetry relations as the Vignale-Kohn functional. In contrast to the Vignale-Kohn functional, this nonlocal functional is completely determined by f^h_{xcL}, the longitudinal part of the exchange-correlation kernel of the homogeneous electron gas, at small frequency, whereas the Vignale-Kohn functional is mainly determined by f^h_{xcT}, the transverse part of the exchange-correlation kernel of the homogeneous electron gas at small frequency. The dielectric functions of silicon and GaP that we obtain using this nonlocal functional collapse in a similar manner as the optical spectra we obtained using the Vignale-Kohn functional. Using our nonlocal functional with solely the uniform part of the current density remaining we obtain results close to those obtained with experiment provided we use an empirical prefactor.

9.1 Introduction

In previous chapters we discussed the Vignale-Kohn functional in its application within time-dependent current-density-functional theory to calculate the optical spectra of semiconductors, metals, and infinite polymer chains. In these analyses two main problems came to light. First, the Vignale-Kohn (VK) functional was derived under

the constraints $k, q \ll k_F, \omega/v_F$, where k is the length of the wave vector of the external perturbation, q is the length of the wave vector of the inhomogeneity of the ground-state density and k_F and v_F are the local Fermi wave vector and velocity, respectively. The constraint $q \ll k_F, \omega/v_F$ means that formally the application of the VK functional is only justified if the ground-state density is slowly varying and the constraint $k \ll k_F, \omega/v_F$ means we are formally allowed to use the VK functional if the induced current density is slowly varying. Furthermore, the constraint $k \ll \omega/v_F$ implies the region above the particle-hole continuum of the homogeneous electron gas. As we showed in chapter 7 these constraints are violated almost everywhere for real systems. Second, the VK functional requires knowledge of the longitudinal and transverse parts of the exchange-correlation kernel of the homogeneous electron gas $f^h_{xcL,T}(\rho,\omega)$ with ρ the density of the electron gas. In chapters 5 and 7 we showed that in the calculation of optical spectra of semiconductors and infinite polymer chains the Vignale-Kohn functional is very sensitive to the values of $f^h_{xcT}(\rho,\omega)$. In fact, surprisingly, the influence on the optical spectra of the terms in the VK functional involving the transverse kernel $f^h_{xcT}(\omega)$ is much bigger than the terms involving the longitudinal kernel $f^h_{xcL}(\omega)$. The transverse part of the exchange-correlation kernel at $\omega = 0$ is related to μ_{xc} which is the exchange-correlation part of the shear modulus. For the values of μ_{xc} that are available in the literature [15,48] the optical spectra, in general, collapse. However, if we make the approximation $\mu_{xc} = 0$ we obtain results close to the results obtained within the adiabatic local density approximation (ALDA). Moreover, in chapter 8 we showed that in the calculation of the optical spectra of metals we need to make the approximation $\mu_{xc} = 0$ in order to describe correctly the Drude-like tail in the low-frequency range. The fact that terms of the VK functional involving $f^h_{xcT}(\rho,\omega)$ have a much larger influence on the optical spectra than $f^h_{xcL}(\rho,\omega)$ is related to the fact that due to the constraint $k \ll \omega/v_F$ we have to evaluate $f^h_{xcL,T}(\rho,0)$ above the particle-hole continuum in $(\mathbf{k},\omega) = (0,0)$. This is important because there exists a singularity in the origin of the $(\mathbf{k},\omega)$ plane the size of which is proportional to μ_{xc}. The approximation $\mu_{xc} = 0$ therefore effectively removes this singularity.

From the above considerations we argue that it might be desirable to search for a nonlocal VK-type functional since for such a nonlocal functional both constraints on k as well as the constraint $q \ll \omega/v_F$ dissappear. We are then left with the constraint $q \ll k_F$ which is the same constraint under which the ALDA is valid. Therefore our aim in this chapter is to obtain a nonlocal expression for $\delta\mathbf{A}_{xc}(\mathbf{r},\omega)$ with a similar viscoelastic strucure as the Vignale-Kohn functional that satisfies the same conservation laws and symmetry relations as the Vignale-Kohn functional. We construct such a nonlocal functional starting from the exchange-correlation potential of the homogeneous electron gas and by studying the restrictions that conservation

laws and symmetry relations impose on the form of $\delta\mathbf{A}_{xc}(\mathbf{r},\omega)$ for general systems. We note that although the nonlocal functional derived in this way is formally less restricted by constraints than the VK functional, the latter is exact when applied to systems that satisfy the constraints $k, q \ll k_F, \omega/v_F$ whereas the former is not necessarily exact when the constraint $q \ll k_F$ is satisfied.

The outline of this chapter is as follows. In Sec. 9.2 we give the derivation of our nonlocal functional. In Sec. 9.3 we then give the main aspects of the implementation. The computational details of the calculations are the subject of Sec. 9.4. We have tested our method on silicon and GaP, the results of which can be found in Sec. 9.5. Finally we present our conclusions in Sec. 9.6.

9.2 Theory

9.2.1 TDCDFT

Within TDCDFT an interacting many-particle system in an external electromagnetic field is replaced by an auxiliary non-interacting many-particle system in an effective field desribed by the set of Kohn-Sham potentials $\{v_s(\mathbf{r},t), \mathbf{A}_s(\mathbf{r},t)\}$. This set of potentials has the property that it produces the exact time-dependent current density $\mathbf{j}(\mathbf{r},t)$ and the exact time-dependent density $\rho(\mathbf{r},t)$ for a given initial state. If the initial state is the ground state, it is already determined by the ground-state density on the basis of the Hohenberg-Kohn theorem [1]. In the Kohn-Sham scheme the time-dependent single-particle wave functions are solutions of the following equation

$$i\frac{\partial}{\partial t}\phi_n(\mathbf{r},t) = \left(\frac{1}{2}\left[\hat{\mathbf{p}} + \mathbf{A}_s(\mathbf{r},t)\right]^2 + v_s(\mathbf{r},t)\right)\phi_n(\mathbf{r},t). \tag{9.1}$$

Given the initial state, the time-dependent potentials $v_s(\mathbf{r},t)$ and $\mathbf{A}_s(\mathbf{r},t)$ produce the exact time-dependent density and current density,

$$\rho(\mathbf{r},t) = \sum_n f_n \phi_n^*(\mathbf{r},t)\phi_n(\mathbf{r},t), \tag{9.2}$$

$$\mathbf{j}(\mathbf{r},t) = \sum_n f_n \mathrm{Re}[-i\phi_n^*(\mathbf{r},t)\nabla\phi_n(\mathbf{r},t)] + \rho(\mathbf{r},t)\mathbf{A}_s(\mathbf{r},t), \tag{9.3}$$

where f_n are the occupation numbers of the Kohn-Sham wave functions. Here we assumed that our initial state is nondegenerate and is described by a single Slater determinant. The first and second terms on the right-hand side of Eq. (9.3) correspond to the paramagnetic and diamagnetic current, respectively. Both the density and the current density are gauge invariant.

The set of Kohn-Sham potentials $\{v_s(\mathbf{r},t), \mathbf{A}_s(\mathbf{r},t)\}$ is defined in our gauge by [76],

$$v_s(\mathbf{r},t) = v_{H,mic}(\mathbf{r},t) + v_{xc,mic}(\mathbf{r},t), \tag{9.4}$$

$$\mathbf{A}_s(\mathbf{r},t) = \mathbf{A}_{mac}(\mathbf{r},t) + \mathbf{A}_{xc}(\mathbf{r},t). \tag{9.5}$$

Here $v_{H,mic}(\mathbf{r},t)$ is the microscopic part of the Hartree potential and $v_{xc,mic}(\mathbf{r},t)$ is the microscopic part of the exchange-correlation potential. The term $\mathbf{A}_{mac}(\mathbf{r},t)$ denotes the macroscopic vector potential,

$$\mathbf{A}_{mac}(\mathbf{r},t) = \mathbf{A}_{ext}(\mathbf{r},t) + \mathbf{A}_{ind}(\mathbf{r},t), \tag{9.6}$$

where $\mathbf{A}_{ext}(\mathbf{r},t)$ is the external vector potential and $\mathbf{A}_{ind}(\mathbf{r},t)$ is the induced macroscopic vector potential. The latter potential accounts for the long-range contribution of the Hartree potential of the surface charge as well as the retarded contribution of the induced transverse current density. We can neglect the microscopic part of the vector potential which is consistent with the Breit approximation used in the ground-state calculation [76,78,79]. We choose the field $\mathbf{E}_{mac}(\mathbf{r},t)$ to be fixed and its relation to $\mathbf{A}_{mac}(\mathbf{r},t)$ is given by $\partial_t \mathbf{A}_{mac}(\mathbf{r},t) = -\mathbf{E}_{mac}(\mathbf{r},t)$. We leave the relation between $\mathbf{E}_{mac}(\mathbf{r},t)$ and $\mathbf{E}_{ext}(t)$ unspecified as this depends on the sample size and shape and requires knowledge of χ_e. Finally, $\mathbf{A}_{xc}(\mathbf{r},t)$ is the exchange-correlation vector potential. In practice approximations are required for the set of exchange-correlation potentials $\{v_{xc}(\mathbf{r},t), \mathbf{A}_{xc}(\mathbf{r},t)\}$. The form of this set of exchange-correlation potentials is restricted by some exact constraints. In the next section we will discuss how the constraints set by the zero-force and zero-torque theorems restrict the form of $\{v_{xc}(\mathbf{r},t), \mathbf{A}_{xc}(\mathbf{r},t)\}$.

9.2.2 Zero-Force and Zero-Torque Theorems

In accordance with Newton's third law the net force and net torque acting on a system should have no contribution from the system itself. Since the net force and the net torque due to the Hartree potential are equal to zero, the net force and the net torque due to the set of exchange correlation potentials $\{v_{xc}(\mathbf{r},t), \mathbf{A}_{xc}(\mathbf{r},t)\}$ should be equal to zero as well [42]. This leads to constraints on the form of $\{v_{xc}(\mathbf{r},t), \mathbf{A}_{xc}(\mathbf{r},t)\}$. These constraints are made explicit by the zero-force and zero-torque theorems which read

$$\mathbf{F}_{xc}(t) = \int d\mathbf{r}[\rho(\mathbf{r},t)\mathbf{E}_{xc}(\mathbf{r},t) + \mathbf{j}(\mathbf{r},t) \times \mathbf{B}_{xc}(\mathbf{r},t)] = 0 \tag{9.7}$$

$$\mathbf{T}_{xc}(t) = \int d\mathbf{r}[\rho(\mathbf{r},t)\mathbf{r} \times \mathbf{E}_{xc}(\mathbf{r},t) + \mathbf{r} \times (\mathbf{j}(\mathbf{r},t) \times \mathbf{B}_{xc}(\mathbf{r},t))] = 0, \tag{9.8}$$

where $\mathbf{F}_{xc}(t)$ and $\mathbf{T}_{xc}(t)$ are the exchange-correlation parts of the force and the torque, respectively and the exchange-correlation parts of the electric and magnetic fields are given by

$$\mathbf{E}_{xc}(\mathbf{r},t) = \nabla v_{xc,0}(\mathbf{r}) - \frac{\partial}{\partial t}\mathbf{A}_{xc}(\mathbf{r},t) \quad (9.9)$$

$$\mathbf{B}_{xc}(\mathbf{r},t) = \nabla \times \mathbf{A}_{xc}(\mathbf{r},t), \quad (9.10)$$

where we chose the gauge such that all perturbations are included in the vector potential. We note that if the zero-force theorem is satisfied this automatically guarantees that the harmonic-potential theorem is satisfied. The harmonic-potential theorem states that the density of a system of electrons confined in a static parabolic potential well follows rigidly the classical motion of the center of mass when subjected to a uniform time-dependent perturbation [43]. In the following the exchange-correlation scalar potential will be taken within the local density approximation (LDA), i.e., $v_{xc,0}(\mathbf{r}) = v_{xc,0}^{LDA}(\mathbf{r})$. Evaluating Eqs. (9.7) and (9.8) for the density $\rho(\mathbf{r},t) = \rho_0(\mathbf{r}) + \delta\rho(\mathbf{r},t)$ we obtain up to first order in $\delta\rho(\mathbf{r},t)$

$$\mathbf{F}_{xc}(t) = -\int d\mathbf{r}\rho_0(\mathbf{r})\frac{\partial}{\partial t}\delta\mathbf{A}_{xc}(\mathbf{r},t) = 0 \quad (9.11)$$

$$\mathbf{T}_{xc}(t) = -\int d\mathbf{r}\rho_0(\mathbf{r})\mathbf{r}\times\frac{\partial}{\partial t}\delta\mathbf{A}_{xc}(\mathbf{r},t) = 0, \quad (9.12)$$

since the LDA exchange-correlation scalar potential exerts no force and no torque on the system. Doing a Fourier transform with respect to t we obtain the following constraints,

$$\mathbf{F}_{xc}(\omega) = i\omega\int d\mathbf{r}\rho_0(\mathbf{r})\delta\mathbf{A}_{xc}(\mathbf{r},\omega) = 0 \quad (9.13)$$

$$\mathbf{T}_{xc}(\omega) = i\omega\int d\mathbf{r}\rho_0(\mathbf{r})\mathbf{r}\times\delta\mathbf{A}_{xc}(\mathbf{r},\omega) = 0, \quad (9.14)$$

where the Fourier tranform and its inverse are given by

$$f(\mathbf{k},\omega) = \int d\mathbf{r}e^{-i(\mathbf{k}\cdot\mathbf{r}-\omega t)}f(\mathbf{r},t) \quad (9.15)$$

$$f(\mathbf{r},t) = \int\frac{d\mathbf{k}d\omega}{(2\pi)^4}e^{i(\mathbf{k}\cdot\mathbf{r}-\omega t)}f(\mathbf{k},\omega). \quad (9.16)$$

Let us now look for a general form of $\delta\mathbf{A}_{xc}(\mathbf{r},\omega)$ that fulfills these constraints. We write

$$\mathbf{F}_{xc}(\omega) = \int d\mathbf{r}\mathcal{F}_{xc}(\mathbf{r},\omega) = 0 \quad (9.17)$$

$$\mathbf{T}_{xc}(\omega) = \int d\mathbf{r}\mathbf{r}\times\mathcal{F}_{xc}(\mathbf{r},\omega) = 0, \quad (9.18)$$

where

$$\mathcal{F}_{xc}(\mathbf{r},\omega) = i\omega\rho_0(\mathbf{r})\delta\mathbf{A}_{xc}(\mathbf{r},\omega). \tag{9.19}$$

We can write $\mathcal{F}_{xc}(\mathbf{r},\omega)$ as the divergence of a second rank tensor according to

$$\mathcal{F}_{xc,i}(\mathbf{r},\omega) = \sum_j \partial_j \sigma_{xc,ij}(\mathbf{r},\omega), \tag{9.20}$$

where we assumed that $\sigma_{xc}(\mathbf{r},\omega)$ can be chosen such that the boundary conditions for $\mathcal{F}_{xc}(\mathbf{r},\omega)$ are satisfied. The tensor $\sigma_{xc}(\mathbf{r},\omega)$ is not completely determined by $\mathcal{F}_{xc}$, there is freedom in choosing its components. Using the divergence theorem we can now write the zero-force theorem as

$$F_{xc,i}(\omega) = \sum_j \int dS \sigma_{xc,ij}(\mathbf{r},\omega). \tag{9.21}$$

This integral vanishes if $\sigma_{xc}(\mathbf{r},\omega)$ decays near the boundaries or if its values at opposite boundaries are the same as occurs when periodic boundary conditions are used. The tensor $\sigma_{xc}(\mathbf{r},\omega)$ can be written as

$$\sigma_{xc,ij}(\mathbf{r},\omega) = \partial_i \phi_j(\mathbf{r},\omega) + \sum_{kl} \epsilon_{ikl}\partial_k \Phi_{lj}(\mathbf{r},\omega), \tag{9.22}$$

where ϕ and Φ are an arbitrary vector and second rank tensor, respectively. So $\mathcal{F}_{xc}$ is completely determined by ϕ since the divergence of a curl vanishes. The freedom we have in choosing Φ will be convenient now that we turn to the zero-torque theorem. We have

$$T_{xc,i}(\omega) = \sum_{jkl} \epsilon_{ijk} \int d\mathbf{r} r_j \partial_l \sigma_{xc,kl}(\mathbf{r},\omega), \tag{9.23}$$

where ϵ_{ijk} is the Levi-Civita antisymmetric tensor. Performing an integration by parts we arrive at

$$T_{xc,i}(\omega) = \sum_{jkl} \epsilon_{ijk} \int d\mathbf{r} \partial_l \left[r_j \sigma_{xc,kl}(\mathbf{r},\omega)\right] - \sum_{jkl} \epsilon_{ijk} \int d\mathbf{r} \left(\partial_l r_j\right) \sigma_{xc,kl}(\mathbf{r},\omega). \tag{9.24}$$

This can be rewritten as

$$T_{xc,i}(\omega) = \sum_{jkl} \epsilon_{ijk} \int dS \left[r_j \sigma_{xc,kl}(\mathbf{r},\omega)\right] - \sum_{jk} \epsilon_{ijk} \int d\mathbf{r} \sigma_{xc,kj}(\mathbf{r},\omega). \tag{9.25}$$

We can now use the freedom we have in choosing the components of Φ to get rid of the second term on the right-hand side. This term vanishes if $\sigma_{xc}(\mathbf{r},\omega)$ is symmetric. So we have that

$$\begin{aligned} \sigma_{xc,ij}(\mathbf{r},\omega) - \sigma_{xc,ji}(\mathbf{r},\omega) &= \partial_i \phi_j(\mathbf{r},\omega) - \partial_j \phi_i(\mathbf{r},\omega) \\ &+ \sum_{kl} \epsilon_{ikl}\partial_k \Phi_{lj}(\mathbf{r},\omega) - \sum_{kl} \epsilon_{jkl}\partial_k \Phi_{li}(\mathbf{r},\omega) = 0. \end{aligned} \tag{9.26}$$

If we now choose $\Phi_{ji} = \sum_k \epsilon_{ijk}\phi_k$ then the second term on the right-hand side of Eq. (9.25) vanishes.

So we have transformed the zero-force and zero-torque theorems for $\mathcal{F}_{xc}$ into the following two constraints on the symmetric tensor $\sigma_{xc}(\mathbf{r},\omega)$,

$$\sum_j \int dS \sigma_{xc,ij}(\mathbf{r},\omega) = 0 \tag{9.27}$$

$$\sum_{jkl} \epsilon_{ijk} \int dS \left[r_j \sigma_{xc,kl}(\mathbf{r},\omega)\right] = 0. \tag{9.28}$$

If these constraints are satisfied we see from Eq. (9.19) that we have the following form for $\delta\mathbf{A}_{xc}(\mathbf{r},\omega)$,

$$i\omega\delta A_{xc,i}(\mathbf{r},\omega) = \frac{1}{\rho_0(\mathbf{r})} \sum_j \partial_j \sigma_{xc,ij}(\mathbf{r},\omega). \tag{9.29}$$

In the next sections we will show that this form follows quite naturally from an analysis of $\delta\mathbf{A}_{xc}(\mathbf{r},\omega)$ in the case of the homogeneous electron gas.

9.2.3 The Exchange-Correlation Vector Potential of the Homogeneous Electron Gas

The general expression for the exchange-correlation vector potential to first order is

$$\delta A_{xc,i}(\mathbf{r},\omega) = \int d\mathbf{r}' \sum_j f_{xc,ij}(\mathbf{r},\mathbf{r}',\omega)\delta j_j(\mathbf{r}',\omega). \tag{9.30}$$

In the case of the homogeneous electron gas we have

$$\delta A_{xc,i}(\mathbf{r},\omega) = \int d\mathbf{r}' \sum_j f^h_{xc,ij}(\rho,|\mathbf{r}-\mathbf{r}'|,\omega)\delta j_j(\mathbf{r}',\omega), \tag{9.31}$$

where ρ is the density of the homogeneous electron gas. Fourier transforming with respect to $(\mathbf{r}-\mathbf{r}')$ we obtain

$$\delta A_{xc,i}(\mathbf{r},\omega) = \int \frac{d\mathbf{k}}{(2\pi)^3} e^{i\mathbf{k}\cdot\mathbf{r}} \sum_j f^h_{xc,ij}(\rho,k,\omega)\delta j_j(\mathbf{k},\omega), \tag{9.32}$$

where $k = |\mathbf{k}|$. Inserting the relation

$$f^h_{xc,ij}(\rho,k,\omega) = \frac{1}{\omega^2}\left[k_i k_j f^h_{xcL}(\rho,k,\omega) + \left(\delta_{ij}k^2 - k_i k_j\right) f^h_{xcT}(\rho,k,\omega)\right], \tag{9.33}$$

which defines the longitudinal and transverse part of the exchange-correlation kernel denoted by $f^h_{xcL}(\rho,k,\omega)$ and $f^h_{xcT}(\rho,k,\omega)$, respectively, we obtain

$$\delta A_{xc,i}(\mathbf{r},\omega) = \frac{1}{\omega^2}\int \frac{d\mathbf{k}}{(2\pi)^3} e^{i\mathbf{k}\cdot\mathbf{r}} \sum_j k_i k_j f^h_{xcL}(\rho,k,\omega)\delta j_j(\mathbf{k},\omega) + \frac{1}{\omega^2}\int \frac{d\mathbf{k}}{(2\pi)^3} e^{i\mathbf{k}\cdot\mathbf{r}} \sum_j \left(\delta_{ij}k^2 - k_i k_j\right) f^h_{xcT}(\rho,k,\omega)\delta j_j(\mathbf{k},\omega). \quad (9.34)$$

Doing the inverse Fourier transform we arrive at

$$\delta A_{xc,i}(\mathbf{r},\omega) = \frac{1}{\omega^2}\int d\mathbf{r}' \sum_j \left[\partial'_i\partial_j f^h_{xcL}(\rho,|\mathbf{r}-\mathbf{r}'|,\omega)\right]\delta j_j(\mathbf{r}',\omega) + \frac{1}{\omega^2}\int d\mathbf{r}' \sum_j \left[\left(\delta_{ij}\sum_k \partial'_k\partial_k - \partial'_i\partial_j\right) f^h_{xcT}(\rho,|\mathbf{r}-\mathbf{r}'|,\omega)\right]\delta j_j(\mathbf{r}',\omega). \quad (9.35)$$

Performing some integrations by parts and using the fact that $f^h_{xcL,T}$ only depends on the length of $(\mathbf{r}-\mathbf{r}')$ so that $\partial' f^h_{xcL,T}(\rho,|\mathbf{r}-\mathbf{r}'|,\omega) = -\partial f^h_{xcL,T}(\rho,|\mathbf{r}-\mathbf{r}'|,\omega)$ we obtain

$$\delta A_{xc,i}(\mathbf{r},\omega) = -\frac{1}{\omega^2}\sum_j \partial_j \int d\mathbf{r}' f^h_{xcL}(\rho,|\mathbf{r}-\mathbf{r}'|,\omega)\delta_{ij}\sum_k \partial'_k \delta j_k(\mathbf{r}',\omega) + \frac{2}{\omega^2}\sum_j \partial_j \int d\mathbf{r}' f^h_{xcT}(\rho,|\mathbf{r}-\mathbf{r}'|,\omega)\delta_{ij}\sum_k \partial'_k \delta j_k(\mathbf{r}',\omega) - \frac{1}{\omega^2}\sum_j \partial_j \int d\mathbf{r}' f^h_{xcT}(\rho,|\mathbf{r}-\mathbf{r}'|,\omega)\left[\partial'_j\delta j_i(\mathbf{r}',\omega) + \partial'_i\delta j_j(\mathbf{r}',\omega)\right]. \quad (9.36)$$

This can then be rewritten in the form

$$i\omega\delta A_{xc,i}(\mathbf{r},\omega) = -\sum_j \partial_j S_{xc,ij}(\mathbf{r},\omega), \quad (9.37)$$

where $S_{xc}(\mathbf{r},\omega)$ is a symmetric tensor given by

$$S_{xc,ij}(\mathbf{r},\omega) = \int d\mathbf{r}'\alpha_{xc}(\mathbf{r},\mathbf{r}',\omega)\left[\partial'_j\delta j_i(\mathbf{r}',\omega) + \partial'_i\delta j_j(\mathbf{r}',\omega) - \frac{2}{3}\delta_{ij}\sum_k \partial'_k\delta j_k(\mathbf{r}',\omega)\right] + \int d\mathbf{r}'\beta_{xc}(\mathbf{r},\mathbf{r}',\omega)\delta_{ij}\sum_k \partial'_k\delta j_k(\mathbf{r}',\omega), \quad (9.38)$$

in which

$$\alpha_{xc}(\mathbf{r},\mathbf{r}',\omega) = \frac{i}{\omega} f^h_{xcT}(\rho,|\mathbf{r}-\mathbf{r}'|,\omega) \quad (9.39)$$

$$\beta_{xc}(\mathbf{r},\mathbf{r}',\omega) = \frac{i}{\omega}\left[f^h_{xcL}(\rho,|\mathbf{r}-\mathbf{r}'|,\omega) - \frac{4}{3}f^h_{xcT}(\rho,|\mathbf{r}-\mathbf{r}'|,\omega)\right]. \quad (9.40)$$

We have arrived at an expression that is very similar to the viscoelastic form of $\delta A_{xc}(\mathbf{r},\omega)$ derived by Vignale and Kohn. In the next section we will discuss how to perform a local density approximation in Eq. (9.37) in such a way that all the constraints that are satisfied by the Vignale-Kohn functional are also satisfied by our nonlocal functional.

9.2.4 A Nonlocal Current-Denstity Functional

From a comparison between Eq. (9.29) and Eq. (9.37) we see that if we divide the right-hand side of Eq. (9.37) by ρ and subsequently make the local approximation $\rho = \rho_0(\mathbf{r})$ we have obtained a nonlocal functional for general density profiles that satisfies the zero-force and zero-torque theorems. Another constraint satisfied by the Vignale-Kohn functional is the so-called generalized translational invariance. This states that

$$\delta\mathbf{A}_{xc}[\delta\mathbf{j}'](\mathbf{r},\omega) = \delta\mathbf{A}_{xc}[\delta\mathbf{j}](\mathbf{r}-\mathbf{x}(\omega),\omega), \tag{9.41}$$

where

$$\delta\mathbf{j}'(\mathbf{r},\omega) = \delta\mathbf{j}(\mathbf{r},\omega) - i\omega\mathbf{x}(\omega)\rho_0(\mathbf{r}-\mathbf{x}(\omega)), \tag{9.42}$$

with $\mathbf{x}(\omega)$ a purely frequency-dependent vector. The above equations simply state that a rigid translation of the current density implies the same rigid translation of the exchange-correlation vector potential. Therefore by dividing the induced current density on the right-hand side of Eq. (9.37) by ρ', and subsequently making the local approximation $\rho' = \rho_0(\mathbf{r}')$ we satisfy this constraint since $\mathbf{x}$ only depends on ω and its space derivative vanishes. In order to keep our expression for $\delta\mathbf{A}_{xc}(\mathbf{r},\omega)$ exact in the limit of constant density we have to multiply $\sigma_{xc}(\mathbf{r},\omega)$ by $\rho_0(\mathbf{r})\rho_0(\mathbf{r}')$. Finally, we have to satisfy the Onsager symmetry relation for the exchange correlation kernel $\mathbf{f}_{xc}(\mathbf{r},\mathbf{r}',\omega)$. It is given by

$$f_{xc,ij}(\mathbf{r},\mathbf{r}',\omega) = f_{xc,ji}(\mathbf{r}',\mathbf{r},\omega). \tag{9.43}$$

In order to satisfy this constraint we have to symmetrize our result with respect to $f^h_{xcL,T}$. Our final expression becomes

$$i\omega\delta A_{xc,i}(\mathbf{r},\omega) = -\frac{1}{\rho_0(\mathbf{r})}\sum_j \partial_j \sigma_{xc,ij}(\mathbf{r},\omega), \tag{9.44}$$

where

$$\begin{aligned}\sigma_{xc,ij}(\mathbf{r},\omega) = &\int d\mathbf{r}'\eta_{xc}(\mathbf{r},\mathbf{r}',\omega)\left[\partial'_j u_i(\mathbf{r}',\omega) + \partial'_i u_j(\mathbf{r}',\omega) - \frac{2}{3}\delta_{ij}\sum_k \partial'_k u_k(\mathbf{r}',\omega)\right] \\ &+ \int d\mathbf{r}'\zeta_{xc}(\mathbf{r},\mathbf{r}',\omega)\delta_{ij}\sum_k \partial'_k u_k(\mathbf{r}',\omega),\end{aligned} \tag{9.45}$$

in which

$$u_i(\mathbf{r},\omega) = \frac{\delta j_i(\mathbf{r},\omega)}{\rho_0(\mathbf{r})}, \tag{9.46}$$

and

$$\eta_{xc}(\mathbf{r},\mathbf{r}',\omega) = \frac{i}{2\omega}\rho_0(\mathbf{r})\rho_0(\mathbf{r}')\left[f^h_{xcT}(\rho_0(\mathbf{r}),|\mathbf{r}-\mathbf{r}'|,\omega) + f^h_{xcT}(\rho_0(\mathbf{r}'),|\mathbf{r}-\mathbf{r}'|,\omega)\right] \tag{9.47}$$

$$\begin{aligned}\zeta_{xc}(\mathbf{r},\mathbf{r}',\omega) = \frac{i}{2\omega}\rho_0(\mathbf{r})\rho_0(\mathbf{r}')\Bigg\{ & f^h_{xcL}(\rho_0(\mathbf{r}),|\mathbf{r}-\mathbf{r}'|,\omega) - \frac{4}{3}f^h_{xcT}(\rho_0(\mathbf{r}),|\mathbf{r}-\mathbf{r}'|,\omega) \\ + \; & f^h_{xcL}(\rho_0(\mathbf{r}'),|\mathbf{r}-\mathbf{r}'|,\omega) - \frac{4}{3}f^h_{xcT}(\rho_0(\mathbf{r}'),|\mathbf{r}-\mathbf{r}'|,\omega)\Bigg\}.\end{aligned} \tag{9.48}$$

Let us now determine the behavior of $\eta_{xc}(\mathbf{r},\omega)$ and $\zeta_{xc}(\mathbf{r},\omega)$ in the limit $\omega \to 0$. In Fourier space we have the following expression for $f^h_{xcT}(\mathbf{k},\omega)$ in the limit $\omega \to 0$ for finite $\mathbf{k}$,

$$\lim_{\omega\to 0} f^h_{xcT}(\mathbf{k},\omega) = \lim_{\omega\to 0}\frac{\omega^2}{k^2}\left(\frac{1}{\chi_{T,s}(\mathbf{k},\omega)} - \frac{1}{\chi_T(\mathbf{k},\omega)}\right) = 0 \tag{9.49}$$

The right-hand side of this equation vanishes because in the limit $\omega \to 0$ both $\chi_{T,s}(\mathbf{k},\omega)$ and $\chi_T(\mathbf{k},\omega)$ have finite values [10, 51]. Therefore, also in real space the transverse part of the exchange-correlation kernel vanishes in the limit $\omega \to 0$ (unless $|\mathbf{r}-\mathbf{r}'| \to \infty$). We thus obtain for $\eta_{xc}(\mathbf{r},\omega)$ and $\zeta_{xc}(\mathbf{r},\omega)$ in the limit $\omega \to 0$,

$$\lim_{\omega\to 0}\omega\eta_{xc}(\mathbf{r},\mathbf{r}',\omega) = 0, \tag{9.50}$$

and

$$\begin{aligned}\lim_{\omega\to 0}\omega\zeta_{xc}(\mathbf{r},\mathbf{r}',\omega) &= \frac{i}{2}\rho_0(\mathbf{r})\rho_0(\mathbf{r}')\left\{f^h_{xcL}(\rho_0(\mathbf{r}),|\mathbf{r}-\mathbf{r}'|,\omega=0)\right. \\ &+ \left. f^h_{xcL}(\rho_0(\mathbf{r}'),|\mathbf{r}-\mathbf{r}'|,\omega=0)\right\}.\end{aligned} \tag{9.51}$$

This result shows an important difference between our nonlocal functional and the VK functional. Whereas the viscoelastic part of the VK functional is solely determined by f^h_{xcT} in the limit $\omega \to 0$, the viscoelastic part of our nonlocal functional is solely determined by f^h_{xcL} in this limit.

From Eq. (9.44) we can derive an expression for the exchange-correlation kernel in real space. We obtain

$$\begin{aligned}f_{xc,ij}(\mathbf{r},\mathbf{r}',\omega) &= \frac{1}{i\omega}\frac{1}{\rho_0(\mathbf{r})\rho_0(\mathbf{r}')}\left(\partial_j\partial'_i + \delta_{ij}\sum_k \partial_k\partial'_k - \frac{2}{3}\partial_i\partial'_j\right)\eta_{xc}(\mathbf{r},\mathbf{r}',\omega) \\ &+ \frac{1}{i\omega}\frac{1}{\rho_0(\mathbf{r})\rho_0(\mathbf{r}')}\partial_i\partial'_j\zeta_{xc}(\mathbf{r},\mathbf{r}',\omega).\end{aligned} \tag{9.52}$$

The functional in Eq. (9.44) reduces to the exact expression for $\delta\mathbf{A}_{xc}(\mathbf{r},\omega)$ of the homogeneous electron gas in the limit of constant density. However, in practice we have to make approximations for $f^h_{xcL,T}(\rho,|\mathbf{r}-\mathbf{r}'|,\omega)$ which enter $\delta\mathbf{A}_{xc}(\mathbf{r},\omega)$ since their exact expressions are not known. We will discuss the approximations we use for these kernels in the next section.

9.2.5 The Exchange-Correlation Kernel of the Homogeneous Electron Gas

We evaluate $f^h_{xcL,T}(\mathbf{k},\omega)$ in the limit $\omega\to 0$ since in this limit the exchange part of $f^h_{xcL}(\mathbf{k},\omega)$ is known exactly. Furthermore, $f^h_{xcT}(\mathbf{k},\omega)$ vanishes in this limit for finite $\mathbf{k}$ which simplifies our expression for $\delta\mathbf{A}_{xc}(\mathbf{r},\omega)$ given in Eq. (9.44) considerably. The longitudinal part of the exchange-correlation kernel of the homogeneous electron gas is given in the exchange-only limit by the following expression at $\omega=0$,

$$f^h_{xL}(\mathbf{k},0)=\frac{\Pi_1(\mathbf{k},0)}{[\Pi_0(\mathbf{k},0)]^2}, \tag{9.53}$$

where $\Pi_0(\mathbf{k},0)$ is the Lindhard function at $\omega=0$ and $\Pi_1(\mathbf{k},0)$ is the lowest order correction to $\Pi_0(\mathbf{k},0)$. The analytic expression for $\Pi_1(\mathbf{k},0)$ was derived by Engel and Vosko [134]. The kernel $f^h_{xL}(\mathbf{k},0)$ can be written in terms of the dimensionless variable $K=k/2k_F$ with $k=|\mathbf{k}|$ and k_F the Fermi momentum given by $k_F^3=(3\pi^2\rho)$. In Fig. (9.1) we show $f^h_{xL}(K)$ as a function of K for $\rho=1$. In practice we need to evaluate semi-infinite integrals over $f^h_{xL}(K)$. These integrals are difficult to evaluate since in the limit $K\to 1$ the slope of $f^h_{xL}(K)$ goes to $-\infty$ due to a logarithmic singularity at $K=1$. However, since $f^h_{xL}(K)$ has known asymptotic expansions around $\omega=0$ and $\omega=\infty$ we can approximate $f^h_{xL}(K)$ by a two-point Padé approximant. In general a two-point Padé approximant of a function $f(x)$ is a rational function of the form

$$P^N_M(x)=\frac{\sum_{n=0}^{N}a_n x^n}{\sum_{n=0}^{M}b_n x^n}. \tag{9.54}$$

which reproduces the asymptotic expansions of $f(x)$ around two arbitrary points x_0 and x_1. The coefficient b_0 may be fixed to one without loss of generality. The remaining $N+M+1$ coefficients are then chosen such that the first J terms of the Taylor expansion around x_0 of $P^N_M(x)$ agree with the first J terms of the Taylor expansion of $f(x)$ around x_0 and the first K terms of the Taylor expansion around x_1 of $P^N_M(x)$ agree with the first K terms of the Taylor expansion of $f(x)$ around x_1, where $J+K=N+M+1$. Following the procedure described in Ref. [135] we obtain the following expression for the two-point Padé approximant $P^6_4(K)$ which is

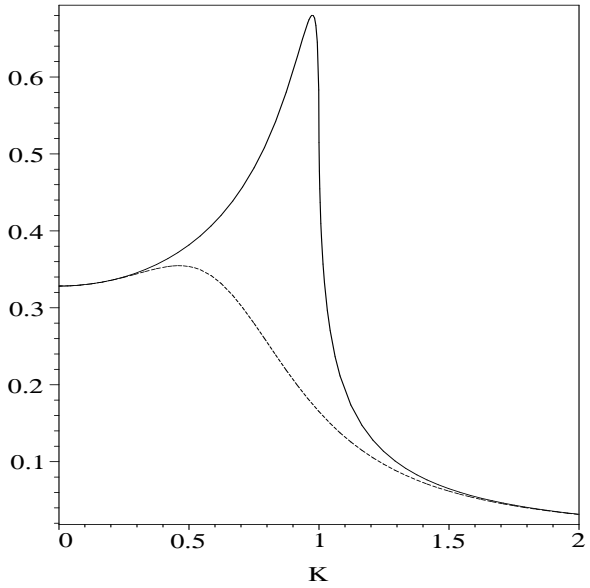

Figure 9.1: $-f_{xL}^h(K)$ of the homogeneous electron gas for $\rho = 1$. Continuous line: Exact Result; Dashed line: Padé approximant $P_4^6(K)$ of $f_{xL}^h(K)$.

an approximation of $f_{xL}^h(K)$,

$$f_{xL}^h(K) \approx P_4^6(K) = \frac{-4\pi}{k_F^2} \frac{a_0 + a_2 K^2 + a_4 K^4}{b_0 + b_2 K^2 + b_4 K^4 + b_6 K^6}, \tag{9.55}$$

where we isolated the common factor $-4\pi/k_F^2$. The odd-numbered coefficients entering the right-hand side of Eq. (9.55) are equal to zero and the even-numbered coefficients are given by

$$\begin{aligned} a_0 &= \frac{1}{4}, a_2 = \frac{2783}{9000}, a_4 = \frac{931}{2160} \\ b_0 &= 1, b_2 = \frac{511}{750}, b_4 = \frac{919}{900}, b_6 = \frac{931}{180}. \end{aligned} \tag{9.56}$$

The first 5 terms of the Taylor expansion of $P_4^6(K)$ around $x = 0$ match the first 5 terms of the Taylor expansion of $f_{xL}^h(K)$ and the first 6 terms of the Taylor expansion of $P_4^6(K)$ around $x = \infty$ match the first 6 terms of the Taylor expansion of $f_{xL}^h(K)$. In Fig. (9.1) we show $P_4^6(K)$ and compare it to $f_{xL}^h(K)$. It is clear that the sharp peak of $f_{xL}^h(K)$ around $K = 1$ is poorly described by the Padé aproximant $P_4^6(K)$. However, in order to describe this peak within a reasonable accuracy we have to use Padé aprroximants with polynomials of much higher order. Furthermore, it is known

from Monte Carlo simulations [136] that addition of correlation to $f^h_{xL}(K)$ results in the disappearance of the peak around $K = 1$. The true $f^h_{xcL}(K)$ is actually well approximated by its value at $K = 0$ for $K \lesssim 1$. Therefore $P^6_4(K)$ is much closer to the true $f^h_{xcL}(K)$ than it is to $f^h_{xL}(K)$. For these reasons we will use $P^6_4(K)$ as an approximation to $f^h_{xcL}(K)$.

9.3 Implementation

9.3.1 Evaluation of the Exchange-Correlation Vector Potential

As we show in the appendix we can rewrite $\delta\mathbf{A}_{xc}(\mathbf{r},\omega)$ according to

$$-\frac{1}{\rho_0(\mathbf{r})}\nabla\cdot\sigma_{xc}(\mathbf{r}) \doteq i\omega\delta\mathbf{A}_{xc}(\mathbf{r}) = \nabla\delta u_{xc}(\mathbf{r}) + i\omega\delta\mathbf{a}_{xc}(\mathbf{r}) + i\omega\nabla\times\delta\mathbf{b}_{xc}(\mathbf{r}), \quad (9.57)$$

where $\delta u_{xc}(\mathbf{r})$, $\delta\mathbf{a}_{xc}(\mathbf{r})$, and $\delta\mathbf{b}_{xc}(\mathbf{r})$ are given by

$$\begin{aligned}\delta u_{xc}(\mathbf{r}) = \int d\mathbf{r}'\Bigg\{ &- i\omega\frac{-\frac{2}{3}\eta_{xc}(\mathbf{r},\mathbf{r}') + \zeta_{xc}(\mathbf{r},\mathbf{r}')}{\rho_0(\mathbf{r})\rho_0(\mathbf{r}')}\delta\rho(\mathbf{r}') \\ &+\frac{-\frac{2}{3}\eta_{xc}(\mathbf{r},\mathbf{r}') + \zeta_{xc}(\mathbf{r},\mathbf{r}')}{\rho_0(\mathbf{r})\rho_0(\mathbf{r}')}\frac{\nabla'\rho_0(\mathbf{r}')}{\rho_0(\mathbf{r}')}\cdot\delta\mathbf{j}(\mathbf{r}')\Bigg\}, \quad (9.58)\end{aligned}$$

$$\begin{aligned}i\omega\delta\mathbf{a}_{xc}(\mathbf{r}) = \int d\mathbf{r}'\Bigg\{ &- i\omega\frac{-\frac{2}{3}\eta_{xc}(\mathbf{r},\mathbf{r}') + \zeta_{xc}(\mathbf{r},\mathbf{r}')}{\rho_0(\mathbf{r})\rho_0(\mathbf{r}')}\frac{\nabla\rho_0(\mathbf{r})}{\rho_0(\mathbf{r})}\delta\rho(\mathbf{r}') \\ &+\frac{\eta_{xc}(\mathbf{r},\mathbf{r}')}{\rho_0(\mathbf{r})\rho_0(\mathbf{r}')}\frac{\nabla\rho_0(\mathbf{r})}{\rho_0(\mathbf{r})}\times\delta\mathbf{m}(\mathbf{r}') \\ &+\frac{\nabla\rho_0(\mathbf{r})}{\rho_0(\mathbf{r})}\frac{-\frac{5}{3}\eta_{xc}(\mathbf{r},\mathbf{r}') + \zeta_{xc}(\mathbf{r},\mathbf{r}')}{\rho_0(\mathbf{r})\rho_0(\mathbf{r}')}\frac{\nabla'\rho_0(\mathbf{r}')}{\rho_0(\mathbf{r}')}\cdot\delta\mathbf{j}(\mathbf{r}') \\ &+\left(2\frac{\nabla\otimes\nabla'\eta_{xc}(\mathbf{r},\mathbf{r}')}{\rho_0(\mathbf{r})\rho_0(\mathbf{r}')} + \frac{\eta_{xc}(\mathbf{r},\mathbf{r}')}{\rho_0(\mathbf{r})\rho_0(\mathbf{r}')}\frac{\nabla\rho_0(\mathbf{r})\cdot\nabla'\rho_0(\mathbf{r}')}{\rho_0(\mathbf{r})\rho_0(\mathbf{r}')}\mathbf{I}\right)\cdot\delta\mathbf{j}(\mathbf{r})\Bigg\}, \quad (9.59)\end{aligned}$$

$$i\omega\delta\mathbf{b}_{xc}(\mathbf{r}) = \int d\mathbf{r}'\left\{\frac{\eta_{xc}(\mathbf{r},\mathbf{r}')}{\rho_0(\mathbf{r})\rho(\mathbf{r}')}\delta\mathbf{m}(\mathbf{r}') - \frac{\eta_{xc}(\mathbf{r},\mathbf{r}')}{\rho_0(\mathbf{r})\rho_0(\mathbf{r}')}\frac{\nabla'\rho_0(\mathbf{r}')}{\rho_0(\mathbf{r}')}\times\delta\mathbf{j}(\mathbf{r}')\right\}, \quad (9.60)$$

where $\delta\mathbf{m}(\mathbf{r},\omega) = \nabla\times\mathbf{j}(\mathbf{r},\omega)$. In the above expressions we suppressed the ω dependence for convenience and we will continue to do so in the following. The functions $\delta\rho(\mathbf{r},\omega)$, $\delta\mathbf{j}(\mathbf{r},\omega)$, and $\delta\mathbf{m}(\mathbf{r},\omega)$ can all be obtained by using at most first-order derivatives of the orbitals.

We are now able to write Eqs. (9.58), (9.59) and (9.60) in the following compact and elegant matrix vector product

$$\begin{pmatrix}\delta u_{xc}(\mathbf{r})\\ i\omega\delta\mathbf{a}_{xc}(\mathbf{r})/c\\ i\omega\delta\mathbf{b}_{xc}(\mathbf{r})/c\end{pmatrix} = \int d\mathbf{r}'\begin{pmatrix}y_{\rho\rho}(\mathbf{r},\mathbf{r}') & y_{\rho\mathbf{j}}(\mathbf{r},\mathbf{r}') & 0\\ y_{\mathbf{j}\rho}(\mathbf{r},\mathbf{r}') & y_{\mathbf{jj}}(\mathbf{r},\mathbf{r}') & y_{\mathbf{jm}}(\mathbf{r},\mathbf{r}')\\ 0 & y_{\mathbf{mj}}(\mathbf{r},\mathbf{r}') & y_{\mathbf{mm}}(\mathbf{r},\mathbf{r}')\end{pmatrix}\cdot\begin{pmatrix}\delta\rho(\mathbf{r}')\\ i\delta\mathbf{j}(\mathbf{r}')/\omega\\ i\delta\mathbf{m}(\mathbf{r}')/\omega\end{pmatrix}. \quad (9.61)$$

The matrix entries are given as

$$y_{\rho\rho}(\mathbf{r},\mathbf{r}') = -i\omega\frac{-\frac{2}{3}\eta_{xc}(\mathbf{r},\mathbf{r}')+\zeta_{xc}(\mathbf{r},\mathbf{r}')}{\rho_0(\mathbf{r})\rho_0(\mathbf{r}')}, \tag{9.62}$$

$$y_{\rho\mathbf{j}}(\mathbf{r},\mathbf{r}') = -i\omega\frac{-\frac{2}{3}\eta_{xc}(\mathbf{r},\mathbf{r}')+\zeta_{xc}(\mathbf{r},\mathbf{r}')}{\rho_0(\mathbf{r})\rho_0(\mathbf{r}')}\frac{\nabla'\rho_0(\mathbf{r}')}{\rho_0(\mathbf{r}')} = y^T_{\mathbf{j}\rho}(\mathbf{r}',\mathbf{r}), \tag{9.63}$$

$$\begin{aligned} y_{\mathbf{jj}}(\mathbf{r},\mathbf{r}') = {} & -i\omega\left(\frac{-\frac{5}{3}\eta_{xc}(\mathbf{r},\mathbf{r}')+\zeta_{xc}(\mathbf{r},\mathbf{r}')}{\rho_0(\mathbf{r})\rho_0(\mathbf{r}')}+2\frac{\partial^2\eta_{xc}(\mathbf{r},\mathbf{r}')}{\partial\rho_0(\mathbf{r})\partial\rho_0(\mathbf{r}')}\right)\frac{\nabla\rho_0(\mathbf{r})\otimes\nabla'\rho_0(\mathbf{r}')}{\rho_0(\mathbf{r})\rho_0(\mathbf{r}')} \\ & -i\omega\frac{\eta_{xc}(\mathbf{r},\mathbf{r}')}{\rho_0(\mathbf{r})\rho_0(\mathbf{r}')}\frac{\nabla\rho_0(\mathbf{r})\cdot\nabla'\rho_0(\mathbf{r}')}{\rho_0(\mathbf{r})\rho_0(\mathbf{r}')}\mathbf{I}, \end{aligned} \tag{9.64}$$

$$y_{\mathbf{jm}}(\mathbf{r},\mathbf{r}') = -i\omega\frac{\eta_{xc}(\mathbf{r},\mathbf{r}')}{\rho_0(\mathbf{r})\rho_0(\mathbf{r}')}\left[\frac{\nabla\rho_0(\mathbf{r})}{\rho_0(\mathbf{r})}\times\right] = y^T_{\mathbf{mj}}(\mathbf{r}',\mathbf{r}), \tag{9.65}$$

$$y_{\mathbf{mm}}(\mathbf{r},\mathbf{r}') = -i\omega\frac{\eta_{xc}(\mathbf{r},\mathbf{r}')}{\rho_0(\mathbf{r})\rho_0(\mathbf{r}')}\mathbf{I}, \tag{9.66}$$

in which we define the antisymmetric 3×3 matrix $[\nabla\rho_0/\rho_0\times]_{ij} = -\sum_k \epsilon_{ijk}(\partial_k\rho_0)/\rho_0$. In the next section we discuss how the integrals in Eq. (9.61) can be evaluated using fitfunctions.

9.3.2 Fitfunctions

In Eq. (9.61) we have to evaluate terms of the following forms

$$g(\mathbf{r}) = \int d\mathbf{r}' f^h_{xcL,T}(\rho_0(\mathbf{r}),|\mathbf{r}-\mathbf{r}'|)h(\mathbf{r}') \tag{9.67}$$

$$g'(\mathbf{r}) = \int d\mathbf{r}' f^h_{xcL,T}(\rho_0(\mathbf{r}'),|\mathbf{r}-\mathbf{r}'|)h(\mathbf{r}'). \tag{9.68}$$

To evaluate these integrals we use an orthonormal set of fit functions $f_i(\mathbf{r})$. Therefore we can write

$$h(\mathbf{r}) = \sum_i c_i f_i(\mathbf{r}), \tag{9.69}$$

where the coefficients c_i are obtained from

$$c_i = \int d\mathbf{r} f_i(\mathbf{r})h(\mathbf{r}). \tag{9.70}$$

We can now write $g(\mathbf{r})$ as

$$g(\mathbf{r}) = \sum_i c_i f^c_i(\mathbf{r}), \tag{9.71}$$

where $f^c_i(\mathbf{r})$ is given by

$$f^c_i(\mathbf{r}) = \int d\mathbf{r}' f^h_{xcL,T}(\rho_0(\mathbf{r}),|\mathbf{r}-\mathbf{r}'|)f_i(\mathbf{r}'). \tag{9.72}$$

Once the functions $f_i^c(\mathbf{r})$ are known we can calculate $g(\mathbf{r})$ from Eq. (9.71). To obtain an equivalent expression for $g'(\mathbf{r})$ we substitute Eq. (9.70) into Eq. (9.71). We obtain

$$g(\mathbf{r}) = \sum_i f_i^c(\mathbf{r}) \int d\mathbf{r}' f_i(\mathbf{r}) h(\mathbf{r}'). \tag{9.73}$$

Comparing this expression with Eq. (9.67) we see that $f^h_{xcL,T}(\rho_0(\mathbf{r}), |\mathbf{r} - \mathbf{r}'|)$ can be rewritten as

$$f^h_{xcL,T}(\rho_0(\mathbf{r}), |\mathbf{r} - \mathbf{r}'|) = \sum_i f_i^c(\mathbf{r}) f_i(\mathbf{r}'). \tag{9.74}$$

By interchanging $\mathbf{r}$ and $\mathbf{r}'$ we then obtain for $f^h_{xcL,T}(\rho_0(\mathbf{r}'), |\mathbf{r} - \mathbf{r}'|)$,

$$f^h_{xcL,T}(\rho_0(\mathbf{r}'), |\mathbf{r} - \mathbf{r}'|) = \sum_i f_i^c(\mathbf{r}') f_i(\mathbf{r}). \tag{9.75}$$

We now get the following expression for $g'(\mathbf{r})$

$$g'(\mathbf{r}) = \sum_i \tilde{c}_i f_i(\mathbf{r}), \tag{9.76}$$

where the coefficients $\tilde{c}_i$ are obtained from

$$\tilde{c}_i = \int d\mathbf{r} f_i^c(\mathbf{r}) h(\mathbf{r}). \tag{9.77}$$

We note that Eqs. (9.74) and (9.75) are only true if we have a complete basis. In practice the set of fitfunctions f_i is finite and chosen such to fit $h(\mathbf{r})$ as accurately as possible. Therefore Eq. (9.74) still holds approximately for a finite basis. However, this is, in general, not true for Eq. (9.75). For the basis we use in practice we indeed encounter this problem. In the following we will therefore assume that $g'(\mathbf{r})$ is approximately equal to $g(\mathbf{r})$ which is true if $\rho(\mathbf{r})$ is slowly varying. We believe that our results will not be seriously affected by this approximation.

It remains to calculate the functions $f_i^c(\mathbf{r})$. The fit functions we will use are

$$f_i(\mathbf{r}) = Z_{lm}(\theta, \phi) R_n(r), \tag{9.78}$$

where $Z_{lm}(\theta, \phi)$ are the real spherical harmonics and $R_n(r) = r^{n-1} e^{-\zeta r}$. Using the Fourier transform and its inverse given in Eqs. (9.15) and (9.16) we can rewrite $f_i^c(\mathbf{r})$ as

$$f_i^c(\mathbf{r}) = \int \frac{d\mathbf{k}}{(2\pi)^3} f_{xcL,T}(\rho_0(\mathbf{r}), k) f_i(\mathbf{k}) e^{i\mathbf{k}\cdot\mathbf{r}}. \tag{9.79}$$

Using the following identity for $e^{-i\mathbf{k}\cdot\mathbf{r}}$ [137],

$$e^{-i\mathbf{k}\cdot\mathbf{r}} = 4\pi \sum_{l,m} (-i)^l j_l(kr) Z_{lm}(\theta_\mathbf{r}, \phi_\mathbf{r}) Z_{lm}(\theta_\mathbf{k}, \phi_\mathbf{k}), \tag{9.80}$$

where $j_l(kr)$ is a spherical Bessel function, we can write $f_i(\mathbf{k})$ as

$$f_i(\mathbf{k}) = 4\pi(-i)^l Z_{lm}(\theta_\mathbf{k}, \phi_\mathbf{k}) \int_0^\infty dr r^2 j_l(kr) R_n(r), \tag{9.81}$$

where we used the orthogonality of the spherical harmonics. We can rewrite this as

$$f_i(\mathbf{k}) = 4\pi(-i)^l Z_{lm}(\theta_\mathbf{k}, \phi_\mathbf{k}) M_{nl}(k), \tag{9.82}$$

with

$$M_{nl}(k) = \int_0^\infty dr r^{n+1} j_l(kr) e^{-\zeta r}. \tag{9.83}$$

The functions $M_{nl}(k)$ can be obtained from recursion relations for $n \geq l$ and $l \geq 0$ [138]. For $n = l$ we have

$$M_{00} = \frac{1}{k^2 + \zeta^2} \tag{9.84}$$

$$M_{ll} = \frac{2kl}{k^2 + \zeta^2} M_{l-1,l-1}, \tag{9.85}$$

and for $n > l$ we have

$$M_{nl} = \frac{n + l + 1}{\zeta} M_{n-1,l} - \frac{k}{\zeta} M_{n,l+1}. \tag{9.86}$$

Inserting Eq. (9.82) in Eq. (9.79) and using the complex conjugate of Eq. (9.80) we obtain

$$f_i^c(\mathbf{r}) = \frac{2}{\pi} Z_{lm}(\theta, \phi) \int_0^\infty dk k^2 j_l(kr) f_{xcL,T}(\rho_0(\mathbf{r}), k) M_{nl}(k), \tag{9.87}$$

where we once more made use of the orthogonality of the spherical harmonics.

The integrand in Eq. (9.87) is a highly oscillatory function due to the spherical Bessel function which might make it difficult to calculate numerically. However, the integrand also decays rapidly for $k \to \infty$. In this limit the integrand decays as $1/k^3$ for $n = l = 0$ and faster for higher values of n and l. For small values of r the integral in the above expression can therefore be efficiently calculated using a Gauss-Legendre quadrature since the integrand oscillates only a couple of times before it has decayed. For larger values of r the number of oscillations of the integrand before it has decayed become too big and the integral is slowly converging and can no longer be efficiently calculated with a Gauss-Legendre quadrature. For these values of r we therefore employ a nonlinear transformation to accelerate the convergence. We use the so-called $H\bar{D}$ method of Safouhi [139, 140] which is an efficient way to calculate highly oscillatory semi-infinite integrals involving a spherical Bessel function. We do not use the more efficient $S\bar{D}$ method [141, 142] since our integrand does not meet the criteria for application of this method for $l > 2$.

9.4 Computational Details

The implementation was done in the ADF-BAND program [76, 81–83] and we performed our calculations with this modified version. We made use of Slater-type orbitals (STO) in combination with frozen cores and a hybrid valence basis set consisting of the numerical solutions of a free-atom Herman-Skillman program [84] that solves the radial Kohn-Sham equations. The spatial resolution of this basis is equivalent to a STO triple-zeta basis set augmented with two polarization functions. This valence basis set was made orthogonal to the core states. The Herman-Skillman program also provides us with the free-atom effective potential. The Hartree potential was evaluated using an auxiliary basis set of STO functions to fit the deformation density in the ground-state calculation and the induced density in the response calculation. For the evaluation of the **k**-space integrals we used a numerical integration scheme with 369 symmetry-unique sample points in the irreducible wedge of the Brillouin zone which was constructed by adopting a Lehmann-Taut tetrahedron scheme [85]. We checked the convergence with respect to the number of conduction bands used and found that ten conduction bands are sufficient. This number was used in all our calculations. We made use of the Vosko-Wilk-Nusair parametrization [55] of the LDA exchange-correlation potential for the calculation of the ground state.

9.5 Results

In Figs. 9.2 and 9.3 we report the macroscopic dielectric functions of silicon and GaP obtained with TDCDFT using the nonlocal functional in Eq. (9.44). The macroscopic dielectric function is obtained from

$$\epsilon(\omega) = 1 + 4\pi\chi_e(\omega). \tag{9.88}$$

Here $\chi_e(\omega)$ is the electric susceptibility which is the constant of proportionality between the macroscopic polarization $\mathbf{P}_{mac}(\omega)$ and the macroscopic field $\mathbf{E}_{mac}(\omega)$ according to

$$\mathbf{P}_{mac}(\omega) = \chi_e(\omega) \cdot \mathbf{E}_{mac}(\omega), \tag{9.89}$$

where $\mathbf{E}_{mac}(\omega)$ is related to the macroscopic vector potential, $\mathbf{E}_{mac}(\omega) = i\omega\mathbf{A}_{mac}(\omega)$. The macroscopic polarization $\mathbf{P}_{mac}(\omega)$ is calculated from the induced current density $\delta\mathbf{j}(\mathbf{r},\omega)$ as

$$\mathbf{P}_{mac}(\omega) = \frac{-i}{\omega V}\int_V \delta\mathbf{j}(\mathbf{r},\omega)d\mathbf{r}. \tag{9.90}$$

We compare the results obtained with our nonlocal functional with our ALDA results, and with the best available results obtained from experiment [109, 143]. In order to

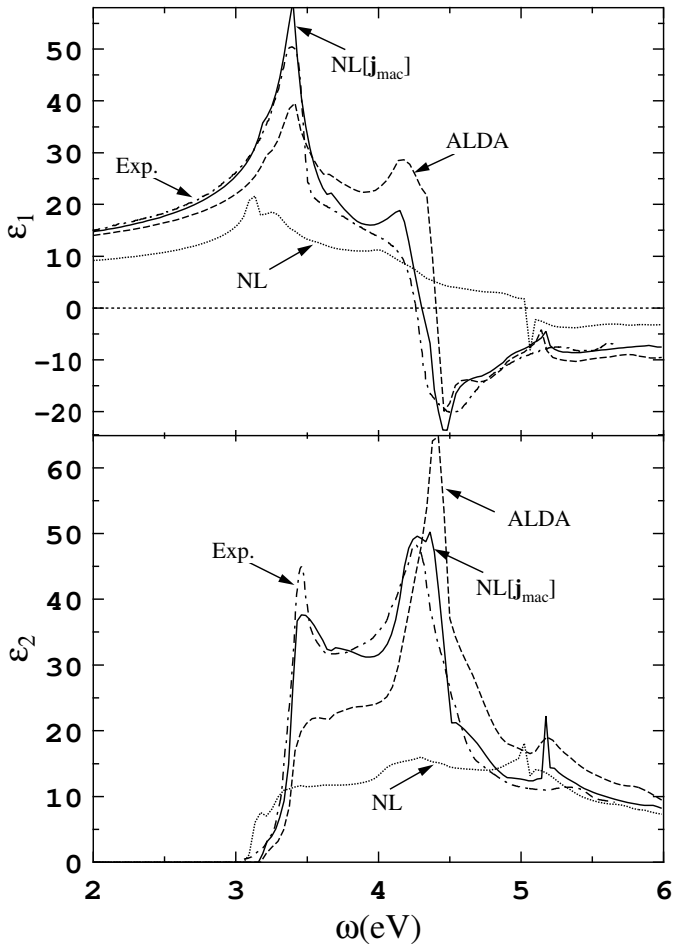

Figure 9.2: The dielectric function of silicon. Dotted curve: nonlocal functional (NL); Continuous curve: nonlocal functional (NL[$\mathbf{j}_{mac}$]) with uniform current density; Dashed curve: ALDA; Dot-dashed curve: experimental result from Ref. [109].

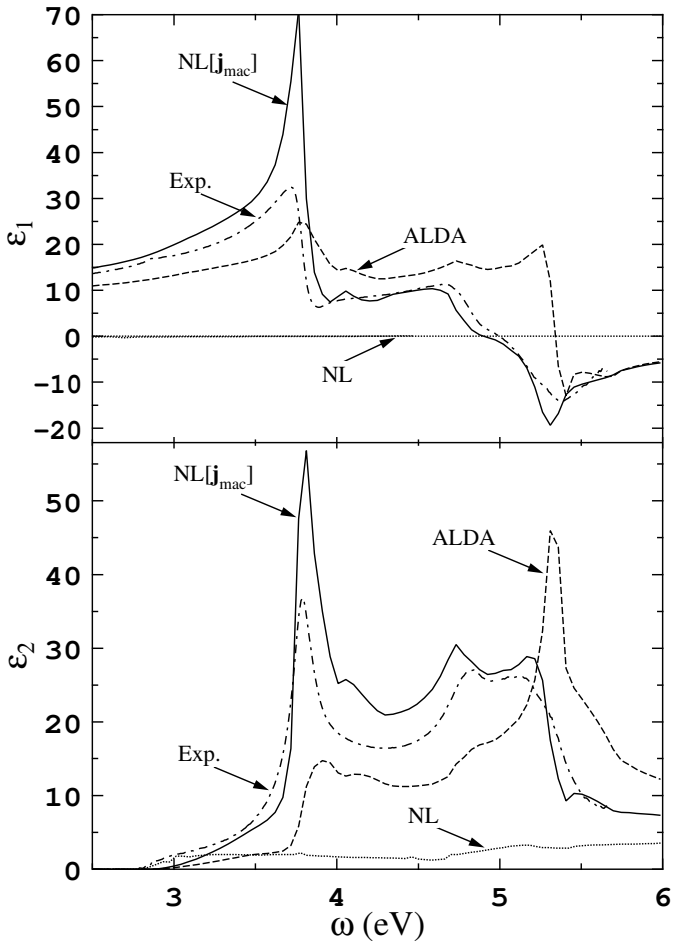

Figure 9.3: The dielectric function of GaP. Dotted curve: nonlocal functional (NL); Continuous curve: nonlocal functional with uniform current density (NL[$\mathbf{j}_{mac}$]); Dashed curve: ALDA; Dot-dashed curve: experimental result from Ref. [143].

facilitate comparison we have used a scissors operator in our calculations to coincide the calculated optical gap with that found in experiment. The scissors operator shifts upwards the energies of the unoccupied Kohn-Sham orbitals and changes the matrix elements of the current operator. It is clear from Figs. 9.2 and 9.3 that by relieving the constraints $k \ll k_F, \omega/v_F$ by employing our nonlocal functional we do not resolve the problems of the Vignale-Kohn functional in the description of optical spectra since the spectra of silicon and GaP obtained with this functional collapse in a similar manner as the optical spectra obtained with the Vignale-Kohn functional. The reason is that the current density can locally have very large values. Since $\omega\zeta_{xc}(\mathbf{r}, \mathbf{r}', \omega)$ does not vanish in the limit $\omega \to 0$, as does the corresponding term in the Vignale-Kohn functional, certain terms in Eqs. (9.57) - (9.60) involving the current density become very large causing the spectra to collapse. A similar situation arises when using the Vignale-Kohn functional. However, in that case it is the term corresponding to $\omega\eta_{xc}(\mathbf{r}, \mathbf{r}', \omega)$ that does not vanish in the limit $\omega \to 0$ together with the large local current densities that causes the spectra to collapse.

To illustrate that we are considering the correct physics by using a functional of the current density instead of the density we also give our results obtained by substituting in Eq. (9.44) the induced current density $\delta\mathbf{j}(\mathbf{r}, \omega)$ with its uniform part $\overline{\delta\mathbf{j}}(\omega) = 1/V \int_V d\mathbf{r}\delta\mathbf{j}(\mathbf{r}, \omega)$. This approximation is similar to the one-band effective mass approximation that Ullrich and Vignale [50, 80] apply in their study of the line widths of intersubband plasmons in quantum wells using the Vignale-Kohn functional. Within this approximation only the macroscopic density and current density are considered. They obtain a quantitative agreement with the experimentally observed line widths of the intersubband plasmons. Furthermore, we avoid the problems due to large local current densities mentioned above. With this approximation we obtain results close to the experimental results provided we apply an empirical prefactor of 1/3. These results are reported in Figs. 9.2 and 9.3. Even the first peaks in the absorption spectra of Si and GaP that are attributed to excitonic effects [71,144,145] are well described qualitatively. We note that these peaks are absent if a similar approximation is used for the Vignale-Kohn functional because the VK functional generates a counteracting field, whereas the field corresponding to our nonlocal functional is in the direction of the applied field. This difference is a consequence of the fact that $f^h_{xcT}(\rho, \omega = 0)$, which mainly determines the effect of the Vignale-Kohn functional on the optical spectra, and $f^h_{xcL}(\rho, \omega = 0)$, which determines the effect of our nonlocal functional on these spectra, have opposite signs. The uniform part of the current density is directly related to the macroscopic polarization of the system as is clear from Eq. (9.90). If this part of the current density is described correctly one obtains the exact dielectric function. Therefore it is important to take into account correctly

the uniform part of the current density in the exchange-correlation vector potential. Unfortunately, a good current-density functional is not available at the moment.

9.6 Conclusions

In this chapter we relieved the constraint on the length of the wave vector of the perturbation, i.e., $k \ll k_F, \omega/v_F$, that limits the formal range of applicability of the local Vignale-Kohn current-density functional by introducing a nonlocal functional of the current density with a similar viscoelastic structure as the Vignale-Kohn functional. This nonlocal functional was constructed such that it satisfies the same conservation laws and symmetry relations as the Vignale-Kohn functional. In contrast to the Vignale-Kohn functional, this nonlocal functional is almost completely determined by f_{xcL}^h for small frequencies whereas the Vignale-Kohn functional is mainly determined by f_{xcT}^h in this frequency range. The dielectric functions of silicon and GaP that we obtain using this nonlocal functional collapse in a similar manner as the optical spectra we obtained using the Vignale-Kohn functional. Using our nonlocal functional with solely the uniform part of the current density remaining we obtain results close to those obtained with experiment provided we use an empirical prefactor. We therefore conclude that we are considering the correct physics by using a functional of the current density instead of a functional of the density, but that a good current-density functional is not available at the moment.

Appendix: Derivation of the exchange-correlation vector potential

We start from the following identity

$$
\begin{aligned}
\left[\nabla \times \left[\eta_{xc}(\mathbf{r},\mathbf{r}')(\nabla' \times \mathbf{u}(\mathbf{r}'))\right]\right]_i &= \sum_{jk} \epsilon_{ijk} \partial_j \left[\eta_{xc}(\mathbf{r},\mathbf{r}') \left[\nabla' \times \mathbf{u}(\mathbf{r}')\right]\right]_k && (9.91)\\
&= \sum_{jk} \epsilon_{ijk} \partial_j \left[\eta_{xc}(\mathbf{r},\mathbf{r}') \sum_{lm} \epsilon_{klm} \partial_l' u_m(\mathbf{r}')\right] && (9.92)\\
&= \sum_{jklm} \epsilon_{ijk}\epsilon_{klm} \partial_j \left[\eta_{xc}(\mathbf{r},\mathbf{r}') \partial_l' u_m(\mathbf{r}')\right] && (9.93)\\
&= \sum_{j} \left(\delta_{il}\delta_{jm} - \delta_{im}\delta_{jl}\right) \partial_j \left[\eta_{xc}(\mathbf{r},\mathbf{r}') \partial_l' u_m(\mathbf{r}')\right] && (9.94)\\
&= \sum_{j} \left[\partial_j \eta_{xc}(\mathbf{r},\mathbf{r}') \partial_i' u_j(\mathbf{r}') - \partial_j \eta_{xc}(\mathbf{r},\mathbf{r}') \partial_j' u_i(\mathbf{r}')\right] && (9.95)
\end{aligned}
$$

Let us work out the first term on the righthand side a bit further,

$$\partial_j \eta_{xc}(\mathbf{r},\mathbf{r}')\partial'_i u_j(\mathbf{r}') = \partial'_i[(\partial_j \eta_{xc}(\mathbf{r},\mathbf{r}'))u_j(\mathbf{r}')] - (\partial'_i \partial_j \eta_{xc}(\mathbf{r},\mathbf{r}'))u_j(\mathbf{r}'). \tag{9.96}$$

We can now combine the two results, Eqs. (9.95) and (9.96), to arrive at the following expression

$$\begin{aligned}
\sum_j \partial_j \sigma_{xc,ij}(\mathbf{r}) &= \int d\mathbf{r}' \left\{-\nabla \times [\eta_{xc}(\mathbf{r},\mathbf{r}')(\nabla' \times \mathbf{u}(\mathbf{r}'))]\right\}_i + \\
&\int d\mathbf{r}' \sum_j \Big\{ 2\partial_j(\eta_{xc}(\mathbf{r},\mathbf{r}')\partial'_i u_j(\mathbf{r}')) - \frac{2}{3}\partial_i(\eta_{xc}(\mathbf{r},\mathbf{r}')\partial'_j u_j(\mathbf{r}')) \\
&+\partial_i(\zeta_{xc}(\mathbf{r},\mathbf{r}')\partial'_j u_j(\mathbf{r}'))\Big\} \qquad (9.97) \\
&= \int d\mathbf{r}' \left\{-\nabla \times [\eta_{xc}(\mathbf{r},\mathbf{r}')(\nabla' \times \mathbf{u}(\mathbf{r}'))]\right\}_i + \\
&\int d\mathbf{r} \sum_j \partial_i \left[\left(-\frac{2}{3}\eta_{xc}(\mathbf{r},\mathbf{r}') + \zeta_{xc}(\mathbf{r},\mathbf{r}')\right)\partial'_j u_j(\mathbf{r}')\right] - \\
&\int d\mathbf{r}' 2 \sum_j \left[\partial'_i \partial_j \eta_{xc}(\mathbf{r},\mathbf{r}')u_j(\mathbf{r}')\right]. \qquad (9.98)
\end{aligned}$$

Note that the integral of the first term on the right hand of Eq. (9.96) vanishes.

Using the nabla operator, we arrive at the following result for the exchange-correlation vector potential field,

$$\begin{aligned}
-\frac{1}{\rho_0(\mathbf{r})}\nabla \cdot \sigma_{xc}(\mathbf{r}) &= \int d\mathbf{r}' \Big\{-\nabla\left[\frac{1}{\rho_0(\mathbf{r})}\left(-\frac{2}{3}\eta_{xc}(\mathbf{r},\mathbf{r}') + \zeta_{xc}(\mathbf{r},\mathbf{r}')\right)(\nabla' \cdot \mathbf{u}(\mathbf{r}'))\right] \\
&+\nabla \times \left(\frac{1}{\rho_0(\mathbf{r})}\eta_{xc}(\mathbf{r},\mathbf{r}')(\nabla' \times \mathbf{u}(\mathbf{r}'))\right) \\
&-\frac{\nabla\rho_0(\mathbf{r})}{\rho_0^2(\mathbf{r})}\left[\left(-\frac{2}{3}\eta_{xc}(\mathbf{r},\mathbf{r}') + \zeta_{xc}(\mathbf{r},\mathbf{r}')\right)(\nabla' \cdot \mathbf{u}(\mathbf{r}'))\right] \\
&+\eta_{xc}\frac{\nabla\rho_0(\mathbf{r})}{\rho_0^2(\mathbf{r})} \times (\nabla' \times \mathbf{u}(\mathbf{r}')) \\
&+\frac{2}{\rho_0(\mathbf{r})}\left[\nabla \otimes \nabla'\eta_{xc} \cdot \mathbf{u}(\mathbf{r}')\right]\Big\}. \qquad (9.99)
\end{aligned}$$

This equation can be rewritten according to Eq. (9.57).

List of Acronyms

ADF	Amsterdam Density Functional [program package]
ALDA	adiabatic local density approximation
BSE	Bethe-Salpeter equation
CNT	Conti-Nifosì-Tosi [parametrization]
DFT	density-functional theory
EELS	electron energy loss spectroscopy/spectrum
GEA	gradient-expansion approximation
GGA	generalized gradient approximation
GK	Gross-Kohn [parametrization]
LDA	local density approximation
MP2	second-order Møller-Plesset [perturbation theory]
NCT	Nifosì-Conti-Tosi [parametrization]
PA	polyacetylene
PBC	periodic boundary conditions
PBT	polybutatriene
PDA	polydiacetylene
PE	polyethylene
PMI	polymethineimine
PSi	polysilane
PSi2	polysilene
PT	polythiophene
PY	polyyne
QV	Qian-Vignale [parametrization]
QV0	Qian-Vignale [parametrization] (frequency-independent)
QVA	Qian-Vignale [parametrization] (μ_{xc}=0)
SCF	self-consistent field
STO	Slater-type orbital

TDCDFT	time-dependent current-density-functional theory
TDDFT	time-dependent density-functional theory
VK	Vignale-Kohn [functional]
VWN	Vosko-Wilk-Nusair [parametrization]
ZORA	zeroth order regular approximation

Samenvatting

Dit proefschrift bediscussieert stroomdichtheidsfunctionalen in tijdsafhankelijke stroomdichtheidsfunctionaaltheorie (TDCDFT) voor systemen met periodiciteit in één of drie dimensies. Dichtheidsfunctionaaltheorie (DFT) is een methode die ontwikkeld is in de jaren '60 door Hohenberg, Kohn en Sham. Het waren Hohenberg en Kohn die in 1964 lieten zien dat de eigenschappen van een niet-ontaarde grondtoestand van een veelelektronensysteem volledig kunnen worden beschreven door enkel de elektronendichtheid, zonder daarbij expliciet gebruik te maken van de veeldeeltjesgolffunctie. De voordelen van DFT ten opzichte van golffunctietheorieën zijn duidelijk. Terwijl de ingewikkelde veeldeeltjesgolffunctie afhangt van de drie ruimtecoördinaten van elk van de N elektronen, hangt de elektronendichtheid slechts af van de drie ruimtecoördinaten, waardoor de elektronendichtheid in de praktijk makkelijker is om mee om te gaan. Verder is de elektronendichtheid ook makkelijker om mee om te gaan vanuit een conceptueel oogpunt. Het Hohenberg-Kohn theorema zegt dat de grondtoestandsdichtheid de externe potentiaal uniek bepaalt op een constante na. Dit betekent dat de externe potentiaal een functionaal is van de dichtheid. Voor systemen met een niet-ontaarde grondtoestand is ook de grondtoestandsgolffunctie uniek bepaald door de dichtheid en is de externe potentiaal dus een unieke functionaal van de dichtheid. Verder betekent dit dat alle grondtoestandseigenschappen, en in het bijzonder de grondtoestandsenergie, functionalen zijn van de elektronendichtheid in het geval van een niet-ontaarde grondtoestand. Kohn en Sham kwamen vervolgens met het idee dat de elektronendichtheid van een systeem bestaande uit deeltjes met onderlinge wisselwerking onder de invloed van een bepaalde externe potentiaal kan worden gereproduceerd in een systeem bestaande uit deeltjes zonder wisselwerking onder de invloed van een effectieve potentiaal, de zogenaamde Kohn-Sham potentiaal. Deze Kohn-Sham potentiaal is dus ook een unieke functionaal van de elektronendichtheid volgens het Hohenberg-Kohn theorema. Hierbij hebben Kohn en Sham aangenomen dat de energiefunctionalen van de twee systemen met en zonder wisselwerking tussen de deeltjes gedefinieerd zijn op hetzelfde domein. De

Kohn-Sham potentiaal bestaat uit de externe potentiaal, de Hartree potentiaal en de zogenaamde uitwisseling-correlatiepotentiaal. Deze laatste potentiaal is de functionele afgeleide van de uitwisseling-correlatie-energie naar de elektronendichtheid. Voor de uitwisseling-correlatie-energie en dus ook voor de bijbehorende potentiaal zullen in de praktijk benaderingen moeten worden gebruikt. Met behulp van de Kohn-Sham theorie kan de Schrödinger vergelijking worden herschreven als een set van ééndeeltjesvergelijkingen. De elektronendichtheid kan dan simpel verkregen worden uit de som van de kwadraten van de bezette Kohn-Sham orbitalen. Deze twee vergelijkingen kunnen zelfconsistent worden opgelost. Met de op deze manier gevonden dichtheid kunnen vervolgens de grondtoestandsenergie en andere eigenschappen van de grondtoestand berekend worden. In het geval van een ontaarde grondtoestand geldt het Hohenberg-Kohn theorema zoals hierboven geformuleerd nog steeds. Echter voor deze systemen bepaalt de externe potentiaal niet langer uniek de grondtoestandsgolffunctie. Dit betekent dat de verwachtingswaarde van welke operator dan ook (natuurlijk met uitzondering van de totale energie) afhangt van de gekozen grondtoestand uit de verzameling van grondtoestanden. In het bijzonder geldt dat de dichtheidsoperator, in het algemeen, verschillende dichtheden oplevert voor verschillende grondtoestanden uit de verzameling grondtoestanden. Daarom is de elektronendichtheid van de grondtoestand geen unieke functionaal van de externe potentiaal voor systemen met een ontaarde grondtoestand. De meest eenvoudige en meest gebruikte benadering voor de uitwisseling-correlatie-energiefunctionaal is de zogenaamde lokale dichtheidsbenadering. In deze benadering wordt het echte inhomogene systeem lokaal beschreven door een homogeen elektronengas. Men zou verwachten dat deze ruwe benadering alleen goed werkt in systemen met een bijna homogene dichtheid. Echter, deze benadering blijkt ook goed te werken in erg inhomogene systemen zoals atomen en moleculen. We bespreken DFT uitvoerig in hoofdstuk 1.

De tijdsafhankelijke versie van de DFT (TDDFT) werd in 1984 geformuleerd door Runge en Gross. Zij lieten zien dat twee dichtheden die evolueren vanuit een gezamenlijke begintoestand en worden gegenereerd door twee scalaire potentialen die beide een Taylor-expansie hebben rond de initiële tijd en die meer verschillen dan een additieve tijdsafhankelijke functie niet hetzelfde kunnen zijn. Dit betekent dat de tijdsafhankelijke scalaire potentiaal een unieke functionaal is van de tijdsafhankelijke dichtheid en de begintoestand. Als gevolg van een generalisatie van het Runge-Gross theorema door van Leeuwen weten we dat, onder bepaalde aannamen, er voor elk systeem bestaande uit deeltjes met onderlinge wisselwerking met tijdsafhankelijke dichtheid er een systeem van deeltjes zonder onderlinge wisselwerking bestaat met dezelfde dichtheid. Op basis hiervan kunnen vervolgens de tijdsafhankelijke Kohn-Sham vergelijkingen worden opgesteld. De tijdsafhankelijke uitwisseling-correlatiepotentiaal

die in deze vergelijkingen voorkomt kan echter niet geschreven worden als functionele afgeleide van een actie die gedefinieerd is op de normale tijdas. Dit betekent dat voor de praktische toepassing van TDDFT we geen gebruik kunnen maken van de symmetrie van de actie in de zoektocht naar een goede benadering voor de tijdsafhankelijke uitwisseling-correlatiepotentiaal. Echter, er zijn een aantal fysische restricties op de vorm van de tijdsafhankelijke uitwisseling-correlatiepotentiaal waarmee we benaderingen kunnen afleiden. We merken op dat van Leeuwen heeft laten zien dat de tijdsafhankelijke uitwisseling-correlatiepotentiaal geschreven kan worden als functionele afgeleide van een actie die gedefinieerd is op een Keldysh contour. De meest eenvoudige benadering voor de tijdsafhankelijke uitwisseling-correlatiepotentiaal is de zogenaamde adiabatische lokale dichtheidsbenadering. In deze benadering is de functionale vorm van de tijdsafhankelijke uitwisseling-correlatiepotentiaal gelijk aan die van de tijdsonafhankelijke uitwisseling-correlatiepotentiaal in de lokale dichtheidsbenadering. Echter, deze wordt nu geëvalueerd op de instantane tijdsafhankelijke dichtheid.

TDDFT zoals geformuleerd door Runge en Gross beschouwt alleen systemen waarin het tijdsafhankelijke externe veld beschreven kan worden door een tijdsafhankelijke scalaire potentiaal. De generalisatie naar algemene tijdsafhankelijke potentialen werd gegeven door Ghosh en Dhara. Zij lieten zien dat twee stroomdichtheden die evolueren vanuit een gezamenlijke begintoestand die gegenereerd worden door twee sets potentialen bestaande uit een tijdsafhankelijke scalaire potentiaal en een tijdsafhankelijke vectorpotentiaal die meer verschillen dan een ijktransformatie en waar in beide sets alle potentialen een Taylor-expansie hebben rond de initiële tijd niet hetzelfde kunnen zijn. De dichtheid is dan uniek bepaald door de stroomdichtheid vanwege de continuïteitsvergelijking. Echter, de dichtheid bepaalt niet uniek de stroomdichtheid. Hierdoor is het handiger om de theorie te herformuleren in termen van de stroomdichtheid wat leidt tot de zogenaamde TDCDFT. Recentelijk heeft Vignale een generalisatie gegeven van van Leeuwen's theorema voor algemene tijdsafhankelijke potentialen. Op dezelfde manier als voorheen in stationaire DFT kan op basis hiervan de tijdsafhankelijke Kohn-Sham vergelijkingen worden opgesteld voor algemene tijdsafhankelijke potentialen. Er zijn voornamelijk drie redenen om TDCDFT te gebruiken in plaats van TDDFT. De eerste reden is gerelateerd aan het gebruik van periodieke randvoorwaarden die op kunstmatige wijze de dichtheidsveranderingen op het oppervlak van het systeem verwijderen. Een macroscopische afschermend veld in de bulk van het systeem ten gevolge van een dichtheidsverandering op het oppervlak van het systeem kan niet beschreven worden als functionaal van de bulkdichtheid alleen. Dit fenomeen kan wel beschreven worden door een functionaal van de stroomdichtheid in de bulk aangezien deze is gerelateerd aan de dichtheidsver-

anderingen op het oppervlak via de continuïteitsvergelijking. De tweede reden is dat met TDCDFT ook de respons ten gevolge van transversale velden kan worden berekend wat niet mogelijk is met TDCDFT. De derde reden is dat het beschrijven van uitwisseling-correlatie-effecten makkelijker en efficiënter kan zijn met een lokale functionaal van de stroomdichtheid dan met een niet-lokale functionaal van de dichtheid. We bespreken TDDFT en TDCDFT uitgebreid in hoofdstuk 2.

In dit proefschrift zijn we geïnteresseerd in de respons van een veeldeeltjessysteem op een kleine externe storing, bijv. een elektromagnetisch veld. De eerst term in een expansie in machten van de sterkte van de storing leidt tot een respons als lineaire functie van de storing. Als de storing inderdaad klein is dan is deze lineaire respons een goede benadering voor de hele respons. De lineaire respons kan uitgedrukt worden in zogenaamde lineaire responsfuncties. Deze worden geheel bepaald door eigenwaarden en eigenfuncties van het onverstoorde systeem. Op deze manier kunnen de Kohn-Sham lineaire responsvergelijkingen worden opgesteld. We bespreken de lineaire responsformulering van TD(C)DFT in hoofdstuk 3.

De ijk kan zo gekozen worden dat de scalaire uitwisseling-correlatiepotentiaal verdwijnt voor alle frequenties. Wat overblijft is het kiezen van een goede benadering van de uitwisseling-correlatievectorpotentiaal. Vignale en Kohn hebben een uitwisseling-correlatievectorpotentiaal afgeleid door het bestuderen van een zwak verstoord elektron gas. Hun uitdrukking voldoet aan verscheidene exacte behoudswetten en symmetrierelaties. Zij voldoet aan de behoudswetten die eisen dat de uitwisseling-correlatiepotentialen geen netto kracht en koppel uitoefenen op het systeem. Verder voldoet zij aan de gegeneraliseerde translatie-invariantie die eist dat een rigide translatie van de stroomdichtheid dezelfde rigide translatie van uitwisseling-correlatiepotentialen impliceert. Ook voldoet de bijbehorende uitwisseling-correlatietensorkern van de uitwisseling-correlatievectorpotentiaal aan de Onsager symmetrierelatie die eist dat deze kern symmetrisch is onder het gelijktijdig verwisselen van de plaatscoördinaten en het transponeren van de tensorkern.

In de Vignale-Kohn (VK) functionaal komen de frequentieafhankelijke longitudinale en transversale uitwisseling-correlatiekernen van het homogene elektronengas voor. Zowel Conti, Nifosì en Tosi (CNT) als Qian en Vignale (QV) geven parameterisaties voor beide kernen. CNT berekenden de imaginaire gedeelten van de longitudinale en transversale uitwisseling-correlatiekernen door directe evaluatie van de imaginaire gedeelten van de longitudinale and transversale responsfuncties. Verder introduceerden zij parameterisaties voor de imaginaire gedeelten van de longitudinale en transversale uitwisseling-correlatiekernen die hun numerieke resultaten reproduceren. De reële gedeelten kunnen vervolgens met behulp van de Kramers-Krönig dispersierelaties berekend worden waarin de hoge-frequentielimiet werden verkregen uit

derde-frequentiemoment somregels. QV gebruiken een interpolatieformula waarin de coefficiënten worden bepaald door exacte relaties die bekend zijn voor de longitudinale en transversale uitwisseling-correlatiekernen in bepaalde limieten. Een belangrijk verschil in het lage-frequentiegebied tussen beide parameterisaties is dat, in tegenstelling tot QV, CNT de discontinuïteiten die er bestaan in de oorsprong van het $(\mathbf{k}, \omega)$-vlak van de longitudinale en transversale uitwisseling-correlatiekernen verwaarlozen. Beide discontinuïteiten zijn proportioneel met het uitwisseling-correlatiegedeelte van de schuifmodulus. De VK functionaal en de longitudinale en transversale uitwisseling-correlatiekernen die erin voorkomen worden uitvoerig besproken in hoofdstuk 4.

In hoofdstuk 5 vergelijken we de invloed van de CNT en QV parameterisaties voor de longitudinale en transversale uitwisseling-correlatiekernen van het homogene elektronengas in de toepassing van de VK functionaal in de berekening van de lineaire responseigenschappen van één-dimensionale en drie-dimensionale oneindige polyacetyleenketens. We laten zien dat de resultaten sterk afhangen van de waarden voor het uitwisseling-correlatiegedeelte van de schuifmodulus. De spectra verkregen met CNT parameterisatie liggen relatief dichtbij de spectra verkregen met de adiabatische lokale dichtheidsbenadering, terwijl de spectra verkregen met de QV parameterisatie sterk verschillen van deze spectra. Geen van beide spectra ligt echter dichtbij de spectra verkregen in andere werken waarin de Bethe-Salpeter vergelijking wordt opgelost. We verkrijgen ongeveer dezelfde resultaten wanneer we de frequentieafhankelijkheid van de twee parameterisaties verwaarlozen. Dit betekent dat de verklaring voor het verschil van de QV spectra met de spectra verkregen met de adiabatische lokale dichtheidsbenadering gezocht moet worden in de afhankelijkheid van de resultaten van de transversale uitwisseling-correlatiekern van het homogene elektron gas in de limiet dat de frequentie naar nul gaat, aangezien het longitudinale stuk reduceert tot de adiabatische lokale dichtheidsbenadering in deze limiet. De transversale uitwisseling-correlatiekern is in deze limiet gerelateerd aan het uitwisseling-correlatiegedeelte van de schuifmodulus. Helaas zijn de waarden voor deze grootheid slechts bij benadering bekend.

Om onze resultaten voor de polariseerbaarheid per eenheidscel van oneindige polymeerketens te kunnen vergelijken met de resultaten voor eindige polymeerketens introduceren we in hoofdstuk 6 een extrapolatiemodel. In tegenstelling tot veel extrapolatiemodellen in de literatuur is ons model gebaseerd op de fysieke eigenschappen van polymeerketens. In ons model nemen we aan dat een polymeerketen goed beschreven kan worden door een niet-geleidende cilinder met een radius die veel kleiner is dan zijn lengte, het zogenaamde diëlektrische naaldmodel. We laten zien dat binnen dit model de macroscopische afscherming verdwijnt in de limiet van een oneindige cilinder. Deze constatering leidt tot een relatie tussen de polariseerbaarheid per eenheidscel en de

elektrische susceptibiliteit van een oneindige polymeerketen. Dit betekent dat we de polariseerbaarheid per eenheidscel van een oneindige polymeerketen direct kunnen berekenen met behulp van een berekening met periodieke randvoorwaarden. Uit onze analyse blijkt verder dat eindeffecten, die in de limiet van oneindige keten uiteindelijk zullen verdwijnen, slechts langzaam afvallen voor toenemende ketenlengte. Het diëlektrische naaldmodel verschaft ons ook een procedure om de polariseerbaarheid per eenheidscel van eindige polymeerketens te extrapoleren naar de waarde voor oneindige polymeerketens. Een vergelijking van deze geëxtrapoleerde waarde met de waarde verkregen door een berekening met periodieke randvoorwaarden geeft een maat voor de geldigheid van het gebruik van het diëlektrische naaldmodel. We hebben ons diëlektrische naaldmodel getest op polyacetyleen en de waterstofketen en vonden dat de waarden voor de polariseerbaarheid per eenheidscel verkregen met deze twee methoden nagenoeg hetzelfde zijn. Dit betekent dat ons diëlektrisch naaldmodel een goede benadering verschaft om de diëlektrische eigenschappen van lange polymeerketens te beschrijven.

In hoofdstuk 7 passen we de VK functionaal toe op de berekening van de optische spectra van halfgeleiders. We bespreken de resultaten voor silicium wat een typisch geval is. Als we de QV parameterisatie gebruiken voor de longitudinale en transversale uitwisseling-correlatiekernen van het homogene elektronengas dan stort het optische spectrum ineen. We bediscussiëren mogelijke redenen voor dit resultaat. We laten zien dat de voorwaarden voor de mate van niet-uniformiteit van de grondtoestandsdichtheid en de mate van de ruimtelijke variatie van de externe potentiaal waaronder de VK functionaal is afgeleid bijna allemaal worden geschonden. Bovendien, omdat de VK functionaal is afgeleid voor een zwak verstoord elektronengas in het regime boven het continuüm van excitatie-energieën, beargumenteren we dat het niet geschikt is voor het berekenen van optische spectra aangezien die sterk gerelateerd zijn aan het continuüm van excitatie-energieën. Als we de benadering maken dat het uitwisseling-correlatiegedeelte van de schuifmodulus gelijk is aan nul, zoals in de CNT parameterisatie, verkrijgen we optische spectra die dichtbij de spectra verkregen in de adiabatische lokale dichtheidsbenadering liggen. Dit is simpelweg een gevolg van het feit dat in deze benadering de VK functionaal reduceert tot de adiabatische lokale dichtheidsbenadering in de limiet dat de frequentie verdwijnt en het feit dat voor de relevante frequenties in optische spectra de waarden voor de de longitudinale en transversale uitwisseling-correlatiekernen van het homogene elektronengas niet veel verschillen van hun waarden in de limiet dat de frequentie verdwijnt.

In hoofdstuk 8 laten we zien hoe we de VK uitdrukking meenemen in onze formulering voor de lineaire respons van metalen. Aangezien deze functionaal niet lokaal is in de tijd kunnen we op deze manier relaxatie-effecten ten gevolge van elektron-

elektronverstrooiing in onze beschrijving meenemen. We bediscussiëren het verschillende gedrag van de inter- en intraband processen in het geval dat de golfvector van de storing klein is. In de optische limiet waarin deze golfvector verdwijnt zijn de twee sets van zelfconsistente vergelijkingen die de inter- en intraband bijdragen aan de respons beschrijven gekoppeld wanneer we de VK functionaal in onze formulering meenemen. Vanwege de hierboven genoemde resultaten voor de optische spectra van halfgeleiders en het feit dat we met name geïnteresseerd zijn in de frequentieafhankelijkheid van de uitwisseling-correlatievectorpotentiaal om relaxatie-effecten te kunnen beschrijven maken we in alle berekening de benadering dat het uitwisseling-correlatiegedeelte van de schuifmodulus gelijk is aan nul. Op deze manier hebben we met de CNT en QV parameterisaties de diëlektrische functie en de elektronenergieverliesfunctie berekend van koper, zilver en goud. De verkregen resultaten zijn in goede overeenstemming met de experimenteel verkregen resultaten. In tegenstelling tot de resultaten verkregen in de adiabatische lokale dichtheidsbenadering verkrijgen we nu wel de Drude-achtige staart in het imaginaire gedeelte van de diëlektrische functie. Verder verkrijgen we nu ook de experimenteel gevonden scherpe plasmonpiek in het elektronenenergieverliesspectrum van zilver.

In hoofdstuk 9 verlichten we de voorwaarden op de golfvector van de storing die het formele toepassingsgebied van de lokale VK stroomdichtheidsfunctionaal beperkt door een niet-lokale functionaal van de stroomdichtheid met een soortgelijke viscoelastische structuur als de VK functionaal te introduceren. Deze niet-lokale functionaal is zo geconstrueerd dat hij voldoet aan dezelfde behoudswetten en symmetrierelaties als de VK functionaal. In tegenstelling tot de VK functionaal wordt deze niet-lokale functionaal voor lage frequenties bijna volledig bepaald door de longitudinale uitwisseling-correlatiekern van het homogene elektronengas, terwijl de VK functionaal voornamelijk wordt bepaald door de transversale uitwisseling-correlatiekern in dit frequentiegebied. De optische spectra van silicium en galliumfosfide berekend met deze niet-lokale functionaal vertonen eenzelfde soort ineenstorting als we verkregen door de VK functionaal te gebruiken. Wanneer we onze niet-lokale functionaal gebruiken waarin we alleen de uniforme component van de stroomdichtheid meenemen, verkrijgen we resultaten die dichtbij de experimenteel verkregen resultaten liggen op voorwaarde dat we een empirisch bepaalde voorfactor gebruiken. We concluderen daarom dat we de juiste fysica beschouwen door een functionaal van de stroomdichtheid gebruiken in plaats van een functionaal van de dichtheid, maar dat een goede stroomdichtheidsfunctionaal op dit moment nog niet beschikbaar is.

List of Publications

J. A. Berger, P. L. de Boeij, and R. van Leeuwen, *A nonlocal current-density functional*, Phys. Rev. B, to be submitted; see Chapter 9.

J. A. Berger, P. Romaniello, R. van Leeuwen, and P. L. de Boeij, *Performance of the Vignale-Kohn functional in the linear response of metals*, Phys. Rev. B, submitted; see Chapter 8.

J. A. Berger, P. L. de Boeij, and R. van Leeuwen, *Analysis of the Vignale-Kohn current functional in the calculation of optical spectra*, Phys. Rev. B, submitted; see Chapter 7.

J. A. Berger, P. L. de Boeij, and R. van Leeuwen, *A physical model for the longitudinal polarizabilities of polymer chains*, J. Chem. Phys. **123**, 174910 (2005); see Chapter 6.

J. A. Berger, P. L. de Boeij, and R. van Leeuwen, *Analysis of the viscoelastic coefficients in the Vignale-Kohn functional: The cases of one- and three-dimenstional polyacetylene*, Phys. Rev. B **71**, 155104 (2005); see Chapter 5.

M. van Faassen, L. Jensen, J. A. Berger, and P. L. de Boeij, *Size-scaling of the polarizability of tubular fullerenes investigated with time-dependent (current)-density-functional theory*, Chem. Phys. Lett. **395**, 274 (2004).

M. van Faassen, P. L. de Boeij, R. van Leeuwen, J. A. Berger, and J. G. Snijders, *Application of time-dependent current-density-functional theory to nonlocal exchange-correlation effects in polymers*, J. Chem. Phys. **118**, 1044 (2003).

M. van Faassen, P. L. de Boeij, R. van Leeuwen, J. A. Berger, and J. G. Snijders, *Ultranonlocality in time-dependent current-density-functional theory: Applications to*

conjugated polymers, Phys. Rev. Lett. **88**, 186401 (2002).

P. L. de Boeij, F. Kootstra, J. A. Berger, R. van Leeuwen, and J. G. Snijders, *Current-density-functional theory for optical spectra: A successful polarization functional*, J. Chem. Phys. **115**, 1995 (2001).

Dankwoord

Hierbij wil ik iedereen bedanken die heeft bijgedragen aan de totstandkoming van dit proefschrift. Als eerste wil ik graag prof. dr. J. G. Snijders bedanken. Jaap, bedankt dat je mij de kans hebt gegeven om hier in Groningen mijn promotieonderzoek te doen. Dit onderzoek was een direct vervolg op het doctoraalonderzoek dat ik bij je had gedaan en wat mij zeer was bevallen. Je had mijn eerste promotor moeten zijn, maar spijtig genoeg zul je de promotie niet meer mee kunnen maken door een vroegtijdig overlijden. Ik zal je blijven herinneren als een goedlachse man met een brede kennis en een scherp inzicht die tijdens discussies en lezingen immer naar voren kwamen.

Ik wil prof. dr. R. Broer graag bedanken voor het opnemen van de taak van eerste promotor. Ria, bedankt dat je zorg hebt willen dragen voor alle lastige bezigheden die de taak van eerste promotor met zich meebrengt en die je zo goed hebt volbracht. Ook wil ik je bedanken voor de goede samenwerking tijdens de colleges Chemische Binding 2, waarvan jij de hoorcolleges verzorgde en waarbij ik één van de werkcollegedocenten was.

Tevens wil ik graag mijn copromotores dr. ir. P. L. de Boeij en dr. R. van Leeuwen bedanken. Paul en Robert, jullie deuren stonden letterlijk en figuurlijk altijd open voor een eindeloze stroom vragen mijnerzijds en daarvoor ben ik jullie zeer dankbaar. Ik heb onze samenwerking de afgelopen jaren altijd als zeer plezierig beschouwd. Paul, bedankt voor de vele tijd die je in dit project hebt gestoken en voor je talrijke praktische oplossingen voor de problemen waar we tegenaan liepen. Daarnaast wil ik je bedanken voor de goede relatie buiten het werk om. Zo diende in de eerste paar jaar jouw appartement aan het Kattendiep regelmatig als 'uitvalsbasis' voor menig cinematografisch en/of culinair uitstapje. Ook schuwde jij zelf het keukengerei niet wat tot menig smakelijk en gezellig etentje heeft geleid. Robert, bedankt voor de vele keren dat je mij de theorie van uiteenlopende zaken zo helder hebt uitgelegd en voor je goede ideeën die dit onderzoek in de juiste richting hebben geholpen. Bovendien wil ik je bedanken voor je altijd humorvolle anekdotes en je interessante triviale feitenkennis

waarvoor, naast zoveel nuttige informatie, jouw hersenpan verbazingwekkend genoeg nog plaats biedt.

Ook wil ik alle overige leden en oud-leden van de theoretische chemie groep bedanken. Adrian, Alex, Alexandrina, Aymeric, Freddie, Henriët, Javier, Johan, Khompat, Klaas, Lasse, Liviu, Marcel, Maya, Meta, Michael, Nienke, Nils, Olena, Piet, Rob, Robbert, Rosanna, Thomas, Tuomas en Wim bedankt voor het bijdragen aan een goede sfeer in de groep en voor de leuke activiteiten die we naast het werk hebben ondernomen. Meta, bedankt voor het verstrekken van extra data polariseerbaarheden van polyacetyleen- en waterstofketens. Rob, bedankt voor het implementeren van de Qian-Vignale interpolatieformule.

Verder wil ik de beoordelingscommissie bestaande uit prof. dr. A. Görling, prof. dr. J. Knoester en prof. dr. G. Vignale bedanken voor het zorgvuldig bestuderen van het proefschrift en voor hun bruikbare suggesties.

Ik wil de leden van het Murphy's Quiz Night team bedanken voor de gezellige dinsdagavonden in Ray's Pub, waar iedere week weer de meest nutteloze maar desalniettemin uiterst interessante feiten uit de donkere krochten van ieders brein worden opgediept. Ook de deelnemers aan de 'kolonistencompetitie' wil ik bedanken voor de leuke spelletjesavonden. De mensen van De Groene Uilen en The Shadows bedank ik voor het met hen (hebben) mogen uitoefenen van de mooiste sport op aard. Verder wil ik mijn oud-huisgenoot Bastiaan graag bedanken voor de goede herinneringen aan de tijd die we hebben doorgebracht in het Vinkhuizer 'getto'.

Cara Pina, voglio ringraziarti per il divertimento e per tutti i bei momenti che abbiamo vissuti finora. Sono molto felice di questi tre anni trascorsi insieme. Grazie per tutto ciò che hai fatto per me, per essere stata così paziente con i miei 'giochi' e, cosa più importante, grazie per il tuo sostegno e il tuo amore. Mille grazie ai genitori di Pina, a suo fratello Leo e a sua sorella Mariantonietta per la loro ospitalità ogni volta che siamo stati lì e per il mangiare, tanto buono e abbondante!

In het bijzonder wil ik graag mijn ouders en mijn zus Corien bedanken voor hun steun en liefde door de jaren heen. Pa en ma, bedankt voor het vertrouwen en de vrijheid die jullie mij altijd hebben gegeven. Corien, bedankt dat je mij net als Pina als paranimf wilt bijstaan tijdens de promotie.

Arjan Berger,
Groningen, 2006.

Bibliography

[1] P. Hohenberg and W. Kohn, Phys. Rev. **136**, B864 (1964).

[2] W. Kohn and L. J. Sham, Phys. Rev. **140**, A1133 (1965).

[3] E. Runge and E. K. U. Gross, Phys. Rev. Lett. **52**, 997 (1984).

[4] A. K. Dhara and S. K. Ghosh, Phys. Rev. A **35**, R442 (1987).

[5] S. K. Ghosh and A. K. Dhara, Phys. Rev. A **38**, 1149 (1988).

[6] G. Vignale, Phys. Rev. B **70**, 201102(R) (2004).

[7] X. Gonze, P. Ghosez, and R.W. Godby, Phys. Rev. Lett. **74**, 4035 (1995), *ibid.* **78**, 294 (1997).

[8] G. Onida, L. Reining, and A. Rubio, Rev. Mod. Phys. **74**, 601 (2002).

[9] Y. -H. Kim and A. Görling, Phys. Rev. B **66**, 035114 (2002); Phys. Rev. Lett. **89**, 096402 (2002).

[10] P. Nozières and D. Pines, *The Theory of Quantum Liquids* (Perseus Books, Cambridge, Massachusetts, 1999).

[11] G. Vignale, Phys. Lett. A **209**, 206 (1995).

[12] G. Vignale and W. Kohn, Phys. Rev. Lett. **77**, 2037 (1996).

[13] G. Vignale and W. Kohn, in *Electronic Density Functional Theory: Recent Progress and New Directions*, edited by J. Dobson, M. P. Das, and G. Vignale. (Plenum Press, New York, 1998).

[14] S. Conti, R. Nifosì, and M. P. Tosi, J. Phys. Condens. Matter **9**, L475 (1997).

[15] Z. Qian and G. Vignale, Phys. Rev. B **65**, 235121 (2002).

[16] R. van Leeuwen, Adv. Quantum Chem. **43**, 26 (2003).

[17] R. G. Parr and W. Yang, *Density-Functional Theory of Atoms and Molecules*, (Oxford University Press, New York, 1989).

[18] R. M. Dreizler and E. K. U. Gross, *Density Functional Theory: An Approach to the Quantum Many-Body Problem*, (Springer-Verlag, Berlin, 1990).

[19] E. H. Lieb, Int. J. Quant. Chem. **24**, 243 (1983).

[20] R. van Leeuwen, Int. J. Mod. Phys. B **15**, 1969 (2001).

[21] H. Hellmann, *Einführung in die QuantenChemie*, Leipzig (1937); R. P. Feynman, Phys. Rev. **56**, 340 (1939).

[22] M. Levy, J. P. Perdew, and V. Sahni, Phys. Rev. A **30**, 2745 (1984).

[23] C.-O. Almbladh and U. von Barth, Phys. Rev. B **31**, 3231 (1985).

[24] O. V. Gritsenko, B. Braïda, and E. J. Baerends, J. Chem. Phys. **119**, 1937 (2003).

[25] G. F. Giuliani and G. Vignale. *Quantum Theory of the Electron Liquid*, (Cambridge University Press, Cambridge, 2005).

[26] D. Mearns, Phys. Rev. B **38**, 5906 (1988).

[27] M. Levy, Phys. Rev. A **26**, 1200 (1982).

[28] P. R. T. Schipper, O. V. Gritsenko, and E. J. Baerends, Theor. Chem. Acc. **99**, 329 (1998).

[29] P. R. T. Schipper, O. V. Gritsenko, and E. J. Baerends, J. Chem. Phys. **111**, 4056 (1999).

[30] M. Levy, Proc. Nat. Acad. Sci. USA **76**, 6062 (1979).

[31] H. Englisch and R. Englisch, Phys. Stat. Solidi B **123**, 711 (1984); **124**, 373 (1984).

[32] C. A. Ullrich and W. Kohn, Phys. Rev. Lett. **87**, 093001 (2001).

[33] D. J. W. Geldart, in *Topics in Current Chemistry* (R. F. Nalewajski, Eds.), Springer, Berlin, Vol. 180, p. 31 (1996).

[34] Y. Osaka, J. Phys. Soc. Japan **36**, 376 (1974).

[35] J. P. Perdew and S. Kurth, *Density Functionals for Non-Relativistic Coulomb Systems*, in *Density Functionals: Theory and Applications*, edited by D. P. Joubert, *Lecture Notes in Physics*, Vol. 500, (Springer, Berlin, 1998).

[36] R. van Leeuwen and E. J. Baerends, Phys. Rev. A **49**, 2421 (1994).

[37] E. K. U. Gross, J. F. Dobson, and M. Petersilka, Top. Curr. Chem. **181**, 81 (1996).

[38] R. van Leeuwen, Phys. Rev. Lett. **82**, 3863 (1999).

[39] L. V. Keldysh, Sov. Phys. JETP **20**, 1018 (1965).

[40] R. D'Agosta and G. Vignale, Phys. Rev. B **71**, 245103 (2005).

[41] R. van Leeuwen, in *The Fundamentals of Electron Density, Density Matrix and Density Functional Theory in Atoms, Molecules and the Solid State*, edited by N. I. Gidopoulos and S. Wilson, Progress in Theoretical Chemistry and Physics, (Kluwer Academic Publishers, Dordrecht, 2003), Vol. 24.

[42] G. Vignale, Phys. Rev. Lett. **74**, 3233 (1995).

[43] J. Dobson, Phys. Rev. Lett. **73**, 2244 (1994).

[44] H. Lehmann, Nuovo Cimento **11**, 342 (1954).

[45] E. K. U. Gross and W. Kohn, Phys. Rev. Lett. **55**, 2850 (1985); **57**, 923(E) (1986).

[46] G. Vignale, C. A. Ullrich, and S. Conti, Phys. Rev. Lett. **79**, 4878 (1997).

[47] H. M. Böhm, S. Conti, and M. P. Tosi, J. Phys. Condens. Matter **8**, 781 (1996).

[48] R. Nifosì, S. Conti, and M. P. Tosi, Phys. Rev. B **58**, 12758 (1998).

[49] S. Conti and G. Vignale, Phys. Rev. B **60**, 7966 (1999).

[50] C. A. Ullrich and G. Vignale, Phys. Rev. B **65**, 245102 (2002).

[51] J. Lindhard, Kgl. Danske Videnskab. Selskab, Mat.-Fys. Medd. **28**, no.8, (1954).

[52] N. Iwamoto and E. K. U. Gross, Phys. Rev. B **35**, 3003 (1987).

[53] S. Ichimaru, Rev. Mod. Phys. **54**, 2850 (1982).

[54] D. M. Ceperley, Phys. Rev. B **18**, 3126 (1978).

[55] S. H. Vosko, L. Wilk, and M. Nusair, Can. J. Phys. **58**, 1200 (1980).

[56] A. J. Glick and W. F. Long, Phys. Rev. B **4**, 3455 (1971).

[57] H. Yasuhara and Y. Ousaka, Int. J. Mod. Phys. B **6**, 3089 (1992).

[58] E. K. U. Gross and W. Kohn, Adv. Quantum Chem. **21**, 255 (1990).

[59] G. D. Mahan and K. R. Subbaswami, *Local Density Theory of Polarizability* (Plenum Press, New York, 1990).

[60] O. -J. Wacker, R. Kümmel, and E. K. U. Gross, Phys. Rev. Lett. **73**, 2915 (1994).

[61] R. van Leeuwen, in *Progress in Nonequilibrium Green's Functions II*, edited by M. Bonitz and D. Semkat, (World Scientific, Singapore, 2003), p. 427-435.

[62] F. Sottile, V. Olevano, and L. Reining, Phys. Rev. Lett. **91**, 056402 (2003).

[63] G. Adragna, R. del Sole, and A. Marini, Phys. Rev. B **68**, 165108 (2003).

[64] M. van Faassen, P. L. de Boeij, R. van Leeuwen, J. A. Berger, and J. G. Snijders, Phys. Rev. Lett. **88**, 186401 (2002).

[65] M. van Faassen, P. L. de Boeij, R. van Leeuwen, J. A. Berger, and J. G. Snijders, J. Chem. Phys. **118**, 1044 (2003).

[66] M. van Faassen and P. L. de Boeij, J. Chem. Phys. **121**, 10707 (2004).

[67] S. J. A. van Gisbergen, P. R. T. Schipper, O. V. Gritsenko, E. J. Baerends, J. G. Snijders, B. Champagne, and B. Kirtman, Phys. Rev. Lett. **83**, 694 (1999).

[68] P. L. de Boeij, F. Kootstra, J. A. Berger, R. van Leeuwen, and J. G. Snijders, J. Chem. Phys. **115**, 1995 (2001).

[69] D. M. Ceperley and B. J. Alder, Phys. Rev. Lett. **45**, 566 (1980).

[70] P. Vogl and D. K. Campbell, Phys. Rev. B **41**, 12797 (1990).

[71] M. Rohlfing and S. G. Louie, Phys. Rev. Lett. **82**, 1959 (1999).

[72] P. Puschnig and C. Ambrosch-Draxl, Phys. Rev. Lett. **89**, 056405 (2002); Synth. Met. **135-136**, 415 (2003).

[73] M. L. Tiago, M. Rohlfing, and S. G. Louie, Phys. Rev. B **70**, 193204 (2004).

[74] G. Leising, Phys. Rev. B **38**, 10313 (1988).

[75] J.-W. van der Horst, P. A. Bobbert, and M. A. J. Michels, Phys. Rev. B **66**, 035206 (2002).

[76] F. Kootstra, P. L. de Boeij, and J. G. Snijders, J. Chem. Phys. **112**, 6517 (2000).

[77] F. Kootstra, P. L. de Boeij, and J. G. Snijders, Phys. Rev. B **62**, 7071 (2000).

[78] G. Breit, Phys. Rev. **34**, 553 (1929); **39**, 616 (1932).

[79] O. L. Brill and B. Goodman, Am. J. Phys. **35**, 832 (1967).

[80] C. A. Ullrich and G. Vignale, Phys. Rev. Lett. **87**, 037402 (2001).

[81] G. te Velde and E. J. Baerends, Phys. Rev. B **44**, 7888 (1991); J. Comput. Phys. **99**, 84 (1992).

[82] C. Fonseca Guerra, O. Visser, J. G. Snijders, G. te Velde, and E. J. Baerends, in *Methods and Techniques in Computational Chemistry*, edited by E. Clementi and G. Corongiu, (STEF, Cagliary, 1995), p. 305.

[83] G. te Velde, F. M. Bickelhaupt, E. J. Baerends, C. Fonseca Guerra, S. J. A. van Gisbergen, J. G. Snijders, and T. Ziegler, J. Comput. Chem. **22**, 931 (2001).

[84] F. Herman and S. Skillman, *Atomic Structure Calculations*, (Prentice-Hall, Englewood Cliffs NJ, 1963)

[85] G. Lehmann and M. Taut, Phys. Status. Solidi B **54**, 469 (1972).

[86] B. Kirtman, W. B. Nilsson, and W. E. Palke, Solid State Commun. **46**, 791 (1983).

[87] B. Kirtman, Chem. Phys. Lett. **143**, 81 (1988).

[88] G. J. B. Hurst, M. Dupuis, and E. Clementi, J. Chem. Phys. **89**, 385 (1988).

[89] B. Champagne, D. H. Mosley, and J.-M. André, Int. J. Quantum Chem. Symp. **27**, 667 (1993).

[90] K. N. Kudin, R. Car, and R. Resta, J. Chem. Phys. **122** 134907 (2005).

[91] A. G. Rojo and G. D. Mahan, Phys. Rev. B **47**, 1794 (1993); G. D. Mahan and A. G. Rojo, Phys. Rev. B **50**, 2642 (1994);

[92] S. Tretiak, V. Chernyak, and S. Mukamel, Phys. Rev. Lett. **77**, 4656 (1996).

[93] J. A. Berger, P. L. de Boeij, and R. van Leeuwen, Phys. Rev. B **71**, 155104 (2005).

[94] B. Champagne, D. Jacquemin, J.-M. André, and B. Kirtman, J. Phys. Chem. A **101**, 3158 (1997).

[95] E. Dalskov, J. Oddershede, and D. M. Bishop, J. Chem. Phys. **108**, 2152 (1998).

[96] E. J. Weniger and B. Kirtman, Comput. Math. Appl. **45**, 189 (2003).

[97] B. Kirtman, F. L. Gu, and D. M. Bishop, J. Chem. Phys. **113**, 1294 (2000).

[98] D. M. Bishop, F. L. Gu, and B. Kirtman, J. Chem. Phys. **114**, 7633 (2001).

[99] M. Fixman, J. Chem. Phys. **75**, 4040 (1981).

[100] M. A. Gusmão, Phys. Rev. B **35**, 1682 (1987).

[101] E. R. Love, Q. J. Mech. Appl. Maths **2**, 428 (1949); Mathematika **37**, 217 (1990).

[102] D. F. Bartlett and R. Corle, J. Phys. A: Math. Gen. **18**, 1337 (1985).

[103] Y. Ren, B. Zhang, and H. Qiao, J. Comput. Appl. Math. **110**, 15 (1999).

[104] M. van Faassen, private communication.

[105] C. A. Ullrich and G. Vignale, Phys. Rev. B **58**, 7141 (1998).

[106] C. A. Ullrich and G. Vignale, Phys. Rev. B **58**, 15756 (1998).

[107] M. van Faassen and P. L. de Boeij, J. Chem. Phys. **120**, 8353 (2004).

[108] C. A. Ullrich and K. Burke, J. Chem. Phys. **121**, 28 (2004).

[109] P. Lautenschlager, M. Garriga, L. Viña, and M. Cardona, Phys. Rev. B **36**, 4821 (1987).

[110] P. Romaniello and P. L. de Boeij, Phys. Rev. B **71**, 155108 (2005)

[111] T. Kreibich and E. K. U. Gross, Phys. Rev. Lett. **86**, 2984 (2001).

[112] R. van Leeuwen, Phys. Rev. B **69**, 115110 (2004).

[113] J. A. Berger, P. L. de Boeij, and R. van Leeuwen, *submitted*

[114] H. J. Hagemann, W. Gudat, and C. Kunz, J. Opt. Soc. Am. **65**, 742 (1975).

[115] B. Dold and R. Mecke, Optik Am. **65**, 742 (1975).

[116] K. Stahrenberg, Th. Herrmann, K. Wilmers, N. Esser, and W. Richter, Phys. Rev. B **64**, 115111 (2001).

[117] P. B. Johnson and R. W. Christy, Phys. Rev. B **6**, 4370 (1972).

[118] E. D. Palik, *Handbook of optical constants of solids*, Vol. I and II (Academic Press Inc., 1985/1991).

[119] J. H. Weaver, C. Krafka, D. W. Lynch, and E. E. Koch, in *Optical properties of Metals* (Physics Data, Fachinformationszentrum, Karlsruhe, 1981).

[120] H. Ehrenreich and H. R. Philipp, Phys. Rev. **128**, 1622 (1962).

[121] E. van Lenthe, E. J. Baerends, and J. G. Snijders, J. Chem. Phys. **101**, 9783 (1994).

[122] E. van Lenthe, R. van Leeuwen, E. J. Baerends, and J. G. Snijders, Int. J. Quant. Chem. **57**, 281 (1996).

[123] P. H. T. Philipsen, E. van Lenthe, J. G. Snijders, and E. J. Baerends, Phys. Rev. B **56**, 13556 (1997).

[124] F. Kootstra, P. L. de Boeij, H. Aissa, and J. G. Snijders, J. Chem. Phys. **114**, 1860 (2001).

[125] P. L. de Boeij, F. Kootstra, and J. G. Snijders, Int. J. Quant. Chem. **85**, 449 (2001).

[126] P. Romaniello and P. L. de Boeij, J. Chem. Phys. **122** 164303 (2005)

[127] P. Romaniello and P. L. de Boeij, *in preparation.*

[128] E. van Lenthe and E. J. Baerends, J. Comput. Chem. **24**, 1142 (2003).

[129] G. Wiesenekker and E. J. Baerends, J. Phys.: Condens. Matter **3**, 6721 (1991); G. Wiesenekker, G. te Velde, and E. J. Baerends, J. Phys. C **21**, 4263 (1988).

[130] J. B. Smith and H. Ehrenreich, Phys. Rev. B **25**, 923 (1982).

[131] G. R. Parkins, W. E. Lawrence, and R. W. Christy, Phys. Rev. B **23**, 6408 (1981).

[132] R. T. Beach and R. W. Christy, Phys. Rev. B **12**, 5277 (1977).

[133] S. R. Nagel and S. E. Schnatterly, Phys. Rev. B **9**, 1299 (1974).

[134] E. Engel and S. H. Vosko, Phys. Rev. B **42**, 4940 (1990).

[135] A. Gonzalez, J. Phys. Condens. Matter **9**, 4643 (1997).

[136] S. Moroni, D. M. Ceperley, and G. Senatore, Phys. Rev. Lett. **75**, 689 (1995).

[137] A. Messiah, *Quantum Mechanics*, (North Holland, Amsterdam, 1961).

[138] P. O. Ellison, J. Chem. Phys. **61**, 507 (1974).

[139] H. Safouhi, J. Comput. Phys. **165**, 473 (2000).

[140] H. Safouhi, J. Math. Chem. **29**, 213 (2000).

[141] H. Safouhi, J. Phys. A: Math. Gen. **34**, 2801 (2001).

[142] H. Safouhi, J. Phys. A: Math. Gen. **35**, 9685 (2002).

[143] S. Zollner, M. Garriga, J. Kircher, J. Humliček, and M. Cardona, Phys. Rev. B **48**, 7915 (1993).

[144] L. X. Benedict, E. L. Shirley, and R. B. Bohn, Phys. Rev. Lett. **80**, 4514 (1998); Phys. Rev. B **57**, R9385 (1998).

[145] L. Reining, V. Olevano, A. Rubio, and G. Onida, Phys. Rev. B **88**, 066404 (2002).